



Universiteit
Leiden
The Netherlands

Development of kinase inhibitors and activity-based probes

Liu, N.

Citation

Liu, N. (2016, December 15). *Development of kinase inhibitors and activity-based probes*. Retrieved from <https://hdl.handle.net/1887/44807>

Version: Not Applicable (or Unknown)

License: [Licence agreement concerning inclusion of doctoral thesis in the Institutional Repository of the University of Leiden](#)

Downloaded from: <https://hdl.handle.net/1887/44807>

Note: To cite this publication please use the final published version (if applicable).

Cover Page



Universiteit Leiden



The handle <http://hdl.handle.net/1887/44807> holds various files of this Leiden University dissertation.

Author: Liu, N.

Title: Development of kinase inhibitors and activity-based probes

Issue Date: 2016-12-15

Development of Kinase Inhibitors and Activity-based Probes

PROEFSCHRIFT

ter verkrijging van
de graad van Doctor aan de Universiteit van Leiden,
op gezag van Rector Magnificus Prof. mr. C. J. J. M. Stolker,
volgens het besluit van het College voor Promoties
te verdedigen op 15 december 2016
klokke 12:30 uur

door

Nora Liu

geboren te 's-Gravenhage in 1986

Promotiecommissie

Promotor	Prof. dr. H. S. Overkleeft Prof. dr. J. Neefjes
Co-promotor	Dr. M. van der Stelt
Overige leden	Prof. dr. J. M. F. G. Aerts Prof. dr. G. A. van der Marel Prof. dr. J. Brouwer Dr. I. Berlin Dr. C. Kuijl, VUmc, Amsterdam

Cover Design Kai Fung Yu

Drukker Ridderprint B.V., Ridderkerk, Nederland

Table of contents

List of Abbreviations	6
Chapter 1 General Introduction	11
Chapter 2 Chemical tools to label kinases	23
Chapter 3 Synthesis of FLT3 kinase inhibitors: isoquinolinesulfonamide-based library	47
Chapter 4 Biological evaluation of H-89-analogues: searching for selective AKT1 and FLT3 inhibitors	85
Chapter 5 Direct and two-step bioorthogonal probes for Bruton's tyrosine kinase based on ibrutinib: a comparative study	111

Chapter 6	135
Probing for PKA and AKT1 using photoaffinity probes	
Chapter 7	155
An affinity-based probe for kinase profiling: Fishing for Dasatinib targets	
Chapter 8	165
Summary and Future Prospects	
Samenvatting	185
List of Publications	188
Curriculum Vitae	189

List of Abbreviations

Å	Ångström	Boc	<i>tert</i> -butyloxycarbonyl
ab	antibody	Boc ₂ O	<i>tert</i> -butyloxycarbonic anhydride
ABP	activity-based probe		
ABPP	activity-based protein profiling	bs	broad singlet
abs	absorption	BTK	bruton's tyrosine kinase
Ac	acetyl	CaMK	Ca ²⁺ /Calmodulin dependent kinase
ACN	acetonitrile	cAMP	cyclic adenosine monophosphate'
ADP	adenosine diphosphate	CBB	Coomassie brilliant blue
AfBP	affinity-based probe	Cbz-Cl	carbobenzoxoy chloride
AGC	PKA, PKG and PKC	CCMS	capture compound mass spectrometry
AKT	V-AKT murine thymoma viral oncogene homolog 1		
ALL	acute lymphoblastic leukemia	CDK	cyclin-dependent kinase
AML	acute myeloid leukemia	cGMP	cyclic guanosine monophosphate
AMP	adenosine monophosphate	CLL	chronic lymphocytic leukemia
aq.	aqueous	CLK	Cdc-like kinase
ARG	arginine	CK1	casein kinase 1
arom , ar	aromatic	c/m	chloroform/methanol
ATM	ataxia telangiectasia mutated	CMGC	CDK, MAPK, GSK3 and CLK
ATP	adenosine triphosphate	CML	chronic myeloid leukemia
ATR	ataxia telangiectasia and Rad3-related	CSK	C-terminal Scr kinase
βARK	β-andrenergic receptor kinase	CSNK1D	casein kinase 1 delta
BMSC	bone marrow stromal cell	CuAAC	copper(I)-catalyzed alkyne-azide [2+3] cycloaddition
BCR	B-cell receptor		
BCR-Abl	breakpoint cluster region Abelson	Cy	cyanine dye
		Cys	cysteine
		Δ	heating (reflux)
		δ	chemical shift
		d	doublet
BODIPY	4,4-difluoro-4-bora-3a,4a-diaza-s-indacene	Da	Dalton
		Das.	dasatinib

DC	dual color molecular weight marker SDS-PAGE	FGFR	fibroblast growth factor receptor
DCE	dichloroethane	FL	FLT3 ligand
DCM	dichloromethane	FLT3	FMS-like tyrosine kinase 3
dd	doublet of doublets	FMS	Feline McDonough
DDR	discoidin domain receptor		Sarcoma
DIAD	diisopropyl azadicarboxylate	FOXO3	forkhead box O3
DiBAL-H	diisobutylaluminium hydride	FSBA	5'-fluorosulfonylbenzoyl 5'-adenosine
DiPEA	<i>N, N</i> -diisopropyl- <i>N</i> -ethylamine	FYN	Fgr/Yes related novel protein
DLBCL	diffuse large B-cell lymphoma	GABA	γ -aminobutyric acid
DMEM	Dulbecco's modified eagle medium	GSK3	glycogen synthase kinase
DMF	<i>N,N</i> -dimethylformamide	GTP	guanosine triphosphate
DMSO	dimethylsulfoxide	H	hour(s)
DNA	deoxyribonucleic acid	HATU	1-[Bis(dimethylamino)-methylene]-1 <i>H</i> -1,2,3-triazolo[4,5- <i>b</i>]pyridinium 3-oxid
dt	double triplet		hexafluorophosphate
DTT	dithiothreitol	HEK	human embryonic kidney cell line
DUS2	dihydrouridine synthase 2		
EGFR	epidermal growth factor receptor	HEPES	4-(2-hydroxyethyl)-1-piperazineethanesulfonic acid
em	emission		
EPHA	ephrin receptor kinase	HPLC	high performance liquid chromatography
eq.	equivalents		
ERK	extracellular signal-regulated kinase	HRMS	high-resolution mass spectrometry
ESI	electrospray ionization	HWE	Horner-Wadsworth-Emmons
Et	ethyl		
Et ₂ O	diethyl ether	Hz	hertz
EtOAc	ethylacetate	lbr.	ibrutinib
EtOH	ethanol	IC ₅₀	half maximal inhibitory concentration
FACS	fluorescence activated cell sorting	ICAP	isotope-coded ATP ABPP probe
FAK	focal adhesion kinase		
FDA	Food and Drug Administration	IEDDA	inverse-electron demand Diels-Alder

Im.	imatinib	NMR	nuclear magnetic resonance
IMAP	immobilized metal ion affinity-based fluorescence polarization	NQO2	NAD(P)H quinone dehydrogenase 2
Ig	immunoglobulin	PBS	phosphate buffered saline
IR	infrared-spectrometry	PDB	protein data bank
ITAM	immunoreceptor tyrosine-based activation motif	PDGFRB	platelet derived growth factor receptor beta
ITD	internal tandem duplication	PDK1	phosphoinositide- dependent protein kinase 1
<i>J</i>	coupling constant	PE	petroleum ether
JAK	Janus kinase	PET	positron emission tomography
K_i	inhibitor constant	PH	pleckstrin homology
KR	kinase reaction	Ph	phenyl
Lck	lymphocyte-specific protein tyrosine kinase	PI	phophoinositide
LCMS	liquid chromatography mass spectrometry	PI3K	phophatidylinositol-3- kinase
LIMK	LIM domain kinase	PIKK	PI3K-related kinase
LY N	Lck/Yes novel	PIM	proviral integration site
Lys	lysine		MuLV (murine leukemia virus)
M	molar		
m	multiplet	PIP3	phosphatidylinositol 3,4,5 triphosphate
MAPK	mitogen-activated protein kinase	PKA	protein kinase A
MCL	mantle cell lymphoma	PKB	protein kinase B
MDS	myelodysplasia	PKC	protein kinase C
MEK	MAPK/ERK kinase	PKG	protein kinase G
MeOH	methanol	PLC γ 2	phospholipase C gamma 2
min	minutes		
mTor	mechanistic target of rapamycin	PNP	para-nitrophenyl
m/z	mass-to-charge ratio	ppm	parts per million
NFAT	nuclear factor of activated T cells	PTK	protein tyrosine kinase
NF κ B	nuclear factor κ B	q	quartet
NHS	<i>N</i> -hydroxysuccinimide	quant.	quantitative
		Ras	Rat sarcoma
		Raf	rapidly accelerated fibrosarcoma

R _f	retention factor		triazolylmethyl amine
RGC	receptor guanylate cyclase	Thr	threonine
		TLC	thin layer chromatography
ROCK	Rho-associated, coiled-coil containing protein kinase	TK	tyrosine kinase
		TKD	tyrosine kinase domain
RP	reversed phase	TKL	TK-like
RT	room temperature	TR-FRET	time resolved fluorescence resonance energy transfer
Rt	retention time		
RTK	receptor tyrosine kinase		
S	substrate	Tris	2-amino-2-(hydroxymethyl)-1,3-propanediol
s	singlet		
S6K	p70 S6 kinase		
SAR	structure-activity relationships	Ts	tosyl
		Tyr	tyrosine
sat.	saturated	UV	ultra violet
SDS-PAGE	sodium dodecyl sulfate polyacrylamide gel	v	volume
		Val	valine
Ser	serine	YES	Yamaguchi (Y73 virus), Esh avian sarcoma oncogene
SH	Src homology		
Src	sarcoma		
STAT-5	signal transducer and activator of transcription 5	WM	Waldenström's macroglobulinemia
		ZAK	α motif leucine zipper containing kinase
STE	homologues of yeast sterile kinase		
STK	serine/threonine kinase 25		
Su	succinimide		
Syk	spleen tyrosine kinase		
t	triplet		
tBu	<i>tert</i> -butyl		
tBuOH	<i>tert</i> -butanol		
td	triplet of doublets		
TEA	triethylamine		
TFA	trifluoroacetic acid		
TH	Tec homology		
THF	tetrahydrofuran		
THPTA	Tris (3-hydroxypropyl		

1

General introduction

Kinases

A wide array of intracellular signaling events in eukaryotic cells, including metabolism, growth, division, differentiation, motility, organelle trafficking, membrane transport, muscle contraction, immunity, learning and memory, are mediated by protein phosphorylation.¹ The diversity of processes regulated by this post-translational modification is reflected by the large number of protein kinases (about 600) encoded by the human genome.² Protein kinases are related by their conserved homologous kinase domains; a catalytic core that consists of 250 – 350 residues.³ The site of phosphate transfer is located between a N-terminal lobe composed of a β -sheet and a

single α -helix (the “C-helix”) and a larger C-terminal lobe consisting of α -helices, connected by a linker referred to as the hinge region (Figure 1A). Within the conserved, narrow and hydrophobic ATP-binding pocket, the adenine ring of ATP makes a number of hydrophobic contacts in the ATP-binding cleft and forms at least one hydrogen bond with the backbone of the hinge region.⁴ The triphosphate group of ATP points out of the adenosine pocket towards the hydrophilic medium. When the substrate (peptide, lipid or carbohydrate) binds to its kinase, a set of conserved residues within the kinase catalytic domain catalyses the transfer of the terminal γ -phosphate of ATP to the hydroxyl oxygen of Ser, Thr or Tyr residue of the substrate. Phosphorylation may result in significant changes in either structural features or function of the target protein (Figure 1B).

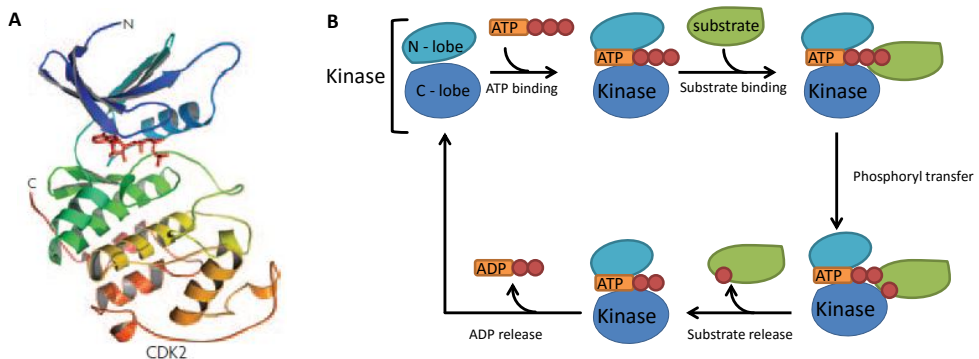


Figure 1. A) In general, protein kinases consist of a N-terminal (blue) and a C-terminal lobe (green, yellow, orange). The crystal structure of cyclin-dependent kinase 2 (CDK2) (Protein Data Bank (PDB) ID: 1QMZ) shows the representative fold. ATP is modeled bound in the cleft (red ball and stick model). B) The general catalytic cycle for substrate phosphorylation by a kinase.

The kinase superfamily consists of four major families, namely AGC, Ca^{2+} /calmodulin-dependent protein kinases (CaMK), CMGC and tyrosine kinases (TK), and four minor families, namely casein kinase 1 (CK1), STE, receptor guanylate cyclase (RGC) and TK-like (TKL) kinase.⁵

The AGC group of kinases comprises more than 60 members including the cyclic-nucleotide-dependent family protein kinases A (PKA) and G (PKG), the protein kinase C (PKC) family, the β -adrenergic receptor kinase (β ARK) family, the ribosomal S6 kinase family, and other close relatives. In general, this group of kinases tends to be basic amino acid-directed enzymes by phosphorylating at Ser/Thr residues, which are near Arg and Lys. The AGC kinases participate in a variety of well-known signaling processes. They mediate cyclic AMP signaling, the response to insulin, protection against apoptosis, diacylglycerol signaling and control of protein translation.^{6,7}

The CaMK group protein kinases are Ser/Thr protein kinases. Almost all are activated by Ca^{2+} /calmodulin binding to a small domain located near the COOH-terminal to the catalytic domain. CaMKs are particularly abundant in the brain and the nervous system, where they are involved in synaptic development and plasticity, gene transcription, muscle contraction and learning and memory processes by targeting various factors including structural proteins, ion channels and protein pumps.^{8, 9, 10}

CMCG is a major category of Ser/Thr kinases. Mostly, CMCG members phosphorylate substrates at proline-rich sites. This group includes the protein kinases cyclin-dependent kinase (CDK), mitogen-activated protein kinase (MAPK), glycogen synthase kinase (GSK3), CDC-like kinase (CLK). These kinases are known for controlling the cell cycle, activity of human tumor suppressors and cell-fate decisions.^{11, 12}

The protein tyrosine kinase family phosphorylates, in contrast to the families described above, on Tyr residues. Family members play a role in mitogenesis, differentiation and development, angiogenesis, cell cycle control, growth control, cell survival and apoptosis, transcriptional regulation, and glucose uptake.¹³

TKL kinases are a diverse group of Ser/Thr protein kinases with sequence similarity to TK, but lacking TK-specific motifs.¹ These kinases are involved in programmed cell death, growth and immune system.¹⁴

CK1 represents an unique group within the superfamily of Ser/Thr kinases. They have been implicated in the control of cytoplasmic and nuclear processes, including DNA replication and repair.^{15, 16}

Members of the STE kinase family include the homologues of yeast sterile 7, sterile 11 and sterile 20 kinases. This group of kinases prefers to phosphorylate serine and threonine residues with an arginine residue N-terminal to the phosphorylation site. They form the MAPK cascade and transduce signals from the cell surface to the nucleus.¹⁷

The kinases of the RGC family contain an active guanylate cyclase domain, which generates the cGMP second messenger. This second messenger is a key signaling molecule that in turn modulates the activity of cGMP dependent kinases, ion channels, and phosphodiesterases. They also contain a catalytically inactive kinase domain, which appears to have a regulatory domain.¹⁸ RGCs have attracted considerable interest due to their roles in the cardiovascular and nervous systems, bone development and vision.¹⁹

Kinases as drug targets

Since protein kinases are key components of most signal transduction networks, this makes them therapeutically relevant drug targets and interesting to explore their biological roles and functions in detail. A few kinases together with their inhibitors relevant to studies described in this thesis are highlighted below.

PKB/AKT1 and FLT3

AKT, also known as protein kinase B (PKB), is an intracellular anti-apoptotic serine/threonine kinase belonging to the AGC family of kinases. Three isoforms of AKT are known to exist, namely AKT1, AKT2 and AKT3. These isoforms exhibit about 90% sequence identity in the kinase domain and 97-100% sequence identity in the ATP-binding site.²⁰ PKB/AKT is a key component of the PI3K-AKT-mTor kinase pathway, which is responsible for cell proliferation, survival, cell growth, apoptosis and metabolism.²¹

Full activation of PKB is a multi-step process that uses the PI3K signaling pathway. First, extracellular ligands (hormones and growth factors) bind to receptor tyrosine kinase (RTK), which in turn forms homo-oligomers.²² In response, phosphatidylinositol-3 kinase (PI3K) is activated through binding to phosphotyrosine residues in the receptor and phosphorylates in turn phosphoinositides (PI) to generate phosphatidylinositol 3,4,5 triphosphate (PIP3). PIP3 organizes PKB/AKT, PDK1 and Ser473-kinase on the plasma membrane, where PKB/AKT becomes phosphorylated and activated. Then, the activated PKB/AKT translocates from the cytosol to the nucleus (Figure 2).^{23, 24, 25}

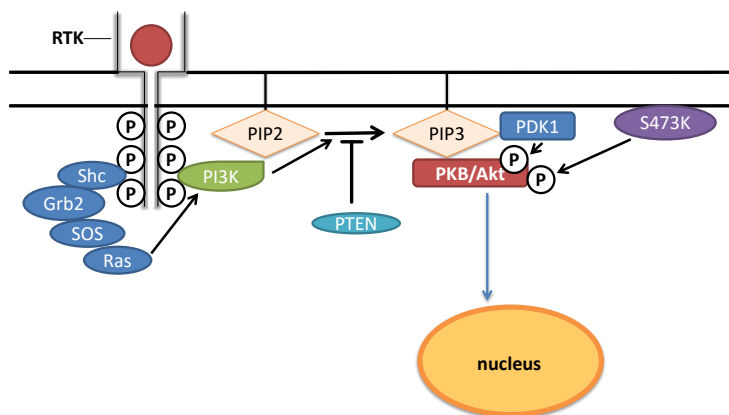


Figure 2. Schematic representation of PKB activation.

PKB/AKT is recognized as an important therapeutic target for the treatment of human cancers, such as breast, ovarian, prostate and pancreatic cancers,²⁶ as well as diabetes.²⁷ In addition, one of the three PKB/AKT isomers has been identified as a potential target to prevent intracellular growth of *Salmonella typhimurium* and *Mycobacterium tuberculosis*. Kuijl *et al.* have shown that inhibition of PKB/AKT1 resulted in less infection, which makes it a potential antibiotic drug target.²⁸ However, the major bottleneck is to find selective PKB/AKT1 inhibitors, since elimination of both AKT1 and AKT2 is lethal whereas genetic elimination of AKT1 had no impact on the health of the mice.

Studies have revealed that the PKA inhibitor H-89 (**1**, Figure 3) has a higher selectivity towards AKT1 than AKT2, which makes this compound an interesting lead compound. Many analogues of H-89 have been synthesized, however a nanomolar inhibitor needs still to be developed.

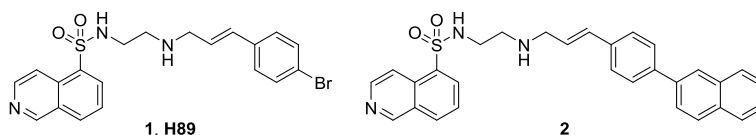


Figure 3. Structures of lead compounds **1** (PKB/AKT1) and **2** (FLT3).

Within many synthesized analogues of H-89, one interesting compound that was identified comprises naphthalene analogue **2** (Figure 3). This bulky aromatic compound showed hardly any PKB/AKT1 inhibition, but inhibited another interesting kinase named FMS-like tyrosine kinase 3 (FLT3) with an IC_{50} of 1.01 μ M. FLT3 is a type III receptor tyrosine kinase and consists of five immunoglobulin-like domains in the extracellular region, a juxtamembrane domain, a tyrosine kinase domain separated by a kinase insert domain and a C-terminal domain in the intracellular region.²⁹ This kinase is expressed on the surface of normal hematopoietic stem/progenitor cells and plays a well-established role in normal growth, survival and differentiation of hematopoietic precursor cells. Like other RTKs, upon binding of FLT3 ligand (FL), which is expressed by bone marrow stroma cells, the FLT3 receptor dimerizes at the plasma membrane (Figure 2).³⁰ This leads to autophosphorylation and activation of multitude downstream effector signaling cascades, including Ras/Mek, PI3K/AKT/mTor, and STAT-5 pathways. All these pathways play important roles in the promotion of cell cycle progression, inhibition of apoptosis, and activation of differentiation. FLT3 is an important key regulator in multiple hematopoietic pathways, and mutated FLT3 causes altered mechanisms of cellular proliferation and apoptosis that promote cell survival thereby conferring a substantial growth advantage to leukemic stem and progenitor cells. FLT3 mutations are mostly found in patients with acute myeloid leukemia (AML)^{31,32,33}, myelodysplasia (MDS),^{34,35} and acute lymphoblastic leukemia (ALL).^{36,37} Potent and selective FLT3 inhibitors may form the starting point for therapeutics for these diseases.

Bruton's tyrosine kinase (BTK)

Another tyrosine kinase that plays a major role in the pathogenesis of hematological malignancies, such as chronic lymphocytic leukaemia (CLL) and mantle cell lymphoma (MCL), and autoimmune diseases as well is Bruton's tyrosine kinase (BTK).³⁸ BTK is a member of the Tec tyrosine kinase family and is expressed in most hematopoietic cells

such as B-cells, mast cells and microphages, except in T-cells and plasma cells. It is predominantly situated in the cytosol and has several conserved domains from the N-terminus: pleckstrin homology (PH), Tec homology (TH), Src homology 2 and 3 (SH2 and SH3) and a carboxyl-terminal regulatory and catalytic region that contains the tyrosine kinase (TK) or SH1 domains.³⁹ BTK functions downstream of multiple receptors including growth factors, B-cell antigen, chemokine and innate immune receptors. BTK initiates a diverse range of cellular processes, such as cell proliferation, survival, differentiation, motility, angiogenesis, cytokine production and antigen presentation.⁴⁰

From the many pathways, the B-cell receptor (BCR) signaling pathway is crucial for the pathogenesis of many B-cell malignancies. BCR plays a fundamental role in B-cell proliferation, differentiation and function including production of antibodies.⁴¹ It serves as an antigen receptor, which consists of a surface transmembrane immunoglobulin (Ig) receptor associated with the Ig-alpha (CD79a) and Ig-beta (CD79b) heterodimers.⁴² In normal B-cells, antigen binding to the receptor leads to receptor aggregation and recruits other kinases such as spleen tyrosine kinase (SYK) and LYN kinases. These in turn, phosphorylate the receptor's cytoplasmic tyrosine-based activation motifs (ITAMs) on the cytoplasmic Ig domains of the receptor. ITAM phosphorylation sets off a cascade of downstream events including activation of downstream kinases, adaptor molecules, and generation of second messengers. SYK propagates the signal by activation of PI3K, which stimulates the production of PIP3. Once an adequate amount of PIP3 is produced, BTK is mobilized to the plasma membrane. At this site, BTK is activated by phosphorylation at the Y551 site by the Src family kinases, especially LYN and FYN. BTK amplifies the signal via phosphorylation of phospholipase gamma C2 (PLCγ2), mobilization of calcium secondary messengers, PKC, and finally activation of MAP kinase pathways, nuclear factor of activated T cells (NFAT) and nuclear factor κB (NFκB). These signals regulate patterns of gene expression necessary for B cell survival and proliferation (Figure 4).^{40, 42}

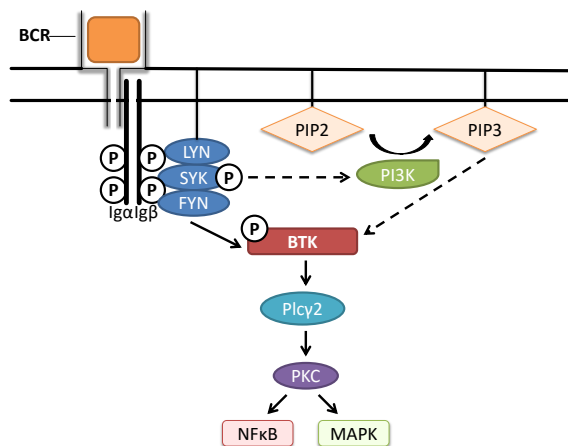


Figure 4. Schematic representation of BCR/BTK signaling pathway.

Among the many kinases involved in BCR signaling, BTK is a unique therapeutic target for treatment of B-cell malignancies. This is due to the fact that BTK inhibition leads to inhibition of NF κ B DNA binding, reduction of integrin-mediated cell adhesion and migration, limitation of cell production of chemokines and, ultimately, apoptosis. The first-in-class BTK-inhibitor ibrutinib (Imbruvica®, PCI-32765, **3**, Figure 5) has recently been approved for the treatment of Waldenström's macroglobulinemia (WM), MCL and CLL by the FDA.^{43,44,45,46} Apart from its clinical efficacy, ibrutinib is of interest because of its mechanism of action. Ibrutinib irreversibly blocks BTK activity through covalent modification of Cys481 within the enzyme ATP-binding pocket following conjugate addition of the cysteine thiol to the acrylamide moiety in **3** (Figure 5), an event that prevents phosphorylation of Tyr223, an essential step for BTK activation.⁴⁷ Even though the action of this drug has been studied in detail for BTK, it would also be interesting to investigate whether this drug has other cellular targets. This will give insight into the mechanism of side effects.

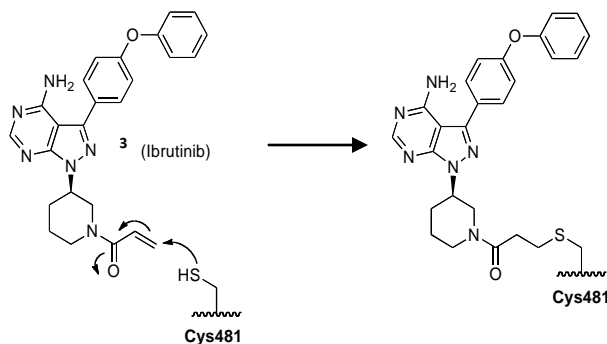


Figure 5. Covalent binding of ibrutinib (**3**) to Cys481 in the active site of BTK.

Dasatinib as inhibitor for Bcr-Abl

Chronic myeloid leukemia (CML) is a hematological malignancy, which is defined to be Philadelphia chromosome/Bcr-Abl positive. In 1960, the Philadelphia chromosome was first discovered in cell cultures from CML patients.⁴⁸ A Philadelphia chromosome is a truncated version of chromosome 22 produced by a reciprocal translocation between the Abl gene on chromosome 9 and the breakpoint cluster region (BCR) on chromosome 22, which leads to the formation of the novel Bcr Abelson tyrosine kinase (Bcr-Abl) fusion gene. This fusion kinase possesses the tyrosine kinase activity of Abl, which is constitutively active in the cytosol. As a result, the downstream signaling pathways are dysregulated and proliferation and survival of leukemic cells are increased.⁴⁹

BCR is a serine/threonine kinase with several interactions domains for proteins such as actin, lipids and GTP. C-Abl protein, which has a molecular weight of 140 kDa, shuttles

between the nucleus and cytoplasm. It is involved in many processes such as regulation of cell growth and survival, oxidative stress reaction, response to DNA damage and regulation of actin dynamics and cell migration. Specific breakpoints in the chromosomal translocation lead to distinct forms of Bcr-Abl protein: p185 Bcr-Abl, p210 Bcr-Abl and P230 Bcr-Abl. Each type is found in different types of leukemia; the p210 form is associated with CML, whereas p230 and p185 are associated with neutrophilic leukemia and acute lymphoblastic leukemia, respectively.⁵⁰

Up to now, there are three generation of BCR-Abl inhibitors approved by the FDA. One of the many inhibitors is dasatinib (**4**), which is a dual-specificity Abl- and Src-family kinases inhibitor having a substituted thiazole-carboxamide (Figure 6). However, the molecule is not selective for Bcr-Abl and Src, since it has been successively reported that this compound also inhibits other TKs.⁴⁸ This information provides a rationale for investigating it in other hematologic malignancies, such as CLL.

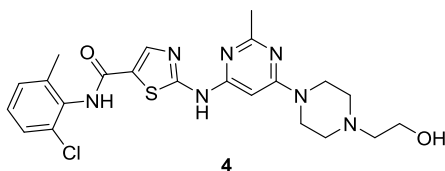


Figure 6. Structure of dasatinib (**4**).

Finally, it should be mentioned that kinase inhibitors are important not just for the treatment of diseases, but also as reagents for gaining understanding about the physiological roles of protein kinases and additional targets that cause side effects or synergy. In these cases, the use of chemo-proteomic tools, also known as activity-based probes (ABPs), for performing activity-based protein profiling (ABPP) comes to a rescue. These chemical tools need to bind or have affinity for the target(s) of interest and contain a reporter group, such as the fluorescent group Bodipy-FL or biotin for detection, quantification, and/or enrichment/identification of labeled proteins. In cases where enzyme activities in living cells or organisms are subject of study, the use of reporter groups with a small, latent chemical handle (alkyne, azide or norbornene) may be a solution, because bulky reporter groups may hamper cell permeability feature of an ABP. Since the inhibitors (H-89, ibrutinib and dasatinib) that are discussed above bind (non)covalently to their specific subset (or family) of catalytically related enzymes, these compounds are interesting candidates to turn into an affinity- or activity-based probe. This will provide more insight into the additional drug targets and mechanism of the various types of cancers, diabetes and immune diseases.

Aim and outline of this thesis

The central role of protein kinases in many signal transduction pathways has generated intense interest in targeting these enzymes for a wide range of diseases. This thesis focuses on both the development of more potent kinase inhibitors and the development of ABPs to study the roles of kinases, inhibitor selectivity profile and the additional targets of known kinase inhibitors.

In **Chapter 2**, an overview will be provided about three kinase profiling methods that are published in literature, namely activity-based protein profiling, photoaffinity protein profiling and affinity-based protein profiling. The fundamentals of these profiling methods will be explained in detail.

More potent inhibitors towards FLT3 are needed to treat certain types of leukemia.

Chapter 3 describes the design and synthesis of 102 isoquinolinesulfonamide compounds, which share the same core as H-89 (**1**). The variations between these related compounds were created by substitution of the phenyl bromide with bulky (hetero)aromatic groups at the ortho, meta or para phenyl site under Suzuki coupling conditions.

The biological activities of these 102 compounds together with 137 structurally related isoquinolinesulfonamides were evaluated in **Chapter 4**. IC₅₀ and K_i values towards the kinases PKA, AKT1, AKT2 and FLT3 are given. Based on these findings, structure-activity relationships (SAR) are discussed and the most active and selective inhibitors shown.

In the second part of the thesis, three ways to label kinases are outlined. In **Chapter 5** the synthesis of two direct (Bodipy-FL and Bodipy-TMR) and three two-step labeling ibrutinib-based probes (azide, alkyne and norbornene) are discussed. These probes are used to label BTK and act as activity-based probes, since they bind covalently to BTK after a nucleophilic attack of the thiol-group in the active site of BTK. Furthermore, labeling of BTK in Ramos cells and lysate is visualized on SDS-PAGE gel.

Chapter 6 focuses on the synthesis of photoaffinity-based probes for PKB/AKT1 and PKA. These core of the probes are based on the PKA inhibitor H-89 (**1**) and they also contain a diazine group as the photoaffinity group, which bind covalently to its target after exposure to UV. In addition, these probes also contain an azide ligation handle, which is useful for visualization and/or enrichment of proteins. Labeling of recombinant PKA and AKT1 kinases and competition assays will be shown.

A third way to label kinases is by affinity-based protein profiling, which is discussed in **Chapter 7**. The synthesis of an affinity-based probe based on dasatinib, which is immobilized on NHS-activated beads, will be discussed. Furthermore, information about the targets of this probe will be provided by Western blot analysis.

Finally, **Chapter 8** provides a summary of the results gained in this thesis and projects some future prospects.

References

- ¹ J. A. Ubersax and J. E. Ferrell Jr, *Nature Rev. Mol. Cell. Biol.*, 2007, **8**, 530.
- ² P. Blume-Jensen and T. Hunter, *Nature*, 2001, **411**, 355.
- ³ S. K. Hanks and T. Hunter, *Faseb. J.*, 1995, **9**, 576.
- ⁴ J. A. Endicott, M. E. M. Noble and L. N. Johnson, *Annu. Rev. Biochem.*, 2012, **81**, 587.
- ⁵ E. D. G. Fleuren, L. Zhang, J. Wu and R. J. Daly, *Nature Rev. Canc.*, 2016, **16**, 83.
- ⁶ R. T. Peterson and S. L. Schreiber, *Curr. Biol.*, 1999, **9**, R521.
- ⁷ J. M. Arencibia, D. Pastor-Flores, A. F. Bauer, J. O. Schulze and R. M. Biondi, *Biochim. Biophys. Act.*, 2013, **1834**, 1302.
- ⁸ G. A. Wayman, Y-S Lee, H. Tokumitsu, A. Silva and T. R. Soderling, *Neuron.*, 2008, **56**, 914.
- ⁹ G. A. Wayman, H. Tokumitsu, M. A. Davare and T. R. Soderling, *Cell Calcium*, 2011, **50**, 1.
- ¹⁰ K. A. Skelding, J. A. P. Rostas and N. M. Verrills, *Cell Cycle*, 2011, **10**, 631.
- ¹¹ N. Kannan and A. F. Neuwald, *Prot. Sci.*, 2004, **13**, 2059.
- ¹² M. Varjosalo, K. S. Keskitalo, A. van Drogen, H. Nurkkala, A. Vichalkovski, R. Aebersold and M. Gstaiger, *Cell. Rep.*, 2013, **3**, 1306.
- ¹³ F. A. Al-Obeidi, J. J. Wu and K. S. Lam, *Biopolymers*, 1998, **47**, 197.
- ¹⁴ M. E. Handley, J. Rasaiyaah, B. M. Chain and D. R. Katz, 2007, **88**, 111.
- ¹⁵ U. Knippschild, A. Gocht, S. Wolff, N. Huber, J. Lohler and M. Stoter, *Cell. Sign.*, 2005, **17**, 675.
- ¹⁶ K. J. Fish, A. Cegielska, M. E. Getman, G. M. Landes and D. M. Virshup, *J. Biol. Chem.*, 1995, **270**, 14875.
- ¹⁷ G. Zhu, K. Kuijl, Y. Liu, V. Codrea, J. Herrero, and S. Shaw, *J. Biol. Chem.*, 2005, **280**, 36372.
- ¹⁸ L. R. Potter, *Pharmacol. Ther.*, 2011, **130**, 71.
- ¹⁹ P. S. Padayatti, P. Pattanaik, X. Ma and F. van den Akker, *Pharm. Ther.*, 2004, **104**, 83.
- ²⁰ N. C. Kallan, K. L. Spencer, J. F. Blake, R. Xu, J. Heizer, J. R. Bencsik, I. S. Mitchell, S. L. Gloor, M. Martinson, T. Risom, S. D. Gross, T. H. Morales, W-I Wu, G. P. A. Vigers, B. J. Brandhuber and N. J. Skelton, *Bioorg. Med. Chem. Lett.*, 2011, **21**, 2410.
- ²¹ T. G. Davies, M. L. Verdonk, B. Graham, S. Saalau-Bethell, C. C. F. Hamlett, T. McHardy, I. Collins, M. D. Garrett, P. Workman, S. J. Woodhead, H. Jhoti and D. Barford, *J. Mol. Biol.*, 2007, **367**, 882.
- ²² T. O. Chan, S. E. Rittenhouse and P. N. Tsichlis, *Annu. Rev. Biochem.*, 1999, **68**, 965.
- ²³ E. S. Kandel and N. Hay, *Exp. Cell. Res.*, 1999, **253**, 210.
- ²⁴ M. Hanada, J. Feng and B. A. Hemmings, *Biochim. Biophys. Acta.*, 2004, **1697**, 3.
- ²⁵ J. Downward, *Curr. Opin. Cell. Biol.*, 1998, **10**, 262.
- ²⁶ H. Reuveni, N. Livnah, T. Geiger, S. Klein, O. Ohne, I. Cohen, M. Benhar, G. Gellerman and A. Levitzki, *Biochem.*, 2002, **41**, 10304.
- ²⁷ L. Logie, A. J. Ruiz-Alcaraz, M. Keane, Y. L. Woods, J. Bain, R. Marquez, D. R. Alessi and C. Sutherland, *Diabetes*, 2007, **56**, 2218.

- ²⁸ C. Kuijl, N. D. L. Savage, M. Marsman, A. W. Tuin, L. Janssen, D. A. Egan, M. Ketema, R. van den Nieuwendijk, S. J. F. van den Eeden, A. Geluk, A. Poot, G. van der Marel, R. L. Beijersbergen, H. S. Overkleef, T. H. M. Ottenhof and J. Neefjes, *Nature*, 2007, **450**, 725.
- ²⁹ J. Nagoya, *J. Med. Sci.*, 2015, **77**, 7.
- ³⁰ S. A. Wander, M. J. Levis and A. T. Fathi, *Ther. Adv. Hematol.*, 2014, **5**, 65.
- ³¹ H. Kiyoi, M. Towatari, S. Yokota, M. Hamaguchi, R. Ohno, H. Saito and T. Naoe, *Leukemia*, 1998, **12**, 1333.
- ³² D. L. Stirewalt, K. J. Kopecky, S. Meshinchi, F. R. Appelbaum, M. L. Slovak, C. L. Willman and J. P. Radich, *Blood*, 2001, **97**, 3589.
- ³³ S. Meshinchi, W. G. Woods, D. L. Stirewalt, D. A. Sweetser, J. D. Buckley, T. K. Tjoa, I. D. Bernstein and J. P. Radich, *Blood*, 2001, **97**, 89.
- ³⁴ S. Horiike, S. Yokota, M. Nakao, T. Iwai, Y. Sasai, H. Kaneko, M. Taniwaki, K. Kashima, H. Fujii, T. Abe and S. Misawa, *Leukemia*, 1997, **11**, 1442.
- ³⁵ S. Yokota, H. Kiyoi, M. Nakao, T. Iwai, S. Misawa, T. Okuda, Y. Sonoda, T. Abe, K. Kahsima, Y. Matsuo and T. Naoe, *Leukemia*, 1997, **11**, 1605.
- ³⁶ C. Thiede, C. Steudel, B. Mohr, M. Schaich, U. Schakel, U. Platzbecker, M. Wermke, M. Bornhauser, M. Ritter, A. Neubauer, G. Ehninger and T. Illmer, *Blood*, 2002, **99**, 4326.
- ³⁷ Y. Yamamoto, H. Kiyoi, Y. Nakano, R. Suzuki, Y. Kodera, S. Miyawaki, N. Asou, K. Kuriyama, F. Yagasaki, C. Shimazaki, H. Akiyama, K. Saito, M. Nishimura, T. Motoji, K. Shinagawa, A. Takeshita, H. Saito, R. Ueda, R. Ohno and T. Naoe, *Blood*, 2001, **97**, 2434.
- ³⁸ U. Gaygo, M. Fung, F. Clow, S. Sun, E. Faust, S. Price, D. James, M. Doyle, S. Bari and S. H. Zhuang, *Ann. N. Y. Acad. Sci.*, 2015, **1358**, 82.
- ³⁹ A. Akinleye, M. Furqan and O. Adekunle, *Clin. Lymph. Myel. Leuk.*, 2014, **14**, 253.
- ⁴⁰ M. S. Davids and J. R. Brown, *Leuk. Lymphoma*, 2012, **53**, 2362.
- ⁴¹ A. Novero, P. M. Ravello, Y. Chen, G. Dous and D. Liu, *Exp. Hematol. Onc.*, 2014, **3**, 4.
- ⁴² A. Aalipour and R. H. Advani, *Brit. J. Haematol.*, 2013, **163**, 436.
- ⁴³ F. Cameron and M. Sanford, *Drugs*, 2014, **74**, 263.
- ⁴⁴ US Food and Drug Administration, Imbruvica, 2013, (Accessed 9 December 2013).
- ⁴⁵ L. A. Honigberg, A. M. Smith, M. Sirisawas, E. Verner, D. Loury, B. Chang, S. Li, Z. Pan, D. H. Thamm, R. A. Miller and J. J. Buggy, *PNAS*, 2010, **107**, 13075 – 13080.
- ⁴⁶ Z. Pan, H. Scheerens, S.-J. Li, B. E. Schultz, P. A. Sprengeler, L. C. Burrill, R. V. Mendonca, M. D. Seeney, K. C. K. Scott, P. G. Grothaus, D. A. Jeffery, J. M. Spoerke, L. A. Honigberg, P. R. Young, S. A. Dalrymple and J. T. Palmer, *Chem. Med. Chem.*, 2007, **2**, 58.
- ⁴⁷ L. A. Honigberg, A. M. Smith, M. Sirisawad, E. Verner, D. Loury, B. Chang, S. Li, Z. Pan, D. H. Thamm, R. A. Miller and J. J. Buggy, *PNAS*, 2010, **117**, 13075.
- ⁴⁸ K. Yang and L.-W. Fu, *Crit. Rev. Onc. Hematol.*, 2015, **93**, 277.
- ⁴⁹ A. Desogus, S. Schenone, C. Brullo, C. Tintori and F. Musumeci, *Exp. Opin. Ther. Pat.*, 2015, **25**, 397.
- ⁵⁰ T. S. Ross and V. E. Mgbemena, *Mol. Cell. Oncol.*, 2014, **1**, e963450.

2

Chemical tools to label kinases

2.1 Introduction

The protein kinase family is one of the largest protein superfamilies in eukaryotic genomes. Due to their central role in cell signaling, physiology and pathophysiology, there is need for biomarker discovery or development of selective kinase agonists or antagonists as therapeutics. To be able to develop more potent kinase inhibitors or to identify and assign function to the whole kinome completely, it is essential to determine the substrates of each individual protein kinase, to define how signaling pathways operate and to determine the (off)targets of kinase inhibitors. For this reason, there is interest in the development and application of chemical biology tools that allow the global analysis of the

protein expression and activity in complex biological samples. Three major strategies used for profiling of small molecule-protein interactions are: affinity-based protein profiling, activity-based protein profiling (ABPP), and photoaffinity labeling. Affinity-based probes (AfBP) are bi-functional small molecules that create a reversible interaction with the target proteins and are linked to either a sorting function or directly to a solid phase. After binding, non-binding proteins are washed away, and the bound proteins are analyzed with an analytical technique (e.g. LC-MS/MS) after elution (Figure 1A).^{1,2}

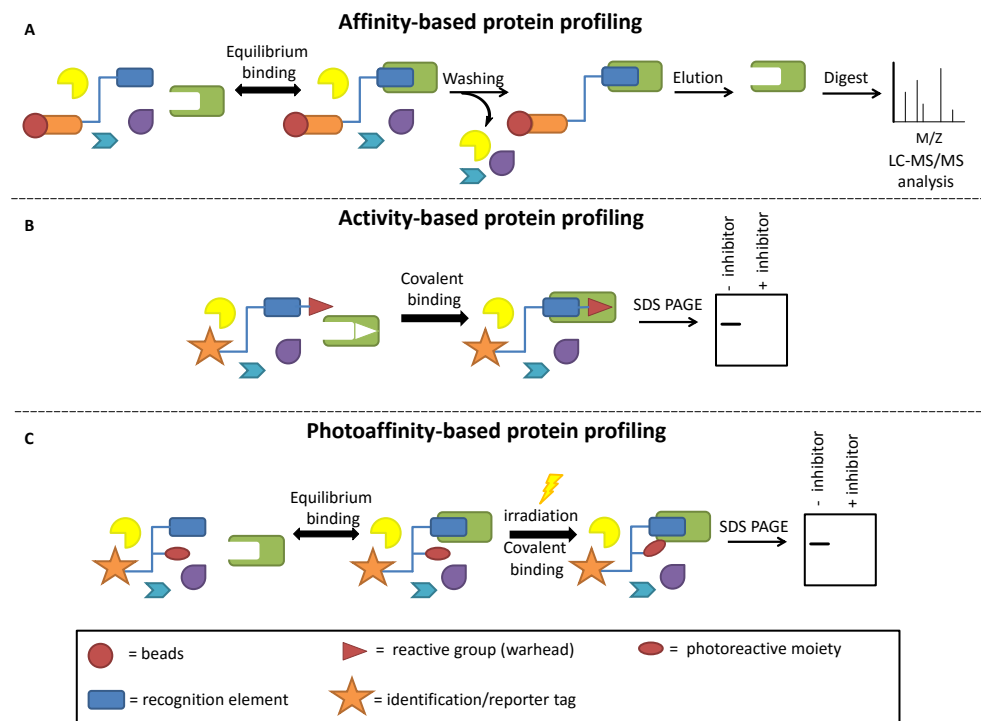


Figure 1. Schematic workflow for affinity pull down (A), activity-based protein profiling (B) and photoaffinity based profiling (C).

In ABPP the probe design consists of three general elements, namely a reactive group (the “warhead”), a recognition site and a chemical tag. The reactive group, which is an electrophilic group, binds and covalently modifies nucleophilic amino acids in the active sites of a single enzyme or a broad range of enzymes from a particular protein class (or classes). Due to the covalent and irreversible nature of this interaction, it enables subsequent sample processing steps employing other parts of the probe such as detection or sorting functions. The structure of the recognition site is in most cases based on the structure of the natural substrate of the target(s) or a known inhibitor (Figure 1B).³ Finally, photoaffinity probes contain three functional modules: 1) the selectivity function

accomplishes an equilibrium-driven affinity binding to target proteins, 2) the photo-reactivity function binds covalently to the active site of the target protein through photo-activation, and 3) the tag function is necessary for isolation or visualization of the targeted proteins (Figure 1C).⁴

Various techniques are available to visualize the probe-labeled proteins, such as fluorescence scanning of SDS-PAGE gels, fluorescence microscopy, fluorescence assisted cell sorting (FACS), and positron emission tomography (PET). Furthermore, labeling can also be used for enrichment of the sample for subsequent analysis by MS/MS or NMR techniques. For the visualization and/or isolation of the labeled enzymes, numerous reporter tags have been used. Commonly used reporter tags include fluorescent tags (e.g. BODIPY and cyanine dyes (Cy2, Cy3 and Cy5)) and affinity tags such as biotin.^{1,3,5,6} Even though the vast majority of chemical proteomics studies have been conducted on lysate samples, it is preferably to probe intracellular proteins in intact cells with membrane-permeable probes. Since only a minority of probes has been reported to be cell permeable and in some cases the bulkiness of the reporter group hampers recognition by the target enzymes, reporter tags in probes are replaced by markedly smaller bio-orthogonal ligation handles to overcome these problems. This strategy uses a two-step labeling method to label proteins in a chemoselective manner. Ligation handles that are frequently used are azide, alkyne and norbornene. Azides and alkynes can be used to perform a copper(I)-catalyzed Huisgen 1,3-dipolar cycloaddition ("click" reaction). Azides can also be used for Staudinger ligation. Norbornenes are used for an inverse-electron demand Diels-Alder reaction. All these ligation methods can be performed in the same biological sample in a chemoselective way (Figure 2).^{7,8,9,10}

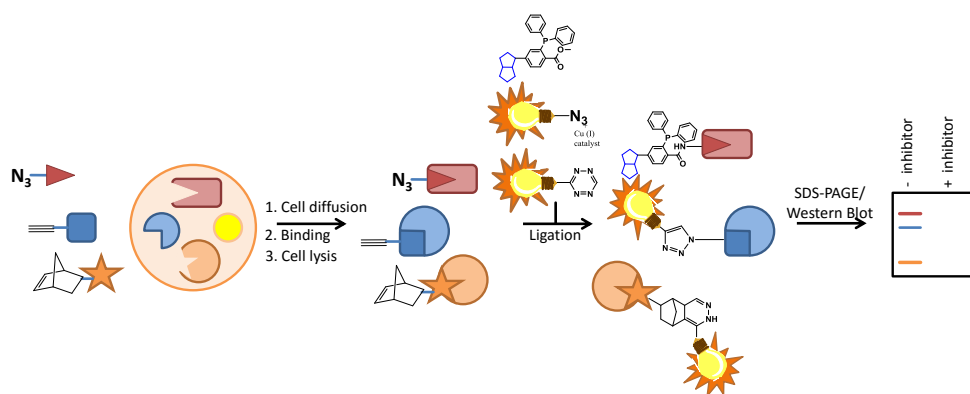


Figure 2. Schematic representation of three different bioorthogonal ligation methods: copper(I)-catalyzed click reaction, Staudinger-Bertozzi ligation and inverse-electron demand Diels-Alder ligation.

Affinity-based protein profiling

A powerful technique for the identification of the intracellular targets of small molecules and substrates is affinity chromatography. This methodology uses affinity-based probes, which contain a molecule of interest that can be immobilized on a solid support, to enrich ligand-binding proteins from cell lysates. This technique is attractive for determining the specificity of protein kinase inhibitors. For these studies, a known protein kinase inhibitor is immobilized on a solid support.¹¹ A number of notable examples of the application of this methodology are described below.

The first example that uses affinity chromatography to study the intracellular targets of a protein kinase inhibitor was performed with an analog of the CDK-family inhibitor purvalanol B (Figure 3, **1** en **2**).¹² Based on the crystal structure of CDK2-purvalanol, a linker could be attached to the carboxylic acid of the 6-anilino substituent of the inhibitor without interfering with its interaction with the kinase.¹³ This site was used to link purvalonal B to an agarose matrix through a polyethylene glycol linker (**2**). As a negative control, an inactive N6-methylated purvalanol (**3**) was synthesized and immobilized on agarose (**4**) (Figure 3). The immobilized purvalanol **2** was used to affinity purify interacting proteins from starfish oocytes, diverse mammalian tissues and protozoan parasites. The bound proteins were eluted, resolved by SDS-PAGE and analyzed by Western blotting or microsequencing. As a result, immobilized purvalanol **2** targets next to CDK1, CDK2, CDK5 also ERK1, ERK2, calcium/calmodulin-dependent protein kinase II (CamKII), p70 S6 kinase (S6K) and casein kinase 1 (CK1). The only non-protein kinase identified is the enzyme biliverdin reductase. *In vitro* assays have been performed to validate the interaction of purvalanol B (**1**) with ERK1, ERK2, CamKII, S6K and CK1. It should be noted that soluble purvalanol B (**1**) was less potent for ERK1, ERK2, CamKII, S6K and CK1 than CDK1, CDK2 and CDK5.

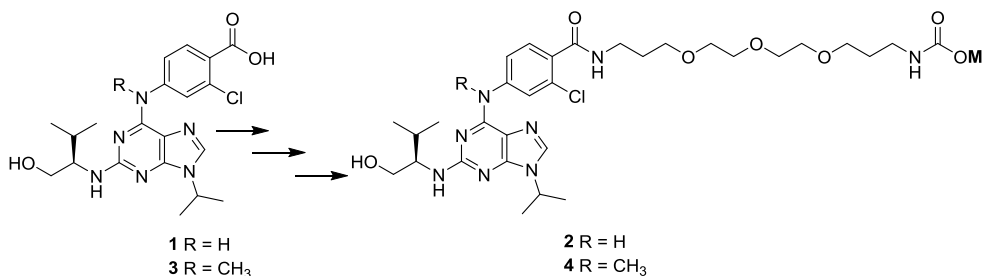


Figure 3. Structures of Purvalanol B (**1**), immobilized purvalanol **2**, the N6-methylated negative control **3** and its immobilized analogue **4**. **M** = agarose matrix.

Following a similar concept for the identification of protein kinase inhibitor targets in order to predict side effects and novel medical uses, Rix *et al.*¹⁴ have immobilized three BCR-ABL tyrosine kinase inhibitors that are used in the current frontline therapy in chronic myeloid leukemia (CML): imatinib (**5**), nilotinib (**6**) and dasatinib (**7**) (Figure 4). These three drugs (**5-6**) were converted into their coupleable analogues **8-10**, respectively, before being immobilized on NHS-activated Sepharose 4 Fast Flow beads via their amino functionalities to yield immobilized imatinib, nilotinib and dasatinib **11-13** (Figure 4). Since the acetylated analogues **14-16**, which are mimicking the immobilized compounds, did not display significantly altered activities, it was assumed that the immobilized drugs would act the same as their soluble analogue. Lysates of K562 and CML primary cells were subjected to affinity chromatography with immobilized drugs (**11-13**), and matrix-bound proteins were identified by liquid chromatography electrospray ionization tandem mass spectrometry (LC-ESI-MS/MS) and/or western blot analysis after being resolved by SDS-PAGE. According to mass spectrometry analysis, imatinib has 11, nilotinib has 14 and dasatinib 38 targets. Among the most prominent targets of dasatinib were the TEC family kinases TEC and BTK, next to BCR-ABL. Since imatinib and nilotinib displayed much more specific target profiles compared with dasatinib, the latter is thus more likely to have a more pronounced impact on multiple biologic processes.

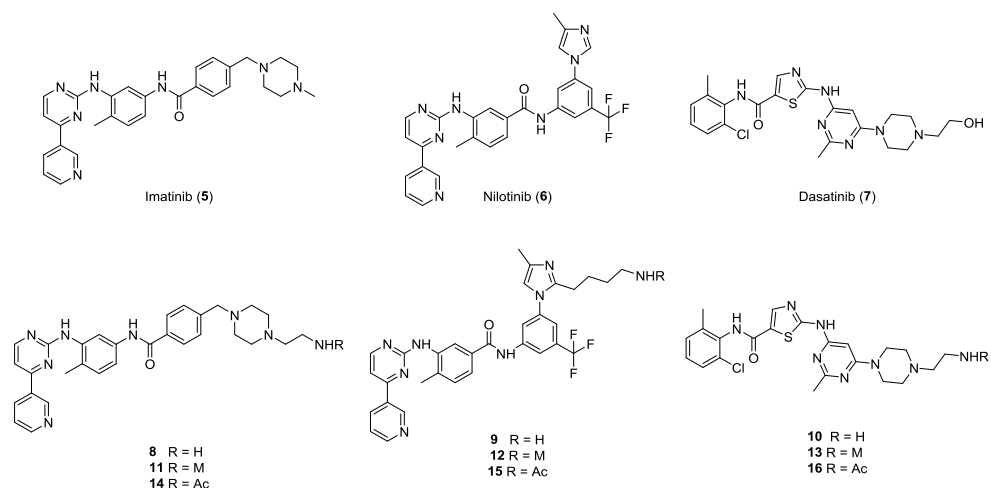


Figure 4. Structures of BCR-ABL inhibitors imatinib (**5**), nilotinib (**6**) and Dasatinib (**7**), their coupleable analogues (**8-10**), their immobilized analogues (**11-13**) (on NHS-activated Sepharose 4 Fast Flow beads) and their acetylated positive controls **14-16**. **M** = sepharose matrix

Other BCR-ABL inhibitors, INNO-406 (**17**)¹⁵ and bosutinib (**18**)¹⁶ were converted into coupleable precursors (**19** and **20**, respectively) prior to immobilization on sepharose beads (**21** and **22**, respectively) and were used to enrich for interacting proteins in human CML K562 cells (Figure 5). INNO-406 is known to inhibit BCR-ABL and LYN efficiently, but

this study additionally identified several novel kinases targets including ZAK, the receptor tyrosine kinases DDR1 and DDR2, and various ephrin receptor kinases (predominantly EPHA2, EPHA5 and EPHA8). Found interaction partners of bosutinib were BCR-ABL, SRC kinases LYN and YES, CSK, BTK, GAK, EPHB4 and PTK2.

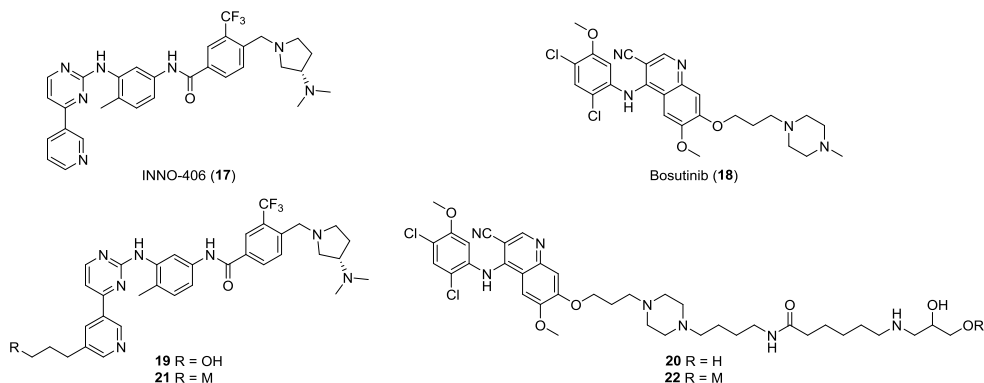


Figure 5. Structures of BCR-ABL inhibitors INNO-406 (**17**) and bosutinib (**18**), their coupleable analogues **19** and **20** and their immobilized analogues **21** and **22** (on NHS-activated Sepharose 4 Fast Flow beads). **M** = sepharose matrix.

Recently, Sewald *et al.* developed an affinity probe in order to understand new links of Janus Kinase (JAK) family members with other signaling pathways, because the JAK signaling pathways play a key role in many cellular processes, and was recently associated with neuronal disorders.¹⁷ The developed probe **24** is an aminopyrimidine derivative based on the known JAK inhibitor **23** (Figure 6), which is known to have high affinity towards all JAK isoforms. To design a probe to address all JAK isoforms, the acetanilide moiety in inhibitor **23** was substituted for an alcohol group and an additional methyl ester group, leading to probe **24**. Probe **24** was immobilized on NHS-activated sepharose beads through covalent linkage using the primary amine group, and pull down experiments were performed using the acute monocytic leukemia cell line MV4-11. The eluted target proteins were digested with trypsin into peptide fragments and analyzed by LC-MS/MS. By this method 133 kinases were identified with probe **24**, and these included the JAK isoforms JAK1, JAK2 and Tyk2. Next to the JAK kinases, a large number of other kinases related to signaling pathways, including MAPK1, MAPK3, MAPK8, MAPK9, MAPK14, MAP4K4, MKNK1 and PI3K, were identified. Due to the broad kinase coverage of probe **24**, it can be applied for the selectivity profiling of kinase inhibitors for the identified 133 kinases.

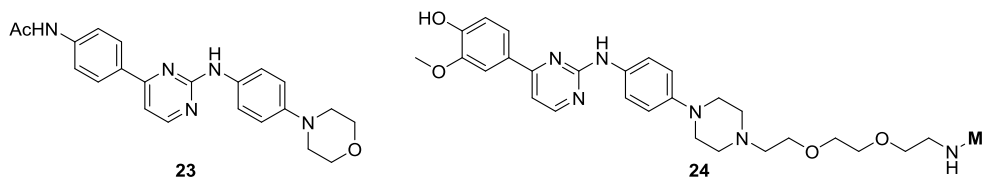


Figure 6. Structures of JAK inhibitor **23** and affinity based probe **24**. **M** = matrix (sepharose bead).

Other studies have also focused on the broadband-isolation of protein kinases combined with quantitative mass spectrometry. Herein, a mixed inhibitor affinity matrix, termed Kinobeads, that carry a collection of >100 ATP-competitive kinase inhibitors including chemical scaffolds, research tool compounds, drug candidates in development, as well as approved drugs, is used to map kinases from complex biological samples and to assess the selectivity profiles of kinase inhibitor drugs. For example, Bantscheff and colleagues applied this methodology to three drugs targeting the oncogenic BCR-ABL kinase, which induces CML.¹⁸ The immobilized compounds were first incubated with lysates of HeLa or K562 CML cells to allow protein binding, which was followed by separation of the beads from the lysate. The bound proteins were eluted, digested with trypsin, and identified by MS. The kinobeads matrix specifically captures roughly 200 protein kinases (two-thirds of the expressed kinome) from any given cell type. This data set works as a control sample (Figure 7a).

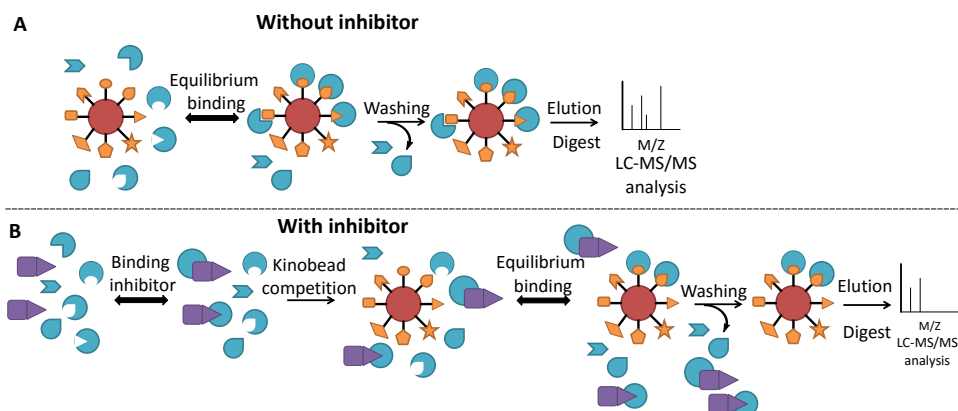


Figure 7. Schematic workflow of proteomic drug target profiling by a kinobead competition assay.

To quantitatively profiling the targets of the three BCR-ABL drugs, namely bosutinib, imatinib and dasatinib, these drugs were added to K562 cell lysates and the lysates were subsequently subjected to kinobeads. When the drug in the lysate has bound to its target and thus has blocked the ATP-binding site, a reduced amount of the free target has been available for capturing by kinobeads, whereas the binding of nontargeted kinases and

other proteins has been unaffected. The kinobead-bound material was subjected for quantification by MS. The selectivity drug profile can be determined by comparing this labeling profile with the control profile (Figure 7b). As a result, for imatinib 13 proteins exhibited >50% binding reduction on kinobeads. These proteins include ABL, BCR-ABL, the ABL family kinase ARG and two novel target candidates DDR1 and NQO2. Dasatinib and bosutinib labeled more targets than imatinib (39 and 53 proteins respectively), including BCR-ABL, ARG and DDR1, BTK, EphB4, focal adhesion kinase (FAK), FER, MER and Syk. Thus, the combination of a mixed-affinity matrix with quantitative MS provides a convenient tool to map a drug's direct and indirect targets in a single set of experiments.

Activity-based protein profiling

Many ABPs have been developed for numerous enzyme classes up to now, including serine hydrolases, cysteine proteases, metallohydrolases, phosphatases, glycosidases, deubiquitylating enzymes, penicillin-binding proteins, palmitoyl transferases, various oxidoreductases and for kinases as well. A characteristic feature of ABPP probes is that they contain a selectivity function capable of covalently reacting with the active site of target enzymes driven by the catalytic mechanism of the enzyme. However, kinases catalyze phosphate transfer from ATP to their substrate by a direct transfer mechanism that does not involve covalent enzyme intermediates. Thus, the kinase active site does not contain conserved nucleophilic residues for catalysis. In these cases, electrophilic ABPs that react with native or engineered noncatalytic nucleophilic residues must be used. Based on sequence comparisons, it is known that almost all protein kinases have at least one conserved lysine residue within their active sites that represents a possible modification site for an appropriate probe. These lysine residues are situated close to β - and γ -phosphates of bound ATP, suggesting that the positively charged ϵ -amino groups of these lysines provide electrostatic interactions with the phosphate backbone. Therefore, it has been reasoned that kinase ABPP probes based on ATP might take advantage of the conserved lysine.¹⁹ In an approach by Patricelli and colleagues, ABPs were used with a biotinylated acyl group positioned at the terminal phosphate of ATP (**25**) or ADP (**26**) to provide broad proteome coverage (Figure 8A).²⁰ These acyl phosphates have appropriate reactivity with amines and are stable in aqueous solution. Upon addition of the acyl phosphate probes to cell lysates, a stable amide bond with the biotin tag has been formed and an ATP or ADP has been released by a reaction between the active-site lysine(s) and the activated acyl phosphate (Figure 8B). Subsequently, the biotinylated kinases were subjected to proteolytic digestion with trypsin. The labeled peptides were purified on streptavidin-agarose beads prior to analysis by LC-MS/MS to determine the identity of the labeled protein as well as the site of labeling. The acyl phosphate probes were shown to selectively label at least 75% (~ 400) of human kinases in cell lysates. This method is thus

able to profile the functional state of many kinases in native proteomes in a parallel manner.

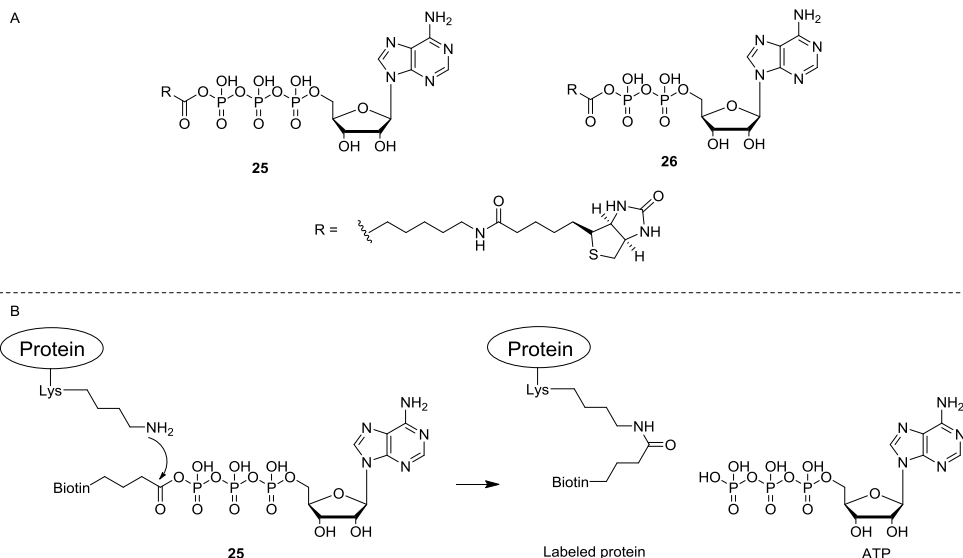


Figure 8. A) Structures of ATP-Biotin probe **25** and ADP-Biotin probe **26**. **B)** Mechanism of labeling of ATP-biotin probe **25** with target lysine.

Another ATP containing ABP has been developed and used for enrichment and identification of kinases and other ATP-binding proteins from complex protein mixtures, namely the isotope-coded ATP ABPP probes (ICAPs) **27** and **28** (Figure 9).²¹ The differences between this probe and the ATP probe **25** are that this probe contains a desthiobiotin as the tag instead of biotin and a linker with isotopes. Since chemical isotopic labeling methods like dimethyl labeling are prone to additional experimental errors due to late stage incorporation of the isotopes during sample preparation, the isotopes are already incorporated into the ATP-probe. Two different probes have been developed, one containing a heavy linker (containing six deuterons, **27**) and the other containing a light linker (containing six hydrogens, **28**).

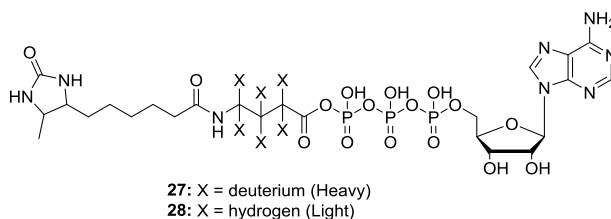


Figure 9. Structures of isotope-coded ATP probes (ICAP).

By using two different ATP probes, two protein labeling profiles of two different samples can be compared. The general procedure with the use of ICAP is as follows: 1) ATP-binding proteins from a sample representing one experimental state are obtained with the isotopically light form ATP probe **28**, whereas the ATP-binding proteins from a sample representing another experimental state are labeled with the isotopically heavy form ATP probe **27**. 2) The two protein samples are mixed and digested with trypsin, and the resulting light/heavy isotope-coded desthiobiotin-labeled proteins are enriched with streptavidin agarose beads. 3) The purified peptides are analyzed by LC-MS/MS. Quantification results can be obtained by comparing the MS peak intensity ratios of the light and heavy forms of desthiobiotin-modified peptide pairs (Figure 10).

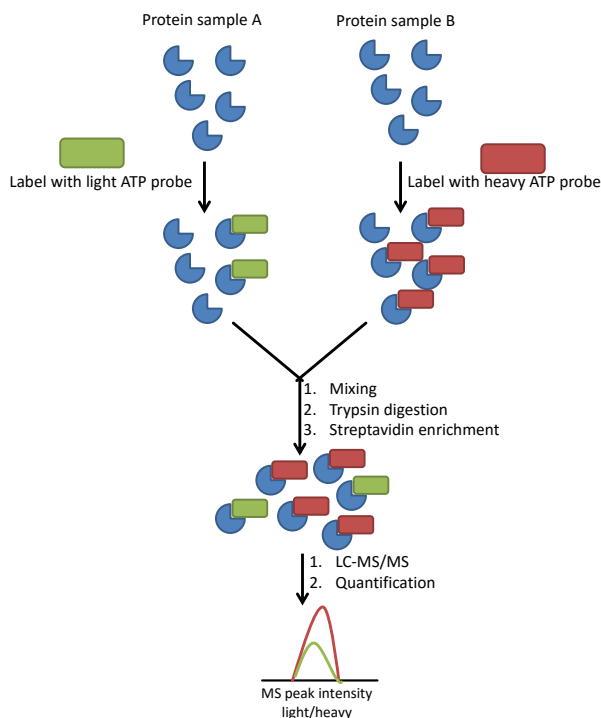
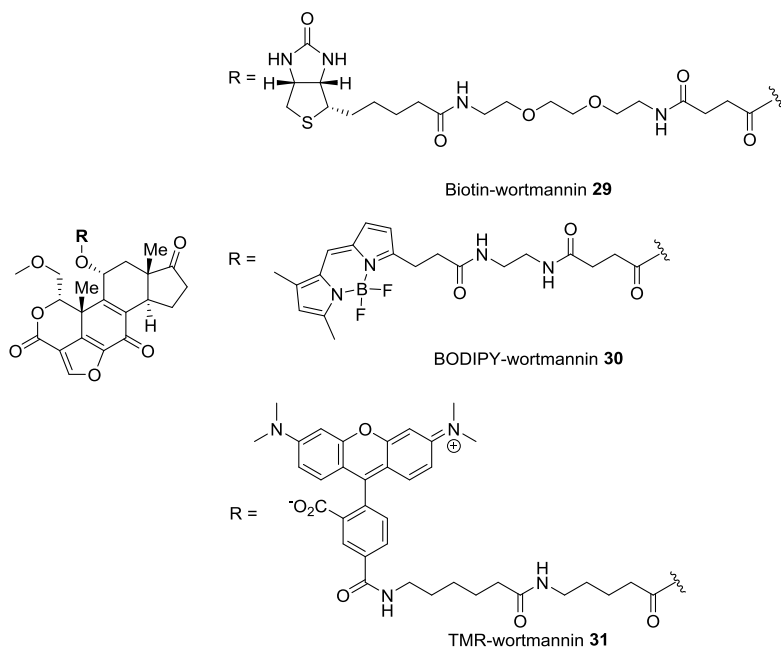


Figure 10. General strategy for quantitative ATP-ABPP using ICAP.

A disadvantage of the ATP-containing probes is that they also label other non-kinase proteins, since ATP is a substrate not only for kinases, but for other ATP-binding proteins as well. Therefore, many studies have focused on the development of kinase-selective ABPP to overcome this problem by using probes based on covalent kinase inhibitors. Wortmannin, which is a metabolite of the fungus *Penicillium funiculosum*, irreversibly inhibits phosphoinositide-3-kinases (PI3Ks) and the PI3K-related kinases (PIKK) families by covalent modification of a lysine in the active site. This lysine is conserved in the different



Another ATP analogue, namely 5'-fluorosulfonylbenzoyl 5'-adenosine (**32**, FSBA) (Figure 11), which is used to study the mechanism of action of wortmannin, has been used as a general ABP for the protein kinase family.²³ FSBA covalently modifies most protein kinases

by binding irreversibly to the ϵ -amino group of a conserved ATP pocket lysine. This reagent is structurally similar to ATP, but the phosphoryl groups of ATP are replaced by a fluorosulfonylbenzoyl moiety. To profile protein kinases, biotin-tagged FSBA ABPs have been designed and synthesized.²⁴ Biotin groups were introduced by modifying the free hydroxyl groups of the ribose ring of FSBA, which resulted in the three different FSBA-biotin probes **33-35**, whereof probe **35** carries two biotin tags (Figure 11). Biotin-tagged ABPs allow visualization of labeled proteins after Western blotting and can also be used as handle for protein isolation by streptavidin-coated beads. Ratcliffe *et al.* have proven that FSBA and its biotin-tagged probes can be used to screen and validate ATP competitive kinases inhibitors using LC/MS or Western blot techniques.

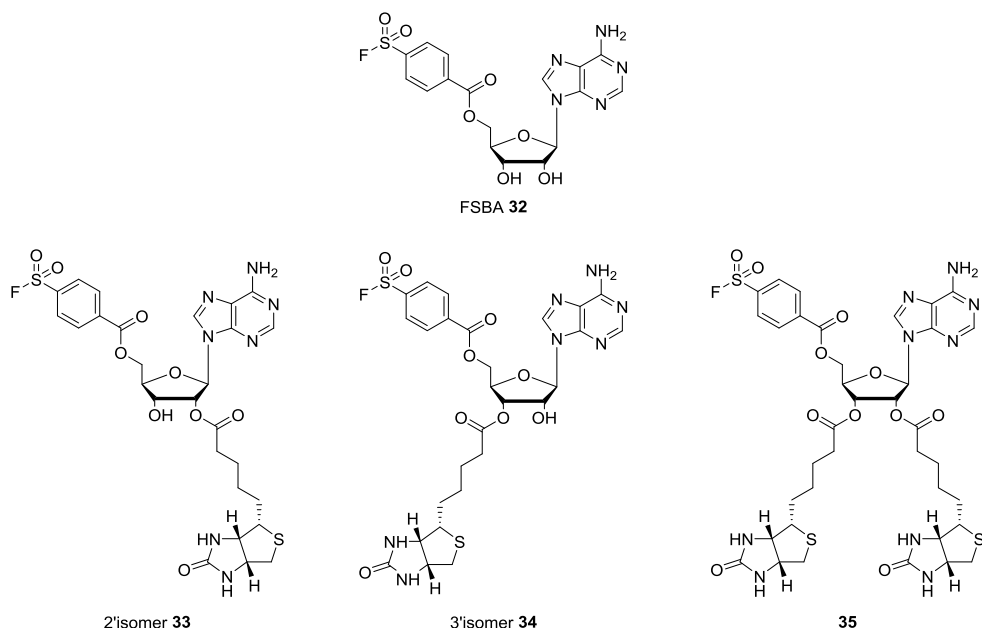


Figure 11. Structures of FSBA (**32**) and its biotin-labeled ABPs **33-35**.

Taunton *et al.* have developed irreversible selective Src-family kinase probes by modification of FSBA (**32**).²⁵ The Src active site contains at least two potentially nucleophilic side chains Lys295 and Cys277. It is known that Lys295 reacts with millimolar concentration of FSBA. The second nucleophile in the Src active site, Cys277, is situated proximal to both Lys295 and the γ -phosphate of ATP. Since this cysteine is poorly conserved, it is an attractive target for selective covalent inhibition. Only nine human kinases contain an equivalent cysteine, including Src, Yes, FGFR1-4, LIMK1 and TNK1. To improve the selectivity of FSBA for the Src-family kinases, two hybrid nucleosides (**36** and **37**) which borrowing structural elements from FSBA and the Src-family inhibitor PP1 (**38**)

(Figure 12), have been developed. Since the *p*-tolyl substituent in PP1 exploits a hydrophobic pocket found in all Src-family kinases, this group has been introduced in FSBA. For monitoring of covalent binding to proteins using copper-catalyzed click chemistry, a propargyl ether has been included as bioorthogonal tag. These modifications gave ABPs **36** and **37**. Of note, compound **37** contains a vinylsulfone as the electrophilic trap instead of the fluorosulfonylbenzoyl group. The two probes were compared for their selectivity and their reactivity. Both the probes were able to capture multiple Src-family kinases in intact cells, along with robust competition by kinases inhibitors including the clinical Bcr-Abl inhibitor ponatinib. The fluorosulfonylbenzoyl probe **36** reacts with the conserved lysine and shows little discrimination among related kinases. However, the 5'-vinylsulfonate **37** reacts with the poorly conserved cysteine.

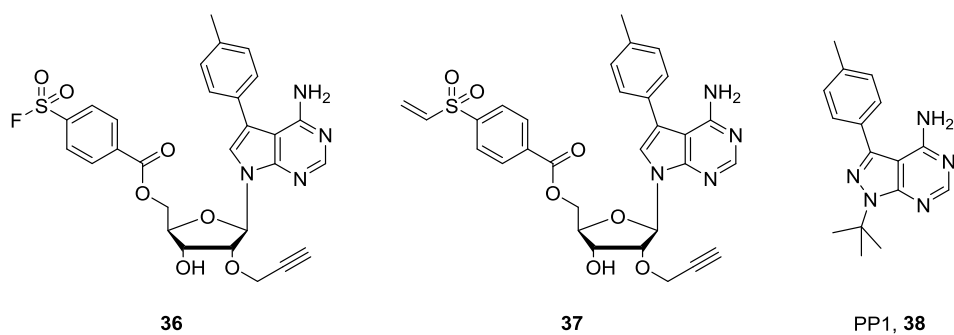


Figure 12. Structures of two alkyne containing Src-family kinase ABPs based on FSBA (**32**) and PP1 (**38**): 5'-fluorosulfonylbenzoyl probe **36** and 5'-vinylsulfonate **37**.

Other cysteine protein kinases have been targeted by covalent kinase inhibitors as well. The targeted active site cysteines offer a potential selectivity filter, since these residues are not uniformly conserved across the kinome. Thus far, irreversible inhibitors have been developed for some protein kinases, including oncogenic drug targets like the epidermal growth factor receptor (EGFR) and Bruton's tyrosine kinase (BTK), for which the corresponding irreversible inhibitors afatinib and ibrutinib have shown to treat non-small cell lung cancer and chronic lymphocytic leukemia (CLL), respectively. Recently, ABPP combined with quantitative MS was used to perform global and in-depth analysis of proteins targeted by the covalent EGFR inhibitor PF-6271184 (**39**) and BTK inhibitor ibrutinib (**40**) (Figure 13). Both the inhibitors **39** and **40** use Michael receptors ($\alpha\beta$ -unsaturated amide) for covalent binding with the nucleophilic active-site cysteines in the ATP-binding pockets. To use these inhibitors as ABPs, an alkyne group was installed as the ligation handle to yield probes **41** and **42** (Figure 13).²⁶ Rhodamine azide was used as their ligation partner for visualization of targeted enzymes and off targets in A431 and Ramos cells, which possess high levels of the primary inhibitor targets EGFR and BTK, respectively. SDS-PAGE and in-gel fluorescence scanning revealed that the probes **41** and **42** were able

to probe their corresponding on-targets EGFR and BTK, and to detect off-targets. To identify all the targets of these probes, ABPP was combined with MS. Consistent with other studies, EGFR and ERB2 were identified as specific targets for both the probes. However, BTK was primarily labeled by the ibrutinib-probe **41**. Most of the off-targets identified contain the active-site cysteine residue except for MLTK. Non-kinase targets were found as well, including FAM213A and DUS2L for probes **41** and **42**, respectively.

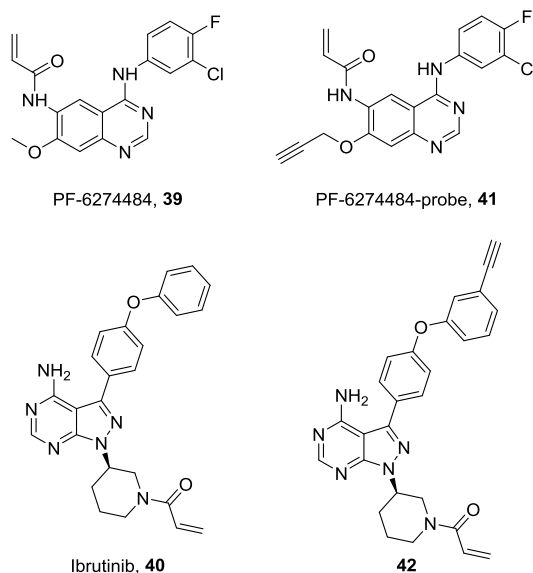


Figure 13. Structures of cysteine kinase inhibitors PF-6274484 (**39**) and ibrutinib (**40**) and their corresponding alkyne-labeled ABPs **41** and **42**.

More ibrutinib-based ABPs have been developed both direct and two-step bioorthogonal probes. Both Honigberg *et al.*²⁷ and Turetsky *et al.*²⁸ used a Bodipy-FL containing ibrutinib probe (**43** or **44**, respectively, Figure 14A). Both studies have proven that the direct Bodipy-FL ibrutinib probes were able to label BTK in several BTK-positive tumor cell lines. Recently, Liu *et al.* developed two fluorescent ibrutinib probes (BodipyFL-like **45** and Bodipy-TMR **46**) and three two-step bioorthogonal probes (alkyne **47**, azide **48** and norbornene **49**) to compare the direct and two-step labeling ABPP methodologies in labeling of BTK using Ramos cells and lysates (Figure 14A).²⁹ The ligation partners of the alkyne **47**, the azide **48** and norbornene **49** were azido Bodipy-FL **50**, alkyne Bodipy-FL **51** and tetrazine Bodipy-FL **52**, respectively (Figure 14B). Cu(I)-catalyzed azide-alkyne [2+3] cycloaddition reactions were performed for the ligation of the bioorthogonal ABPP pairs **47/50** and **48/51**, and an inverse-electron demand Diels-Alder reaction was performed for the ligation of **49/52**. All the five probes (**45** – **49**) were able to label BTK in *in vitro* and *in situ* experiments. Direct imaging using Bodipy-ibrutinib **45** and **46** appears most effective

and with less background labeling in *in situ* experiments than the two-step bioorthogonal analogues. A more detailed discussion will be given in Chapter 5 of this thesis.

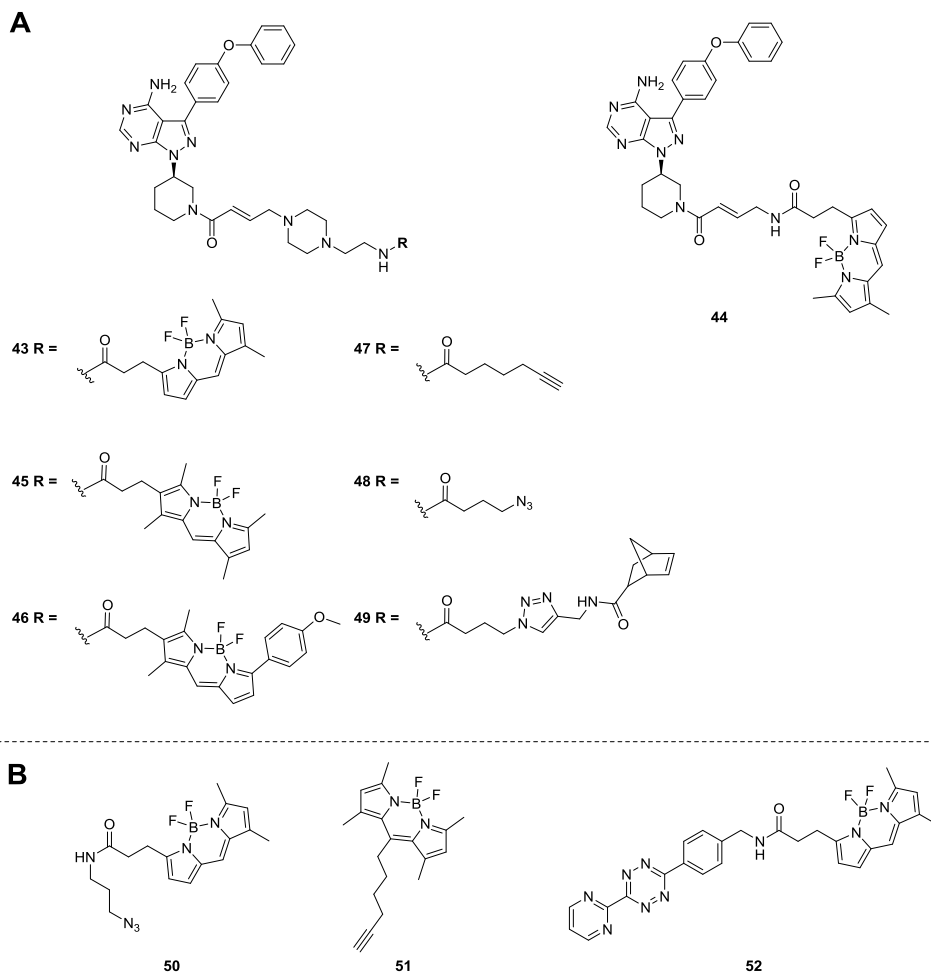


Figure 14. Structures of ibrutinib-based direct and two-step bioorthogonal ABPs and ligation reagents. A) Compounds **43** – **46** are fluorescent probes and compounds **47** – **49** are two-step labeling probes. B) Corresponding ligation reagents **50** – **52** for probes **47** – **49**, respectively.

Photoaffinity labeling

Since not every kinase possesses a conserved and reactive active-site residue for targeting by ABPs, a photochemical group can be used to form a covalent bond between the probe and the kinase. Under UV-exposure conditions, the photoreactive group forms a reactive

intermediate that rapidly reacts and binds to the nearest molecule, which ideally will be the target protein. Probes contain in general three functionalities: an affinity unit (small molecule of interest), a photoreactive moiety and an identification/reporter tag. The affinity unit is responsible for reversible binding to the target kinase, the photoreactive moiety allows permanent attachment to its target and the identification tag is necessary for the detection and isolation of probe-protein complexes. The main photoreactive moieties used for photoaffinity labeling are phenylazides, phenyldiazirines and benzophenones, where under irradiation condition a nitrene, a carbene and a diradical, respectively, are formed as intermediates (Figure 15).³⁰

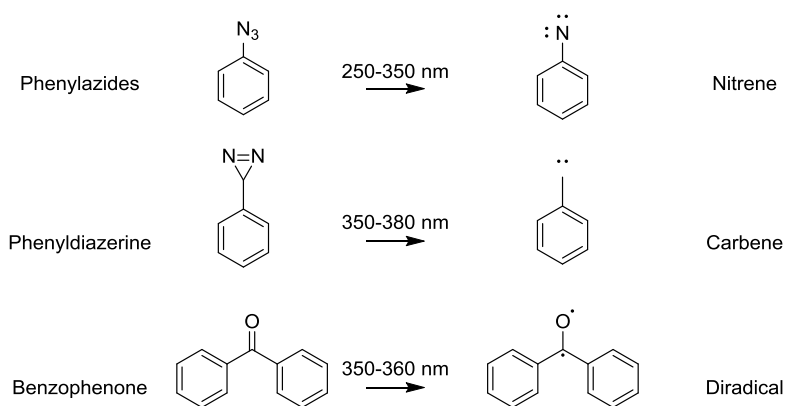


Figure 15. The major photoaffinity groups: phenylazide, phenyldiazirine and benzophenone.

Phenylazides are frequently used as photoaffinity moiety, since they are easily synthesized and are commercially available. However, damage to biological molecules can be caused by the use of the shorter wavelengths required to excite the phenylazide probes. In addition, the formed nitrene intermediates after expelling molecular nitrogen (N_2) decrease photoaffinity yields compared with carbenes, which might be due to that nitrenes are less reactive than carbenes. Rearrangement of nitrenes can also form benzazirines and dehydroazepines/ketenimines as undesired side products. To prevent the formation of ketenimines, substituted arylazides such as tetrafluorophenylazides have been developed.

Benzophenones are activated by a long wavelength (350-360 nm), which lowers the risk of damaging biomolecules, and thereby a reactive triplet diradical is formed upon UV irradiation. However, the drawbacks of benzophenones are: 1) it is relatively bulky, which can affect the interaction between the affinity pharmacophore and the target protein, 2) the steric hindrance can lead to increased nonspecific labeling and capture, 3) a longer irradiation period is required which can lead to increased nonspecific labeling.

Aryldiazirines are the most commonly used photoaffinity group, since they are highly resistant towards a number of factors such as temperature, nucleophiles, acidic and basic conditions as well as oxidizing and reducing agents. In addition, the photolabile diazine group absorbs most efficiently at a wavelength of 350-380 nm, at which hardly no significant cell damage would occur. Upon irradiation of diazine, molecular nitrogen is expelled and a singlet carbene is formed. This intermediate is extremely reactive and has a short half life, which leads to fast insertion reactions and less discrimination between reaction sites.

Other functionalities that have been used for photoaffinity labeling include diazo groups, diazocarbonyls, enones, sulfur radicals, halogenated substrates, nitrobenzenes, diazonium salts and alkyl derivatives of azides and diazirines. In the following part, some examples of photoaffinity labeling of kinases using both direct and two-step bioorthogonal probes containing one of the above mentioned photoreactive moieties will be discussed.

Also in the case of photoaffinity labeling, adenine-based probes have been developed. Biotinylated adenine-benzophenone conjugates **53** and **54** (Figure 16) were synthesized to label selectively Lck kinase, which belongs to the Src-family and plays roles in thymocyte differentiation and T-cell activation.³¹ These two probes were incubated with six commercially available kinases, PKA, GSK3, CK1, Src, Fyn and Lck. Upon irradiation at 350 nm, the biotinylated proteins were blotted onto PVDF membrane and visualized after treatment of anti-biotin horseradish peroxidase-conjugated antibody. The *S*-configured probe **53** showed to label Lck only and the *R*-configured probe **54** does not label any of the kinases. This proves that a simple configuration change leads to a drastic change in selectivity and activity of the probe. Based on these findings, five other adenine-benzophenone conjugates were developed to gain insights into the relative importance between target-binding affinity and conformational flexibility of the probe for labeling of LCK kinase. In this study the central Gly residue has been replaced by five other D-amino acids, namely proline (**55**), serine (**56**), piperidine (**57**), glutamic acid (**58**) and γ -aminobutyric acid (GABA, **59**) (Figure 16).³² This study showed that binding-affinity did not predict photolabeling efficiency of the LCK probes. However, conformational flexibility showed to have correlation with labeling efficiency, since compound **59**, which has the most flexibility around benzophenone, showed to have the highest labeling efficiency. The proline containing probe **55** did not label Lck, because of the conformational constraint on the backbone.

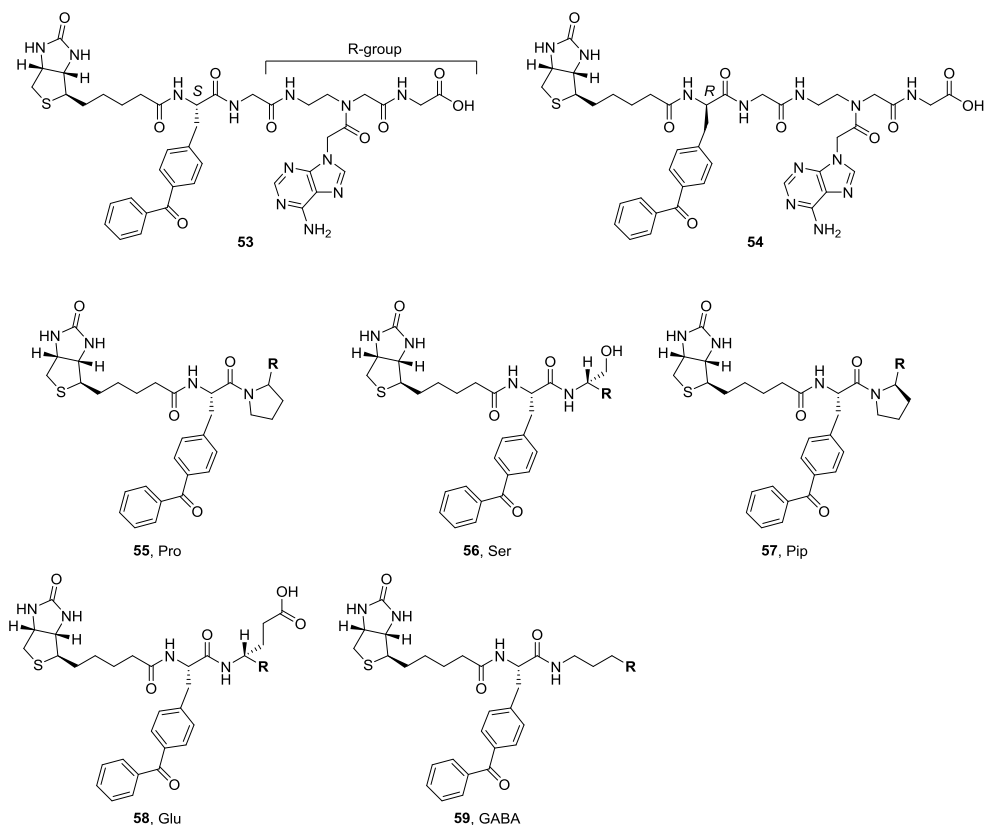


Figure 16. Structure of the biotinylated adenine-benzophenone probes for labeling of LCK **53** – **59**.

The use of known reversible kinase inhibitors as the affinity moiety has been done by many studies. Sewald and co-workers have developed the direct photoaffinity probe **61** by using H-9 (**60**), which is an isoquinolinesulfonamide of the H-series, as the reversible inhibitor (affinity moiety), a benzophenone as the photoreactive group and the isomeric mixture of 5- and 6-carboxyfluorescein as the reporter tag (Figure 17).³³ This study has shown that this isoquinolinesulfonamide benzophenone probe was able to label and visualize four purified proteins, namely hexokinase, creatine kinase, 3PGA phosphokinase and cAMP-dependent protein kinase A. However, a very low binding tendency for the probe has been seen for 3PGA phosphokinase.

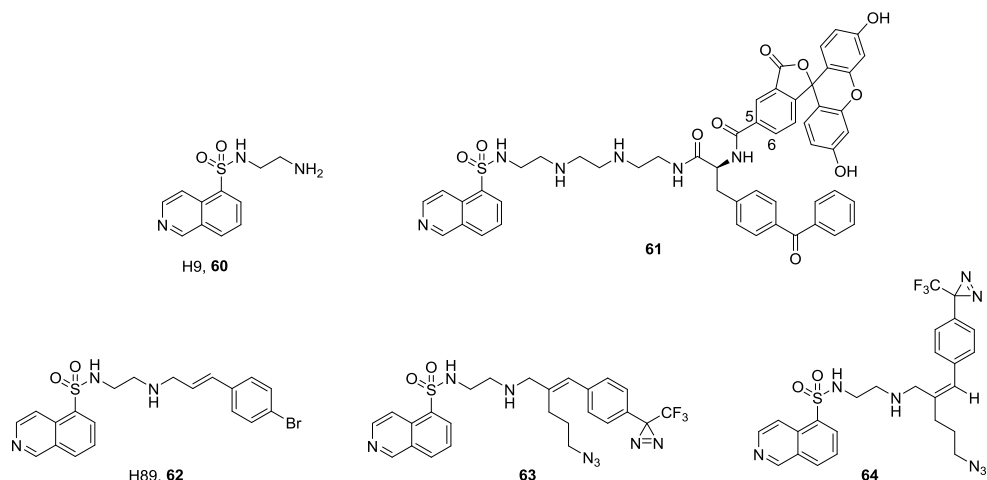


Figure 17. Structures of isoquinolinesulfonamide kinase inhibitors H9 (**60**) and H-89 (**62**) and their corresponding photoaffinity labeling probes **61** and **63** – **64**, respectively.

Another group also has developed photoaffinity labeling probes based on an isoquinolinesulfonamide of the H-series, namely H-89 (**62**, Figure 17), which is known for its inhibition towards PKA and other kinases including AKT1 and AKT2. In this case, the two-step bioorthogonal probes **63** and **64** are developed and contain a trifluoromethylphenyldiazirine, which is a more stable version of the original phenyldiazirine, as the photoaffinity reactive group and an azide group that functions as the ligation handle (Figure 17).³⁴ Both the probes showed inhibition activity against PKA and AKT1, and for AKT2 and AKT3 in a much lower extent. To prove that these probes were able to be used as photoaffinity labeling probes, both the probes **63** and **64** were incubated with recombinant PKA and AKT1, followed by photo-crosslinking at 350 nm and a final click reaction with an alkyne-modified Cy5 reporter for in-gel analysis. Probe **63** labels both kinases with a higher affinity than probe **64**, which can be explained by the fact that probe **63** is structurally more similar to the lead compound H-89 (**62**) than probe **64**. This study will be discussed in more detail in Chapter 6.

Since most kinase inhibitors target the highly conserved ATP-binding site of kinases, they tend to inhibit multiple cellular targets. To better understand the cellular selectivity of anti-kinase drugs and to anticipate potential side effects of these drugs, known reversible kinase drugs were converted into a photoaffinity labeling probe.³⁵ An example is the dual Src/Abl inhibitor dasatinib, which is used for the treatment of imatinib-resistant CML. Related method to profile the off-targets of dasatinib has already been performed using immobilized dasatinib on sepharose beads (**7**), which is discussed above. However, disadvantages of this method are: 1) the heavy reliance on a small number of bead-immobilized kinase baits, which affects the accessibility of some target kinases, and leads

to missed targets, 2) due to non-covalent inhibition between the immobilized probe and the kinases, relatively mild wash conditions must be applied, which often leads to accumulation of false positives, as well as exclusion of weaker kinase-drug interaction. Therefore, alkynylated dasatinib-photoreactive labeling probes, which bind covalently to its target have been used to profile the off-targets of dasatinib. Yao and co-workers³⁶ have designed and synthesized two-step bioorthogonal alkynylated-dasatinib probes, one contains an aliphatic diazirine moiety (**65**) and the other a benzophenone (**66**) as the photoreactive group. For protein profiling and pull-down/target identification, the small terminal alkyne handle was ligated to rhodamine-N₃ (**67**) or biotin-N₃ (**68**), respectively (Figure 18). First, to prove that these probes can be used to profile the targets of dasatinib, docking experiments and *in vitro* kinase assays were performed to determine the binding site and IC₅₀ values respectively. As a result, both the probes were able to inhibit c-Src/c-Abl kinase domains in the same range as dasatinib, however only the aliphatic diazirine probe **65** was much more cell-permeable than the benzophenone probe **66**. Therefore, further protein profiling experiments were performed using the cell-permeable diazirine probe **65** only. This aliphatic diazirine probe (**65**) was capable of proteome-wide profiling of potential cellular targets of Dasatinib. Results obtained from different proteomic setups (cell lysates, live cells and immobilized affinity matrix) were compared and it has been found that under similar experimental settings, the photoaffinity probe (**65**) was able to identify more putative kinase targets over immobilized dasatinib affinity matrix. In addition to Abl and Src family tyrosine kinase, six serine/threonine kinases were identified by pull-down/immunoblotting experiments as new targets, namely PCKT3, STK25, eIF-2A, PIM3, PKA C α and PKN2.

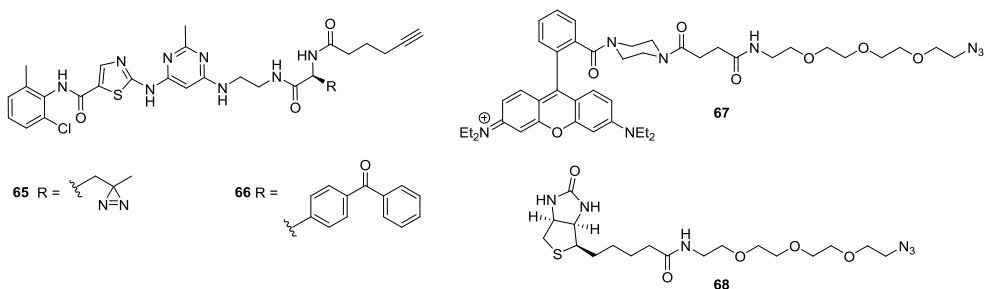


Figure 18. Structures of two-step bioorthogonal photoaffinity-group containing dasatinib-probes **65** and **66**. Rhodamine-N₃ (**67**) and biotin-N₃ served as the ligation reagents for visualization and pull-down of targets, respectively.

Instead of labeling one particular kinase or kinase family, in some cases large scale labeling of kinases are preferable. For the labeling of kinases in broad-scale, many studies have already done this by using bead affinity-driven techniques as mentioned above. To

overcome the disadvantages of the bead affinity-driven approach, biological samples may be profiled in solution by soluble, multitargeted small molecule probes. To allow labeling of the ATP-binding sites of as much as possible kinases, a few studies have used the reversible ATP mimetic kinase inhibitor staurosporine, which is known for inhibiting at least 253 kinases, as the affinity group.^{37, 38} An example is the biotinylated staurosporine-arylazide **69** developed by Fisher *et al.* (Figure 19). The staurosporine probe **69** were incubated with human liver cancer cell line HepG2 whole cell lysates prior to irradiation at 312 nm. Streptavidin coated magnetic beads were used to isolate the covalently cross-linked protein-probe complexes. According to the LC-MS/MS results 101 kinase and 144 non-kinases were labeled. Among these identified kinases, the majority are members of the serine/threonine kinase family.

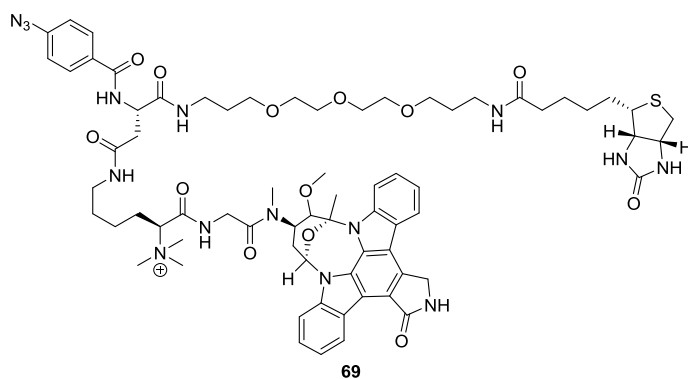


Figure 19. Structure of the biotinylated staurosporine photoaffinity probe, which contains an arylazide as the photoaffinity moiety.

Conclusion

Three methods of chemical profiling are applied for the labeling and identification of kinases. Each method has its own advantages and disadvantages. Thus, dependent on the purpose of the study and under which conditions the experiments need to be performed, one of these methods will suit the best for the experiment and kinase(s) of interest. Even though many studies have already been done up to now, much more experiments need to be done in the future. Not every kinase or kinase subset can be labeled and not every function of the many kinases are determined yet due to the complexity of the kinome and the low abundance of most kinases. Therefore, there is need for the development of more selective and active probes, which in turn can be analyzed using highly sensitive and efficient read-out methods.

References

- ¹ M. J. Niphakis and B. F. Cravatt, *Annu. Rev. Biochem.*, 2014, **83**, 341.
- ² C. H. S. Lu, K. Liu, L. P. Tan and S. Q. Yao, *Chem. Eur. J.*, 2012, **18**, 28.
- ³ B. F. Cravatt, A. T. Wright, and J. W. Kozarich, *Annu. Rev. Biochem.*, 2008, **77**, 383.
- ⁴ T. Lenz, J. J. Fischer and M. Dreger, *J. Prot.*, 2011, **75**, 100.
- ⁵ W. Shi and H. Ma, *Chem. Comm.*, 2012, **48**, 8732.
- ⁶ A. Loudet and K. Burgess, *Chem. Rev.*, 2007, **107**, 4891.
- ⁷ L. I. Willems, N. Li, B. I. Florea, M. Ruben, G. A. van der Marel and H. S. Overkleeft, *Angew. Chem. Int. Ed.*, 2012, **51**, 4431.
- ⁸ L. I. Willems, W. A. van der Linden, N. Li, K.-Y. Li, N. Liu, S. Hoogendoorn, G. A. van der Marel, B. I. Florea and H. S. Overkleeft, *Acc. Chem. Res.*, 2011, **44**, 718.
- ⁹ M. Kohn and R. Breinbauer, *Angew. Chem. Int. Ed.*, 2004, **43**, 3106.
- ¹⁰ J. A. Prescher and C. R. Bertozzi, *Nat. Chem. Biol.*, 2005, **1**, 13.
- ¹¹ R. Krishnamurty and D. J. Maly, *Comb. Chem. High. Throughput. Screen.*, 2007, **10**, 652.
- ¹² M. Knockaert, N. Gray, E. Damiens, Y-T. Chang, P. Grellier, K. Grant, D. Fergusson, J. Mottram, M. Soete, J-F. Dubremetz, K. Le. Roch, C. Doerig, PG. Schultz and L. Meijer, *Chem. Biol.*, 2000, **7**, 411.
- ¹³ Y-T. Chang, N. S. Gray, G. R. Rosania, D. P. Sutherlin, S. Kwon, T. C. Norman, R. Sarohia, M. Leost, L. Meijer and P. G. Schultz, *Chem. Biol.*, 1999, **6**, 361.
- ¹⁴ U. Rix, O. Hantschel, G. Durnberger, L. L. Remsing Rix, M. Planyavsky, N. V. Fernbach, I. Kaupe, K. L. Bennett, P. Valent, J. Colinge, T. Kocher and G. Superti-Furga, *Blood*, **110**, 4055.
- ¹⁵ U. Rix, L. L. Remsing Rix, A. S. Terker, N. V. Fernbach, O. Hantschel, M. Planyavsky, F. P. Breitwieser, H. Hermann, J. Colinge, K. L. Bennett, M. Augusin, J. H. Till, M. C. Heinrich, P. Valent and G. Superti-Furga, *Leukemia*, 2010, **24**, 44.
- ¹⁶ I. Chamrad, U. Rix, A. Stukalov, M. Gridling, K. Parapatics, A. C. Muller, S. Altiok, J. Colinge, G. Superti-Furga, E. B. Haura and K. L. Bennett, *J. Proteome. Res.*, 2013, **12**, 4005.
- ¹⁷ M. Hofener, F. Pachl, B. Kuster and N. Sewald, *Proteomics*, 2015, **15**, 3066.
- ¹⁸ M. Bantscheff, D. Eberhard, Y. Abraham, S. Bastuck, M. Boesche, S. Hobson, T. Mathieson, J. Perrin, M. Raida, C. Rau, V. Reader, G. Sweetman, A. Bauer, T. Bouwmeester, C. Hopf, U. Kruse, G. Neubauer, N. Ramsden, J. Rick, B. Kuster and G. Drewes, *Nat. Biotech.*, 2007, **25**, 1035.
- ¹⁹ Y. Xiao, L. Guo, X. Jlang and Y. Wang, *Anal. Chem.*, 2013, **85**, 3198.
- ²⁰ M. P. Patricelli, A. K. Szardenings, M. Liyanage, T. K. Nomanbhoy, M. Wu, H. Weissig, A. Aban, D. Chun, S. Tanner and J. W. Kozarich, *Biochem.*, 2007, **46**, 350.
- ²¹ Y. Xiao, L. Guo and Y. Wang, *Anal. Chem.*, 2013, **85**, 7478.
- ²² M-C Yee, S. C. Fas, M. M. Stohlmeyer, T. J. Wandless and K. A. Cimprich, *J. Biol. Chem.*, 2005, **280**, 29053.
- ²³ S. S. Khandekar, B. Feng, T. Yi, S. Chen, N. Laping and N. Bramson, *J. Biomol. Screen.*, 2005, **10**, 447.
- ²⁴ S. J. Ratcliffe, T. Yi and S. S. Khandekar, *J. Biomol. Screen.*, 2007, **12**, 126.
- ²⁵ N. N. Gushwa, S. Kang, J. Chen and J. Taunton, *J. Am. Chem. Soc.*, 2012, **134**, 20214.

- ²⁶ B. R. Lanning, L. R. Whitby, M. M. Dix, J. Douhan, A. M. Gilbert, E. C. Hett, T. O. Johnson, C. Joslyn, J. C. Kath, S. Niessen, L. R. Roberts, M. E. Schnute, C. Wang, J. J. Hulce, B. Wei, L. O. Whiteley, M. M. Hayward and B. F. Cravatt, *Nat. Chem. Biol.*, 2014, **10**, 760.
- ²⁷ L. A. Honingberg, A. M. Smith, M. Sirisawad, E. Verner, D. Loury, B. Chang, S. Li, Z. Pan, D. H. Thamm, R. A. Miller and J. J. Buggy, *PNAS*, 2010, **107**, 13075.
- ²⁸ A. Turetsky, E. Kim, R. H. Kohler, M. A. Miller and R. Weissleder, *Sci. Rep.*, 2014, **4**, 4782.
- ²⁹ N. Liu, S. Hoogendoorn, B. van de Kar, A. Kaptein, T. Barf, C. Driessen, D. V. Filippov, G. A. van der Marel, M. van der Stelt and H. S. Overkleeft, *Org. Biomol. Chem.*, 2015, **13**, 5147.
- ³⁰ E. Smith and I. Collins, *Future. Med. Chem.*, 2015, **7**, 159.
- ³¹ S. Hindi, H. Deng, L. James and A. Kawamura, *Bioorg. Med. Chem. Lett.*, 2006, **16**, 5625.
- ³² A. Kawamura, S. Hindi, D. M. Mihai, L. James and O. Aminova, *Bioorg. Med. Chem.*, 2008, **16**, 8824.
- ³³ M. C. Hagenstein, J. H. Mussgnug, K. Lotte, R. Plessow, A. Brockhinke, O. Kruse and N. Sewald, *Angew. Chem. Int. Ed.*, 2003, **42**, 5635.52
- ³⁴ S. C. Stolze, N. Liu, R. H. Wijdeven, A. W. Tuin, A. M. C. H. van den Nieuwendijk, B. I. Florea, M. van der Stelt, G. A. van der Marel, J. J. Neefjes and H. S. Overkleeft, *Mol. Biosyst.*, 2016, **12**, 1809.
- ³⁵ K. A. Kalesh, D. S. B. Sim, J. Wang, K. Liu, Q. Lin and S. Q. Yao, *Chem. Comm.*, 2010, **46**, 1118.
- ³⁶ H. Shi, C.-J. Zhang, G. Y. J. Chen and S. Q. Yao, *J. Am. Chem. Soc.*, 2012, **134**, 3001.
- ³⁷ H. Shi, X. Cheng, S. K. Sze and S. Q. Yao, *Chem. Comm.*, 2011, **47**, 11306.
- ³⁸ J. J. Fisher, O. Graebner, M. Dreger, M. Glinski, S. Baumgart and H. Koester, *J. Biomed. Biotechnol.*, 2011, **2011**, 850589.

3

Synthesis of FLT3 kinase inhibitors: isoquinolinesulfonamide-based library

3.1 Introduction

Hematopoietic cells express specific receptors, which are activated by a variety of cytokines leading to cell proliferation, differentiation and survival. FMS (Feline McDonough Sarcoma)-like tyrosine kinase 3 (FLT3) ligand is one of the cytokines that regulates the hematopoietic system and the corresponding FLT3 receptor is expressed on both stem cells and progenitors.¹ FLT3 belongs to the receptor tyrosine kinase (RTK) family (subclass III) and is 993 amino acids in length. FLT3 is composed of five immunoglobulin-like extracellular domains, a transmembrane domain, a juxtamembrane domain and two intracellular tyrosine-kinase domains

(TKDs) linked by a kinase-insert domain. Non-stimulated FLT3 receptors are present as monomers in the plasma membrane. After stimulation with FLT3 ligand, membrane-bound FLT3 receptors quickly change conformation and form homodimers. Activated, homodimerized FLT3 receptors trigger the phosphatidylinositol 3-kinase (PI3K) and RAS/RAF pathways, thereby stimulate downstream proteins such as 3-phosphoinositide-dependent protein kinase 1 (PDK1) and protein kinase B (PKB/AKT), which ultimately leads to increased cell proliferation and inhibition of apoptosis.²

Despite the many checks and balances that are in place to regulate hematopoiesis, mutations of regulatory genes including FLT3 can disrupt hematopoiesis and promote leukemogenesis. FLT3 mutations occur in several hematopoietic malignancies, and may result in FLT3-ligand independent tyrosine kinase activation of the FLT3 receptor,³ as first described Nakao *et al.*⁴ The most common form of FLT3 mutation comprises internal tandem duplication (ITD) in exons 14 and 15, which occurs in 15-35% of patients suffering from acute myeloid leukemia (AML)^{5,6,7} and 5-10% of patients with myelodysplasia (MDS).^{8,9} The second most common type of FLT3 mutation concerns missense point mutations in exon 20 of the TKD. TKD mutations occur in patients suffering from AML (5-10%), MDS (2-5%) and acute lymphoblastic leukemia (ALL) (1-3%).^{10,11} Thus, the wild-type and mutant FLT3 receptors are appealing drug targets for inhibition. Several small molecule inhibitors of tyrosine kinase such as the indolocarbazole derivatives lestaurtinib and midostaurin, which inhibit both the wild-type and mutant FLT3 next to a small spectrum of other tyrosine kinases, were studied in early phase clinical trials.¹²

At the basis of the work described in this chapter is the discovery of the isoquinolines **2** and **3** (Figure 1) as a new structural class of FLT3 kinase inhibitors. Compounds **2** and **3** are analogues of the known PKA inhibitor H-89 (**1**) and were identified from a focused library of H-89 analogues, which were assessed on their PKB/AKT1 inhibitory properties.

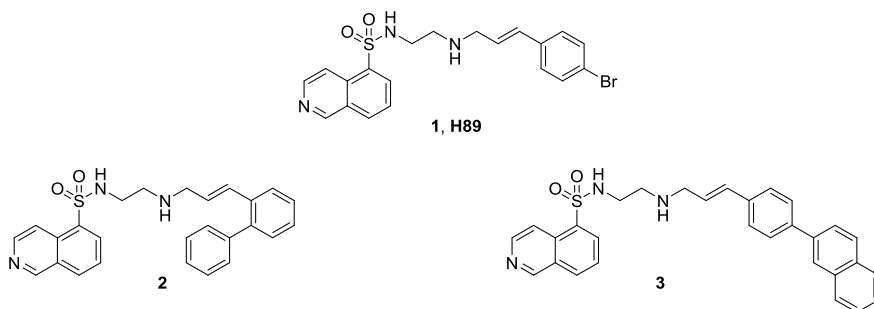


Figure 1. Lead compounds **1** (H-89), **2** and **3**.

In this screen, the *in vitro* activity of the compounds against PKB/AKT1 was determined together with the translocation activity of the AKT-regulated forkhead transcription factor, FOXO3a, into the nucleus. The latter is a way to measure the cellular activity of an inhibitor, since nuclear translocation of FOXO3a is correlated to inactivation of the AKT pathway. Apart from the identification of **2** as the most potent PKB/AKT1 inhibitor of the compounds tested (Figure 1), a set of compounds was discovered that showed hardly any PKB/AKT1 inhibition, but a high translocation activity of FOXO3a into the nucleus. In subsequent studies, it was found that these compounds, exemplified by **3**, inhibit FLT3, which is upstream of AKT1 in the same pathway. Therefore, a higher FOXO3a translocation into the nucleus has been observed without inhibition of PKB/AKT1. The most potent inhibitor of this set of compounds proved to be isoquinolinesulfonamide **3** (Figure 1), with an IC_{50} against FLT3 of 1.01 μ M. To obtain insight in the specificity of this compound, the activities of compound **2** and **3** towards a panel of 111 human kinases were determined using the KinomescanTM assay, which was performed by the company LeadHunter discovery services.¹³ Briefly, the Kinomescan assay is conducted as follows. Purified recombinant kinases (111 in total) tagged with DNA for qPCR detection are incubated with 10 μ M of test compound (here: **2** or **3**) for 1 hour. Subsequently the mixture of kinases and test compound is transferred to an immobilized ligand that binds to the panel of kinases. Compounds that bind the kinase active site will prevent kinase binding to the immobilized ligand. As a result, the amount of kinase captured on the solid support will be reduced (Figure 2A and C). Compounds that do not bind the kinase have no effect on the amount of kinase captured on the solid support (Figure 2B). Potential inhibitors are identified by measuring the amount of kinase captured in test versus control samples by quantitative qPCR.

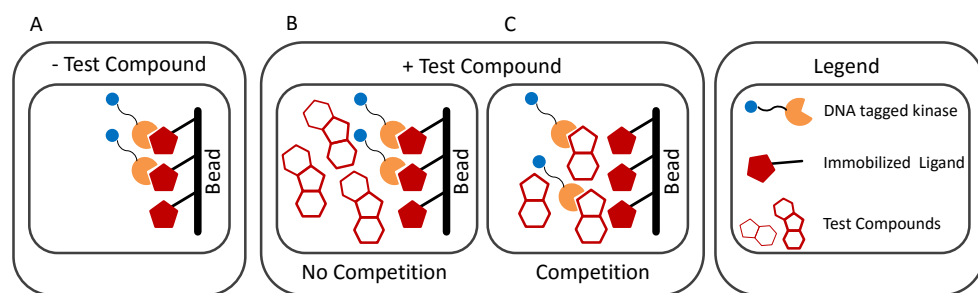


Figure 2. General outline of the KinomescanTM kinase assay applied to identify off targets of compounds **2** and **3**.

Chapter 3

Table 1. Kinase activity relative to control sample (%) after inhibition by compounds **2** and **3** (10 μ M).^a

Kinase	2	3	Kinase	2	3	Kinase	2	3
ABL1	87	79	FLT1	78	70	PDPK1	56	67
ACVR1B	28	83	FLT3	28	1.6	PIK3C2B	100	94
ADCK3	15	87	GSK3B	100	100	PIK3CA	96	76
AKT1	1.3	46	HIPK2	100	75	PIK3CG	100	100
AKT2	24	94	IGF1R	75	100	PIK4CB	100	100
AKT3	4.3	40	IKK-alpha	100	100	PIM1	84	74
ALK	78	36	IKK-beta	87	97	PIM2	100	72
AMPK- α 2	60	60	INSR	95	97	PIM3	85	60
AURKA	100	96	JAK2	91	70	PIP5K1A	17	52
AURKB	28	77	JAK3	82	75	PKAC-alpha	1.6	19
AXL	64	54	JNK1	93	73	PLK1	100	100
BMPR2	100	100	JNK2	100	76	PLK3	100	97
BRAF	67	96	JNK3	80	100	PLK4	70	76
BTK	52	100	KIT	66	55	PRKCD	5	40
CDK11	4.3	64	LKB1	100	100	PRKCE	67	26
CDK2	93	78	MAP3K4	11	96	PRKCH	2.8	16
CDK3	97	58	MAPKAPK2	60	59	PRKCI	30	77
CDK7	5.6	54	MARK3	15	41	PRKCQ	12	100
CDK9	100	95	MEK1	60	93	RAF1	38	68
CHEK1	46	87	MEK2	54	88	RET	71	51
CLK2	45	92	MET	89	93	RIOK2	67	90
CSF1R	47	69	MKNK1	59	100	ROCK2	0.6	5
CSNK1D	3.4	6.6	MKNK2	24	85	RSK2	71	78
CSNK1G2	66	100	MLCK	73	32	SGK3	63	74
CSNK1G3	97	96	MLK1	93	90	SNARK	10	39
DCAMKL1	80	100	MST2	51	92	SRC	69	78
DYRK1A	70	75	MTOR	97	67	SRPK3	93	63
DYRK1B	54	74	MUSK	0.2	62	TAOK1	10	84
EGFR	29	91	MYO3A	87	100	TGFBR1	34	48
EPHA2	48	84	p38-alpha	95	86	TIE2	18	91
ERBB2	38	100	p38-beta	40	93	TRKA	85	83
ERBB4	87	97	PAK1	59	77	TSSK1B	88	61
ERK1	77	100	PAK2	63	69	TYK2	100	100
ERN1	80	77	PAK4	72	91	ULK2	42	81
FAK	83	75	PCTK1	1.1	74	VEGFR2	59	98
FGFR2	33	54	PDGFRA	84	96	YANK3	56	68
FGFR3	25	68	PDGFRB	16	5.4	ZAP70	100	100

The results for binding interactions are reported as relative activity percentage, where lower numbers indicate stronger hits in the matrix (Table 1). Compound **3** proved 18 times more activity towards FLT3 than compound **2** and near 30 times more specific for FLT3 over PKB/AKT1. Since compound **3** also has affinity for other kinases including ROCK2, PDGFRB and CSNK1D, more active and specific FLT3 inhibitors would be desirable. With the purpose to discover such entities, a set of isoquinolinesulfonamide compounds were designed based on compound **3**.

This chapter describes the synthesis of a focused FLT3 inhibitor library, the core structures of which are given in Figure 3. The naphthalene moiety in **3** is either modified or substituted for by thiophene or pyrrole moieties. Since the FLT3 inhibitor library consists of compound **3** and H-89 (**1**) analogues, more potent PKB/AKT1 inhibitors might arise from the focused library as well.

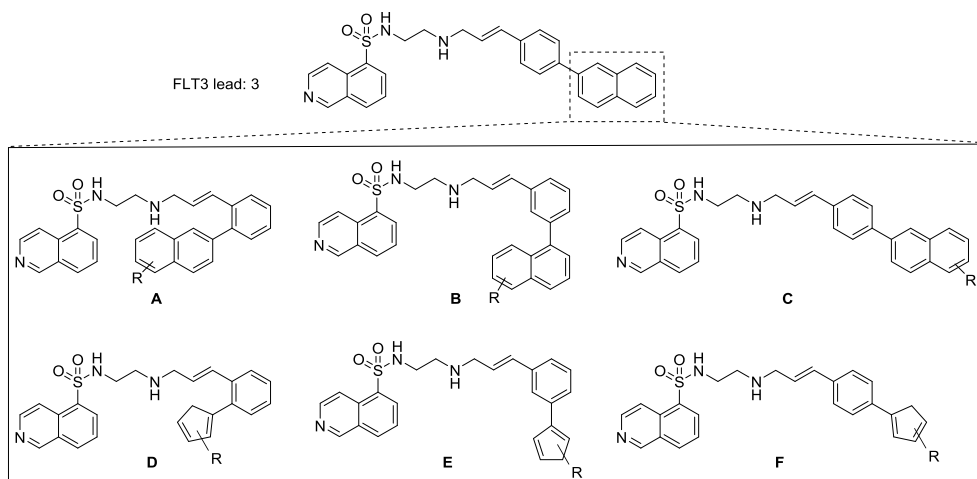
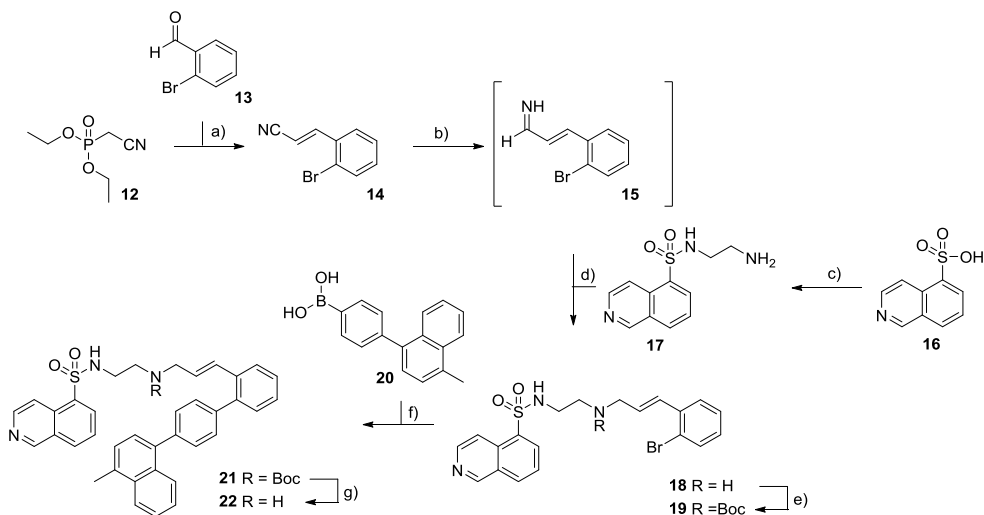


Figure 3. Target structures of the isoquinolinesulfonamide library described here and based on the scaffold of lead compound **3**. The naphthalene in **3** was modified (**A – C**) or substituted for thiophene or pyrrole containing moieties (**D – F**).

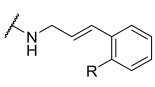
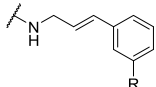
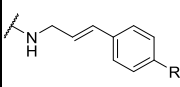
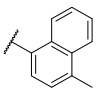
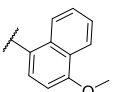
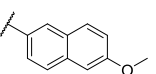
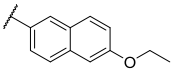
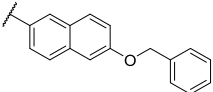
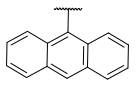
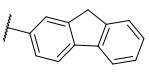
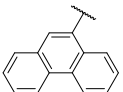
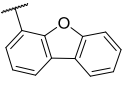
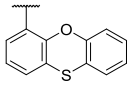
3.2 Results and discussion

The focused isoquinoline library is synthesized in a similar way as compound **22**, the synthesis of which is depicted in scheme 1. The synthesis of compound **22** commenced with a Horner-Wadsworth-Emmons (HWE) reaction between commercially available diethyl cyanomethylphosphonate **12** and *o*-bromobenzaldehyde **13** to obtain the corresponding E-isomer cinnamitrile **14** in 77% yield after column purification and recrystallization. Subsequently, E-isomer **14** was used in the four-step-one-pot trans-imation procedure according to Brussee *et al.*¹⁴ This sequence started with reduction of nitrile **14** using DIBALH to form imine **15**. The latter was reacted with amine **17**, which was obtained by conversion of isoquinoline sulfonic amine **16** into the corresponding isoquinoline sulfonic chloride, which was in turn reacted with ethylenediamine. Next, the resulting secondary imine was reduced by NaBH₄ and the crude isoquinolinesulfonamide **18** was protected with a Boc-group to yield pure E-isoquinolinesulfonamide **19**. A Suzuki reaction (Pd(PPh₃)₄, K₂CO₃) was used to couple aryl bromide **19** with aryl boronic acid **20** to form the Boc-protected isoquinolinesulfonamide **21**. Removal of the Boc protective group, and final HPLC purification, furnished isoquinolinesulfonamide **22** in 13% yield. The yields of the complete library are given in Table 2 and in the experimental section.

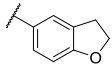
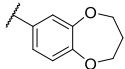
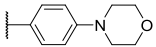
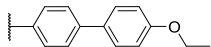
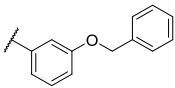
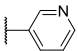
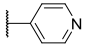
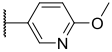
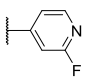
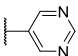
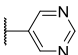
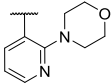


Scheme 1. Exemplified synthesis of bulky arylated isoquinolinesulfonamides. Reagents and conditions: a) NaH, **13**, 0 °C, THF, 77%; b) DIBALH, -78 °C, Et₂O/DCM 1:1 v/v; c) i) SOCl₂, reflux, DMF; ii) ethylenediamine, DCM, 0 °C, 69%; d) i) MeOH, -100 °C; ii) **17**, MeOH, RT; iv) NaBH₄, -10 °C – RT; e) Boc₂O, TEA, DCM, 0 °C, 48%; f) **20**, K₂CO₃, Pd(PPh₃)₄, DMF, 90 °C; g) TFA, DCM, H₂O, 13%.

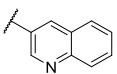
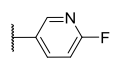
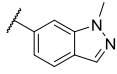
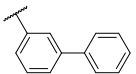
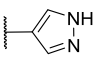
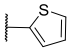
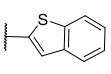
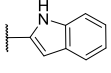
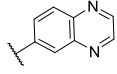
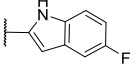
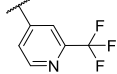
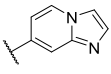
Table 2. Yields (%) of the Suzuki cross coupling reaction.

						
R =		yield (%)		yield (%)		yield (%)
	22	12.7	56	10.1	90	6.4
	23	14.3	57	11.6	91	9.6
	24	18.2	58	13.6	92	6.4
	25	16.1	59	12.9	93	6.5
	26	5.3	60	6.6	94	1.5
	27	5.5	61	9.3	95	2.6
	28	15.1	62	7.2	96	8.0
	29	17.9	63	17.0	97	9.9
	30	26.8	64	13.8	98	15.3
	31	24.6	65	15.3	99	13.7

Chapter 3

	32	24.3	66	12.3	100	13.3
	33	28.5	67	17.1	101	14.6
	34	16.3	68	17.1	102	16.5
	35	15.6	69	10.2	103	7.3
	36	11.0	70	8.9	104	7.2
	37	18.2	71	15.6	105	7.2
	38	27.4	72	19.1	106	16.2
	39	22.1	73	16.0	107	15.1
	40	24.9	74	16.5	108	13.8
	41	24.8	75	14.9	109	21.1
	42	23.4	76	13.0	110	18.5
	43	12.9	77	16.5	111	12.6

Synthesis of FLT3 kinase inhibitors: isoquinolinesulfonamide-based library

	44	24.4	78	16.9	112	21.2
	45	38.9	79	12.8	113	20.9
	46	35.5	80	31.9	114	71.1
	47	50.2	81	34.2	115	43.9
	48	32.1	82	23.4	116	34.4
	49	34.6	83	30.2	117	6.6
	50	26.1	84	27.6	118	40.7
	51	12.0	85	13.9	119	26.6
	52	78.4	86	40.6	120	67.8
	53	15.8	87	10.4	121	22.3
	54	26.5	88	18.4	122	26.0
	55	62.4	89	20.6	123	22.7

3.3 Conclusion

In this chapter the synthesis of 102 new analogues of lead compound **3** is described. The library was assembled in a parallel synthesis fashion using 34 heterocyclic aromatic boronic acids and three isoquinolinesulfonamide-modified aryl bromides using Suzuki cross-coupling methodology. The biological evaluation of the 102 compounds as inhibitors of the four kinases, PKA, AKT1, AKT2 and FLT3 is described in Chapter 4.

Experimental

General: Tetrahydrofuran (THF) was distilled over LiAlH_4 before use. Acetonitrile (ACN), dichloromethane (DCM), N,N-dimethylformamide (DMF), methanol (MeOH) and trifluoroacetic acid (TFA) were of peptide synthesis grade, purchased at Biosolve, and used as received. All general chemicals (Fluka, Acros, Merck, Aldrich, Sigma) were used as received. Traces of water were removed from reagents used in reactions that require anhydrous conditions by coevaporation with toluene. Solvents that were used in reactions were stored over 4 Å molecular sieves, except methanol and acetonitrile, which were stored over 3 Å molecular sieves. Molecular sieves were flame dried before use. Unless noted otherwise all reactions were performed under an argon atmosphere. Column chromatography was performed on Silicycle Silia-P Flash Silica Gel, with a particle size of 40 – 63 μm . The eluents toluene and ethyl acetate were distilled prior to use. TLC analysis was conducted on Merck aluminium sheets (Silica gel 60 F254). Compounds were visualized by UV absorption (254 nm), by spraying with a solution of $(\text{NH}_4)_6\text{Mo}_7\text{O}_{24} \cdot 4\text{H}_2\text{O}$ (25 g/L) and $(\text{NH}_4)_4\text{Ce}(\text{SO}_4)_4 \cdot 2\text{H}_2\text{O}$ (10 g/L) in 10% sulphuric acid, a solution of KMnO_4 (20 g/L) and K_2CO_3 (10 g/L) in water, or ninhydrin (0.75 g/L) and acetic acid (12.5 mL/L) in ethanol, where appropriate, followed by charring at ca. 150°C. ^1H - and ^{13}C -NMR spectra were recorded on a Bruker DMX-400 (400 MHz) or a Bruker DMX-600 (600 MHz) spectrometer. Chemical shifts are given in ppm (δ) relative to tetramethylsilane (^1H -NMR) or CDCl_3 (^{13}C -NMR) as internal standard. Mass spectra were recorded on a PE/Sciex API 165 instrument equipped with an Electrospray Interface (ESI) (Perkin-Elmer). High-resolution MS (HRMS) spectra were recorded with a Finnigan LTQ-FT (Thermo Electron). IR spectra were recorded on a Shimadzu FTIR-8300 and absorptions are given in cm^{-1} . Optical rotations $[\alpha]_D^{23}$ were recorded on a Propol automatic polarimeter at room temperature. LC-MS analysis was performed on a Jasco HPLC system with a Phenomenex Gemini 3 μm C18 50 x 4.6 mm column (detection simultaneously at 214 and 254 nm), coupled to a PE Sciex API 165 mass spectrometer with ESI. HPLC gradients were 10 \rightarrow 90%, 0 \rightarrow 50% or 10 \rightarrow 50% ACN in 0.1% TFA/ H_2O . Chiral HPLC analysis was performed on a Spectroflow 757 system (ABI Analytical Kratos Division, detection at 254 nm) equipped with a Chiralcel OD column (150 x 4.6 mm). The compounds were purified on a Gilson HPLC system coupled to a Phenomenex Gemini 5 μm 250 x 10 mm column and a GX281 fraction collector. The used gradients were either 0 \rightarrow 30% or 10 \rightarrow 40% ACN in 0.1% TFA/water, depending on the lipophilicity of the product. Appropriate fractions were pooled, and concentrated in a Christ rotary vacuum concentrator overnight at room temperature at 0.1 mbar.

(E)-3-(4-bromophenyl)acrylonitrile: ortho-14

Diethyl cyanomethylphosphonate (35.43 g, 200 mmol) was slowly added to an ice-cold solution of NaH (1.1 eq., 8.80 g, 220 mmol, 60% mineral oil) in DMF (900 mL) and the mixture was allowed to stir for 30 min. Hereafter, a solution of 2-bromobenzaldehyde **13** (1.1 eq., 40.70 g, 220 mmol) in DMF (100 mL) was dropwise added. The reaction was allowed to warm to RT and stirred overnight before being quenched with freshly prepared sat. aq. Na₂HSO₃ (800 mL). The mixture was diluted with H₂O (800 mL) and Et₂O (800 mL) and the layers were separated. The aqueous phase was extracted with Et₂O (3 x 600 mL) and the combined organic phases were washed with sat. aq. NaHCO₃ and brine, dried over MgSO₄, filtered and concentrated *in vacuo*. The resulting residue was purified by crystallization from EtOAc/PE (9/1, v/v) to provide ortho-**14** as a white solid (yield: 32.0 g, 154.0 mmol, 77%). ¹H NMR (400 MHz, CDCl₃) δ 7.72 (d, *J* = 16.4 Hz, 1H), 7.58 (dd, *J*₁ = 1.2 Hz, *J*₂ = 8.4 Hz, 1H), 7.50 (dd, *J*₁ = 1.6 Hz, *J*₂ = 8.0 Hz, 1H), 7.34 (t, *J* = 6.8 Hz, 1H), 7.26 (td, *J*₁ = 1.6 Hz, *J*₂ = 8.0 Hz, 1H), 5.84 (d, *J* = 16.4 Hz, 1H). ¹³C NMR (101 MHz, CDCl₃) δ 148.45, 133.19, 132.95, 131.87, 127.66, 126.70, 124.38, 117.35, 98.73.

(E)-3-(3-bromophenyl)acrylonitrile: meta-14

The same procedure as described for ortho-**14** was applied for the preparation of meta-**14**. The resulting residue was purified by crystallization from EtOAc/PE (9/1, v/v) to provide ortho-**14** as a white solid (yield: 33.8 g, 162.6 mmol, 81.3%). ¹H NMR (400 MHz, CDCl₃) δ 7.57 – 7.53 (m, 2H), 7.37 (d, *J* = 8.0 Hz, 1H), 7.32 – 7.26 (m, 2H), 5.88 (d, *J* = 16.4 Hz, 1H). ¹³C NMR (101 MHz, CDCl₃) δ 148.61, 135.22, 133.74, 130.43, 129.85, 125.85, 122.97, 117.45, 97.82.

(E)-3-(2-bromophenyl)acrylonitrile: para-14

The same procedure as described for ortho-**14** was applied for the preparation of para-**14**. The title compound was afforded by crystallization from EtOAc/PE (9/1, v/v) as a white solid (yield: 25.4 g, 122.0 mmol, 61%). ¹H NMR (400 MHz, CDCl₃) δ 7.51 (d, *J* = 8.8 Hz, 2H), 7.33 – 7.29 (m, 3H), 5.89 (d, *J* = 16.8 Hz, 1H). ¹³C NMR (101 MHz, CDCl₃) δ 149.89, 132.12, 132.03, 128.52, 125.26, 117.67, 96.84.

N-(2-aminoethyl)isoquinoline-5-sulfonamide 17

Isoquinoline-5-sulfonic acid **16** (20.92 g, 100 mmol) was treated with thionylchloride (13 eq., 91.5 mL, 1300 mmol) and a catalytic amount of DMF for 2 h at reflux. The reaction mixture was concentrated and the residue was thoroughly washed with DCM before being resuspended in H₂O (300 mL) at 0 °C. NaHCO₃ (1 eq., 8.42 g, 100.2 mmol) was added portion-wise. Next, the mixture was extracted with DCM (3x 500 mL) and dried over MgSO₄. The filtrate was dropwise added to a cooled solution of ethylenediamine (5 eq., 33.4 mL, 500 mL) in DCM (250 mL) and the reaction mixture was allowed to warm to RT and stirred for 1 h. The mixture was then evaporated partially before being washed with brine (50 mL). The aqueous layer was extracted with DCM (10 x 50 mL) and the combined organic layers were washed with brine (50 mL), dried over MgSO₄, filtered and concentrated. The title compound was obtained as a thick yellowish oil (yield: 17.3 g, 69 mmol, 69%) and was used without further purification. ¹H NMR (400 MHz, CDCl₃, Me₄Si) δ 9.36 (1H, s, CH_{ar}), 8.67 (1H, d, *J* = 8.4 Hz, CH_{ar}), 8.47 – 8.43 (2H, m, 2 x CH_{ar}), 8.21 (1H, d, *J* = 11.2 Hz, CH_{ar}), 7.71, (1H, t, *J* = 10.0 Hz, CH_{ar}), 3.45 (3H, bs, NH₂

and NH), 3.00 (2H, t, $J = 5.2$ Hz, CH₂), 2.76 (2H, t, $J = 6.0$ Hz, CH₂). ¹³C NMR (101 MHz, CDCl₃) δ 153.26, 145.06, 133.46, 133.19, 131.23, 129.01, 125.91, 117.22, 45.12, 40.76.

***Tert*-butyl (E)-(3-(4-bromophenyl)allyl)(2-(isoquinoline-5-sulfonamido)ethyl)carbamate: ortho-19**

A solution of nitrile ortho-4 (11.18 g, 53.72 mmol) in anhydrous Et₂O (250 mL) was cooled to -78 °C before dropwise addition of DiBAL-H (2 eq., 100 mL, 100 mmol, 1M solution in hexanes) and the reaction mixture was allowed to warm to 0 °C and was stirred for 2 h, after which TLC analysis showed complete consumption of starting material. Next, the mixture was cooled to -100 °C followed by rapid addition of MeOH (100 mL). After 5 min a solution of isoquinoline amine **17** (2 eq., 25.18 g, 100 mmol) in MeOH (100 mL) was dropwise added and the reaction mixture was allowed to stir at RT overnight. Hereafter, the reaction was cooled to -10 °C and NaBH₄ (2 eq., 3.78 g, 100 mmol) was added and the mixture was allowed to stir at RT for 4 h. The reaction mixture was diluted with 0.5M aq. NaOH (250 mL) and the layers were separated. The aqueous layer was extracted with DCM (3 x 250 mL) and the combined organic phases were washed with H₂O (3 x 250 mL) and brine before being dried, filtered and evaporated. The crude product was subjected to the next step without further purification.

To the ice-cooled solution of crude product in THF (250 mL) Boc₂O (2.5 eq., 27.28 g, 125 mmol) was added and the reaction was allowed to warm to RT and was stirred overnight. The reaction mixture was diluted with H₂O (250 mL) and EtOAc (250 mL) were added before being separated. The aqueous phase was extracted with EtOAc (3x 250 mL). The combined organic layers were washed with sat. aq. NaHCO₃ (2x 250 mL) and brine, dried over MgSO₄, filtered and concentrated *in vacuo*. The title compound was obtained after purification by silica gel column chromatography (0.5 – 3% MeOH/DCM) as a white solid (yield: 14.0 g, 25.6 mmol, 47.6%). ¹H NMR (400 MHz, CDCl₃) δ 9.30 (s, 1H), 8.59 (d, $J = 6.0$ Hz, 1H), 8.44 (d, $J = 6.0$ Hz, 1H), 8.40 (d, $J = 7.2$ Hz, 1H), 8.11 (d, $J = 8.0$ Hz, 1H), 7.60 (t, $J = 8.0$ Hz, 1H), 7.50 (d, $J = 7.6$ Hz, 1H), 7.38 (d, $J = 7.6$ Hz, 1H), 7.23 (br s, 1H), 7.09 (t, $J = 7.2$ Hz, 1H), 6.67 (d, $J = 14.8$ Hz, 1H), 5.97 – 5.90 (m, 1H), 3.89 (d, $J = 6.0$ Hz, 2H), 3.37 (s, 2H), 3.17 – 3.13 (m, 2H), 1.43 (s, 9H). ¹³C NMR (101 MHz, CDCl₃) δ 152.98, 144.68, 136.09, 134.32, 133.22, 132.87, 132.64, 131.01, 130.58, 128.84, 128.81, 127.88, 127.37, 126.96, 125.71, 123.23, 117.21, 80.49, 50.17, 46.54, 42.42, 28.16.

***Tert*-butyl (E)-(3-(3-bromophenyl)allyl)(2-(isoquinoline-5-sulfonamido)ethyl)carbamate: meta-19**

An identical method was used as for the synthesis of ortho-19 except that compound meta-4 (12.48 g, 60 mmol) was used as starting material and the amounts of the other materials were adjusted accordingly. The title compound was obtained after purification by silica gel column chromatography (25 – 50% EtOAc/PE) as a white solid (yield: 13.4 g, 24.6 mmol, 41.0%). ¹H NMR (400 MHz, CDCl₃) δ 9.29 (s, 1H), 8.57 (d, $J = 6.0$ Hz, 1H), 8.42 (d, $J = 6.0$ Hz, 1H), 8.36 (d, $J = 7.2$ Hz, 1H), 8.14 (d, $J = 8.4$ Hz, 1H), 7.59 (t, $J = 7.6$ Hz, 1H), 7.42 (s, 1H), 7.33 – 7.31 (m, 2H), 7.21 – 7.17 (m, 2H), 6.29 (d, $J = 16.4$ Hz, 1H), 6.04 – 6.00 (m, 1H), 3.87 (d, $J = 5.2$ Hz, 2H), 3.33 (s, 2H), 3.10 (s, 2H), 1.42 (s, 9H). ¹³C NMR (101 MHz, CDCl₃) δ 152.87, 144.53, 138.35, 134.25, 133.21, 132.78, 130.94, 130.28, 129.90, 128.89, 128.75, 126.46, 125.67, 124.86, 122.46, 117.18, 80.33, 50.09, 46.39, 42.16, 28.09.

***Tert*-butyl (E)-(3-(2-bromophenyl)allyl)(2-(isoquinoline-5-sulfonamido)ethyl)carbamate: para-19**

An identical method was used as for the synthesis of ortho-19 except that compound para-4 (10.40 g, 50 mmol) was used as starting material and the amounts of the other materials were adjusted accordingly. The title

compound was obtained after purification by silica gel column chromatography (0.1 – 2% MeOH/DCM) as a white solid (yield: 14.9 g, 27.4 mmol, 54.7%). ¹H NMR (400 MHz, CDCl₃) δ 9.32 (s, 1H), 8.59 (d, *J* = 6.4 Hz, 1H), 8.44 (d, *J* = 6.0 Hz, 1H), 8.36 (d, *J* = 7.2 Hz, 1H), 8.14 (d, *J* = 8.0 Hz, 1H), 7.59 (t, *J* = 7.6 Hz, 1H), 7.38 (s, 2H), 7.15 (d, *J* = 7.6 Hz, 2H), 6.77 (br s, 1H), 6.30 (d, *J* = 16.0 Hz, 1H), 6.06 – 5.99 (m, 1H), 3.87 (d, *J* = 5.2 Hz, 2H), 3.35 (s, 2H), 3.12 (s, 2H), 1.42 (s, 9H). ¹³C NMR (101 MHz, CDCl₃) δ 152.93, 144.54, 135.13, 134.33, 133.23, 132.82, 131.43, 131.00, 128.80, 127.70, 125.72, 121.23, 117.25, 80.38, 50.16, 46.45, 42.11, 29.41, 28.12.

General procedure for the Suzuki coupling:

Stock solutions of ortho-**19** (1M in DCM), K₂CO₃ (2M in H₂O) and Pd(PPh₃)₄ (0.017M in DCM) were thoroughly degassed in a sonication bath for 15 minutes. K₂CO₃ (2.5 eq., 0.14 g, 1.0 mmol, 0.5 mL stock), ortho-**19** (0.22 g, 0.4 mmol, 0.4 mL stock) and Pd(PPh₃)₄ (0.05 eq., 0.02 g, 0.02 mmol, 1.2 mL stock) were added to arylbromide **20** (1.5 eq., 0.11 g, 0.6 mmol) and the resulting mixture was stirred at 90 °C overnight. The mixture was filtered over a short plug of silica and eluted with DCM/MeOH (4x column volume, 1:1, v/v). The eluent was evaporated and the residue was subjected to the next step without further purification.

The residue was dissolved in DCM (2.5 mL) and TFA (2.5 mL) and the reaction mixture was stirred for 1 hr. before being evaporated and coevaporated with toluene thrice. The resulting residue was purified by RP-HPLC gradient.

(E)-N-(2-((3-(2-(4-methylnaphthalen-1-yl)phenyl)allyl)amino)ethyl)isoquinoline-5-sulfonamide **22**

Prepared according to the general procedure. Yield: 25.8 mg, 50.8 μmol, 12.7%. ¹H NMR (400 MHz, CD₃OD) δ 9.42 (s, 1H), 8.64 (d, *J* = 6.0 Hz, 1H), 8.51 (d, *J* = 6.4 Hz, 1H), 8.44 (dd, *J*₁ = 8.4 Hz, *J*₂ = 12.0 Hz, 2H), 8.00 (d, *J* = 16.0 Hz, 1H), 7.85 (t, *J* = 7.6 Hz, 1H), 7.78 (d, *J* = 7.2 Hz, 1H), 7.51 – 7.43 (m, 3H), 7.40 – 7.34 (m, 3H), 7.28 (d, *J* = 7.2 Hz, 1H), 7.21 (d, *J* = 7.2 Hz, 1H), 6.39 (d, *J* = 15.6 Hz, 1H), 6.17 – 6.09 (m, 1H), 3.56 – 3.43 (m, 2H), 2.94 – 2.86 (m, 2H), 2.68 (s, 3H). ¹³C NMR (101 MHz, CD₃OD) δ 154.27, 144.73, 141.51, 138.86, 137.85, 136.04, 135.54, 135.44, 135.23, 135.15, 133.96, 133.60, 132.67, 132.69, 130.71, 129.76, 129.19, 128.17, 127.85, 127.66, 127.16, 126.94, 126.89, 126.74, 125.48, 119.76, 119.10, 50.08, 46.96, 39.69, 19.52. HRMS: calculated for C₃₁H₂₉N₃O₂S [M+H]⁺: 508.20532; found: 508.20508.

(E)-N-(2-((3-(2-(4-methoxynaphthalen-1-yl)phenyl)allyl)amino)ethyl)isoquinoline-5-sulfonamide **23**

Prepared according to the general procedure. Yield: 30.0 mg, 57.2 μmol, 14.3%. ¹H NMR (400 MHz, CD₃OD) δ 9.47 (s, 1H), 8.64 (d, *J* = 6.0 Hz, 1H), 8.54 (d, *J* = 6.0 Hz, 1H), 8.45 (dd, *J*₁ = 8.4 Hz, *J*₂ = 16.4 Hz, 2H), 8.20 (d, *J* = 9.2 Hz, 1H), 7.86 (t, *J* = 8.0 Hz, 1H), 7.76 (d, *J* = 7.2 Hz, 1H), 7.49 – 7.43 (m, 2H), 7.39 – 7.32 (m, 2H), 7.29 – 7.22 (m, 3H), 6.97 (d, *J* = 7.6 Hz, 1H), 6.42 (d, *J* = 16.0 Hz, 1H), 6.16 – 6.08 (m, 1H), 4.02 (s, 3H), 3.57 – 3.44 (m, 2H), 2.88 – 2.77 (m, 4H). ¹³C NMR (101 MHz, CD₃OD) δ 156.59, 154.02, 144.18, 141.37, 139.07, 136.31, 135.53, 135.38, 135.29, 134.40, 132.83, 132.56, 131.59, 129.77, 129.08, 128.70, 128.02, 127.70, 126.85, 126.15, 123.23, 119.61, 104.49, 56.10, 50.07, 46.88, 39.66. HRMS: calculated for C₃₁H₂₉N₃O₃S [M+H]⁺: 524.20024; found: 524.20000.

(E)-N-(2-((3-(2-(6-methoxynaphthalen-2-yl)phenyl)allyl)amino)ethyl)isoquinoline-5-sulfonamide **24**

Prepared according to the general procedure. Yield: 38.1 mg, 72.8 μmol, 18.2%. ¹H NMR (400 MHz, CD₃OD) δ 9.39 (s, 1H), 8.60 – 8.55 (m, 2H), 8.38 (dd, *J*₁ = 7.2 Hz, *J*₂ = 23.6 Hz, 2H), 7.78 (t, *J* = 8.0 Hz, 2H), 7.73 – 7.71 (m, 1H),

7.68 – 7.66 (m, 1H), 7.63 (s, 1H), 7.41 – 7.33 (m, 4H), 7.22 (s, 1H), 7.09 (dd, $J_1 = 2.4$ Hz, $J_2 = 8.8$ Hz, 1H), 6.79 (d, $J = 16.0$ Hz, 1H), 6.22 – 6.15 (m, 1H), 3.89 (s, 3H), 3.68 (d, $J = 7.2$ Hz, 2H), 3.08 (s, 4H). ^{13}C NMR (101 MHz, CD_3OD) δ 159.43, 153.78, 143.85, 142.95, 139.24, 136.94, 135.44, 135.18, 134.88, 132.83, 131.54, 130.53, 130.03, 129.32, 128.70, 128.00, 127.87, 127.51, 120.27, 119.97, 119.47, 106.63, 55.80, 50.41, 47.33, 39.93. HRMS: calculated for $\text{C}_{31}\text{H}_{29}\text{N}_3\text{O}_3\text{S}$ $[\text{M}+\text{H}]^+$: 524.20024; found: 524.19987.

(E)-N-(2-((3-(2-(6-ethoxynaphthalen-2-yl)phenyl)allyl)amino)ethyl)isoquinoline-5-sulfonamide 25

Prepared according to the general procedure. Yield: 34.6 mg, 64.4 μmol , 16.1%. ^1H NMR (400 MHz, CD_3OD) δ 9.33 (s, 1H), 8.58 (s, 1H), 8.50 (d, $J = 6.0$ Hz, 1H), 8.38 (d, $J = 7.2$ Hz, 1H), 8.32 – 8.30 (m, 1H), 7.77 – 7.67 (m, 4H), 7.62 (s, 1H), 7.38 – 7.28 (m, 4H), 7.19 (s, 1H), 7.09 (d, $J = 8.8$ Hz, 1H), 6.79 (d, $J = 15.6$ Hz, 1H), 6.22 – 6.14 (m, 1H), 4.11 (q, $J = 6.8$ Hz, 2H), 3.68 (d, $J = 7.2$ Hz, 2H), 3.08 (s, 4H), 1.43 (t, $J = 6.8$ Hz, 3H). ^{13}C NMR (101 MHz, CD_3OD) δ 158.66, 154.16, 144.70, 142.95, 139.23, 136.84, 135.28, 135.20, 135.00, 134.86, 132.55, 131.54, 130.51, 129.97, 129.78, 129.28, 128.69, 127.83, 127.72, 127.51, 120.55, 119.94, 119.08, 107.36, 64.55, 50.40, 47.33, 39.91, 15.12. HRMS: calculated for $\text{C}_{32}\text{H}_{31}\text{N}_3\text{O}_3\text{S}$ $[\text{M}+\text{H}]^+$: 538.21589; found: 538.21569.

(E)-N-(2-((3-(2-(6-benzyloxy)naphthalen-2-yl)phenyl)allyl)amino)ethyl)isoquinoline-5-sulfonamide 26

Prepared according to the general procedure. Yield: 12.7 mg, 21.2 μmol , 5.3%. ^1H NMR (400 MHz, CD_3OD) δ 9.50 (s, 1H), 8.64 (s, 2H), 8.45 (t, $J = 8.0$ Hz, 2H), 7.88 (d, $J = 8.4$ Hz, 1H), 7.81 (t, $J = 7.6$ Hz, 1H), 7.69 – 7.64 (m, 3H), 7.39 – 7.35 (m, 3H), 7.29 (d, $J = 8.8$ Hz, 1H), 7.22 – 7.19 (m, 3H), 7.14 (t, $J = 7.2$ Hz, 2H), 7.04 (t, $J = 6.8$ Hz, 1H), 6.80 (d, $J = 15.6$ Hz, 1H), 6.21 – 6.13 (m, 1H), 4.41 (s, 2H), 3.66 (d, $J = 7.2$ Hz, 2H), 3.05 (s, 4H). ^{13}C NMR (101 MHz, CD_3OD) δ 154.30, 153.37, 143.04, 142.81, 142.75, 139.45, 135.91, 135.80, 135.71, 135.55, 134.87, 134.21, 133.21, 131.63, 130.13, 130.06, 129.80, 129.39, 129.17, 129.05, 128.62, 128.41, 127.43, 126.57, 124.48, 119.77, 119.66, 119.53, 50.36, 47.32, 39.92, 31.42. HRMS: calculated for $\text{C}_{37}\text{H}_{33}\text{N}_3\text{O}_3\text{S}$ $[\text{M}+\text{H}]^+$: 600.23154; found: 600.23150.

(E)-N-(2-((3-(2-(anthracen-9-yl)phenyl)allyl)amino)ethyl)isoquinoline-5-sulfonamide 27

Prepared according to the general procedure. Yield: 12.0 mg, 22.0 μmol , 5.5%. ^1H NMR (400 MHz, CD_3OD) δ 9.50 (s, 1H), 8.67 (s, 1H), 8.60 – 8.58 (m, 1H), 8.53 (d, $J = 8.0$ Hz, 1H), 8.49 (s, 1H), 8.42 (d, $J = 7.2$ Hz, 1H), 8.01 (d, $J = 8.4$ Hz, 2H), 7.93 – 7.89 (m, 2H), 7.60 – 7.55 (m, 2H), 7.43 – 7.27 (m, 7H), 3.35 – 3.34 (m, 2H), 3.67 (dd, $J_1 = 5.2$ Hz, $J_2 = 18.4$ Hz, 4H). ^{13}C NMR (101 MHz, CD_3OD) δ 153.33, 142.67, 139.21, 138.39, 137.03, 136.01, 135.80, 135.67, 135.49, 133.28, 132.99, 132.81, 131.60, 130.07, 129.71, 128.52, 128.17, 127.24, 127.11, 127.02, 126.39, 120.36, 49.75, 46.62, 39.47. HRMS: calculated for $\text{C}_{34}\text{H}_{29}\text{N}_3\text{O}_2\text{S}$ $[\text{M}+\text{H}]^+$: 544.20532; found: 544.20506.

(E)-N-(2-((3-(2-(9H-fluoren-2-yl)phenyl)allyl)amino)ethyl)isoquinoline-5-sulfonamide 28

Prepared according to the general procedure. Yield: 32.1 mg, 60.4 μmol , 15.1%. ^1H NMR (400 MHz, CD_3OD) δ 9.41 (s, 1H), 8.56 (s, 2H), 8.42 (d, $J = 7.2$ Hz, 1H), 8.35 (d, $J = 8.0$ Hz, 1H), 7.82 – 7.74 (m, 3H), 7.68 – 7.66 (m, 1H), 7.49 (d, $J = 7.2$ Hz, 1H), 7.43 (s, 1H), 7.38 – 7.33 (m, 4H), 7.27 (t, $J = 7.2$ Hz, 2H), 6.82 (d, $J = 15.6$ Hz, 1H), 6.22 – 6.15 (m, 1H), 3.87 (s, 2H), 3.71 (d, $J = 7.2$ Hz, 2H), 3.16 (s, 4H). ^{13}C NMR (101 MHz, CD_3OD) δ 153.46, 144.71, 143.18, 143.14, 142.34, 142.16, 140.33, 139.24, 135.63, 135.54, 135.44, 134.78, 133.01, 131.39, 130.49, 129.77,

129.67, 128.70, 128.20, 128.02, 127.92, 127.49, 127.37, 126.09, 120.80, 120.57, 119.88, 119.76, 50.40, 47.37, 39.91, 37.65. HRMS: calculated for $C_{33}H_{29}N_3O_2S$ $[M+H]^+$: 532.20532; found: 532.20521.

(E)-N-(2-((3-(2-(phenanthren-9-yl)phenyl)allyl)amino)ethyl)isoquinoline-5-sulfonamide 29

Prepared according to the general procedure. Yield: 38.9 mg, 71.6 μ mol, 17.9%. 1H NMR (400 MHz, CD_3OD) δ 9.44 (s, 1H), 8.68 (t, J = 12.4 Hz, 2H), 8.60 (d, J = 5.6 Hz, 1H), 8.51 (d, J = 6.0 Hz, 1H), 8.41 (d, J = 8.4 Hz, 1H), 8.35 (d, J = 7.2 Hz, 1H), 7.84 (d, J = 8.0 Hz, 1H), 7.81 – 7.78 (m, 2H), 7.62 – 7.40 (m, 7H), 7.35 – 7.30 (m, 2H), 6.42 (d, J = 16 Hz, 1H), 6.18 – 6.11 (m, 1H), 3.49 – 3.37 (m, 2H), 2.81 – 2.69 (m, 4H). ^{13}C NMR (101 MHz, CD_3OD) δ 153.68, 143.60, 141.06, 138.59, 138.07, 136.12, 135.52, 135.26, 132.88, 132.69, 132.05, 131.66, 131.32, 130.53, 129.86, 129.72, 129.41, 129.07, 128.14, 128.11, 128.08, 127.94, 127.85, 126.86, 124.08, 123.59, 120.14, 119.54, 49.88, 46.76, 39.52. HRMS: calculated for $C_{34}H_{29}N_3O_2S$ $[M+H]^+$: 544.20532; found: 544.20519.

(E)-N-(2-((3-(2-(dibenzo[b,d]furan-4-yl)phenyl)allyl)amino)ethyl)isoquinoline-5-sulfonamide 30

Prepared according to the general procedure. Yield: 57.2 mg, 107.2 μ mol, 26.8%. 1H NMR (400 MHz, CD_3OD) δ 9.41 (s, 1H), 8.61 – 8.59 (m, 1H), 8.52 (d, J = 6.4 Hz, 1H), 8.39 – 8.37 (m, 2H), 7.97 (dd, J_1 = 7.6 Hz, J_2 = 18.4 Hz, 2H), 7.80 (d, J = 7.6 Hz, 1H), 7.76 (d, J = 9.2 Hz, 1H), 7.47 – 7.38 (m, 5H), 7.34 – 7.30 (m, 2H), 7.24 (t, J = 7.2 Hz, 1H), 6.63 (d, J = 16.0 Hz, 1H), 6.25 – 6.17 (m, 1H), 3.58 (d, J = 7.2 Hz, 2H), 2.88 (dd, J_1 = 4.4 Hz, J_2 = 11.2 Hz, 4H). ^{13}C NMR (101 MHz, CD_3OD) δ 157.34, 154.76, 153.71, 143.72, 138.65, 137.25, 135.60, 135.45, 135.24, 132.82, 131.99, 130.50, 129.86, 129.76, 129.53, 128.54, 128.06, 127.16, 126.05, 125.52, 125.28, 124.24, 124.12, 121.93, 121.36, 120.23, 119.48, 112.49, 50.14, 46.91, 39.72. HRMS: calculated for $C_{32}H_{27}N_3O_3S$ $[M+H]^+$: 534.18459; found: 534.18422.

(E)-N-(2-((3-(2-(phenoxathiin-4-yl)phenyl)allyl)amino)ethyl)isoquinoline-5-sulfonamide 31

Prepared according to the general procedure. Yield: 55.7 mg, 98.4 μ mol, 24.6%. 1H NMR (400 MHz, CD_3OD) δ 9.64 (s, 1H), 8.76 – 8.71 (m, 2H), 8.58 – 8.55 (m, 2H), 7.96 (t, J = 7.6 Hz, 1H), 7.77 (d, J = 8.4 Hz, 1H), 7.48 – 7.42 (m, 2H), 7.25 (d, J = 8.4 Hz, 1H), 7.20 – 7.05 (m, 5H), 7.01 – 6.97 (m, 1H), 6.65 (d, J = 15.6 Hz, 1H), 6.59 (d, J = 8.0 Hz, 1H), 6.25 – 6.18 (m, 1H), 3.63 – 3.57 (m, 2H), 3.01 (s, 4H). ^{13}C NMR (101 MHz, CD_3OD) δ 153.36, 152.56, 150.62, 140.93, 138.91, 138.05, 136.82, 136.11, 135.82, 135.48, 133.85, 131.78, 131.57, 131.12, 129.72, 129.39, 129.09, 129.00, 127.81, 127.74, 126.70, 126.10, 125.72, 122.54, 121.90, 120.87, 120.17, 118.94, 50.26, 47.11, 39.90. HRMS: calculated for $C_{32}H_{27}N_3O_3S_2$ $[M+H]^+$: 566.15666; found: 566.15650.

(E)-N-(2-((3-(2-(2,3-dihydrobenzofuran-5-yl)phenyl)allyl)amino)ethyl)isoquinoline-5-sulfonamide 32

Prepared according to the general procedure. Yield: 47.2 mg, 97.2 μ mol, 24.3%. 1H NMR (400 MHz, CD_3OD) δ 9.66 (s, 1H), 8.83 (d, J = 6.4 Hz, 1H), 8.69 (d, J = 6.0 Hz, 1H), 8.58 (dd, J_1 = 7.2 Hz, J_2 = 27.2 Hz, 2H), 7.95 (t, J = 8.0 Hz, 1H), 7.62 (d, J = 8.4 Hz, 1H), 7.35 – 7.29 (m, 2H), 7.24 – 7.22 (m, 1H), 7.10 (s, 1H), 6.95 (d, J = 8.4 Hz, 1H), 6.80 (d, J = 15.6 Hz, 1H), 6.73 (d, J = 8.0 Hz, 1H), 6.21 – 6.13 (m, 1H), 4.54 (t, J = 8.8 Hz, 2H), 3.74 (d, J = 7.2 Hz, 2H), 3.22 – 3.14 (m, 6H). ^{13}C NMR (101 MHz, CD_3OD) δ 160.92, 151.89, 143.01, 139.61, 139.31, 137.33, 136.26, 136.03, 134.69, 134.17, 133.98, 131.39, 130.60, 130.34, 129.68, 129.43, 128.73, 128.29, 127.37, 127.32, 121.44, 119.55,

109.70, 72.45, 50.52, 45.59, 40.01, 30.47. HRMS: calculated for $C_{28}H_{27}N_3O_3S$ $[M+H]^+$: 486.18459; found: 486.18411.

(E)-N-(2-((3-(2-(3,4-dihydro-2H-benzo[b][1,4]dioxepin-7-yl)phenyl)allyl)amino)ethyl)isoquinoline-5-sulfonamide 33

Prepared according to the general procedure. Yield: 58.8 mg, 114.0 μ mol, 28.5%. 1H NMR (400 MHz, CD_3OD) δ 9.61 (s, 1H), 8.79 (d, J = 6.4 Hz, 1H), 8.68 (d, J = 6.0 Hz, 1H), 8.56 (dd, J_1 = 7.2 Hz, J_2 = 33.2 Hz, 2H), 7.92 (t, J = 7.6 Hz, 1H), 7.62 – 7.59 (m, 1H), 7.32 (t, J = 4.4 Hz, 2H), 7.23 – 7.21 (m, 1H), 6.97 (d, J = 8.0 Hz, 1H), 6.83 (s, 1H), 6.81 – 6.75 (m, 2H), 6.21 – 6.13 (m, 1H), 4.16 – 4.12 (m, 4H), 3.75 (d, J = 7.2 Hz, 2H), 3.16 (dd, J_1 = 4.4 Hz, J_2 = 12.0 Hz, 4H), 2.15 – 2.10 (m, 2H). ^{13}C NMR (101 MHz, CD_3OD) δ 152.25, 152.14, 152.10, 141.85, 140.21, 139.15, 137.07, 137.03, 136.13, 135.90, 134.66, 133.94, 131.14, 130.34, 129.73, 129.22, 128.68, 127.50, 125.85, 123.94, 122.59, 121.14, 119.96, 71.98, 71.91, 50.42, 47.33, 40.01, 33.14. HRMS: calculated for $C_{29}H_{29}N_3O_4S$ $[M+H]^+$: 516.19515; found: 516.19480.

(E)-N-(2-((3-(4'-morpholino-[1,1'-biphenyl]-2-yl)allyl)amino)ethyl)isoquinoline-5-sulfonamide 34

Prepared according to the general procedure. Yield: 34.5 mg, 65.2 μ mol, 16.3%. 1H NMR (400 MHz, CD_3OD) δ 9.66 (s, 1H), 8.83 (d, J = 6.4 Hz, 1H), 8.70 (d, J = 5.6 Hz, 1H), 8.59 (dd, J_1 = 7.2 Hz, J_2 = 26.8 Hz, 2H), 7.96 (t, J = 8.0 Hz, 1H), 7.64 (d, J = 8.0 Hz, 1H), 7.38 – 7.32 (m, 2H), 7.29 – 7.28 (m, 1H), 7.26 (d, J = 8.4 Hz, 2H), 7.15 (d, J = 8.8 Hz, 2H), 6.82 (d, J = 16.0 Hz, 1H), 6.23 – 6.15 (m, 1H), 3.87 (t, J = 4.4 Hz, 4H), 3.75 (d, J = 7.2 Hz, 2H), 3.26 (t, J = 4.4 Hz, 4H), 3.18 – 3.15 (m, 4H). ^{13}C NMR (101 MHz, CD_3OD) δ 152.06, 150.36, 142.36, 139.89, 139.34, 137.24, 136.24, 136.04, 134.85, 134.71, 134.12, 131.78, 131.27, 130.40, 129.80, 129.37, 128.50, 127.57, 121.34, 119.83, 117.45, 67.48, 51.38, 47.49, 40.05. HRMS: calculated for $C_{30}H_{32}N_4O_3S$ $[M+H]^+$: 529.22679; found: 529.22658.

(E)-N-(2-((3-(4"-ethoxy-[1,1':4':1"-terphenyl]-2-yl)allyl)amino)ethyl)isoquinoline-5-sulfonamide 35

Prepared according to the general procedure. Yield: 35.2 mg, 62.4 μ mol, 15.6%. 1H NMR (400 MHz, $(CD_3)_2SO$) δ 9.47 (s, 1H), 8.70 (d, J = 5.6 Hz, 1H), 8.44 – 8.42 (m, 2H), 8.36 (d, J = 7.2 Hz, 1H), 7.81 (t, J = 7.6 Hz, 1H), 7.69 (d, J = 8.0 Hz, 2H), 7.64 (d, J = 8.0 Hz, 3H), 7.44 – 7.42 (m, 2H), 7.37 (d, J = 8.0 Hz, 3H), 7.03 (d, J = 8.8 Hz, 2H), 6.74 (d, J = 15.6 Hz, 1H), 6.25 – 6.18 (m, 1H), 4.07 (q, J = 6.8 Hz, 2H), 3.71 (d, J = 6.4 Hz, 2H), 3.06 (d, J = 31.6 Hz, 4H), 1.35 (t, J = 6.8 Hz, 3H). ^{13}C NMR (101 MHz, $(CD_3)_2SO$) δ 158.34, 153.43, 144.70, 140.23, 138.76, 138.13, 135.78, 133.87, 133.77, 133.31, 132.75, 131.73, 130.31, 130.08, 128.74, 128.60, 127.69, 126.39, 126.01, 120.75, 117.08, 114.92, 63.12, 49.30, 45.29, 14.67. HRMS: calculated for $C_{34}H_{33}N_3O_3S$ $[M+H]^+$: 564.23154; found: 564.23131.

(E)-N-(2-((3-(3'-(benzyloxy)-[1,1'-biphenyl]-2-yl)allyl)amino)ethyl)isoquinoline-5-sulfonamide 36

Prepared according to the general procedure. Yield: 24.2 mg, 44.0 μ mol, 11.0%. 1H NMR (400 MHz, CD_3OD) δ 9.52 (s, 1H), 8.67 (s, 1H), 8.50 (dd, J_1 = 7.2 Hz, J_2 = 22.0 Hz, 2H), 7.87 (t, J = 7.6 Hz, 1H), 7.65 – 7.63 (m, 1H), 7.37 – 7.32 (m, 2H), 7.29 – 7.17 (m, 6H), 7.13 – 7.10 (m, 1H), 7.04 (d, J = 7.6 Hz, 1H), 6.85 (d, J = 15.6 Hz, 1H), 6.74 (s, 1H), 6.67 (d, J = 7.6 Hz, 1H), 6.19 – 6.12 (m, 1H), 3.94 (s, 2H), 3.72 (d, J = 7.2 Hz, 2H), 3.10 (s, 4H). ^{13}C NMR (101 MHz, CD_3OD) δ 156.09, 153.36, 142.94, 142.76, 142.54, 140.97, 139.45, 136.02, 135.74, 135.61, 134.60, 133.27,

131.28, 129.99, 129.69, 129.24, 128.58, 128.47, 127.28, 126.79, 122.10, 119.54, 117.28, 50.44, 47.37, 39.99, 36.42. HRMS: calculated for $C_{33}H_{31}N_3O_3S$ $[M+H]^+$: 550.21589; found: 550.21576.

(E)-N-(2-((3-(2-(pyridin-3-yl)phenyl)allyl)amino)ethyl)isoquinoline-5-sulfonamide 37

Prepared according to the general procedure. Yield: 32.4 mg, 72.8 μ mol, 18.2%. 1H NMR (400 MHz, CD_3OD) δ 9.62 (s, 1H), 8.84 – 8.76 (m, 3H), 8.68 (s, 1H), 8.61 – 8.52 (m, 2H), 8.48 – 8.46 (m, 1H), 8.06 – 8.04 (m, 1H), 7.96 – 7.91 (m, 1H), 7.74 – 7.73 (m, 1H), 7.54 – 7.41 (m, 3H), 6.77 – 6.73 (m, 1H), 6.33 – 6.26 (m, 1H), 3.86 – 3.75 (m, 2H), 3.21 – 3.14 (m, 4H). ^{13}C NMR (101 MHz, CD_3OD) δ 152.33, 146.81, 144.38, 142.92, 140.88, 140.51, 137.01, 136.75, 136.13, 135.87, 135.57, 135.45, 133.91, 131.53, 131.12, 130.41, 129.16, 128.39, 127.84, 123.37, 121.04, 50.79, 47.67, 40.06. HRMS: calculated for $C_{25}H_{24}N_4O_2S$ $[M+H]^+$: 445.16927; found: 445.16911.

(E)-N-(2-((3-(2-(pyridin-4-yl)phenyl)allyl)amino)ethyl)isoquinoline-5-sulfonamide 38

Prepared according to the general procedure. Yield: 48.7 mg, 109.6 μ mol, 27.4%. 1H NMR (400 MHz, CD_3OD) δ 9.55 (s, 1H), 8.87 (d, J = 5.2 Hz, 2H), 8.69 (s, 2H), 8.54 (dd, J_1 = 7.2 Hz, J_2 = 21.6 Hz, 2H), 8.01 (d, J = 6.0 Hz, 2H), 7.91 (t, J = 7.6 Hz, 1H), 7.78 (d, J = 7.6 Hz, 1H), 7.64 – 7.50 (m, 3H), 6.82 (d, J = 15.6 Hz, 1H), 6.38 – 6.31 (m, 1H), 3.83 (d, J = 6.8 Hz, 2H), 3.19 (s, 4H). ^{13}C NMR (101 MHz, CD_3OD) δ 158.81, 153.15, 143.17, 142.34, 137.12, 136.65, 136.25, 135.84, 135.60, 135.37, 133.38, 131.90, 131.16, 130.47, 128.92, 128.69, 128.61, 123.71, 120.24, 50.01, 47.76, 40.03. HRMS: calculated for $C_{25}H_{24}N_4O_2S$ $[M+H]^+$: 445.16927; found: 445.16914.

(E)-N-(2-((3-(2-(6-methoxypyridin-3-yl)phenyl)allyl)amino)ethyl)isoquinoline-5-sulfonamide 39

Prepared according to the general procedure. Yield: 42.0 mg, 88.4 μ mol, 22.1%. 1H NMR (400 MHz, CD_3OD) δ 9.57 (s, 1H), 8.75 – 8.68 (m, 2H), 8.54 (dd, J_1 = 7.2 Hz, J_2 = 28.4 Hz, 2H), 8.04 (s, 1H), 7.91 (t, J = 8.0 Hz, 1H), 7.67 – 7.65 (m, 2H), 7.40 – 7.38 (m, 2H), 7.29 – 7.27 (m, 1H), 6.89 (d, J = 8.8 Hz, 1H), 6.77 (d, J = 15.6 Hz, 1H), 6.27 – 6.20 (m, 1H), 3.93 (s, 3H), 3.78 (d, J = 7.2 Hz, 2H), 3.21 – 3.15 (m, 4H). ^{13}C NMR (101 MHz, CD_3OD) δ 164.84, 152.64, 147.69, 145.61, 141.91, 141.27, 138.60, 138.33, 136.61, 135.95, 135.79, 135.17, 133.66, 131.37, 130.78, 130.44, 130.01, 129.29, 128.90, 127.79, 120.98, 111.25, 54.38, 50.470, 47.52, 40.04. HRMS: calculated for $C_{26}H_{26}N_4O_3S$ $[M+H]^+$: 475.17984; found: 475.17944.

(E)-N-(2-((3-(2-(2-fluoropyridin-4-yl)phenyl)allyl)amino)ethyl)isoquinoline-5-sulfonamide 40

Prepared according to the general procedure. Yield: 46.1 mg, 99.6 μ mol, 24.9%. 1H NMR (400 MHz, CD_3OD) δ 9.54 (s, 1H), 8.71 – 8.67 (m, 2H), 8.52 (dd, J_1 = 7.2 Hz, J_2 = 25.6 Hz, 2H), 8.24 (d, J = 4.8 Hz, 1H), 7.90 (t, J = 7.6 Hz, 1H), 7.71 (d, J = 7.2 Hz, 1H), 7.49 – 7.43 (m, 2H), 7.35 – 7.33 (m, 1H), 7.27 (d, J = 4.8 Hz, 1H), 7.04 (s, 1H), 6.77 (d, J = 15.6 Hz, 1H), 6.32 – 6.25 (m, 1H), 3.80 (d, J = 7.2 Hz, 2H), 3.18 (s, 4H). ^{13}C NMR (101 MHz, CD_3OD) δ 166.27, 163.90, 156.07, 155.98, 152.90, 148.43, 148.28, 141.85, 138.54, 137.39, 136.34, 135.85, 135.69, 134.73, 133.48, 130.80, 130.56, 130.47, 130.15, 128.72, 128.01, 124.19, 122.11, 120.43, 111.93, 111.16, 50.25, 47.63, 40.05. HRMS: calculated for $C_{25}H_{23}FN_4O_2S$ $[M+H]^+$: 463.15985; found: 463.15949.

(E)-N-(2-((3-(2-(pyrimidin-5-yl)phenyl)allyl)amino)ethyl)isoquinoline-5-sulfonamide 41

Prepared according to the general procedure. Yield: 44.2 mg, 99.2 μmol , 24.8%. ^1H NMR (400 MHz, CD_3OD) δ 9.59 (s, 1H), 9.16 (s, 1H), 8.78 – 8.74 (m, 3H), 8.69 – 8.67 (m, 1H), 8.55 (dd, $J_1 = 7.2$ Hz, $J_2 = 26.4$ Hz, 2H), 7.93 (t, $J = 7.6$ Hz, 1H), 7.75 – 7.73 (m, 1H), 7.51 – 7.46 (m, 2H), 7.38 – 7.36 (m, 1H), 7.76 (d, $J = 15.6$ Hz, 1H), 6.33 – 6.26 (m, 1H), 3.81 (d, $J = 7.2$ Hz, 2H), 3.19 (s, 4H). ^{13}C NMR (101 MHz, CD_3OD) δ 158.19, 158.03, 152.57, 141.10, 137.16, 136.72, 135.99, 135.85, 125.51, 134.76, 133.72, 131.51, 130.61, 130.43, 130.33, 128.97, 128.16, 122.64, 120.78, 50.22, 47.59, 40.08. HRMS: calculated for $\text{C}_{24}\text{H}_{23}\text{N}_5\text{O}_2\text{S}$ $[\text{M}+\text{H}]^+$: 446.16452; found: 446.16414.

(E)-N-(2-((3-(2-(2-methoxypyrimidin-5-yl)phenyl)allyl)amino)ethyl)isoquinoline-5-sulfonamide 42

Prepared according to the general procedure. Yield: 44.5 mg, 93.6 μmol , 23.4%. ^1H NMR (400 MHz, CD_3OD) δ 9.59 (s, 1H), 8.74 (d, $J = 6.0$ Hz, 1H), 8.69 – 8.67 (m, 1H), 8.58 (d, $J = 7.2$ Hz, 1H), 8.53 – 8.51 (m, 3H), 7.92 (t, $J = 7.6$ Hz, 1H), 7.71 – 7.69 (m, 1H), 7.46 – 7.43 (m, 2H), 7.33 – 7.31 (m, 1H), 6.78 (d, $J = 15.6$ Hz, 1H), 6.32 – 6.24 (m, 1H), 4.02 (s, 3H), 3.81 (d, $J = 6.8$ Hz, 2H), 3.19 (s, 4H). ^{13}C NMR (101 MHz, CD_3OD) δ 165.87, 160.56, 152.58, 141.14, 137.49, 136.70, 135.98, 135.78, 135.52, 134.92, 133.70, 131.43, 130.42, 130.24, 130.06, 129.13, 128.96, 128.01, 122.08, 120.77, 55.68, 50.26, 47.57, 40.07. HRMS: calculated for $\text{C}_{25}\text{H}_{25}\text{N}_5\text{O}_3\text{S}$ $[\text{M}+\text{H}]^+$: 476.17509; found: 476.17481.

(E)-N-(2-((3-(2-(morpholinopyridin-3-yl)phenyl)allyl)amino)ethyl)isoquinoline-5-sulfonamide 43

Prepared according to the general procedure. Yield: 27.3 mg, 51.6 μmol , 12.9%. ^1H NMR (400 MHz, CD_3OD) δ 9.66 (s, 1H), 8.79 (d, $J = 6.0$ Hz, 1H), 8.72 (s, 1H), 8.59 (dd, $J_1 = 2.8$ Hz, $J_2 = 10.4$ Hz, 2H), 8.22 – 8.20 (m, 1H), 7.97 (t, $J = 8.0$ Hz, 1H), 7.89 – 7.87 (m, 1H), 7.83 – 7.81 (m, 1H), 7.54 – 7.49 (m, 2H), 7.43 – 7.41 (m, 1H), 7.32 – 7.28 (m, 1H), 6.72 (d, $J = 15.6$ Hz, 1H), 6.39 – 6.31 (m, 1H), 3.87 – 3.77 (m, 2H), 3.54 (s, 4H), 3.23 – 3.21 (m, 4H), 3.17 (s, 4H). ^{13}C NMR (101 MHz, CD_3OD) δ 156.11, 152.38, 148.33, 140.59, 140.31, 136.99, 136.16, 135.88, 134.79, 133.93, 131.07, 130.78, 130.73, 129.91, 129.18, 128.02, 122.39, 121.08, 117.80, 66.90, 49.98, 47.60, 40.03. HRMS: calculated for $\text{C}_{29}\text{H}_{31}\text{N}_5\text{O}_3\text{S}$ $[\text{M}+\text{H}]^+$: 530.22204; found: 530.22178.

(E)-N-(2-((3-(2-(quinolin-2-yl)phenyl)allyl)amino)ethyl)isoquinoline-5-sulfonamide 44

Prepared according to the general procedure. Yield: 48.3 mg, 97.6 μmol , 24.4%. ^1H NMR (400 MHz, CD_3OD) δ 9.65 (s, 1H), 9.16 (s, 1H), 8.94 (s, 1H), 8.77 (d, $J = 6.4$ Hz, 1H), 8.68 – 8.66 (m, 1H), 8.57 – 8.54 (m, 2H), 8.27 (dd, $J_1 = 8.0$ Hz, $J_2 = 16.0$ Hz, 2H), 8.05 (t, $J = 8.0$ Hz, 1H), 7.96 – 7.86 (m, 2H), 7.79 – 7.77 (m, 1H), 7.58 – 7.54 (m, 3H), 6.83 (d, $J = 15.6$ Hz, 1H), 6.39 – 6.32 (m, 1H), 3.80 (d, $J = 7.2$ Hz, 2H), 3.17 (s, 4H). ^{13}C NMR (101 MHz, CD_3OD) δ 151.97, 148.09, 145.26, 140.82, 139.85, 137.26, 136.98, 136.22, 136.04, 135.90, 135.75, 135.59, 134.94, 134.07, 131.79, 130.86, 130.77, 130.41, 130.33, 130.05, 129.35, 128.31, 123.54, 123.17, 121.29, 50.48, 47.59, 40.00. HRMS: calculated for $\text{C}_{29}\text{H}_{26}\text{N}_4\text{O}_2\text{S}$ $[\text{M}+\text{H}]^+$: 495.18492; found: 495.18463.

(E)-N-(2-((3-(2-(6-fluoropyridin-3-yl)phenyl)allyl)amino)ethyl)isoquinoline-5-sulfonamide 45

Prepared according to the general procedure. Yield: 72.0 mg, 155.6 μmol , 38.9%. ^1H NMR (400 MHz, CD_3OD) δ 9.67 (s, 1H), 8.84 (d, $J = 6.8$ Hz, 1H), 8.69 (d, $J = 6.4$ Hz, 1H), 8.60 (dd, $J_1 = 7.2$ Hz, $J_2 = 28.0$ Hz, 2H), 8.10 (s, 1H), 7.97 (t, $J = 8.0$ Hz, 1H), 7.71 (td, $J_1 = 2.0$ Hz, $J_2 = 8.0$ Hz, 1H), 7.69 – 7.67 (m, 1H), 7.44 – 7.39 (m, 2H), 7.30 – 7.28

(m, 1H), 7.13 (dd, $J_1 = 2.0$ Hz, $J_2 = 8.4$ Hz, 1H), 6.73 (d, $J = 16.0$ Hz, 1H), 6.30 – 6.22 (m, 1H), 3.79 (d, $J = 7.2$ Hz, 2H), 3.22 – 3.18 (m, 4H). ^{13}C NMR (101 MHz, CD_3OD) δ 165.41, 163.03, 151.81, 148.58, 148.44, 144.33, 144.25, 139.51, 137.70, 137.35, 136.24, 135.98, 135.69, 135.25, 134.16, 131.39, 130.28, 130.05, 129.84, 129.44, 127.88, 121.72, 121.44, 110.50, 110.14, 50.29, 47.53, 39.84. HRMS: calculated for $\text{C}_{25}\text{H}_{23}\text{FN}_4\text{O}_2\text{S}$ $[\text{M}+\text{H}]^+$: 463.15985; found: 463.15942.

(E)-N-(2-((3-(2-(1-methyl-1H-indazol-6-yl)phenyl)allyl)amino)ethyl)isoquinoline-5-sulfonamide 46

Prepared according to the general procedure. Yield: 70.6 mg, 142.0 μmol , 35.5%. ^1H NMR (400 MHz, CD_3OD) δ 9.53 (s, 1H), 8.69 (d, $J = 6.4$ Hz, 1H), 8.65 – 8.63 (m, 1H), 8.48 (dd, $J_1 = 7.6$ Hz, $J_2 = 18.0$ Hz, 2H), 7.98 (s, 1H), 7.86 (t, $J = 7.6$ Hz, 1H), 7.75 (d, $J = 8.4$ Hz, 1H), 7.72 – 7.68 (m, 1H), 7.41 – 7.33 (m, 4H), 7.05 (dd, $J_1 = 1.2$ Hz, $J_2 = 8.4$ Hz, 1H), 6.78 (d, $J = 16.0$ Hz, 1H), 6.26 – 6.18 (m, 1H), 4.03 (s, 3H), 3.71 (d, $J = 7.2$ Hz, 2H), 3.16 – 3.10 (m, 4H). ^{13}C NMR (101 MHz, CD_3OD) δ 152.69, 142.91, 141.50, 141.28, 140.64, 138.70, 136.43, 135.86, 135.69, 134.86, 133.66, 133.53, 131.55, 130.39, 129.00, 128.78, 127.38, 124.39, 124.22, 121.79, 120.54, 120.28, 110.99, 50.41, 47.43, 39.84, 35.65. HRMS: calculated for $\text{C}_{28}\text{H}_{27}\text{N}_5\text{O}_2\text{S}$ $[\text{M}+\text{H}]^+$: 498.19582; found: 498.19532.

(E)-N-(2-((3-([1,1':3',1''-terphenyl]-2-yl)allyl)amino)ethyl)isoquinoline-5-sulfonamide 47

Prepared according to the general procedure. Yield: 104.3 mg, 200.8 μmol , 50.2%. ^1H NMR (400 MHz, CD_3OD) δ 9.38 (s, 1H), 8.60 (d, $J = 6.4$ Hz, 1H), 8.52 (d, $J = 6.4$ Hz, 1H), 8.41 (d, $J = 7.2$ Hz, 1H), 8.52 (d, $J = 8.0$ Hz, 1H), 7.77 (t, $J = 7.6$ Hz, 1H), 7.69 – 7.65 (m, 1H), 7.60 – 7.53 (m, 3H), 7.49 – 7.45 (m, 2H), 7.41 – 7.36 (m, 2H), 7.34 – 7.30 (m, 3H), 7.26 – 7.23 (m, 1H), 7.21 – 7.18 (m, 1H), 6.79 (d, $J = 16.0$ Hz, 1H), 6.23 – 6.15 (m, 1H), 3.71 (d, $J = 7.2$ Hz, 2H), 3.03 – 2.96 (m, 4H). ^{13}C NMR (101 MHz, CD_3OD) δ 154.08, 144.50, 142.70, 142.40, 141.92, 139.15, 135.34, 135.29, 135.14, 134.78, 132.65, 131.30, 130.57, 129.95, 129.91, 129.84, 129.70, 129.25, 128.50, 128.13, 127.99, 127.84, 127.53, 127.07, 120.17, 119.19, 50.33, 47.18, 39.86. HRMS: calculated for $\text{C}_{32}\text{H}_{29}\text{N}_3\text{O}_2\text{S}$ $[\text{M}+\text{H}]^+$: 520.20532; found: 520.20510.

(E)-N-(2-((3-(2-(1H-pyrazol-4-yl)phenyl)allyl)amino)ethyl)isoquinoline-5-sulfonamide 48

Prepared according to the general procedure. Yield: 55.7 mg, 128.4 μmol , 32.1%. ^1H NMR (400 MHz, CD_3OD) δ 9.63 (s, 1H), 8.81 (d, $J = 6.4$ Hz, 1H), 8.71 (s, 1H), 8.64 (d, $J = 7.2$ Hz, 1H), 8.54 (d, $J = 8.4$ Hz, 1H), 7.95 (t, $J = 8.0$ Hz, 1H), 7.76 (s, 1H), 7.61 (d, $J = 7.2$ Hz, 1H), 7.46 – 7.29 (m, 3H), 7.04 (d, $J = 16.0$ Hz, 1H), 6.29 – 6.18 (m, 1H), 3.84 (d, $J = 7.2$ Hz, 2H), 3.20 (s, 4H). ^{13}C NMR (101 MHz, CD_3OD) δ 152.41, 140.71, 139.04, 139.92, 136.10, 135.96, 134.96, 133.92, 133.28, 131.032, 129.93, 129.13, 128.36, 127.80, 120.54, 50.60, 47.62, 40.12. HRMS: calculated for $\text{C}_{23}\text{H}_{23}\text{N}_5\text{O}_2\text{S}$ $[\text{M}+\text{H}]^+$: 434.16452; found: 434.16395.

(E)-N-(2-((3-(2-(thiophen-2-yl)phenyl)allyl)amino)ethyl)isoquinoline-5-sulfonamide 49

Prepared according to the general procedure. Yield: 62.2 mg, 138.4 μmol , 34.6%. ^1H NMR (400 MHz, CD_3OD) δ 9.52 (s, 1H), 8.11 (d, $J = 6.4$ Hz, 1H), 8.67 (s, 1H), 8.55 (d, $J = 7.2$ Hz, 1H), 8.45 (d, $J = 8.4$ Hz, 1H), 7.87 (t, $J = 8.0$ Hz, 1H), 7.64 – 7.60 (m, 1H), 7.44 (dd, $J_1 = 1.2$ Hz, $J_2 = 5.2$ Hz, 1H), 7.43 – 7.38 (m, 1H), 7.37 – 7.32 (m, 2H), 7.11 – 7.09 (m, 1H), 7.04 – 7.00 (m, 2H), 3.80 (d, $J = 7.2$ Hz, 2H), 3.21 – 3.15 (m, 4H). ^{13}C NMR (101 MHz, CD_3OD) δ 152.89, 142.60, 141.67, 138.80, 136.31, 135.82, 135.73, 135.40, 134.97, 133.46, 131.72, 130.45, 129.77, 129.28, 129.00,

128.68, 128.54, 128.02, 127.28, 120.82, 50.48, 47.53, 40.05. HRMS: calculated for $C_{24}H_{23}N_3O_2S_2$ $[M+H]^+$: 450.13044; found: 450.12986.

(E)-N-(2-((3-(2-(benzo[b]thiophen-2-yl)phenyl)allyl)amino)ethyl)isoquinoline-5-sulfonamide 50

Prepared according to the general procedure. Yield: 52.2 mg, 104.4 μ mol, 26.1%. 1H NMR (400 MHz, CD_3OD) δ 9.55 (s, 1H), 8.73 (d, $J = 6.4$ Hz, 1H), 8.65 – 8.63 (m, 1H), 8.54 (d, $J = 7.2$ Hz, 1H), 8.46 (d, $J = 8.4$ Hz, 1H), 7.88 – 7.76 (m, 3H), 7.68 (dd, $J_1 = 6.0$ Hz, $J_2 = 8.0$ Hz, 1H), 7.50 – 7.48 (m, 1H), 7.42 – 7.38 (m, 2H), 7.37 – 7.28 (m, 2H), 7.25 (s, 1H), 7.07 (d, $J = 15.6$ Hz, 1H), 6.29 – 6.21 (m, 1H), 3.79 (d, $J = 7.2$ Hz, 2H), 3.16 (s, 4H). ^{13}C NMR (101 MHz, CD_3OD) δ 152.53, 142.84, 141.56, 141.10, 138.51, 136.62, 135.93, 135.80, 134.88, 133.67, 131.92, 130.41, 129.91, 129.81, 128.89, 128.05, 125.70, 125.67, 125.61, 124.85, 122.94, 121.22, 120.73, 50.37, 47.51, 39.99. HRMS: calculated for $C_{28}H_{25}N_3O_2S_2$ $[M+H]^+$: 500.14610; found: 500.14576.

(E)-N-(2-((3-(2-(1H-indol-2-yl)phenyl)allyl)amino)ethyl)isoquinoline-5-sulfonamide 51

Prepared according to the general procedure. Yield: 23.2 mg, 48.0 μ mol, 12.0%. 1H NMR (400 MHz, CD_3OD) δ 9.50 (s, 1H), 8.65 (q, $J = 7.6$ Hz, 2H), 8.52 (dd, $J_1 = 1.2$ Hz, $J_2 = 7.6$ Hz, 1H), 8.44 (d, $J = 8.0$ Hz, 1H), 7.84 (t, $J = 7.6$ Hz, 1H), 7.67 (dd, $J_1 = 1.2$ Hz, $J_2 = 7.2$ Hz, 1H), 7.52 (d, $J = 8.0$ Hz, 1H), 7.45 – 7.37 (m, 3H), 7.10 (td, $J_1 = 0.8$ Hz, $J_2 = 6.8$ Hz, 1H), 7.00 (td, $J_1 = 1.2$ Hz, $J_2 = 8.0$ Hz, 1H), 6.26 – 6.18 (m, 1H), 3.81 (d, $J = 6.8$ Hz, 2H), 3.15 (s, 4H). ^{13}C NMR (101 MHz, CD_3OD) δ 153.16, 142.36, 139.35, 138.43, 137.31, 136.15, 135.78, 135.65, 135.41, 134.10, 133.37, 130.63, 130.53, 130.01, 129.79, 129.04, 128.55, 128.08, 122.87, 121.19, 120.53, 120.33, 120.18, 112.13, 50.47, 47.43, 39.98. HRMS: calculated for $C_{28}H_{26}N_4O_2S$ $[M+H]^+$: 483.18492; found: 483.18449.

(E)-N-(2-((3-(2-(quinoxalin-6-yl)phenyl)allyl)amino)ethyl)isoquinoline-5-sulfonamide 52

Prepared according to the general procedure. Yield: 155.4 mg, 313.6 μ mol, 78.4%. 1H NMR (400 MHz, CD_3OD) δ 9.46 (s, 1H), 8.83 (s, 2H), 8.61 (s, 2H), 8.47 (d, $J = 7.2$ Hz, 1H), 8.40 (d, $J = 8.4$ Hz, 1H), 8.09 (d, $J = 8.8$ Hz, 1H), 7.92 (s, 1H), 7.84 – 7.76 (m, 2H), 7.71 – 7.69 (m, 1H), 7.47 – 7.39 (m, 3H), 6.77 (d, $J = 15.6$ Hz, 1H), 6.30 – 6.23 (m, 1H), 3.76 (d, $J = 7.2$ Hz, 2H), 3.17 (s, 4H). ^{13}C NMR (101 MHz, CD_3OD) δ 152.99, 146.95, 146.61, 143.92, 143.32, 142.91, 142.20, 140.70, 138.40, 136.09, 135.69, 135.51, 135.03, 133.50, 133.23, 131.35, 130.42, 130.34, 130.02, 129.71, 128.51, 127.97, 121.37, 120.17, 50.29, 47.49, 39.98. HRMS: calculated for $C_{28}H_{25}N_5O_2S$ $[M+H]^+$: 496.18017; found: 496.17970.

(E)-N-(2-((3-(2-(5-fluoro-1H-indol-2-yl)phenyl)allyl)amino)ethyl)isoquinoline-5-sulfonamide 53

Prepared according to the general procedure. Yield: 31.6 mg, 63.2 μ mol, 15.8%. 1H NMR (400 MHz, CD_3OD) δ 9.52 (s, 1H), 8.66 (s, 2H), 8.61 (s, 2H), 8.52 (d, $J = 7.2$ Hz, 1H), 8.47 (d, $J = 8.0$ Hz, 1H), 7.86 (t, $J = 7.6$ Hz, 1H), 7.70 (d, $J = 7.2$ Hz, 1H), 7.58 (d, $J = 7.6$ Hz, 1H), 7.47 – 7.40 (m, 2H), 7.35 (dd, $J_1 = 4.4$ Hz, $J_2 = 8.8$ Hz, 1H), 7.20 – 7.16 (m, 2H), 6.88 (td, $J_1 = 2.4$ Hz, $J_2 = 9.2$ Hz, 1H), 6.47 (s, 1H), 6.28 – 6.21 (m, 1H), 3.84 (d, $J = 6.8$ Hz, 2H), 3.19 – 3.14 (m, 4H). ^{13}C NMR (101 MHz, CD_3OD) δ 160.36, 158.04, 153.49, 143.02, 139.33, 139.19, 135.89, 135.73, 135.53, 135.45, 135.00, 133.78, 133.17, 130.62, 130.30, 130.26, 129.87, 129.32, 128.38, 128.12, 120.53, 112.97, 111.08, 110.81, 105.68, 105.44, 104.87, 104.82, 50.45, 47.49, 39.98. HRMS: calculated for $C_{28}H_{25}FN_4O_2S$ $[M+H]^+$: 501.17550; found: 501.17528.

(E)-N-(2-((3-(2-(2-(trifluoromethyl)pyridin-4-yl)phenyl)allyl)amino)ethyl)isoquinoline-5-sulfonamide 54

Prepared according to the general procedure. Yield: 54.3 mg, 106.0 μ mol, 26.5%. ^1H NMR (400 MHz, CD_3OD) δ 9.54 (s, 1H), 8.78 (d, J = 3.6 Hz, 1H), 8.68 – 8.66 (m, 2H), 8.54 (d, J = 4.4 Hz, 1H), 8.50 (d, J = 5.2 Hz, 1H), 7.90 (t, J = 5.2 Hz, 1H), 7.79 (s, 1H), 7.76 (d, J = 5.6 Hz, 1H), 7.64 (d, J = 3.6 Hz, 1H), 7.55 – 7.49 (m, 2H), 7.41 (d, J = 4.8 Hz, 1H), 6.32 – 6.27 (m, 1H), 3.80 (d, J = 4.8 Hz, 2H), 3.32 – 3.31 (m, 4H). ^{13}C NMR (101 MHz, CD_3OD) δ 153.45, 152.18, 151.19, 149.14 (q, J = 23.23 Hz), 142.94, 138.52, 137.43, 135.91, 135.75, 135.59, 134.89, 133.25, 131.07, 130.80, 130.38, 129.20, 128.42, 128.15, 123.20 (q, J = 171.7 Hz), 122.55, 122.51, 119.99, 50.22, 47.65, 40.08. HRMS: calculated for $\text{C}_{26}\text{H}_{23}\text{F}_3\text{N}_4\text{O}_2\text{S}$ $[\text{M}+\text{H}]^+$: 513.15666; found: 513.15631.

(E)-N-(2-((3-(2-(imidazo[1,2-a]pyridin-7-yl)phenyl)allyl)amino)ethyl)isoquinoline-5-sulfonamide 55

Prepared according to the general procedure. Yield: 120.7 mg, 249.6 μ mol, 62.4%. ^1H NMR (400 MHz, CD_3OD) δ 9.54 (s, 1H), 8.82 (s, 1H), 8.68 – 8.65 (m, 2H), 8.50 (d, J = 5.2 Hz, 1H), 8.26 (s, 1H), 8.05 (s, 1H), 8.50 (d, J = 6.4 Hz, 1H), 7.94 (d, J = 6.0 Hz, 1H), 7.91 (t, J = 2.4 Hz, 1H), 7.78 (d, J = 5.2 Hz, 1H), 7.56 – 7.49 (m, 2H), 7.45 (d, J = 0.8 Hz, 1H), 6.84 (d, J = 10.8 Hz, 1H), 6.35 – 6.30 (m, 1H), 3.80 (d, J = 4.4 Hz, 2H), 3.18 – 3.14 (m, 4H). ^{13}C NMR (101 MHz, CD_3OD) δ 153.28, 142.55, 140.61, 137.31, 136.97, 136.11, 136.02, 135.82, 135.72, 135.54, 133.30, 132.01, 131.66, 130.72, 130.58, 130.28, 129.50, 128.52, 128.07, 124.14, 122.64, 120.11, 117.13, 112.88, 50.04, 47.66, 40.00. HRMS: calculated for $\text{C}_{27}\text{H}_{25}\text{N}_5\text{O}_2\text{S}$ $[\text{M}+\text{H}]^+$: 484.18017; found: 484.17998.

(E)-N-(2-((3-(3-(4-methylnaphthalen-1-yl)phenyl)allyl)amino)ethyl)isoquinoline-5-sulfonamide 56

Prepared according to the general procedure. Yield: 20.5 mg, 40.4 μ mol, 10.1%. ^1H NMR (400 MHz, CD_3OD) δ 9.50 (s, 1H), 8.67 (s, 2H), 8.54 (d, J = 7.6 Hz, 1H), 8.44 (d, J = 8.0 Hz, 1H), 8.07 (d, J = 8.4 Hz, 1H), 7.86 (t, J = 8.0 Hz, 1H), 7.78 (d, J = 8.4 Hz, 1H), 7.54 – 7.46 (m, 4H), 7.42 – 7.36 (m, 3H), 7.26 (d, J = 7.2 Hz, 1H), 6.93 (d, J = 16.0 Hz, 1H), 6.36 – 6.28 (m, 1H), 3.85 (d, J = 7.2, 2H), 3.18 (s, 4H), 2.71 (s, 3H). ^{13}C NMR (101 MHz, CD_3OD) δ 153.23, 142.98, 140.04, 139.91, 139.32, 137.19, 136.90, 136.05, 135.72, 135.66, 135.25, 134.18, 133.31, 132.86, 131.67, 129.83, 129.49, 128.58, 127.55, 127.19, 127.04, 126.76, 125.48, 120.13, 119.48, 50.78, 47.52, 39.88, 19.59. HRMS: calculated for $\text{C}_{31}\text{H}_{29}\text{N}_3\text{O}_2\text{S}$ $[\text{M}+\text{H}]^+$: 508.20532; found: 508.20510.

(E)-N-(2-((3-(3-(4-methoxynaphthalen-1-yl)phenyl)allyl)amino)ethyl)isoquinoline-5-sulfonamide 57

Prepared according to the general procedure. Yield: 24.3 mg, 46.4 μ mol, 11.6%. ^1H NMR (400 MHz, CD_3OD) δ 9.54 (s, 1H), 8.73 (d, J = 6.0 Hz, 1H), 8.68 (s, 1H), 8.57 (d, J = 7.6 Hz, 1H), 8.47 (d, J = 8.4 Hz, 1H), 8.28 (d, J = 8.4 Hz, 1H), 7.88 (t, J = 8.0 Hz, 1H), 7.73 (d, J = 8.0 Hz, 1H), 7.52 – 7.37 (m, 6H), 7.30 (d, J = 8.0 Hz, 1H), 6.95 – 6.90 (m, 2H), 6.36 – 6.28 (m, 1H), 4.03 (s, 3H), 3.85 (d, J = 6.8 Hz, 2H), 3.18 (s, 4H). ^{13}C NMR (101 MHz, CD_3OD) δ 156.45, 152.85, 142.84, 141.67, 140.12, 136.90, 136.43, 135.88, 135.80, 133.63, 133.22, 131.78, 130.51, 129.84, 129.71, 128.77, 128.11, 127.57, 127.00, 126.54, 126.34, 126.09, 123.25, 120.53, 119.38, 104.51, 56.08, 50.49, 47.52, 40.13. HRMS: calculated for $\text{C}_{31}\text{H}_{29}\text{N}_3\text{O}_3\text{S}$ $[\text{M}+\text{H}]^+$: 524.20024; found: 524.19998.

(E)-N-(2-((3-(3-(6-methoxynaphthalen-2-yl)phenyl)allyl)amino)ethyl)isoquinoline-5-sulfonamide 58

Prepared according to the general procedure. Yield: 28.5 mg, 54.4 μ mol, 13.6%. ^1H NMR (400 MHz, CD_3OD) δ 9.48 (s, 1H), 8.69 (d, J = 6.0 Hz, 1H), 8.64 (s, 1H), 8.54 (d, J = 7.6 Hz, 1H), 8.41 (d, J = 8.4 Hz, 1H), 7.97 (s, 1H), 7.85

– 7.76 (m, 4H), 7.71 – 7.63 (m, 2H), 7.46 – 7.43 (m, 2H), 7.21 (s, 1H), 7.12 (dd, $J_1 = 2.4$ Hz, $J_2 = 8.8$ Hz, 1H), 6.92 (d, $J = 16.0$ Hz, 1H), 6.39 – 6.32 (m, 1H), 3.89 (s, 3H), 3.86 (d, $J = 7.2$ Hz, 2H), 3.19 (s, 4H). ^{13}C NMR (101 MHz, CD_3OD) δ 159.38, 152.98, 142.94, 142.08, 140.14, 137.40, 136.84, 136.21, 135.76, 135.67, 135.47, 133.39, 130.70, 130.54, 130.39, 128.56, 126.64, 126.50, 120.21, 119.38, 106.56, 55.77, 50.49, 47.50, 40.12. HRMS: calculated for $\text{C}_{31}\text{H}_{29}\text{N}_3\text{O}_3\text{S}$ $[\text{M}+\text{H}]^+$: 524.20024; found: 524.19998.

(E)-N-(2-((3-(3-(6-ethoxynaphthalen-2-yl)phenyl)allyl)amino)ethyl)isoquinoline-5-sulfonamide 59

Prepared according to the general procedure. Yield: 27.7 mg, 51.6 μmol , 12.9%. ^1H NMR (400 MHz, CD_3OD) δ 9.53 (s, 1H), 8.71 – 8.67 (m, 2H), 8.58 (d, $J = 7.6$ Hz, 1H), 8.49 (d, $J = 8.0$ Hz, 1H), 8.02 (s, 1H), 7.90 (t, $J = 7.6$ Hz, 1H), 7.85 – 7.81 (m, 3H), 7.74 – 7.69 (m, 2H), 7.50 – 7.47 (m, 2H), 7.24 (s, 1H), 7.15 (dd, $J_1 = 2.4$ Hz, $J_2 = 8.8$ Hz, 1H), 6.97 (d, $J = 16.0$ Hz, 1H), 6.42 – 6.35 (m, 1H), 4.17 (q, $J = 6.8$ Hz, 2H), 3.89 (d, $J = 3.2$ Hz, 2H), 3.14 (s, 4H), 1.46 (t, $J = 7.2$ Hz, 3H). ^{13}C NMR (101 MHz, CD_3OD) δ 158.71, 153.28, 143.14, 142.53, 140.29, 137.43, 136.87, 136.11, 135.80, 135.72, 135.59, 133.39, 130.69, 130.58, 130.44, 128.67, 128.54, 126.69, 126.58, 126.52, 120.53, 120.15, 119.34, 107.35, 64.59, 50.54, 47.56, 40.17, 15.14. HRMS: calculated for $\text{C}_{32}\text{H}_{31}\text{N}_3\text{O}_3\text{S}$ $[\text{M}+\text{H}]^+$: 538.21589; found: 538.21566.

(E)-N-(2-((3-(3-(benzyloxy)naphthalen-2-yl)phenyl)allyl)amino)ethyl)isoquinoline-5-sulfonamide 60

Prepared according to the general procedure. Yield: 15.8 mg, 26.4 μmol , 6.6%. ^1H NMR (400 MHz, CD_3OD) δ 9.47 (s, 1H), 8.65 (s, 2H), 8.53 (d, $J = 7.2$ Hz, 2H), 8.43 (d, $J = 8.4$ Hz, 1H), 8.01 (s, 1H), 7.86 – 7.80 (m, 4H), 7.72 – 7.67 (m, 2H), 7.50 – 7.47 (m, 4H), 7.39 (t, $J = 6.8$ Hz, 2H), 7.33 – 7.30 (m, 2H), 7.22 (dd, $J_1 = 2.4$ Hz, $J_2 = 9.2$ Hz, 1H), 6.95 (d, $J = 15.6$ Hz, 1H), 6.41 – 6.33 (m, 1H), 5.19 (s, 2H), 3.87 (d, $J = 7.2$ Hz, 2H), 3.19 (s, 4H). ^{13}C NMR (101 MHz, CD_3OD) δ 158.46, 153.55, 143.21, 143.03, 140.23, 138.54, 137.43, 137.05, 135.78, 135.64, 135.59, 135.45, 133.13, 130.82, 130.72, 130.43, 129.54, 128.95, 128.68, 128.65, 128.61, 128.29, 126.70, 126.55, 120.53, 119.37, 108.14, 71.09, 50.51, 47.55, 40.14. HRMS: calculated for $\text{C}_{37}\text{H}_{33}\text{N}_3\text{O}_3\text{S}$ $[\text{M}+\text{H}]^+$: 600.23154; found: 600.23139.

(E)-N-(2-((3-(3-(anthracen-9-yl)phenyl)allyl)amino)ethyl)isoquinoline-5-sulfonamide 61

Prepared according to the general procedure. Yield: 20.2 mg, 37.2 μmol , 9.3%. ^1H NMR (400 MHz, CD_3OD) δ 9.40 (s, 1H), 8.63 (d, $J = 6.0$ Hz, 1H), 8.57 (d, $J = 6.0$ Hz, 1H), 8.52 (s, 1H), 8.48 (d, $J = 7.6$ Hz, 1H), 8.37 (d, $J = 8.0$ Hz, 1H), 8.05 (d, $J = 8.4$ Hz, 2H), 7.79 (t, $J = 8.0$ Hz, 1H), 7.66 (d, $J = 7.6$ Hz, 1H), 7.60 (t, $J = 7.2$ Hz, 1H), 7.54 (d, $J = 8.8$ Hz, 2H), 7.48 (s, 1H), 7.43 (t, $J = 7.2$ Hz, 2H), 7.33 – 7.29 (m, 3H), 6.94 (d, $J = 16.0$ Hz, 1H), 6.36 – 6.28 (m, 1H), 3.83 (d, $J = 7.2$ Hz, 2H), 3.15 (s, 4H). ^{13}C NMR (101 MHz, CD_3OD) δ 153.87, 143.98, 140.75, 139.85, 137.33, 137.19, 135.44, 132.85, 132.75, 131.34, 130.61, 130.10, 129.54, 128.10, 128.00, 127.29, 126.61, 126.20, 119.76, 119.44, 50.42, 47.52, 40.09. HRMS: calculated for $\text{C}_{34}\text{H}_{29}\text{N}_3\text{O}_2\text{S}$ $[\text{M}+\text{H}]^+$: 544.20532; found: 544.20504.

(E)-N-(2-((3-(3-(9H-fluoren-2-yl)phenyl)allyl)amino)ethyl)isoquinoline-5-sulfonamide 62

Prepared according to the general procedure. Yield: 15.3 mg, 28.8 μmol , 7.2%. ^1H NMR (400 MHz, CD_3OD) δ 9.37 (s, 1H), 8.62 (d, $J = 6.0$ Hz, 1H), 8.55 (d, $J = 6.0$ Hz, 1H), 8.48 (d, $J = 7.2$ Hz, 1H), 8.36 (d, $J = 8.0$ Hz, 1H), 7.84 – 7.77 (m, 4H), 7.72 (s, 1H), 7.61 – 7.59 (m, 2H), 7.53 (d, $J = 7.6$ Hz, 2H), 7.44 – 7.43 (m, 2H), 7.35 (t, $J = 7.2$ Hz, 1H), 7.28 (d, $J = 7.2$ Hz, 1H), 6.92 (d, $J = 15.6$ Hz, 1H), 6.39 – 6.31 (m, 1H), 3.90 (s, 2H), 3.86 (d, $J = 7.2$ Hz, 2H), 3.18 (s, 4H).

¹³C NMR (101 MHz, CD₃OD) δ 154.14, 145.33, 144.79, 144.57, 143.32, 142.47, 142.43, 140.49, 140.18, 137.35, 135.37, 135.32, 135.16, 132.67, 130.62, 130.36, 128.58, 127.95, 127.91, 127.83, 126.90, 126.65, 126.56, 126.07, 121.13, 120.93, 119.35, 119.17, 50.49, 47.51, 40.10, 37.68. HRMS: calculated for C₃₃H₂₉N₃O₂S [M+H]⁺: 532.20532; found: 532.20509.

(E)-N-(2-((3-(3-(phenanthren-9-yl)phenyl)allyl)amino)ethyl)isoquinoline-5-sulfonamide 63

Prepared according to the general procedure. Yield: 37.0 mg, 68.0 μmol, 17.0%. ¹H NMR (400 MHz, CD₃OD) δ 9.30 (s, 1H), 8.78 – 8.76 (m, 1H), 8.73 – 8.70 (m, 1H), 8.59 (d, *J* = 6.0 Hz, 2H), 8.50 (d, *J* = 6.0 Hz, 1H), 8.42 (d, *J* = 7.6 Hz, 1H), 8.27 (d, *J* = 8.0 Hz, 1H), 7.86 – 7.84 (m, 1H), 7.80 – 7.69 (m, 2H), 7.65 – 7.34 (m, 9H), 6.88 (d, *J* = 16 Hz, 1H), 6.34 – 6.27 (m, 1H), 3.80 (d, *J* = 6.8 Hz, 2H), 3.14 (s, 4H). ¹³C NMR (101 MHz, CD₃OD) δ 154.28, 145.00, 142.60, 139.83, 139.40, 137.02, 135.23, 135.18, 134.90, 132.78, 132.47, 132.06, 131.95, 131.49, 131.26, 130.57, 129.90, 129.73, 129.50, 128.48, 128.01, 127.90, 127.72, 127.63, 127.52, 127.00, 124.12, 123.59, 119.66, 118.98, 50.40, 47.47, 40.06, 31.11. HRMS: calculated for C₃₄H₂₉N₃O₂S [M+H]⁺: 544.20532; found: 544.20519.

(E)-N-(2-((3-(3-(dibenzo[b,d]furan-4-yl)phenyl)allyl)amino)ethyl)isoquinoline-5-sulfonamide 64

Prepared according to the general procedure. Yield: 29.5 mg, 55.2 μmol, 13.8%. ¹H NMR (400 MHz, CD₃OD) δ 9.32 (s, 1H), 8.59 (s, 1H), 8.53 (s, 1H), 8.45 (d, *J* = 7.2 Hz, 1H), 8.30 (d, *J* = 8.0 Hz, 1H), 8.02 – 7.96 (m, 2H), 7.82 – 7.80 (m, 1H), 7.74 (t, *J* = 7.6 Hz, 1H), 7.61 – 7.56 (m, 2H), 7.50 – 7.40 (m, 5H), 7.35 (t, *J* = 7.2 Hz, 1H), 6.93 (d, *J* = 16.0 Hz, 1H), 6.39 – 6.32 (m, 1H), 3.85 (d, *J* = 7.2 Hz, 2H), 3.18 (s, 4H). ¹³C NMR (101 MHz, CD₃OD) δ 157.36, 154.41, 154.16, 144.72, 140.01, 138.21, 137.79, 135.31, 135.26, 135.04, 132.56, 130.20, 130.15, 128.53, 128.34, 127.84, 127.74, 127.15, 126.37, 126.18, 125.23, 124.63, 124.14, 121.82, 121.11, 119.56, 112.58, 50.45, 47.49, 40.08. HRMS: calculated for C₃₂H₂₇N₃O₃S [M+H]⁺: 534.18459; found: 534.18438.

(E)-N-(2-((3-(3-(phenoxathiin-4-yl)phenyl)allyl)amino)ethyl)isoquinoline-5-sulfonamide 65

Prepared according to the general procedure. Yield: 34.6 mg, 61.2 μmol, 15.3%. ¹H NMR (400 MHz, CD₃OD) δ 9.32 (s, 1H), 8.59 (s, 1H), 8.52 – 8.51 (m, 1H), 8.44 (d, *J* = 7.2 Hz, 1H), 8.31 (d, *J* = 8.0 Hz, 1H), 7.74 (d, *J* = 7.6 Hz, 1H), 7.55 (s, 1H), 7.48 – 7.43 (m, 3H), 7.18 – 7.09 (m, 5H), 7.07 – 7.02 (m, 1H), 6.96 (d, *J* = 30.4 Hz, 1H), 6.78 (d, *J* = 8.0 Hz, 1H), 6.35 – 6.28 (m, 1H), 3.85 (d, *J* = 6.8 Hz, 2H), 3.17 (s, 4H). ¹³C NMR (101 MHz, CD₃OD) δ 154.29, 153.79, 150.41, 144.95, 139.96, 138.94, 136.78, 135.26, 135.23, 134.95, 132.51, 132.40, 131.05, 130.84, 130.59, 130.35, 129.69, 129.13, 127.88, 127.68, 127.47, 127.00, 126.06, 125.78, 123.09, 122.34, 119.45, 119.02, 118.47, 50.43, 47.49, 40.07. HRMS: calculated for C₃₂H₂₇N₃O₃S₂ [M+H]⁺: 566.15666; found: 566.15641.

(E)-N-(2-((3-(3-(2,3-dihydrobenzofuran-5-yl)phenyl)allyl)amino)ethyl)isoquinoline-5-sulfonamide 66

Prepared according to the general procedure. Yield: 23.9 mg, 49.2 μmol, 12.3%. ¹H NMR (400 MHz, CD₃OD) δ 9.40 (s, 1H), 8.63 (d, *J* = 6.0 Hz, 1H), 8.58 (d, *J* = 5.6 Hz, 1H), 8.49 (d, *J* = 7.2 Hz, 1H), 8.39 (d, *J* = 8.4 Hz, 1H), 7.81 (t, *J* = 8.0 Hz, 1H), 7.61 (s, 1H), 7.50 – 7.49 (m, 1H), 7.45 (s, 1H), 7.38 (d, *J* = 4.8 Hz, 2H), 7.33 (dd, *J*₁ = 1.6 Hz, *J*₂ = 8.4 Hz, 1H), 6.89 (d, *J* = 16.0 Hz, 1H), 6.78 (d, *J* = 8.0 Hz, 1H), 6.36 – 6.29 (m, 1H), 4.56 (t, *J* = 8.8 Hz, 2H), 3.85 (d, *J* = 7.2 Hz, 2H), 3.23 (t, *J* = 8.8 Hz, 2H), 3.18 (s, 4H). ¹³C NMR (101 MHz, CD₃OD) δ 161.35, 153.79, 143.77, 143.21, 140.47, 137.23, 135.53, 135.48, 134.52, 132.93, 130.60, 130.22, 129.32, 128.17, 128.11, 127.87, 126.23, 125.92,

124.66, 119.57, 119.18, 110.28, 72.52, 50.50, 47.50, 40.11, 30.51. HRMS: calculated for $C_{28}H_{27}N_3O_3S$ $[M+H]^+$: 486.18459; found: 486.18427.

(E)-N-(2-((3-(3,4-dihydro-2H-benzo[b][1,4]dioxepin-7-yl)phenyl)allyl)amino)ethyl)isoquinoline-5-sulfonamide 67

Prepared according to the general procedure. Yield: 35.3 mg, 68.4 μ mol, 17.1%. 1H NMR (400 MHz, CD_3OD) δ 9.47 (s, 1H), 8.65 (s, 2H), 8.53 (d, $J = 7.2$ Hz, 1H), 8.42 (d, $J = 8.4$ Hz, 1H), 7.84 (t, $J = 7.6$ Hz, 1H), 7.60 (s, 1H), 7.51 – 7.47 (m, 1H), 7.39 – 7.36 (m, 2H), 7.21 – 7.16 (m, 2H), 7.01 (d, $J = 8.0$ Hz, 1H), 6.88 (d, $J = 15.6$ Hz, 1H), 6.36 – 6.29 (m, 1H), 4.18 (q, $J = 5.2$ Hz, 4H), 3.85 (d, $J = 7.2$ Hz, 2H), 3.19 (s, 4H), 2.19 – 2.13 (m, 2H). ^{13}C NMR (101 MHz, CD_3OD) δ 152.95, 152.68, 152.49, 142.02, 141.38, 140.06, 137.32, 136.56, 135.93, 135.80, 133.63, 130.31, 128.86, 128.16, 126.49, 126.24, 123.10, 122.89, 121.07, 120.68, 119.41, 71.97, 50.48, 47.50, 40.13, 33.22. HRMS: calculated for $C_{29}H_{29}N_3O_4S$ $[M+H]^+$: 516.19515; found: 516.19490.

(E)-N-(2-((3-(4'-morpholino-[1,1'-biphenyl]-3-yl)allyl)amino)ethyl)isoquinoline-5-sulfonamide 68

Prepared according to the general procedure. Yield: 36.2 mg, 68.4 μ mol, 17.1%. 1H NMR (400 MHz, CD_3OD) δ 9.49 (s, 1H), 8.68 (t, $J = 6.0$ Hz, 2H), 8.55 (d, $J = 6.4$ Hz, 1H), 8.43 (d, $J = 8.0$ Hz, 1H), 7.89 (t, $J = 8.0$ Hz, 1H), 7.63 (s, 1H), 7.55 – 7.50 (m, 3H), 7.39 – 7.38 (m, 2H), 7.07 (d, $J = 8.8$ Hz, 2H), 6.89 (d, $J = 16.0$ Hz, 2H), 6.37 – 6.29 (m, 1H), 3.86 – 3.83 (m, 6H), 3.21 – 3.19 (m, 8H). ^{13}C NMR (101 MHz, CD_3OD) δ 152.47, 150.86, 142.36, 140.89, 140.16, 137.33, 136.78, 136.02, 135.87, 134.58, 133.77, 130.32, 129.01, 128.75, 127.92, 126.14, 126.01, 120.87, 119.32, 117.82, 67.54, 51.18, 50.50, 47.50, 40.13. HRMS: calculated for $C_{30}H_{32}N_4O_3S$ $[M+H]^+$: 529.22679; found: 529.22646.

(E)-N-(2-((3-(4''-ethoxy-[1,1':4',1''-terphenyl]-3-yl)allyl)amino)ethyl)isoquinoline-5-sulfonamide 69

Prepared according to the general procedure. Yield: 23.0 mg, 40.8 μ mol, 10.2%. 1H NMR (400 MHz, CD_3OD) δ 9.49 (s, 1H), 8.66 (s, 2H), 8.55 (dd, $J_1 = 1.2$ Hz, $J_2 = 7.6$ Hz, 1H), 8.45 (d, $J = 8.0$ Hz, 1H), 7.87 (t, $J = 7.6$ Hz, 1H), 7.74 (s, 1H), 7.69 – 7.59 (m, 5H), 7.59 – 7.56 (m, 2H), 7.48 – 7.43 (m, 2H), 7.00 – 6.92 (m, 3H), 6.40 – 6.33 (m, 1H), 4.06 (q, $J = 6.8$ Hz, 2H), 3.87 (d, $J = 7.2$ Hz, 2H), 3.19 (s, 4H), 1.40 (t, $J = 6.8$ Hz, 3H). ^{13}C NMR (101 MHz, CD_3OD) δ 160.17, 153.10, 142.62, 142.20, 141.38, 140.18, 139.97, 137.42, 136.25, 135.84, 135.76, 134.01, 133.47, 130.56, 130.41, 128.86, 128.64, 128.32, 127.93, 126.68, 126.44, 120.31, 119.41, 115.91, 64.55, 50.52, 47.55, 40.15, 15.18. HRMS: calculated for $C_{34}H_{33}N_3O_3S$ $[M+H]^+$: 564.23154; found: 564.23135.

(E)-N-(2-((3-(3'-(benzyloxy)-[1,1'-biphenyl]-3-yl)allyl)amino)ethyl)isoquinoline-5-sulfonamide 70

Prepared according to the general procedure. Yield: 19.6 mg, 35.6 μ mol, 8.9%. 1H NMR (400 MHz, CD_3OD) δ 9.44 (s, 1H), 8.63 (q, $J = 6.0$ Hz, 2H), 8.52 (d, $J = 7.2$ Hz, 1H), 8.42 (d, $J = 8.4$ Hz, 1H), 7.83 (t, $J = 7.6$ Hz, 1H), 7.67 (s, 1H), 7.56 – 7.54 (m, 1H), 7.45 – 7.43 (m, 4H), 7.36 (td, $J_1 = 0.8$ Hz, $J_2 = 6.8$ Hz, 3H), 7.31 – 7.28 (m, 1H), 7.23 – 7.19 (m, 2H), 7.00 (dd, $J_1 = 2.0$ Hz, $J_2 = 7.6$ Hz, 1H), 6.92 (d, $J = 16.0$ Hz, 1H), 6.38 – 6.31 (m, 1H), 5.13 (s, 2H), 3.87 (d, $J = 6.8$ Hz, 2H), 3.18 (s, 4H). ^{13}C NMR (101 MHz, CD_3OD) δ 160.69, 153.79, 148.30, 143.74, 143.41, 142.92, 140.10, 138.86, 137.36, 135.55, 135.48, 132.97, 131.00, 130.61, 130.35, 129.92, 129.51, 128.90, 128.62, 128.21, 126.69,

126.65, 120.70, 119.58, 119.44, 114.96, 114.84, 71.07, 50.46, 47.50, 40.12. HRMS: calculated for $C_{33}H_{31}N_3O_3S$ $[M+H]^+$: 550.21589; found: 550.21565.

(E)-N-(2-((3-(3-(pyridin-3-yl)phenyl)allyl)amino)ethyl)isoquinoline-5-sulfonamide 71

Prepared according to the general procedure. Yield: 27.7 mg, 62.4 μ mol, 15.6%. 1H NMR (400 MHz, CD_3OD) δ 9.47 (s, 1H), 9.07 (s, 1H), 8.75 (d, $J = 5.6$ Hz, 1H), 8.66 – 8.62 (m, 3H), 8.54 (dd, $J_1 = 1.2$ Hz, $J_2 = 7.6$ Hz, 1H), 8.45 (d, $J = 8.0$ Hz, 1H), 7.95 (dd, $J_1 = 5.6$ Hz, $J_2 = 8.0$ Hz, 1H), 7.89 – 7.84 (m, 2H), 7.71 (d, $J = 7.6$ Hz, 1H), 7.62 (d, $J = 8.0$ Hz, 1H), 7.55 (t, $J = 7.6$ Hz, 1H), 6.95 (d, $J = 16.0$ Hz, 1H), 6.48 – 6.40 (m, 1H), 3.89 (d, $J = 6.8$ Hz, 2H), 3.24 – 3.21 (m, 4H). ^{13}C NMR (101 MHz, CD_3OD) δ 153.50, 144.05, 143.61, 143.5, 142.39, 140.35, 139.09, 138.25, 136.85, 135.84, 135.63, 135.54, 133.12, 131.07, 130.55, 128.87, 128.65, 128.32, 127.60, 126.90, 120.77, 119.86, 50.35, 47.63, 40.13. HRMS: calculated for $C_{25}H_{24}N_4O_2S$ $[M+H]^+$: 445.16927; found: 445.16911.

(E)-N-(2-((3-(3-(pyridin-4-yl)phenyl)allyl)amino)ethyl)isoquinoline-5-sulfonamide 72

Prepared according to the general procedure. Yield: 34.0 mg, 76.4 μ mol, 19.1%. 1H NMR (400 MHz, CD_3OD) δ 9.46 (s, 1H), 8.84 (d, $J = 6.8$ Hz, 2H), 8.64 (q, $J = 6.4$ Hz, 2H), 8.53 (dd, $J_1 = 1.2$ Hz, $J_2 = 7.6$ Hz, 1H), 8.45 (d, $J = 8.0$ Hz, 1H), 8.30 (d, $J = 6.8$ Hz, 2H), 8.01 (s, 1H), 7.89 – 7.85 (m, 2H), 7.73 (d, $J = 8.0$ Hz, 1H), 7.61 (t, $J = 7.6$ Hz, 1H), 6.98 (d, $J = 15.6$ Hz, 1H), 6.52 – 6.44 (m, 1H), 3.91 (d, $J = 7.2$ Hz, 2H), 3.25 – 3.20 (m, 4H). ^{13}C NMR (101 MHz, CD_3OD) δ 157.53, 153.65, 144.21, 143.48, 138.75, 138.51, 136.98, 135.70, 135.58, 135.51, 133.04, 131.28, 130.76, 130.59, 129.14, 129.00, 128.23, 127.47, 125.32, 121.29, 119.72, 50.31, 47.67, 40.13. HRMS: calculated for $C_{25}H_{24}N_4O_2S$ $[M+H]^+$: 445.16927; found: 445.16904.

(E)-N-(2-((3-(3-(6-methoxypyridin-3-yl)phenyl)allyl)amino)ethyl)isoquinoline-5-sulfonamide 73

Prepared according to the general procedure. Yield: 30.4 mg, 64.0 μ mol, 16.0%. 1H NMR (400 MHz, CD_3OD) δ 9.62 (s, 1H), 8.80 (d, $J = 6.4$ Hz, 1H), 8.69 (d, $J = 8.0$ Hz, 1H), 8.62 (dd, $J_1 = 1.2$ Hz, $J_2 = 7.6$ Hz, 1H), 8.54 (d, $J = 8.4$ Hz, 1H), 8.38 (d, $J = 2.8$ Hz, 1H), 7.99 – 7.92 (m, 2H), 7.65 (s, 1H), 7.54 – 7.52 (m, 1H), 7.48 – 7.42 (m, 2H), 6.94 – 6.90 (m, 2H), 6.41 – 6.33 (m, 1H), 3.96 (s, 3H), 3.88 (d, $J = 7.2$ Hz, 2H), 3.22 (s, 4H). ^{13}C NMR (101 MHz, CD_3OD) δ 165.06, 152.34, 145.32, 140.53, 139.79, 139.53, 139.24, 137.66, 136.96, 136.10, 135.94, 133.93, 131.16, 130.59, 130.43, 129.16, 128.06, 126.95, 136.16, 121.03, 119.81, 111.70, 54.51, 50.46, 47.57, 40.15. HRMS: calculated for $C_{26}H_{26}N_4O_3S$ $[M+H]^+$: 475.17984; found: 475.17964.

(E)-N-(2-((3-(3-(2-fluoropyridin-4-yl)phenyl)allyl)amino)ethyl)isoquinoline-5-sulfonamide 74

Prepared according to the general procedure. Yield: 30.5 mg, 66.0 μ mol, 16.5%. 1H NMR (400 MHz, CD_3OD) δ 9.63 (s, 1H), 8.80 (d, $J = 6.4$, 1H), 8.70 (d, $J = 6.0$, 1H), 8.63 (dd, $J_1 = 1.2$ Hz, $J_2 = 7.6$ Hz, 1H), 8.55 (d, $J = 8.0$ Hz, 1H), 8.25 (d, $J = 5.2$, 1H), 7.95 (t, $J = 8.0$ Hz, 1H), 7.83 (s, 1H), 7.70 (d, $J = 7.6$ Hz, 1H), 7.61 – 7.60 (m, 2H), 7.52 (t, $J = 7.6$, 1H), 7.36 (s, 1H), 6.95 (d, $J = 16.0$ Hz, 1H), 6.46 – 6.38 (m, 1H), 3.90 (d, $J = 7.2$ Hz, 2H), 3.23 (s, 4H). ^{13}C NMR (101 MHz, CD_3OD) δ 167.07, 164.70, 155.57, 155.48, 152.43, 148.98, 1548.83, 140.71, 139.26, 138.59, 138.01, 136.91, 136.09, 135.94, 133.91, 130.87, 130.47, 129.18, 128.51, 126.72, 120.90, 120.86, 120.52, 108.24, 107.87, 50.40, 47.63, 40.17. HRMS: calculated for $C_{25}H_{23}FN_4O_2S$ $[M+H]^+$: 463.15985; found: 463.15946.

(E)-N-(2-((3-(3-(pyrimidin-5-yl)phenyl)allyl)amino)ethyl)isoquinoline-5-sulfonamide 75

Prepared according to the general procedure. Yield: 26.6 mg, 59.6 μmol , 14.9%. ^1H NMR (400 MHz, CD_3OD) δ 9.62 (s, 1H), 9.15 (s, 1H), 9.07 (s, 2H), 8.79 (d, $J = 6.4$ Hz, 1H), 8.70 (d, $J = 6.0$ Hz, 1H), 8.63 (d, $J = 7.2$ Hz, 1H), 8.55 (d, $J = 8.0$ Hz, 1H), 7.95 (t, $J = 8.4$ Hz, 1H), 7.80 (s, 1H), 7.67 (d, $J = 7.6$ Hz, 1H), 7.60 (d, $J = 8.0$ Hz, 1H), 7.54 (t, $J = 7.6$ Hz, 1H), 6.96 (d, $J = 16.0$ Hz, 1H), 6.47 – 6.39 (m, 1H), 3.90 (d, $J = 7.2$ Hz, 2H), 3.23 (s, 4H). ^{13}C NMR (101 MHz, CD_3OD) δ 158.08, 156.14, 152.48, 140.79, 139.27, 138.17, 136.87, 136.08, 135.93, 135.85, 135.62, 133.88, 131.03, 130.48, 129.10, 128.53, 128.47, 126.63, 120.93, 120.56, 50.40, 47.64, 40.18. HRMS: calculated for $\text{C}_{24}\text{H}_{23}\text{N}_5\text{O}_2\text{S}$ $[\text{M}+\text{H}]^+$: 446.16452; found: 446.16416.

(E)-N-(2-((3-(3-(2-methoxypyrimidin-5-yl)phenyl)allyl)amino)ethyl)isoquinoline-5-sulfonamide 76

Prepared according to the general procedure. Yield: 24.7 mg, 52.0 μmol , 13.0%. ^1H NMR (400 MHz, CD_3OD) δ 9.56 (s, 1H), 8.82 (s, 2H), 8.73 (d, $J = 6.4$ Hz, 1H), 8.68 (d, $J = 6.4$ Hz, 1H), 8.59 (d, $J = 7.2$ Hz, 1H), 8.51 (d, $J = 8.4$ Hz, 1H), 7.92 (t, $J = 8.0$ Hz, 1H), 7.70 (s, 1H), 7.58 (d, $J = 7.2$ Hz, 1H), 7.52 – 7.47 (m, 2H), 6.94 (d, $J = 16.0$ Hz, 1H), 6.43 – 6.35 (m, 1H), 4.05 (s, 3H), 3.89 (d, $J = 7.2$ Hz, 2H), 3.22 (s, 4H). ^{13}C NMR (101 MHz, CD_3OD) δ 166.19, 158.60, 152.90, 141.79, 139.49, 137.97, 136.42, 136.04, 135.90, 135.79, 133.58, 130.86, 130.51, 129.32, 128.77, 127.97, 127.68, 126.09, 120.49, 120.24, 55.69, 50.42, 47.61, 40.16. HRMS: calculated for $\text{C}_{25}\text{H}_{25}\text{N}_5\text{O}_3\text{S}$ $[\text{M}+\text{H}]^+$: 476.17509; found: 476.17474.

(E)-N-(2-((3-(3-(2-morpholinopyridin-3-yl)phenyl)allyl)amino)ethyl)isoquinoline-5-sulfonamide 77

Prepared according to the general procedure. Yield: 35.0 mg, 66.0 μmol , 16.5%. ^1H NMR (400 MHz, CD_3OD) δ 9.63 (s, 1H), 8.79 (d, $J = 6.4$ Hz, 1H), 8.70 (d, $J = 6.4$ Hz, 1H), 8.62 (dd, $J_1 = 0.8$ Hz, $J_2 = 7.2$ Hz, 1H), 8.56 (d, $J = 8.4$ Hz, 1H), 8.18 (dd, $J_1 = 2.0$ Hz, $J_2 = 6.0$ Hz, 1H), 8.00 – 7.94 (m, 2H), 7.71 (s, 1H), 7.59 – 7.54 (m, 3H), 7.31 (dd, $J_1 = 6.0$ Hz, $J_2 = 7.6$ Hz, 1H), 6.95 (d, $J = 16.0$ Hz, 1H), 6.46 – 6.38 (m, 1H), 3.89 (d, $J = 7.2$ Hz, 2H), 3.54 (t, $J = 4.4$ Hz, 4H), 3.25 – 3.23 (m, 8H). ^{13}C NMR (101 MHz, CD_3OD) δ 156.46, 152.50, 147.01, 140.86, 140.02, 138.99, 138.92, 138.13, 136.87, 136.07, 135.90, 133.87, 131.22, 131.05, 130.48, 129.11, 129.08, 128.44, 127.42, 120.92, 120.76, 118.32, 66.85, 50.35, 50.25, 47.03, 40.15. HRMS: calculated for $\text{C}_{29}\text{H}_{31}\text{N}_5\text{O}_3\text{S}$ $[\text{M}+\text{H}]^+$: 530.22204; found: 530.22183.

(E)-N-(2-((3-(3-(quinolin-3-yl)phenyl)allyl)amino)ethyl)isoquinoline-5-sulfonamide 78

Prepared according to the general procedure. Yield: 33.4 mg, 67.6 μmol , 16.9%. ^1H NMR (400 MHz, CD_3OD) δ 9.55 (s, 1H), 9.41 (s, 1H), 9.11 (s, 1H), 8.73 (d, $J = 6.4$ Hz, 1H), 8.66 (d, $J = 6.4$ Hz, 1H), 8.58 (dd, $J_1 = 1.2$ Hz, $J_2 = 7.6$ Hz, 1H), 8.49 (d, $J = 8.4$ Hz, 1H), 8.25 – 8.19 (m, 2H), 8.02 (td, $J_1 = 1.2$ Hz, $J_2 = 6.8$ Hz, 1H), 7.95 – 7.78 (m, 4H), 7.61 – 7.55 (m, 2H), 6.97 (d, $J = 15.6$ Hz, 1H), 6.50 – 6.43 (m, 1H), 3.91 (d, $J = 7.2$ Hz, 2H), 3.24 (s, 4H). ^{13}C NMR (101 MHz, CD_3OD) δ 152.73, 148.30, 146.84, 141.68, 141.45, 139.16, 138.26, 137.04, 136.54, 135.92, 135.77, 135.45, 134.38, 133.61, 131.08, 130.51, 130.44, 130.32, 130.18, 129.92, 128.84, 128.77, 127.02, 124.07, 120.73, 120.59, 50.38, 47.63, 40.15. HRMS: calculated for $\text{C}_{29}\text{H}_{26}\text{N}_4\text{O}_2\text{S}$ $[\text{M}+\text{H}]^+$: 495.18492; found: 495.18465.

(E)-N-(2-((3-(3-(6-fluoropyridin-3-yl)phenyl)allyl)amino)ethyl)isoquinoline-5-sulfonamide 79

Prepared according to the general procedure. Yield: 23.7 mg, 51.2 μ mol, 12.8%. ^1H NMR (400 MHz, CD_3OD) δ 9.58 (s, 1H), 8.75 (d, J = 6.4 Hz, 1H), 8.69 (d, J = 6.0 Hz, 1H), 8.60 (dd, J_1 = 1.2 Hz, J_2 = 7.6 Hz, 1H), 8.52 (d, J = 8.4 Hz, 1H), 8.45 (d, J = 2.4 Hz, 1H), 8.22 – 8.17 (m, 1H), 7.93 (t, J = 8.4 Hz, 1H), 7.71 (s, 1H), 7.60 – 7.47 (m, 3H), 7.16 (dd, J_1 = 2.8 Hz, J_2 = 8.8 Hz, 1H), 6.94 (d, J = 15.6 Hz, 1H), 6.43 – 6.38 (m, 1H), 3.89 (d, J = 7.2 Hz, 2H), 3.21 (s, 4H). ^{13}C NMR (101 MHz, CD_3OD) δ 165.77, 163.38, 152.77, 146.56, 146.42, 141.81, 141.72, 139.58, 138.39, 137.82, 136.57, 136.04, 136.00, 135.96, 133.68, 130.75, 130.51, 128.88, 128.49, 127.66, 126.62, 120.64, 120.13, 110.91, 110.54, 50.44, 47.61, 40.16. HRMS: calculated for $\text{C}_{25}\text{H}_{23}\text{FN}_4\text{O}_2\text{S}$ $[\text{M}+\text{H}]^+$: 463.15985; found: 463.15945.

(E)-N-(2-((3-(3-(1-methyl-1H-indazol-6-yl)phenyl)allyl)amino)ethyl)isoquinoline-5-sulfonamide 80

Prepared according to the general procedure. Yield: 63.4 mg, 127.6 μ mol, 31.9%. ^1H NMR (400 MHz, CD_3OD) δ 9.56 (s, 1H), 8.77 (d, J = 6.8 Hz, 1H), 8.65 (d, J = 6.4 Hz, 1H), 8.59 (d, J = 7.2 Hz, 1H), 8.47 (d, J = 8.0 Hz, 1H), 7.96 (s, 1H), 7.88 (t, J = 8.0 Hz, 1H), 7.76 (s, 1H), 7.74 (s, 1H), 7.67 (s, 1H), 7.63 – 7.61 (m, 1H), 7.45 – 7.42 (m, 2H), 7.38 (dd, J_1 = 1.2 Hz, J_2 = 8.4 Hz, 1H), 6.92 (d, J = 16.0 Hz, 1H), 6.41 – 6.34 (m, 1H), 4.05 (s, 3H), 3.87 (d, J = 7.2 Hz, 2H), 3.22 (m, 4H). ^{13}C NMR (101 MHz, CD_3OD) δ 152.30, 143.05, 141.81, 140.77, 140.63, 139.93, 137.44, 136.89, 136.03, 135.88, 133.85, 133.58, 130.38, 130.34, 129.01, 127.12, 126.93, 124.47, 122.45, 121.80, 120.96, 119.63, 108.27, 50.49, 47.54, 40.14, 35.58. HRMS: calculated for $\text{C}_{28}\text{H}_{27}\text{N}_5\text{O}_2\text{S}$ $[\text{M}+\text{H}]^+$: 498.19582; found: 498.19539.

(E)-N-(2-((3-([1,1':3',1''-terphenyl]-3-yl)allyl)amino)ethyl)isoquinoline-5-sulfonamide 81

Prepared according to the general procedure. Yield: 71.1 mg, 136.8 μ mol, 34.2%. ^1H NMR (400 MHz, $(\text{CD}_3)_2\text{SO}$) δ 9.48 (s, 1H), 8.71 (d, J = 6.4 Hz, 1H), 8.45 – 8.43 (m, 2H), 8.39 (d, J = 7.2 Hz, 1H), 7.90 (s, 1H), 7.85 – 7.81 (m, 2H), 7.75 (d, J = 8.4 Hz, 2H), 7.70 (d, J = 7.2 Hz, 1H), 7.66 (d, J = 7.6 Hz, 1H), 7.57 (d, J = 7.6 Hz, 1H), 7.52 – 7.46 (m, 4H), 7.40 – 7.36 (m, 1H), 6.87 (d, J = 16.0 Hz, 1H), 6.42 – 6.35 (m, 1H), 3.78 (d, J = 6.4 Hz, 2H), 3.13 – 3.07 (m, 4H). ^{13}C NMR (101 MHz, $(\text{CD}_3)_2\text{SO}$) δ 153.49, 144.67, 141.13, 140.80, 140.66, 140.21, 136.94, 136.33, 133.97, 133.93, 133.87, 133.04, 130.50, 129.77, 129.08, 128.85, 127.76, 127.24, 127.05, 126.60, 126.23, 126.03, 125.85, 125.33, 125.30, 120.21, 117.27, 48.45, 45.48, 38.77, 38.69. HRMS: calculated for $\text{C}_{32}\text{H}_{29}\text{N}_3\text{O}_2\text{S}$ $[\text{M}+\text{H}]^+$: 520.20532; found: 520.20573.

(E)-N-(2-((3-(3-(1H-pyrazol-4-yl)phenyl)allyl)amino)ethyl)isoquinoline-5-sulfonamide 82

Prepared according to the general procedure. Yield: 40.6 mg, 93.6 μ mol, 23.4%. ^1H NMR (400 MHz, CD_3OD) δ 9.56 (s, 1H), 8.75 (d, J = 6.4 Hz, 1H), 8.67 (d, J = 6.4 Hz, 1H), 8.60 (dd, J_1 = 1.2 Hz, J_2 = 7.6 Hz, 1H), 8.49 (d, J = 8.4 Hz, 1H), 7.99 (s, 2H), 7.91 (t, J = 8.4 Hz, 1H), 7.65 (s, 1H), 7.52 (d, J = 7.2 Hz, 1H), 7.37 – 7.30 (m, 2H), 6.87 (d, J = 15.6 Hz, 1H), 6.37 – 6.29 (m, 1H), 3.86 (d, J = 6.8 Hz, 2H), 3.21 (s, 4H). ^{13}C NMR (101 MHz, CD_3OD) δ 152.66, 141.26, 140.08, 137.41, 136.63, 135.97, 135.86, 134.51, 133.73, 132.18, 130.46, 130.37, 128.90, 127.05, 125.86, 125.03, 123.21, 120.70, 119.31, 50.51, 47.53, 40.15. HRMS: calculated for $\text{C}_{23}\text{H}_{23}\text{N}_5\text{O}_2\text{S}$ $[\text{M}+\text{H}]^+$: 434.16452; found: 434.16425.

(E)-N-(2-((3-(3-(thiophen-2-yl)phenyl)allyl)amino)ethyl)isoquinoline-5-sulfonamide 83

Prepared according to the general procedure. Yield: 54.3 mg, 120.8 μ mol, 30.2%. ^1H NMR (400 MHz, CD_3OD) δ 9.51 (s, 1H), 8.71 (d, J = 6.4 Hz, 1H), 8.65 (d, J = 6.4 Hz, 1H), 8.56 (dd, J_1 = 1.2 Hz, J_2 = 7.6 Hz, 1H), 8.45 (d, J = 8.4 Hz, 1H), 7.87 (t, J = 8.0 Hz, 1H), 7.66 (s, 1H), 7.57 – 7.54 (m, 1H), 7.40 – 7.33 (m, 4H), 7.08 (dd, J_1 = 3.6 Hz, J_2 = 5.2 Hz, 1H), 6.86 (d, J = 16.0 Hz, 1H), 6.36 – 6.28 (m, 1H), 3.86 (d, J = 7.2 Hz, 2H), 3.20 (s, 4H). ^{13}C NMR (101 MHz, CD_3OD) δ 152.90, 144.71, 141.88, 139.67, 137.53, 136.30, 136.27, 135.81, 135.73, 133.47, 130.48, 130.44, 129.20, 128.66, 127.11, 126.77, 126.21, 125.17, 124.64, 120.38, 119.78, 50.42, 47.53, 40.12. HRMS: calculated for $\text{C}_{24}\text{H}_{23}\text{N}_3\text{O}_2\text{S}_2$ $[\text{M}+\text{H}]^+$: 450.13044; found: 450.13002.

(E)-N-(2-((3-(3-(benzo[b]thiophen-2-yl)phenyl)allyl)amino)ethyl)isoquinoline-5-sulfonamide 84

Prepared according to the general procedure. Yield: 55.2 mg, 110.4 μ mol, 27.6%. ^1H NMR (400 MHz, CD_3OD) δ 9.33 (s, 1H), 8.59 (d, J = 6.4 Hz, 1H), 8.54 (d, J = 6.4 Hz, 1H), 7.46 (dd, J_1 = 0.8 Hz, J_2 = 7.2 Hz, 1H), 8.31 (d, J = 8.4 Hz, 1H), 7.81 – 7.73 (m, 4H), 7.65 – 7.61 (m, 2H), 7.42 – 7.36 (m, 2H), 7.34 – 7.26 (m, 2H), 6.86 (d, J = 16.0 Hz, 1H), 6.37 – 6.30 (m, 1H), 3.84 (d, J = 7.2 Hz, 2H), 3.18 (s, 4H). ^{13}C NMR (101 MHz, CD_3OD) δ 154.06, 144.49, 144.46, 142.07, 140.68, 139.48, 136.04, 135.31, 135.12, 134.99, 132.63, 130.57, 127.77, 127.65, 127.58, 127.40, 125.76, 125.70, 124.79, 123.16, 121.18, 120.01, 119.17, 50.38, 47.53, 40.08. HRMS: calculated for $\text{C}_{28}\text{H}_{25}\text{N}_3\text{O}_2\text{S}_2$ $[\text{M}+\text{H}]^+$: 500.14610; found: 500.14564.

(E)-N-(2-((3-(3-(1H-indol-2-yl)phenyl)allyl)amino)ethyl)isoquinoline-5-sulfonamide 85

Prepared according to the general procedure. Yield: 26.8 mg, 55.6 μ mol, 13.9%. ^1H NMR (400 MHz, CD_3OD) δ 9.50 (s, 1H), 8.70 (d, J = 6.4 Hz, 2H), 8.65 (d, J = 6.0 Hz, 1H), 8.56 (d, J = 7.2 Hz, 1H), 8.44 (d, J = 8.0 Hz, 1H), 7.86 (t, J = 7.2 Hz, 2H), 7.73 (d, J = 7.6 Hz, 1H), 7.52 (d, J = 7.6 Hz, 1H), 7.43 – 7.34 (m, 3H), 7.10 (t, J = 7.6 Hz, 1H), 7.00 (t, J = 7.6 Hz, 1H), 6.90 (d, J = 16.0 Hz, 1H), 6.40 – 6.33 (m, 1H), 3.86 (d, J = 7.2 Hz, 2H), 3.19 (s, 4H). ^{13}C NMR (101 MHz, CD_3OD) δ 153.00, 142.04, 140.02, 138.91, 138.58, 137.42, 136.26, 135.82, 135.73, 134.73, 133.46, 130.50, 130.39, 130.36, 128.64, 126.61, 126.48, 124.72, 122.97, 121.25, 120.63, 120.32, 119.53, 122.16, 50.49, 47.54, 40.13. HRMS: calculated for $\text{C}_{28}\text{H}_{26}\text{N}_4\text{O}_2\text{S}$ $[\text{M}+\text{H}]^+$: 483.18492; found: 483.18448.

(E)-N-(2-((3-(3-(quinoxalin-6-yl)phenyl)allyl)amino)ethyl)isoquinoline-5-sulfonamide 86

Prepared according to the general procedure. Yield: 80.5 mg, 162.4 μ mol, 40.6%. ^1H NMR (400 MHz, CD_3OD) δ 9.44 (s, 1H), 8.86 (d, J = 1.6 Hz, 1H), 8.82 (d, J = 1.6 Hz, 1H), 8.65 – 8.61 (m, 2H), 8.52 (dd, J_1 = 0.8 Hz, J_2 = 7.2 Hz, 1H), 8.40 (d, J = 8.0 Hz, 1H), 8.19 (s, 1H), 8.09 – 8.05 (m, 2H), 7.83 (t, J = 7.6 Hz, 1H), 7.78 (s, 1H), 7.51 – 7.44 (m, 2H), 6.93 (d, J = 16.0 Hz, 1H), 6.44 – 6.36 (m, 1H), 3.90 (d, J = 7.2 Hz, 2H), 3.23 (s, 4H). ^{13}C NMR (101 MHz, CD_3OD) δ 153.27, 146.94, 146.34, 143.91, 143.74, 143.13, 142.76, 140.89, 139.59, 137.72, 135.91, 135.63, 135.50, 133.13, 130.91, 130.67, 130.49, 130.43, 130.13, 128.86, 128.37, 128.20, 127.77, 127.198, 127.03, 120.05, 119.95, 50.44, 47.58, 40.13. HRMS: calculated for $\text{C}_{28}\text{H}_{25}\text{N}_5\text{O}_2\text{S}$ $[\text{M}+\text{H}]^+$: 496.18017; found: 496.17984.

(E)-N-(2-((3-(3-(5-fluoro-1H-indol-2-yl)phenyl)allyl)amino)ethyl)isoquinoline-5-sulfonamide 87

Prepared according to the general procedure. Yield: 20.8 mg, 41.6 μ mol, 10.4%. ^1H NMR (400 MHz, CD_3OD) δ 9.41 (s, 1H), 8.65 (d, J = 4.4 Hz, 1H), 8.57 (d, J = 4.4 Hz, 1H), 8.51 (dd, J_1 = 0.8 Hz, J_2 = 4.8 Hz, 1H), 8.42 (d, J = 5.6

Hz, 1H), 7.89 (s, 1H), 7.84 (t, $J = 5.2$ Hz, 1H), 7.76 (dt, $J_1 = 1.2$ Hz, $J_2 = 4.8$ Hz, 1H), 7.47 – 7.43 (m, 2H), 7.36 (dd, $J_1 = 2.8$ Hz, $J_2 = 5.6$ Hz, 1H), 7.20 (dd, $J_1 = 2.0$ Hz, $J_2 = 6.8$ Hz, 1H), 6.94 (d, $J = 10.4$ Hz, 1H), 6.88 (td, $J_1 = 2.0$ Hz, $J_2 = 6.4$ Hz, 1H), 6.84 (s, 1H), 6.41 – 6.36 (m, 1H), 3.90 (d, $J = 4.8$ Hz, 2H), 3.22 – 3.16 (m, 4H). ^{13}C NMR (101 MHz, CD_3OD) δ 160.12, 158.58, 154.24, 144.71, 140.59, 140.00, 137.49, 135.51, 135.44, 135.35, 135.17, 134.52, 132.70, 130.77, 130.70, 130.48, 127.86, 126.89, 126.77, 126.61, 124.91, 119.61, 119.14, 112.93, 111.10, 110.92, 105.66, 105.50, 100.33, 50.50, 47.59, 40.12. HRMS: calculated for $\text{C}_{28}\text{H}_{25}\text{FN}_4\text{O}_2\text{S}$ $[\text{M}+\text{H}]^+$: 501.17550; found: 501.17552.

(E)-N-(2-((3-(3-(2-(trifluoromethyl)pyridin-4-yl)phenyl)allyl)amino)ethyl)isoquinoline-5-sulfonamide 88

Prepared according to the general procedure. Yield: 37.7 mg, 73.6 μmol , 18.4%. ^1H NMR (400 MHz, CD_3OD) δ 9.43 (s, 1H), 8.77 (d, $J = 3.2$ Hz, 1H), 8.66 (d, $J = 4.0$ Hz, 1H), 8.57 (d, $J = 4.0$ Hz, 1H), 8.51 (dd, $J_1 = 0.4$ Hz, $J_2 = 4.8$ Hz, 1H), 8.44 (d, $J = 5.2$ Hz, 1H), 8.10 (s, 1H), 7.96 (dd, $J_1 = 0.8$ Hz, $J_2 = 3.6$ Hz, 1H), 7.90 (s, 1H), 7.85 (t, $J = 5.2$ Hz, 1H), 7.79 (d, $J = 5.2$ Hz, 1H), 7.66 (d, $J = 5.2$ Hz, 1H), 7.58 (t, $J = 5.2$ Hz, 1H), 6.99 (d, $J = 10.4$ Hz, 1H), 6.46 – 6.41 (m, 1H), 3.91 (d, $J = 4.4$ Hz, 2H), 3.23 – 3.21 (m, 2H), 3.18 – 3.16 (m, 2H). ^{13}C NMR (101 MHz, CD_3OD) δ 154.29, 151.74, 151.64, 149.70 (q, $J = 23.23$ Hz), 144.80, 139.31, 138.61, 138.17, 135.43, 135.34, 135.14, 132.70, 131.07, 130.74, 129.28, 128.72, 128.66, 128.08, 127.83, 126.88, 125.87, 123.20 (q, $J = 171.7$ Hz), 120.58, 119.56, 119.52, 119.12, 50.39, 47.66, 40.14. HRMS: calculated for $\text{C}_{26}\text{H}_{23}\text{F}_3\text{N}_4\text{O}_2\text{S}$ $[\text{M}+\text{H}]^+$: 513.15666; found: 513.15630.

(E)-N-(2-((3-(3-(imidazo[1,2-a]pyridin-7-yl)phenyl)allyl)amino)ethyl)isoquinoline-5-sulfonamide 89

Prepared according to the general procedure. Yield: 39.8 mg, 82.4 μmol , 20.6%. ^1H NMR (400 MHz, CD_3OD) δ 9.43 (s, 1H), 9.14 (s, 1H), 8.66 (d, $J = 4.0$ Hz, 1H), 8.58 (d, $J = 4.0$ Hz, 1H), 8.52 (dd, $J_1 = 0.8$ Hz, $J_2 = 4.8$ Hz, 1H), 8.44 (d, $J = 5.2$ Hz, 1H), 8.30 (dd, $J_1 = 1.2$ Hz, $J_2 = 6.4$ Hz, 1H), 8.26 (s, 1H), 8.08 (s, 1H), 8.03 (d, $J = 6.4$ Hz, 1H), 7.85 (t, $J = 4.8$ Hz, 1H), 7.72 (d, $J = 5.2$ Hz, 1H), 7.64 (d, $J = 5.2$ Hz, 1H), 7.58 (t, $J = 5.2$ Hz, 1H), 6.99 (d, $J = 10.8$ Hz, 1H), 6.48 – 6.43 (m, 1H), 3.91 (d, $J = 4.8$ Hz, 2H), 3.23 – 3.18 (m, 4H). ^{13}C NMR (101 MHz, CD_3OD) δ 154.17, 144.54, 140.80, 139.24, 138.25, 136.95, 135.45, 135.39, 135.25, 134.92, 132.77, 132.39, 131.07, 130.71, 128.70, 128.47, 127.91, 127.59, 127.01, 124.41, 120.70, 119.24, 117.08, 113.32, 50.38, 47.68, 40.13. HRMS: calculated for $\text{C}_{27}\text{H}_{25}\text{N}_5\text{O}_2\text{S}$ $[\text{M}+\text{H}]^+$: 484.18017; found: 484.17986.

(E)-N-(2-((3-(4-(4-methylnaphthalen-1-yl)phenyl)allyl)amino)ethyl)isoquinoline-5-sulfonamide 90

Prepared according to the general procedure. Yield: 13.0 mg, 25.6 μmol , 6.4%. ^1H NMR (400 MHz, CD_3OD) δ 9.46 (s, 1H), 8.66 (s, 1H), 8.62 (d, $J = 6.0$ Hz, 1H), 8.53 (dd, $J_1 = 1.2$ Hz, $J_2 = 7.6$ Hz, 1H), 8.44 (d, $J = 8.0$ Hz, 1H), 8.08 (d, $J = 8.4$ Hz, 1H), 7.88 – 7.82 (m, 2H), 7.60 (d, $J = 8.0$ Hz, 2H), 7.53 (t, $J = 7.2$ Hz, 1H), 7.46 – 7.40 (m, 3H), 7.37 (d, $J = 7.2$ Hz, 1H), 7.28 (d, $J = 7.2$ Hz, 1H), 6.96 (d, $J = 16.0$ Hz, 1H), 6.40 – 6.33 (m, 1H), 3.89 (d, $J = 7.2$, 2H), 3.22 – 3.18 (m, 4H), 2.72 (s, 3H). ^{13}C NMR (101 MHz, CD_3OD) δ 153.92, 144.00, 143.09, 139.90, 139.20, 135.72, 135.52, 135.47, 135.28, 134.23, 132.92, 132.71, 131.61, 130.66, 128.07, 127.90, 127.4, 127.19, 127.16, 126.77, 125.49, 119.51, 119.10, 50.57, 47.58, 40.14. HRMS: calculated for $\text{C}_{31}\text{H}_{29}\text{N}_3\text{O}_2\text{S}$ $[\text{M}+\text{H}]^+$: 508.20532; found: 508.20508.

(E)-N-(2-((3-(4-(4-methoxynaphthalen-1-yl)phenyl)allyl)amino)ethyl)isoquinoline-5-sulfonamide 91

Prepared according to the general procedure. Yield: 20.1 mg, 38.4 μmol , 9.6%. ^1H NMR (400 MHz, CD_3OD) δ 9.49 (s, 1H), 8.67 (s, 1H), 8.56 (dd, $J_1 = 1.2$ Hz, $J_2 = 7.2$ Hz, 1H), 8.45 (d, $J = 8.0$ Hz, 1H), 8.28 (dd, $J_1 = 1.6$ Hz, $J_2 = 8.4$ Hz,

1H), 7.87 (t, $J = 7.6$ Hz, 1H), 7.78 (dd, $J_1 = 1.6$ Hz, $J_2 = 7.6$ Hz, 1H), 7.57 (d, $J = 8.0$ Hz, 1H), 7.47 – 7.39 (m, 4H), 7.30 (d, $J = 8.0$ Hz, 1H), 6.95 – 6.92 (m, 2H), 6.39 – 6.31 (m, 1H), 4.02 (s, 3H), 3.88 (d, $J = 7.2$ Hz, 2H), 3.20 (s, 4H). ^{13}C NMR (101 MHz, CD_3OD) δ 156.46, 153.47, 143.05, 142.93, 139.92, 135.88, 135.66, 135.61, 135.47, 133.51, 133.18, 133.07, 131.64, 128.37, 128.12, 127.91, 127.56, 127.03, 126.32, 126.09, 123.25, 119.94, 118.94, 104.55, 56.06, 50.57, 47.55, 40.13. HRMS: calculated for $\text{C}_{31}\text{H}_{29}\text{N}_3\text{O}_3\text{S}$ $[\text{M}+\text{H}]^+$: 524.20024; found: 524.20000.

(E)-N-(2-((3-(4-(6-methoxynaphthalen-2-yl)phenyl)allyl)amino)ethyl)isoquinoline-5-sulfonamide 92

Prepared according to the general procedure. Yield: 13.4 mg, 25.6 μmol , 6.4%. ^1H NMR (400 MHz, CD_3OD) δ 9.58 (s, 1H), 8.76 (d, $J = 6.0$ Hz, 1H), 8.70 (s, 1H), 8.60 (dd, $J_1 = 1.2$ Hz, $J_2 = 7.6$ Hz, 1H), 8.51 (d, $J = 8.0$ Hz, 1H), 8.02 (d, $J = 1.6$ Hz, 1H), 7.92 (t, $J = 7.6$ Hz, 1H), 7.82 (t, $J = 9.2$ Hz, 2H), 7.75 – 7.71 (m, 3H), 7.57 (d, $J = 8.4$ Hz, 1H), 7.24 (d, $J = 2.4$ Hz, 1H), 7.14 (dd, $J_1 = 2.4$ Hz, $J_2 = 8.8$ Hz, 1H), 6.90 (d, $J = 15.6$ Hz, 1H), 6.36 – 6.29 (m, 1H), 3.91 (s, 3H), 3.87 (d, $J = 7.2$ Hz, 2H), 3.20 (s, 4H). ^{13}C NMR (101 MHz, CD_3OD) δ 159.46, 152.77, 142.85, 141.44, 139.85, 136.57, 136.55, 135.97, 135.86, 135.56, 133.68, 130.77, 130.62, 128.89, 128.56, 128.31, 126.41, 126.33, 120.66, 120.23, 118.79, 106.57, 55.78, 50.60, 47.56, 40.15. HRMS: calculated for $\text{C}_{31}\text{H}_{29}\text{N}_3\text{O}_3\text{S}$ $[\text{M}+\text{H}]^+$: 524.20024; found: 524.20015.

(E)-N-(2-((3-(4-(6-ethoxynaphthalen-2-yl)phenyl)allyl)amino)ethyl)isoquinoline-5-sulfonamide 93

Prepared according to the general procedure. Yield: 14.0 mg, 26.0 μmol , 6.5%. ^1H NMR (400 MHz, CD_3OD) δ 9.53 (s, 1H), 8.71 – 8.67 (m, 2H), 8.57 (dd, $J_1 = 1.2$ Hz, $J_2 = 7.2$ Hz, 1H), 8.48 (d, $J = 8.0$ Hz, 1H), 8.01 (s, 1H), 7.89 (t, $J = 8.0$ Hz, 1H), 7.80 (d, $J = 8.8$ Hz, 2H), 7.75 – 7.70 (m, 3H), 7.56 (d, $J = 8.0$ Hz, 2H), 7.21 (s, 1H), 7.13 (dd, $J_1 = 2.4$ Hz, $J_2 = 9.2$ Hz, 1H), 6.90 (d, $J = 15.6$ Hz, 1H), 6.36 – 6.28 (m, 1H), 4.15 (q, $J = 7.2$ Hz, 2H), 3.86 (d, $J = 6.8$ Hz, 2H), 3.19 (s, 4H), 1.45 (t, $J = 6.8$ Hz, 3H). ^{13}C NMR (101 MHz, CD_3OD) δ 158.70, 153.18, 142.88, 142.46, 139.86, 136.47, 136.18, 135.80, 135.72, 135.59, 135.54, 133.40, 130.74, 130.57, 128.5, 128.30, 128.04, 126.36, 126.32, 120.50, 120.24, 118.77, 107.33, 64.56, 50.36, 47.55, 40.14. HRMS: calculated for $\text{C}_{32}\text{H}_{31}\text{N}_3\text{O}_3\text{S}$ $[\text{M}+\text{H}]^+$: 538.21589; found: 538.21568.

(E)-N-(2-((3-(4-(6-(benzyloxy)naphthalen-2-yl)phenyl)allyl)amino)ethyl)isoquinoline-5-sulfonamide 94

Prepared according to the general procedure. Yield: 3.6 mg, 6.0 μmol , 1.5%. ^1H NMR (400 MHz, CD_3OD) δ 9.46 (s, 1H), 8.67 (br s, 1H), 8.60 (d, $J = 6.4$ Hz, 1H), 8.52 (dd, $J_1 = 1.2$ Hz, $J_2 = 7.6$ Hz, 1H), 8.44 (d, $J = 8.4$ Hz, 1H), 8.02 (d, $J = 2.0$ Hz, 1H), 7.92 – 7.80 (m, 2H), 7.76 – 7.72 (m, 3H), 7.66 (dd, $J_1 = 2.0$ Hz, $J_2 = 8.8$ Hz, 1H), 7.56 (d, $J = 8.4$ Hz, 2H), 7.23 – 7.12 (m, 5H), 7.08 (t, $J = 6.8$ Hz, 1H), 6.90 (d, $J = 15.6$ Hz, 1H), 6.35 – 6.27 (m, 1H), 4.44 (s, 2H), 3.87 (d, $J = 6.8$ Hz, 2H), 3.18 (s, 4H). ^{13}C NMR (101 MHz, CD_3OD) δ 154.30, 154.05, 144.25, 142.94, 142.78, 139.97, 135.51, 135.39, 135.36, 135.30, 134.61, 130.63, 129.54, 129.38, 129.16, 128.50, 128.23, 128.01, 127.10, 126.55, 126.06, 125.26, 119.62, 119.43, 118.60, 50.62, 47.56, 40.13, 31.40. HRMS: calculated for $\text{C}_{37}\text{H}_{33}\text{N}_3\text{O}_3\text{S}$ $[\text{M}+\text{H}]^+$: 600.23154; found: 600.23144.

(E)-N-(2-((3-(4-(anthracen-9-yl)phenyl)allyl)amino)ethyl)isoquinoline-5-sulfonamide 95

Prepared according to the general procedure. Yield: 5.7 mg, 10.4 μmol , 2.6%. ^1H NMR (400 MHz, CD_3OD) δ 9.55 (s, 1H), 8.73 (t, $J = 6.0$ Hz, 2H), 8.60 (dd, $J_1 = 1.2$ Hz, $J_2 = 7.6$ Hz, 1H), 8.51 – 8.49 (m, 2H), 8.05 (d, $J = 8.4$ Hz, 2H),

7.92 (t, $J = 7.6$ Hz, 1H), 7.70 (d, $J = 7.6$ Hz, 2H), 7.57 (d, $J = 8.8$ Hz, 2H), 7.44 (t, $J = 6.8$ Hz, 2H), 7.38 – 7.31 (m, 4H), 7.03 (d, $J = 16.0$ Hz, 1H), 6.48 – 6.40 (m, 1H), 3.93 (d, $J = 7.2$ Hz, 2H), 3.27 – 3.20 (m, 4H). ^{13}C NMR (101 MHz, CD_3OD) δ 153.13, 142.26, 140.83, 139.86, 137.28, 136.27, 136.23, 135.82, 135.74, 133.46, 132.83, 132.79, 131.30, 130.59, 129.55, 128.64, 128.08, 127.89, 127.27, 126.60, 126.20, 120.31, 119.53, 50.56, 47.62, 40.18. HRMS: calculated for $\text{C}_{34}\text{H}_{29}\text{N}_3\text{O}_2\text{S}$ $[\text{M}+\text{H}]^+$: 544.20532; found: 544.20500.

(E)-N-(2-((3-(4-(9H-fluoren-2-yl)phenyl)allyl)amino)ethyl)isoquinoline-5-sulfonamide 96

Prepared according to the general procedure. Yield: 17.0 mg, 32.0 μmol , 8.0%. ^1H NMR (400 MHz, CD_3OD) δ 9.51 (s, 1H), 8.68 (s, 2H), 8.56 (d, $J = 7.2$ Hz, 1H), 8.48 (d, $J = 8.4$ Hz, 1H), 7.91 – 7.80 (m, 4H), 7.69 (d, $J = 8.4$ Hz, 2H), 7.64 (d, $J = 8.0$ Hz, 1H), 7.55 (d, $J = 8.0$ Hz, 3H), 7.64 (t, $J = 7.2$ Hz, 1H), 7.30 (t, $J = 7.2$ Hz, 1H), 6.90 (d, $J = 15.6$ Hz, 1H), 6.35 – 6.28 (m, 1H), 3.93 (s, 2H), 3.87 (d, $J = 7.2$ Hz, 2H), 3.19 (s, 4H). ^{13}C NMR (101 MHz, CD_3OD) δ 153.33, 145.38, 144.85, 143.19, 142.69, 142.55, 142.47, 140.18, 139.85, 136.03, 135.76, 135.66, 135.61, 133.31, 130.58, 128.50, 128.31, 127.98, 127.93, 126.77, 126.09, 124.46, 121.17, 120.94, 120.07, 118.79, 50.60, 47.56, 40.14, 37.69. HRMS: calculated for $\text{C}_{33}\text{H}_{29}\text{N}_3\text{O}_2\text{S}$ $[\text{M}+\text{H}]^+$: 532.20532; found: 532.20511.

(E)-N-(2-((3-(4-(phenanthren-9-yl)phenyl)allyl)amino)ethyl)isoquinoline-5-sulfonamide 97

Prepared according to the general procedure. Yield: 21.5 mg, 39.6 μmol , 9.9%. ^1H NMR (400 MHz, CD_3OD) δ 9.51 (s, 1H), 8.79 (d, $J = 8.4$ Hz, 1H), 8.74 – 8.66 (m, 3H), 8.57 (d, $J = 7.2$ Hz, 1H), 8.46 (d, $J = 8.0$ Hz, 1H), 7.89 – 7.86 (m, 2H), 7.82 (d, $J = 8.0$ Hz, 1H), 7.67 – 7.57 (m, 6H), 7.52 – 7.48 (m, 3H), 6.95 (d, $J = 15.6$ Hz, 1H), 6.41 – 6.33 (m, 1H), 3.88 (d, $J = 7.2$ Hz, 2H), 3.21 (s, 4H). ^{13}C NMR (101 MHz, CD_3OD) δ 153.10, 142.69, 142.27, 139.79, 139.31, 136.18, 136.02, 135.77, 135.69, 133.39, 132.83, 132.00, 131.51, 131.29, 130.52, 129.76, 128.58, 128.46, 128.02, 127.99, 127.92, 127.74, 127.63, 127.50, 124.15, 123.60, 120.24, 119.30, 50.54, 47.58, 40.14. HRMS: calculated for $\text{C}_{34}\text{H}_{29}\text{N}_3\text{O}_2\text{S}$ $[\text{M}+\text{H}]^+$: 544.20532; found: 544.20505.

(E)-N-(2-((3-(4-(dibenzo[b,d]furan-4-yl)phenyl)allyl)amino)ethyl)isoquinoline-5-sulfonamide 98

Prepared according to the general procedure. Yield: 32.7 mg, 61.2 μmol , 15.3%. ^1H NMR (400 MHz, CD_3OD) δ 9.40 (s, 1H), 8.63 (br s, 1H), 8.59 (d, $J = 6.0$ Hz, 1H), 8.49 (d, $J = 7.2$ Hz, 1H), 8.37 (d, $J = 8.4$ Hz, 1H), 8.00 (d, $J = 7.6$ Hz, 1H), 7.96 (d, $J = 7.6$ Hz, 1H), 7.89 (d, $J = 8.0$ Hz, 1H), 7.80 (t, $J = 8.0$ Hz, 1H), 7.62 – 7.57 (m, 4H), 7.47 (t, $J = 7.2$ Hz, 1H), 7.41 (t, $J = 7.6$ Hz, 1H), 7.35 (t, $J = 7.6$ Hz, 1H), 6.89 (d, $J = 16.0$ Hz, 1H), 6.37 – 6.30 (m, 1H), 3.86 (d, $J = 7.2$ Hz, 2H), 3.19 (s, 4H). ^{13}C NMR (101 MHz, CD_3OD) δ 157.36, 154.42, 153.85, 143.96, 139.71, 138.08, 136.16, 135.44, 132.84, 130.57, 130.05, 128.54, 128.18, 128.00, 127.62, 126.23, 126.12, 125.58, 124.14, 121.81, 121.11, 119.46, 119.30, 112.56, 50.52, 47.54, 40.10. HRMS: calculated for $\text{C}_{32}\text{H}_{27}\text{N}_3\text{O}_3\text{S}$ $[\text{M}+\text{H}]^+$: 534.18459; found: 534.18432.

(E)-N-(2-((3-(4-(phenoxathiin-4-yl)phenyl)allyl)amino)ethyl)isoquinoline-5-sulfonamide 99

Prepared according to the general procedure. Yield: 31.0 mg, 54.8 μmol , 13.7%. ^1H NMR (400 MHz, $(\text{CD}_3)_2\text{SO}$) δ 9.50 (s, 1H), 8.73 (d, $J = 5.6$ Hz, 1H), 8.47 – 8.42 (m, 2H), 8.38 (d, $J = 7.2$ Hz, 1H), 7.86 (t, $J = 7.6$ Hz, 1H), 7.60 – 7.56 (m, 4H), 7.35 – 7.31 (m, 3H), 7.27 – 7.21 (m, 2H), 7.15 (t, $J = 7.6$ Hz, 1H), 6.99 (d, $J = 7.6$ Hz, 1H), 6.84 (d, $J = 15.6$ Hz, 1H), 6.35 – 6.28 (m, 1H), 3.79 (d, $J = 6.4$ Hz, 2H), 3.10 (t, $J = 5.2$ Hz, 2H), 3.04 (d, $J = 4.4$ Hz, 2H). ^{13}C NMR (101

MHz, (CD₃)₂SO) δ 153.47, 151.85, 148.52, 144.74, 136.52, 136.41, 134.78, 133.84, 133.79, 132.84, 130.50, 130.31, 129.74, 129.33, 128.74, 128.42, 127.13, 126.60, 126.46, 125.37, 125.13, 121.28, 120.43, 120.01, 117.49, 117.06, 48.34, 45.35, 38.66. HRMS: calculated for C₃₂H₂₇N₃O₃S₂ [M+H]⁺: 566.15666; found: 566.15645.

(E)-N-(2-((3-(4-(2,3-dihydrobenzofuran-5-yl)phenyl)allyl)amino)ethyl)isoquinoline-5-sulfonamide 100

Prepared according to the general procedure. Yield: 25.8 mg, 53.2 μ mol, 13.3%. ¹H NMR (400 MHz, CD₃OD) δ 9.49 (s, 1H), 8.67 (s, 2H), 8.55 (d, *J* = 7.2 Hz, 1H), 8.45 (d, *J* = 8.4 Hz, 1H), 7.87 (d, *J* = 8.0 Hz, 1H), 7.53 (d, *J* = 5.6 Hz, 2H), 7.47 (d, *J* = 8.8 Hz, 3H), 7.34 (dd, *J*₁ = 2.4 Hz, *J*₂ = 8.4 Hz, 1H), 6.85 (d, *J* = 15.6 Hz, 1H), 6.76 (d, *J* = 8.0 Hz, 1H), 6.31 – 6.23 (m, 1H), 4.55 (t, *J* = 8.8 Hz, 2H), 3.85 (d, *J* = 7.2 Hz, 2H), 3.22 (t, *J* = 8.4 Hz, 2H), 3.19 (s, 4H). ¹³C NMR (101 MHz, CD₃OD) δ 161.40, 153.30, 143.05, 142.69, 139.88, 136.00, 135.71, 135.64, 134.91, 134.28, 133.26, 129.35, 128.45, 128.38, 128.00, 127.78, 124.48, 120.06, 118.39, 110.30, 72.52, 50.59, 47.50, 40.11, 30.49. HRMS: calculated for C₂₈H₂₇N₃O₃S [M+H]⁺: 486.18459; found: 486.18437.

(E)-N-(2-((3-(4-(3,4-dihydro-2H-benzo[b][1,4]dioxepin-7-yl)phenyl)allyl)amino)ethyl)isoquinoline-5-sulfonamide 101

Prepared according to the general procedure. Yield: 30.1 mg, 58.4 μ mol, 14.6%. ¹H NMR (400 MHz, CD₃OD) δ 9.51 (s, 1H), 8.67 (t, *J* = 6.0 Hz, 2H), 8.56 (dd, *J*₁ = 1.2 Hz, *J*₂ = 7.6 Hz, 1H), 8.46 (d, *J* = 8.4 Hz, 1H), 7.88 (t, *J* = 7.6 Hz, 1H), 7.54 (d, *J* = 8.0 Hz, 2H), 7.48 (d, *J* = 8.0 Hz, 2H), 7.21 – 7.17 (m, 2H), 6.99 (d, *J* = 8.4 Hz, 1H), 6.85 (d, *J* = 15.6 Hz, 1H), 6.32 – 6.25 (m, 1H), 4.17 (q, *J* = 5.2 Hz, 4H), 3.85 (d, *J* = 7.2 Hz, 2H), 3.19 (s, 4H), 2.19 – 2.13 (m, 2H). ¹³C NMR (101 MHz, CD₃OD) δ 153.09, 152.96, 152.52, 142.23, 140.82, 139.71, 136.95, 136.20, 135.79, 135.69, 135.52, 133.39, 130.52, 128.60, 128.42, 127.89, 127.77, 123.11, 122.74, 120.88, 120.27, 118.82, 71.98, 71.95, 50.54, 47.52, 40.11, 33.20. HRMS: calculated for C₂₉H₂₉N₃O₄S [M+H]⁺: 516.19515; found: 516.19496.

(E)-N-(2-((3-(4'-morpholino-[1,1'-biphenyl]-4-yl)allyl)amino)ethyl)isoquinoline-5-sulfonamide 102

Prepared according to the general procedure. Yield: 34.9 mg, 66.0 μ mol, 16.5%. ¹H NMR (400 MHz, CD₃OD) δ 9.65 (s, 1H), 8.82 (d, *J* = 6.4 Hz, 1H), 8.72 (br s, 1H), 8.64 (d, *J* = 7.6 Hz, 1H), 8.56 (d, *J* = 8.4 Hz, 1H), 7.96 (t, *J* = 8.0 Hz, 1H), 7.61 (dd, *J*₁ = 2.4 Hz, *J*₂ = 9.2 Hz, 4H), 7.52 (d, *J* = 8.0 Hz, 2H), 7.16 (d, *J* = 8.8 Hz, 2H), 6.88 (d, *J* = 15.6 Hz, 1H), 6.33 – 6.26 (m, 1H), 3.90 – 3.85 (m, 6H), 3.28 (t, *J* = 4.8 Hz, 4H), 3.21 (s, 4H). ¹³C NMR (101 MHz, CD₃OD) δ 152.33, 150.64, 142.25, 140.47, 139.87, 137.01, 136.16, 136.05, 135.26, 134.65, 134.01, 130.51, 129.23, 128.67, 128.48, 127.66, 121.13, 118.59, 118.00, 67.50, 51.39, 50.61, 47.55, 40.17. HRMS: calculated for C₃₀H₃₂N₄O₃S [M+H]⁺: 529.22679; found: 529.22648.

(E)-N-(2-((3-(4''-ethoxy-[1,1':4',1''-terphenyl]-4-yl)allyl)amino)ethyl)isoquinoline-5-sulfonamide 103

Prepared according to the general procedure. Yield: 16.5 mg, 29.2 μ mol, 7.3%. ¹H NMR (400 MHz, (CD₃)₂OD) δ 9.51 (s, 1H), 8.73 (d, *J* = 6.0 Hz, 1H), 8.73 (d, *J* = 7.6 Hz, 1H), 8.43 (d, *J* = 6.4 Hz, 1H), 8.38 (d, *J* = 7.6 Hz, 1H), 7.87 (t, *J* = 7.6 Hz, 1H), 7.78 – 7.69 (m, 6H), 7.65 (d, *J* = 8.4 Hz, 2H), 7.55 (d, *J* = 8.4 Hz, 2H), 7.03 (d, *J* = 8.4 Hz, 2H), 6.82 (d, *J* = 16.0 Hz, 1H), 6.32 – 6.24 (m, 1H), 4.07 (q, *J* = 7.2 Hz, 2H), 3.77 (br s, 2H), 3.08 (t, *J* = 5.6 Hz, 2H), 3.03 (s, 2H), 1.35 (t, *J* = 6.8 Hz, 3H). ¹³C NMR (101 MHz, (CD₃)₂OD) δ 158.33, 153.43, 144.64, 139.62, 139.09, 137.54, 136.49, 134.51, 133.88, 133.77, 132.88, 131.66, 130.33, 128.73, 127.65, 127.25, 126.97, 126.63, 126.50, 119.59, 117.07,

114.91, 63.12, 48.40, 45.39, 38.67, 14.67. HRMS: calculated for $C_{34}H_{33}N_3O_3S$ $[M+H]^+$: 564.23154; found: 564.23129.

(E)-N-(2-((3-(3'-(benzyloxy)-[1,1'-biphenyl]-4-yl)allyl)amino)ethyl)isoquinoline-5-sulfonamide 104

Prepared according to the general procedure. Yield: 15.8 mg, 28.8 μ mol, 7.2%. 1H NMR (400 MHz, CD_3OD) δ 9.44 (s, 1H), 8.65 (br s, 1H), 8.59 (d, $J = 6.0$ Hz, 1H), 8.51 (dd, $J_1 = 1.2$ Hz, $J_2 = 7.6$ Hz, 1H), 8.43 (d, $J = 8.4$ Hz, 1H), 7.84 (t, $J = 8.0$ Hz, 1H), 7.61 (d, $J = 8.4$ Hz, 2H), 7.53 (d, $J = 8.4$ Hz, 2H), 7.46 (d, $J = 7.2$ Hz, 2H), 7.39 – 7.32 (m, 4H), 7.23 – 7.20 (m, 2H), 6.99 (dd, $J_1 = 1.2$ Hz, $J_2 = 7.6$ Hz, 1H), 6.89 (d, $J = 16.0$ Hz, 1H), 6.35 – 6.27 (m, 1H), 5.14 (s, 2H), 3.86 (d, $J = 7.2$ Hz, 2H), 3.18 (s, 4H). ^{13}C NMR (101 MHz, CD_3OD) δ 160.72, 154.10, 144.38, 143.06, 142.74, 139.78, 138.72, 135.94, 135.47, 135.29, 132.80, 131.00, 129.52, 128.90, 128.60, 128.44, 128.37, 127.95, 120.56, 119.32, 118.99, 115.09, 114.62, 71.09, 50.56, 47.57, 40.12. HRMS: calculated for $C_{33}H_{31}N_3O_3S$ $[M+H]^+$: 550.21589; found: 550.21560.

(E)-N-(2-((3-(4-(pyridin-3-yl)phenyl)allyl)amino)ethyl)isoquinoline-5-sulfonamide 105

Prepared according to the general procedure. Yield: 12.8 mg, 28.8 μ mol, 7.2%. 1H NMR (400 MHz, CD_3OD) δ 9.57 (s, 1H), 9.14 (s, 1H), 8.77 (d, $J = 8.4$ Hz, 2H), 8.73 – 8.68 (m, 2H), 8.60 (d, $J = 7.2$ Hz, 1H), 8.53 (d, $J = 8.4$ Hz, 1H), 8.05 (t, $J = 6.4$ Hz, 1H), 7.93 (t, $J = 7.6$ Hz, 1H), 7.83 (d, $J = 8.4$ Hz, 2H), 7.69 (d, $J = 8.4$ Hz, 2H), 6.95 (d, $J = 15.6$ Hz, 1H), 6.47 – 6.39 (m, 1H), 3.90 (d, $J = 7.2$ Hz, 2H), 3.21 (s, 4H). ^{13}C NMR (101 MHz, CD_3OD) δ 153.15, 143.40, 142.89, 142.48, 142.25, 138.86, 135.46, 136.25, 135.92, 135.87, 135.78, 133.50, 129.11, 128.86, 128.67, 128.10, 121.06, 120.34, 50.41, 47.73, 40.16. HRMS: calculated for $C_{25}H_{24}N_4O_2S$ $[M+H]^+$: 445.16927; found: 445.16925.

(E)-N-(2-((3-(4-(pyridin-4-yl)phenyl)allyl)amino)ethyl)isoquinoline-5-sulfonamide 106

Prepared according to the general procedure. Yield: 28.8 mg, 64.8 μ mol, 16.2%. 1H NMR (400 MHz, CD_3OD) δ 9.46 (s, 1H), 8.81 (s, 2H), 8.66 (s, 1H), 8.61 (d, $J = 6.0$ Hz, 1H), 8.53 (dd, $J_1 = 1.2$ Hz, $J_2 = 7.2$ Hz, 1H), 8.45 (d, $J = 8.0$ Hz, 1H), 8.29 (d, $J = 6.4$ Hz, 2H), 7.97 (d, $J = 8.4$ Hz, 2H), 7.87 (t, $J = 7.6$ Hz, 1H), 7.72 (d, $J = 8.4$ Hz, 2H), 6.96 (d, $J = 16.0$ Hz, 1H), 6.52 – 6.44 (m, 1H), 3.91 (d, $J = 7.2$ Hz, 2H), 3.23 – 3.18 (m, 4H). ^{13}C NMR (101 MHz, CD_3OD) δ 156.88, 153.92, 144.39, 144.00, 140.17, 138.54, 136.34, 135.53, 135.49, 132.91, 129.44, 127.14, 124.90, 122.05, 119.52, 50.32, 47.74, 40.12. HRMS: calculated for $C_{25}H_{24}N_4O_2S$ $[M+H]^+$: 445.16927; found: 445.16901.

(E)-N-(2-((3-(4-(6-methoxypyridin-3-yl)phenyl)allyl)amino)ethyl)isoquinoline-5-sulfonamide 107

Prepared according to the general procedure. Yield: 28.7 mg, 60.4 μ mol, 15.1%. 1H NMR (400 MHz, CD_3OD) δ 9.56 (s, 1H), 8.73 – 8.68 (m, 2H), 8.59 (dd, $J_1 = 1.2$ Hz, $J_2 = 7.6$ Hz, 1H), 8.52 (d, $J = 8.0$ Hz, 1H), 8.40 (d, $J = 2.4$ Hz, 1H), 7.99 (dd, $J_1 = 2.8$ Hz, $J_2 = 8.8$ Hz, 1H), 7.93 (t, $J = 8.0$ Hz, 1H), 7.62 (d, $J = 8.4$ Hz, 2H), 7.57 (d, $J = 8.0$ Hz, 2H), 6.93 (s, 1H), 6.89 (d, $J = 8.8$ Hz, 1H), 6.37 – 6.29 (m, 1H), 3.96 (s, 3H), 3.87 (d, $J = 7.2$ Hz, 2H), 3.20 (s, 4H). ^{13}C NMR (101 MHz, CD_3OD) δ 165.17, 153.08, 145.41, 142.09, 139.59, 139.19, 139.15, 136.33, 136.04, 135.88, 135.77, 133.51, 130.86, 130.64, 128.68, 127.76, 120.36, 119.25, 111.78, 54.40, 50.54, 47.59, 40.14. HRMS: calculated for $C_{26}H_{26}N_4O_3S$ $[M+H]^+$: 475.17984; found: 475.17958.

(E)-N-(2-((3-(4-(2-fluoropyridin-4-yl)phenyl)allyl)amino)ethyl)isoquinoline-5-sulfonamide 108

Prepared according to the general procedure. Yield: 25.5 mg, 55.2 μmol , 13.8%. ^1H NMR (400 MHz, CD_3OD) δ 9.49 (s, 1H), 8.67 (br s, 1H), 8.62 (d, $J = 5.6$, 1H), 8.54 (dd, $J_1 = 0.8$ Hz, $J_2 = 7.6$ Hz, 1H), 8.47 (d, $J = 8.0$ Hz, 1H), 8.25 (d, $J = 5.2$, 1H), 7.88 (t, $J = 7.6$ Hz, 1H), 7.80 (d, $J = 8.0$ Hz, 2H), 7.65 – 7.62 (m, 3H), 7.39 (s, 1H), 6.94 (d, $J = 16.0$ Hz, 1H), 6.44 – 6.37 (m, 1H), 3.89 (d, $J = 7.2$ Hz, 2H), 3.22 – 3.16 (m, 4H). ^{13}C NMR (101 MHz, CD_3OD) δ 167.15, 164.79, 155.21, 155.13, 153.86, 149.01, 148.87, 143.84, 139.06, 138.46, 135.15, 135.58, 135.49, 132.96, 128.84, 128.65, 128.15, 120.66, 120.62, 107.97, 107.59, 50.41, 47.68, 40.12. HRMS: calculated for $\text{C}_{25}\text{H}_{23}\text{FN}_4\text{O}_2\text{S}$ $[\text{M}+\text{H}]^+$: 463.15985; found: 463.15927.

(E)-N-(2-((3-(4-(pyrimidin-5-yl)phenyl)allyl)amino)ethyl)isoquinoline-5-sulfonamide 109

Prepared according to the general procedure. Yield: 37.6 mg, 84.4 μmol , 21.1%. ^1H NMR (400 MHz, CD_3OD) δ 9.54 (s, 1H), 9.14 (s, 1H), 9.09 (s, 2H), 8.69 (s, 2H), 8.58 (dd, $J_1 = 1.2$ Hz, $J_2 = 7.2$ Hz, 1H), 8.51 (d, $J = 8.0$ Hz, 1H), 7.92 (t, $J = 8.0$ Hz, 1H), 7.76 (d, $J = 8.4$ Hz, 2H), 7.66 (d, $J = 8.4$ Hz, 2H), 6.94 (d, $J = 16.0$ Hz, 1H), 6.44 – 6.36 (m, 1H), 3.89 (d, $J = 7.2$ Hz, 2H), 3.24 – 3.18 (m, 4H). ^{13}C NMR (101 MHz, CD_3OD) δ 158.02, 155.98, 153.31, 142.59, 139.12, 135.75, 136.11, 135.80, 135.68, 135.49, 135.34, 133.36, 129.00, 128.55, 128.51, 120.48, 120.13, 50.43, 47.68, 40.14. HRMS: calculated for $\text{C}_{24}\text{H}_{23}\text{N}_5\text{O}_2\text{S}$ $[\text{M}+\text{H}]^+$: 446.16452; found: 446.16479.

(E)-N-(2-((3-(4-(2-methoxypyrimidin-5-yl)phenyl)allyl)amino)ethyl)isoquinoline-5-sulfonamide 110

Prepared according to the general procedure. Yield: 35.2 mg, 74.0 μmol , 18.5%. ^1H NMR (400 MHz, CD_3OD) δ 9.56 (s, 1H), 8.85 (s, 2H), 8.70 (s, 2H), 8.58 (dd, $J_1 = 1.2$ Hz, $J_2 = 7.2$ Hz, 1H), 8.51 (d, $J = 8.0$ Hz, 1H), 7.92 (d, $J = 8.0$ Hz, 1H), 7.67 (d, $J = 8.4$ Hz, 2H), 7.61 (d, $J = 8.4$ Hz, 2H), 6.92 (d, $J = 15.6$ Hz, 1H), 6.40 – 6.33 (m, 1H), 4.06 (s, 3H), 3.88 (d, $J = 7.6$ Hz, 2H), 3.20 (s, 4H). ^{13}C NMR (101 MHz, CD_3OD) δ 166.21, 158.53, 158.48, 153.31, 142.60, 139.35, 136.84, 136.10, 135.81, 135.71, 133.35, 129.09, 128.89, 128.56, 127.91, 119.86, 55.69, 50.48, 47.65, 40.15. HRMS: calculated for $\text{C}_{25}\text{H}_{25}\text{N}_5\text{O}_3\text{S}$ $[\text{M}+\text{H}]^+$: 476.17509; found: 476.17537.

(E)-N-(2-((3-(4-(2-morpholinopyridin-3-yl)phenyl)allyl)amino)ethyl)isoquinoline-5-sulfonamide 111

Prepared according to the general procedure. Yield: 26.7 mg, 50.4 μmol , 12.6%. ^1H NMR (400 MHz, CD_3OD) δ 9.58 (s, 1H), 8.71 (s, 2H), 8.59 (dd, $J_1 = 1.2$ Hz, $J_2 = 7.2$ Hz, 1H), 8.52 (d, $J = 8.4$ Hz, 1H), 8.16 (dd, $J_1 = 1.6$ Hz, $J_2 = 5.6$ Hz, 1H), 7.95 – 7.91 (m, 2H), 7.68 – 7.61 (m, 4H), 7.27 (dd, $J_1 = 6.0$ Hz, $J_2 = 7.6$ Hz, 1H), 6.93 (d, $J = 16.0$ Hz, 1H), 6.44 – 6.36 (m, 1H), 3.89 (d, $J = 7.2$ Hz, 2H), 3.64 (t, $J = 4.4$ Hz, 4H), 3.23 – 3.18 (m, 8H). ^{13}C NMR (101 MHz, CD_3OD) δ 157.16, 153.30, 146.03, 142.57, 141.13, 139.11, 137.39, 136.12, 135.82, 135.71, 130.74, 129.51, 128.88, 128.57, 120.44, 118.43, 66.95, 50.43, 50.33, 47.71, 40.15. HRMS: calculated for $\text{C}_{29}\text{H}_{31}\text{N}_5\text{O}_3\text{S}$ $[\text{M}+\text{H}]^+$: 530.22204; found: 530.22190.

(E)-N-(2-((3-(4-(isoquinolin-3-yl)phenyl)allyl)amino)ethyl)isoquinoline-5-sulfonamide 112

Prepared according to the general procedure. Yield: 41.9 mg, 84.8 μmol , 21.2%. ^1H NMR (400 MHz, CD_3OD) δ 9.66 (s, 1H), 9.56 (d, $J = 2.4$ Hz, 1H), 9.25 (d, $J = 2.0$ Hz, 1H), 8.82 (d, $J = 6.0$ Hz, 1H), 8.78 (br s, 1H), 8.65 (dd, $J_1 = 1.2$ Hz, $J_2 = 7.6$ Hz, 1H), 8.57 (d, $J = 8.4$ Hz, 1H), 8.31 (d, $J = 8.0$ Hz, 1H), 8.24 (d, $J = 8.4$ Hz, 1H), 8.08 (td, $J_1 = 1.2$ Hz, $J_2 = 6.8$ Hz, 1H), 7.98 (t, $J = 7.6$ Hz, 1H), 7.94 – 7.90 (m, 2H), 7.70 (d, $J = 8.4$ Hz, 2H), 6.95 (d, $J = 16.0$ Hz, 1H), 6.48 –

6.40 (m, 1H), 3.91 (d, $J = 7.2$ Hz, 2H), 3.23 (s, 4H). ^{13}C NMR (101 MHz, CD_3OD) δ 152.28, 146.20, 142.24, 140.56, 140.36, 138.92, 138.06, 137.09, 136.27, 136.18, 136.01, 135.39, 134.93, 134.01, 130.89, 130.50, 130.40, 129.26, 129.12, 128.91, 128.79, 123.25, 121.23, 120.87, 50.43, 47.69, 40.16. HRMS: calculated for $\text{C}_{29}\text{H}_{26}\text{N}_4\text{O}_2\text{S}$ $[\text{M}+\text{H}]^+$: 495.18492; found: 495.18465.

(E)-N-(2-((3-(4-(6-fluoropyridin-3-yl)phenyl)allyl)amino)ethyl)isoquinoline-5-sulfonamide 113

Prepared according to the general procedure. Yield: 38.7 mg, 83.6 μmol , 20.9%. ^1H NMR (400 MHz, CD_3OD) δ 9.67 (s, 1H), 8.84 (d, $J = 6.4$ Hz, 1H), 8.72 (br s, 1H), 8.65 (dd, $J_1 = 1.2$ Hz, $J_2 = 7.6$ Hz, 1H), 8.57 (d, $J = 8.4$ Hz, 1H), 8.43 (d, $J = 2.8$ Hz, 1H), 7.16 (td, $J_1 = 2.4$ Hz, $J_2 = 7.6$ Hz, 1H), 7.98 (t, $J = 7.6$ Hz, 1H), 7.63 (d, $J = 8.4$ Hz, 2H), 7.58 (d, $J = 8.4$ Hz, 2H), 7.14 (dd, $J_1 = 2.4$ Hz, $J_2 = 8.4$ Hz, 1H), 6.90 (d, $J = 16.0$ Hz, 1H), 6.40 – 6.32 (m, 1H), 3.88 (d, $J = 7.2$ Hz, 2H), 3.23 (s, 4H). ^{13}C NMR (101 MHz, CD_3OD) δ 165.70, 163.33, 152.06, 146.39, 146.24, 141.58, 141.50, 139.88, 139.27, 137.99, 137.28, 136.81, 136.24, 136.06, 135.71, 135.67, 134.15, 130.43, 129.39, 128.76, 128.35, 121.37, 119.89, 110.92, 110.55, 50.48, 47.61, 40.15. HRMS: calculated for $\text{C}_{25}\text{H}_{23}\text{FN}_4\text{O}_2\text{S}$ $[\text{M}+\text{H}]^+$: 463.15985; found: 463.15904.

(E)-N-(2-((3-(4-(1-methyl-1H-indazol-6-yl)phenyl)allyl)amino)ethyl)isoquinoline-5-sulfonamide 114

Prepared according to the general procedure. Yield: 141.4 mg, 284.4 μmol , 71.1%. ^1H NMR (400 MHz, CD_3OD) δ 9.49 (s, 1H), 8.74 (d, $J = 6.8$ Hz, 1H), 8.61 (d, $J = 6.4$ Hz, 1H), 8.55 (dd, $J_1 = 1.2$ Hz, $J_2 = 7.2$ Hz, 1H), 8.39 (d, $J = 8.0$ Hz, 1H), 7.89 (s, 1H), 7.82 (t, $J = 8.0$ Hz, 1H), 7.65 (d, $J = 8.4$ Hz, 1H), 7.56 (s, 1H), 7.54 (s, 2H), 7.42 (d, $J = 8.0$ Hz, 2H), 7.29 (dd, $J_1 = 1.2$ Hz, $J_2 = 8.4$ Hz, 1H), 6.80 (d, $J = 16.0$ Hz, 1H), 6.33 – 6.25 (m, 1H), 3.97 (s, 3H), 3.84 (d, $J = 7.2$ Hz, 2H), 3.23 (s, 4H). ^{13}C NMR (101 MHz, CD_3OD) δ 152.10, 142.44, 141.65, 140.46, 140.13, 139.41, 136.79, 136.10, 135.92, 135.88, 135.72, 133.68, 133.48, 130.17, 128.96, 128.62, 128.37, 124.31, 122.36, 121.49, 120.89, 119.19, 107.91, 50.51, 47.52, 40.09, 15.54. HRMS: calculated for $\text{C}_{28}\text{H}_{27}\text{N}_5\text{O}_2\text{S}$ $[\text{M}+\text{H}]^+$: 498.19582; found: 498.19516.

(E)-N-(2-((3-([1,1':3',1''-terphenyl]-4-yl)allyl)amino)ethyl)isoquinoline-5-sulfonamide 115

Prepared according to the general procedure. Yield: 91.3 mg, 175.6 μmol , 43.9%. ^1H NMR (400 MHz, CD_3OD) δ 9.42 (s, 1H), 8.62 (s, 2H), 8.50 (dd, $J_1 = 0.8$ Hz, $J_2 = 7.6$ Hz, 1H), 8.39 (d, $J = 8.0$ Hz, 1H), 7.83 – 7.78 (m, 2H), 7.63 (t, $J = 7.6$ Hz, 4H), 7.57 – 7.53 (m, 3H), 7.51 – 7.47 (m, 2H), 7.45 – 7.41 (m, 2H), 7.33 (t, $J = 7.2$ Hz, 1H), 6.86 (d, $J = 16.0$ Hz, 1H), 6.34 – 6.26 (m, 1H), 3.84 (d, $J = 6.8$ Hz, 2H), 3.18 (s, 4H). ^{13}C NMR (101 MHz, CD_3OD) δ 153.65, 143.54, 143.12, 142.69, 142.23, 142.12, 139.65, 135.92, 135.58, 135.52, 135.48, 132.97, 130.53, 130.45, 129.89, 128.50, 128.40, 128.29, 128.14, 128.09, 127.32, 126.83, 126.54, 126.46, 119.65, 119.06, 50.52, 47.53, 40.09. HRMS: calculated for $\text{C}_{32}\text{H}_{29}\text{N}_3\text{O}_2\text{S}$ $[\text{M}+\text{H}]^+$: 520.20532; found: 520.20502.

(E)-N-(2-((3-(4-(1H-pyrazol-4-yl)phenyl)allyl)amino)ethyl)isoquinoline-5-sulfonamide 116

Prepared according to the general procedure. Yield: 59.7 mg, 137.6 μmol , 34.4%. ^1H NMR (400 MHz, CD_3OD) δ 9.66 (s, 1H), 8.87 (d, $J = 6.8$ Hz, 1H), 8.69 (d, $J = 6.4$ Hz, 1H), 8.65 (d, $J = 7.2$ Hz, 1H), 8.55 (d, $J = 8.4$ Hz, 1H), 8.00 (s, 2H), 7.96 (t, $J = 8.0$ Hz, 1H), 7.54 (d, $J = 8.0$ Hz, 2H), 7.42 (d, $J = 8.0$ Hz, 2H), 6.81 (d, $J = 15.6$ Hz, 1H), 6.29 – 6.21 (m, 1H), 3.84 (d, $J = 7.2$ Hz, 2H), 3.23 – 3.21 (m, 4H). ^{13}C NMR (101 MHz, CD_3OD) δ 151.69, 139.79, 139.34,

137.48, 136.30, 136.10, 134.85, 134.36, 132.18, 130.46, 130.30, 129.52, 128.50, 127.72, 126.73, 123.15, 121.59, 118.30, 50.59, 46.20, 40.14. HRMS: calculated for $C_{23}H_{23}N_5O_2S$ $[M+H]^+$: 434.16452; found: 434.16436.

(E)-N-(2-((3-(4-(thiophen-2-yl)phenyl)allyl)amino)ethyl)isoquinoline-5-sulfonamide 117

Prepared according to the general procedure. Yield: 11.9 mg, 26.4 μ mol, 6.6%. 1H NMR (400 MHz, CD_3OD) δ 9.49 (s, 1H), 8.68 (d, J = 6.0 Hz, 1H), 8.63 (d, J = 6.0 Hz, 1H), 8.54 (dd, J_1 = 1.2 Hz, J_2 = 7.2 Hz, 1H), 8.48 (d, J = 8.0 Hz, 1H), 7.88 (t, J = 7.6 Hz, 1H), 7.66 (dd, J_1 = 2.0 Hz, J_2 = 6.4 Hz, 2H), 7.50 (d, J = 8.0 Hz, 2H), 7.44 – 7.37 (m, 2H), 7.11 (dd, J_1 = 4.0 Hz, J_2 = 5.2 Hz, 1H), 6.88 (d, J = 16.0 Hz, 1H), 6.34 – 6.26 (m, 1H), 3.86 (d, J = 7.2 Hz, 2H), 3.21 – 3.17 (m, 4H). ^{13}C NMR (101 MHz, CD_3OD) δ 153.87, 143.85, 139.68, 136.36, 135.85, 135.61, 135.57, 133.01, 129.30, 128.60, 128.16, 126.99, 126.38, 124.69, 119.58, 118.89, 50.57, 47.60, 40.15. HRMS: calculated for $C_{24}H_{23}N_5O_2S_2$ $[M+H]^+$: 450.13044; found: 450.13040.

(E)-N-(2-((3-(4-(benzo[b]thiophen-2-yl)phenyl)allyl)amino)ethyl)isoquinoline-5-sulfonamide 118

Prepared according to the general procedure. Yield: 81.3 mg, 162.8 μ mol, 40.7%. 1H NMR (400 MHz, CD_3OD) δ 9.51 (s, 1H), 8.73 (d, J = 6.0 Hz, 1H), 8.48 (s, 1H), 8.46 (d, J = 3.2 Hz, 1H), 8.40 (d, J = 7.2 Hz, 1H), 7.94 (d, J = 7.6 Hz, 1H), 7.88 – 7.83 (m, 2H), 7.78 (d, J = 8.4 Hz, 2H), 7.53 (d, J = 8.0 Hz, 2H), 7.40 – 7.32 (m, 2H), 6.80 (d, J = 16.0 Hz, 1H), 6.35 – 6.27 (m, 1H), 3.74 (s, 2H), 3.12 (t, J = 5.6 Hz, 2H), 3.06 (d, J = 5.2 Hz, 2H). ^{13}C NMR (101 MHz, CD_3OD) δ 153.32, 144.30, 142.75, 140.56, 138.75, 136.30, 135.66, 134.05, 133.97, 133.90, 133.59, 133.15, 130.58, 128.83, 127.50, 126.68, 126.49, 124.98, 124.93, 123.92, 122.53, 120.45, 120.28, 117.41, 48.44, 45.54, 38.76. HRMS: calculated for $C_{28}H_{25}N_3O_2S_2$ $[M+H]^+$: 500.14610; found: 500.14564.

(E)-N-(2-((3-(4-(1H-indol-2-yl)phenyl)allyl)amino)ethyl)isoquinoline-5-sulfonamide 119

Prepared according to the general procedure. Yield: 51.3 mg, 106.4 μ mol, 26.6%. 1H NMR (400 MHz, CD_3OD) δ 9.43 (s, 1H), 8.66 (d, J = 6.0 Hz, 1H), 8.62 (d, J = 6.4 Hz, 1H), 8.51 (dd, J_1 = 1.2 Hz, J_2 = 7.6 Hz, 1H), 8.38 (d, J = 8.0 Hz, 1H), 7.81 (d, J = 7.6 Hz, 1H), 7.73 (d, J = 8.4 Hz, 2H), 7.50 (d, J = 8.0 Hz, 1H), 7.46 (d, J = 6.4 Hz, 2H), 7.37 (d, J = 8.0 Hz, 1H), 7.08 (t, J = 8.0 Hz, 1H), 6.98 (t, J = 8.0 Hz, 1H), 6.79 (d, J = 16.0 Hz, 1H), 6.28 – 6.21 (m, 1H), 3.78 (d, J = 6.8 Hz, 2H), 3.15 (s, 4H). ^{13}C NMR (101 MHz, CD_3OD) δ 153.05, 142.27, 139.63, 138.95, 138.44, 136.07, 135.70, 135.58, 134.44, 133.28, 130.42, 128.46, 126.26, 123.04, 121.27, 120.64, 120.14, 118.65, 112.16, 50.52, 47.48, 40.07. HRMS: calculated for $C_{28}H_{26}N_4O_2S$ $[M+H]^+$: 483.18492; found: 483.18492.

(E)-N-(2-((3-(4-(quinoxalin-6-yl)phenyl)allyl)amino)ethyl)isoquinoline-5-sulfonamide 120

Prepared according to the general procedure. Yield: 134.4 mg, 271.2 μ mol, 67.8%. 1H NMR (400 MHz, CD_3OD) δ 9.63 (s, 1H), 8.83 – 8.77 (m, 3H), 8.70 (d, J = 6.4 Hz, 1H), 8.63 (dd, J_1 = 1.2 Hz, J_2 = 7.2 Hz, 1H), 8.53 (d, J = 8.4 Hz, 1H), 8.17 (s, 1H), 8.05 (s, 2H), 7.96 (t, J = 8.0 Hz, 1H), 7.71 (d, J = 8.4 Hz, 2H), 7.53 (d, J = 8.4 Hz, 2H), 6.88 (d, J = 16.0 Hz, 1H), 6.40 – 6.32 (m, 1H), 3.89 (d, J = 7.2 Hz, 2H), 3.25 (s, 4H). ^{13}C NMR (101 MHz, CD_3OD) δ 151.90, 146.93, 146.27, 143.95, 143.34, 143.16, 140.45, 139.71, 139.24, 137.28, 136.93, 136.19, 136.00, 134.10, 130.67, 130.49, 130.30, 129.37, 127.73, 128.68, 127.06, 121.37, 119.97, 50.49, 47.62, 40.16. HRMS: calculated for $C_{28}H_{25}N_5O_2S$ $[M+H]^+$: 496.18017; found: 496.17969.

(E)-N-(2-((3-(4-(5-fluoro-1H-indol-2-yl)phenyl)allyl)amino)ethyl)isoquinoline-5-sulfonamide 121

Prepared according to the general procedure. Yield: 44.7 mg, 89.2 μ mol, 22.3%. ^1H NMR (400 MHz, CD_3OD) δ 9.44 (s, 1H), 8.66 (s, 1H), 8.59 (d, $J = 4.0$ Hz, 1H), 8.52 (d, $J = 4.8$ Hz, 1H), 8.43 (d, $J = 5.2$ Hz, 1H), 7.85 (t, $J = 5.2$ Hz, 1H), 7.80 (d, $J = 5.6$ Hz, 2H), 7.54 (d, $J = 5.6$ Hz, 2H), 7.34 (dd, $J_1 = 3.2$ Hz, $J_2 = 6.0$ Hz, 1H), 7.19 (dd, $J_1 = 2.0$ Hz, $J_2 = 6.8$ Hz, 1H), 6.90 – 6.83 (m, 2H), 6.34 – 6.29 (m, 1H), 3.87 (d, $J = 4.8$ Hz, 2H), 3.20 – 3.16 (m, 4H). ^{13}C NMR (101 MHz, CD_3OD) δ 160.13, 158.59, 154.14, 144.45, 140.38, 139.74, 135.89, 135.62, 135.47, 135.43, 135.28, 134.35, 132.79, 130.73, 130.66, 128.54, 127.94, 126.48, 119.302, 118.89, 112.91, 112.84, 111.17, 111.00, 105.64, 105.48, 50.58, 47.58, 40.13. HRMS: calculated for $\text{C}_{28}\text{H}_{25}\text{FN}_4\text{O}_2\text{S}$ $[\text{M}+\text{H}]^+$: 501.17550; found: 501.17577.

(E)-N-(2-((3-(4-(2-(trifluoromethyl)pyridin-4-yl)phenyl)allyl)amino)ethyl)isoquinoline-5-sulfonamide 122

Prepared according to the general procedure. Yield: 53.3 mg, 104.0 μ mol, 26.0%. ^1H NMR (400 MHz, CD_3OD) δ 9.50 (s, 1H), 8.75 (d, $J = 3.2$ Hz, 1H), 8.68 (s, 1H), 8.64 (d, $J = 4.0$ Hz, 1H), 8.54 (d, $J = 4.8$ Hz, 1H), 8.48 (d, $J = 5.6$ Hz, 1H), 8.09 (s, 1H), 7.96 (d, $J = 3.2$ Hz, 1H), 7.89 (t, $J = 5.2$ Hz, 1H), 7.85 (d, $J = 5.6$ Hz, 2H), 7.67 (d, $J = 5.6$ Hz, 2H), 6.95 (d, $J = 10.4$ Hz, 1H), 6.44 – 6.39 (m, 1H), 3.89 (d, $J = 4.8$ Hz, 2H), 3.22 – 3.18 (m, 4H). ^{13}C NMR (101 MHz, CD_3OD) δ 153.77, 151.73, 151.22, 149.71 (q, $J = 23.23$ Hz), 143.63, 139.03, 138.60, 138.00, 135.63, 135.55, 133.05, 130.71, 128.97, 128.74, 128.22, 125.53, 123.10 (q, $J = 182.81$ Hz), 120.86, 119.70, 119.28, 118.24, 50.42, 47.71, 40.14. HRMS: calculated for $\text{C}_{26}\text{H}_{23}\text{F}_3\text{N}_4\text{O}_2\text{S}$ $[\text{M}+\text{H}]^+$: 513.15666; found: 513.15610.

(E)-N-(2-((3-(4-(imidazo[1,2-a]pyridin-7-yl)phenyl)allyl)amino)ethyl)isoquinoline-5-sulfonamide 123

Prepared according to the general procedure. Yield: 43.9 mg, 90.8 μ mol, 22.7%. ^1H NMR (400 MHz, CD_3OD) δ 9.51 (s, 1H), 9.14 (s, 1H), 8.68 (s, 1H), 8.65 (d, $J = 4.0$ Hz, 1H), 8.56 (dd, $J_1 = 0.8$ Hz, $J_2 = 5.2$ Hz, 1H), 8.48 (d, $J = 5.6$ Hz, 1H), 8.31 (dd, $J_1 = 1.2$ Hz, $J_2 = 6.0$ Hz, 1H), 8.08 (d, $J = 1.2$ Hz, 1H), 8.02 (d, $J = 6.4$ Hz, 1H), 7.90 (t, $J = 4.8$ Hz, 1H), 7.79 (d, $J = 5.6$ Hz, 2H), 7.68 (d, $J = 5.6$ Hz, 1H), 6.95 (d, $J = 10.4$ Hz, 1H), 6.44 – 6.39 (m, 1H), 3.89 (d, $J = 4.8$ Hz, 2H), 3.23 – 3.18 (m, 4H). ^{13}C NMR (101 MHz, CD_3OD) δ 153.62, 143.32, 140.69, 139.00, 137.81, 136.44, 135.79, 135.67, 135.60, 134.80, 133.15, 132.17, 130.67, 129.02, 128.73, 128.32, 127.41, 124.25, 120.63, 119.84, 117.12, 113.27, 50.43, 47.70, 40.14. HRMS: calculated for $\text{C}_{27}\text{H}_{25}\text{N}_5\text{O}_2\text{S}$ $[\text{M}+\text{H}]^+$: 484.18017; found: 484.17986.

References

- ¹ M. Jonsson, M. Engstrom and J.-I. Jonsson, *Biochem. and Biophys Res. Comm.*, 2004, **318**, 899.
- ² D. L. Stirewalt and J. P. Radich, *Nature Rev.*, 2003, **3**, 650.
- ³ D. G. Gilliland and J. D. Griffin, *Blood*, 2002, **100**, 1532.
- ⁴ M. Nakao, S. Yokota, T. Iwai, H. Kaneko, S. Horiike, K. Kashima, Y. Sonoda, T. Fujimoto and S. Misawa, *Leukemia*, 1996, **10**, 1911.
- ⁵ H. Kiyoi, M. Towatari, S. Yokota, M. Hamaguchi, R. Ohno, H. Saito and T. Naoe, *Leukemia*, 1998, **12**, 1333.
- ⁶ D. L. Stirewalt, K. J. Kopecky, S. Meshinchi, F. R. Appelbaum, M. L. Slovak, C. L. Willman and J. P. Radich, *Blood*, 2001, **97**, 3589.

- ⁷ S. Meshinchi, W. G. Woods, D. L. Stirewalt, D. A. Sweetser, J. D. Buckley, T. K. Tjoa, I. D. Bernstein and J. P. Radich, *Blood*, 2001, **97**, 89.
- ⁸ S. Horiike, S. Yokota, M. Nakao, T. Iwai, Y. Sasai, H. Kaneko, M. Taniwaki, K. Kashima, H. Fujii. T. Abe and S. Misawa, *Leukemia*, 1997, **11**, 1442.
- ⁹ S. Yokota, H. Kiyoi, M. Nakao, T. Iwai, S. Misawa, T. Okuda, Y. Sonoda, T. Abe, K. Kahsima, Y. Matsuo and T. Naoe, *Leukemia*, 1997, **11**, 1605.
- ¹⁰ C. Thiede, C. Steudel, B. Mohr, M. Schaich, U. Schakel, U. Platzbecker, M. Wermke, M. Bornhauser, M. Ritter, A. Neubauer, G. Ehninger and T. Illmer, *Blood*, 2002, **99**, 4326.
- ¹¹ Y. Yamamoto, H. Kiyoi, Y. Nakano, R. Suzuki, Y. Kidera, S. Miyawaki. N. Asou, K. Kuriyama, F. Yagasaki, C. Shimazaki, H. Akiyama, K. Saito, M. Nishimura, T. Motoji, K. Shinagawa, A. Takeshita, H. Saito, R. Ueda, R. Ohno and T. Naoe, *Blood*, 2001, **97**, 2434.
- ¹² K. W. Pratz and S. M. Luger, *Curr. Opin. Hematol.*, 2014, **21**, 72.
- ¹³ KINOMEScan[®], A division of DiscoverX, San Diego, United States.
- ¹⁴ P. Zandbergen, A. M. C. H. van den Nieuwendijk, J. Brussee, A. van der Gen and C. G. Kruse, *Tetrahedron*, 1992, **48**, 3977.

4

Biological evaluation of H-89-analogues: searching for selective AKT1 and FLT3 inhibitors

4.1 Introduction

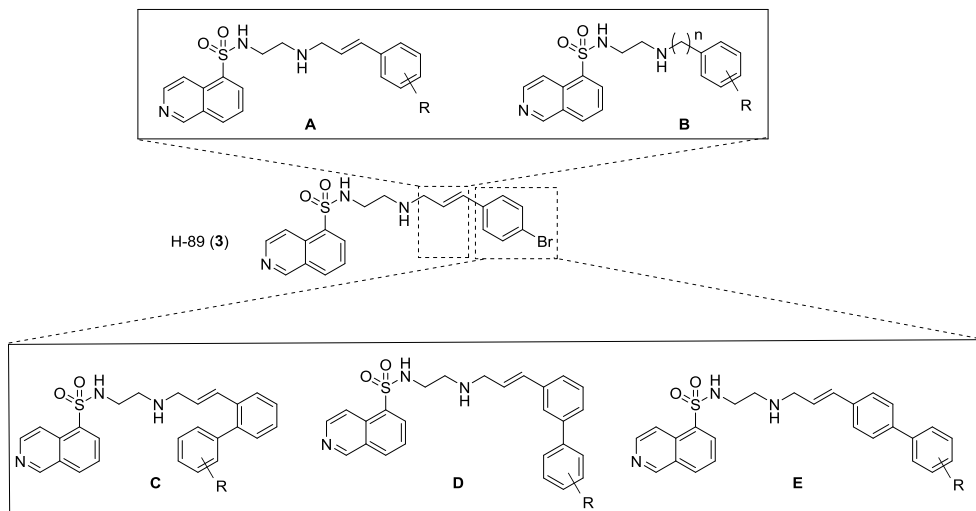
Protein kinase B (PKB/AKT) is an essential factor in the phosphatidylinositol-3-kinase (PI3K)-PKB signaling pathway. This pathway is altered in many human cancers, to include breast, colorectal, ovarian¹ and prostate cancers², and aberrant activation of the PI3K-PKB pathway promotes cell growth and survival, invasion, metastasis and angiogenesis in these tumors. PKB/AKT also plays an important role in diabetes³ and intracellular bacterial infections⁴, underscoring its relevance as a target for clinical drug development.

Most cells express three isoforms of PKB/AKT, namely, AKT1, AKT2 and AKT3.⁵ Genetic deletion of both AKT1 and AKT2 in mice is lethal, whereas elimination of only AKT1

appeared to have no detrimental effect on the development and health of the thus genetically modified mice.⁶ Given the importance of PKB/AKT activation in cancer and other diseases, several studies have been conducted in the past that aimed to develop active and selective PKB/AKT1 inhibitors.⁷ Kuijl *et al.*⁴ have, for instance, revealed that the isoquinoline derivative, H-89 (**3**), which was originally identified as an inhibitor of protein kinase A (PKA),⁸ inhibited AKT1 quite efficiently.⁹

Following the discovery that H-89 inhibits AKT1, a systematic library of H-89 analogues (**1** – **239**)¹⁰ was synthesized with the aim to identify inhibitors selective for AKT1 over both AKT2 and PKA. In this ligand-based drug discovery approach, focused libraries were assembled based on H-89 as a lead structure and by varying the linker in length and distal phenyl ring as well as by modifying the styrene moiety, while keeping the isoquinoline moiety intact (Figure 1). This isoquinoline moiety was kept intact, since co-crystallisation studies of isoquinoline sulfonamides (H-series) complexed with PKA, which shares a close sequence (\pm 68%) homology in the kinase domain and within the adenine binding site itself only three residues differ between AKT2 and PKA, revealed that a single hydrogen bond is formed between the heteroaromatic nitrogen of the isoquinoline and a backbone amide on the kinase hinge (Val123 in PKA), an interaction that is highly conserved in kinase-inhibitor recognition.^{11,12,13} With the aim to establish their selectivity, H-89 and selected members of the focused library that were found to be effective AKT1 inhibitors were tested in a commercial kinase-panel screen (Kinomescan)¹⁴, in which their inhibitory activity at 10 micromolar against 100+ kinases was assessed (see Chapter 2). One of these H-89 analogues that contains a bulky naphthalene group instead of a bromide, namely compound **195** proved to inhibit, next to AKT1, also FMS-like tyrosine kinase 3 (FLT3)¹⁵, which is an interesting drug target in its own right (see Chapter 3). FLT3 is a membrane-bound receptor tyrosine kinase expressed on hematopoietic cells. Upon binding to the FLT3 ligand, the activated receptor triggers both Ras/Raf and PI3K-PKB pathways resulting in cell proliferation and inhibition of apoptosis.^{16,17} FLT3 mutations have been found in acute lymphoblastic leukemia (ALL)¹⁸ and acute myeloid leukemia (AML)¹⁹ patients. FLT3 inhibitors are currently in clinical trials for the treatment of ALL and AML patients. Moreover, inhibitors that target at the same time both AKT1 and FLT3 may act in a synergistic fashion, since both AKT1 and FLT3 activate the PI3K-PKB pathway.

A)



B)

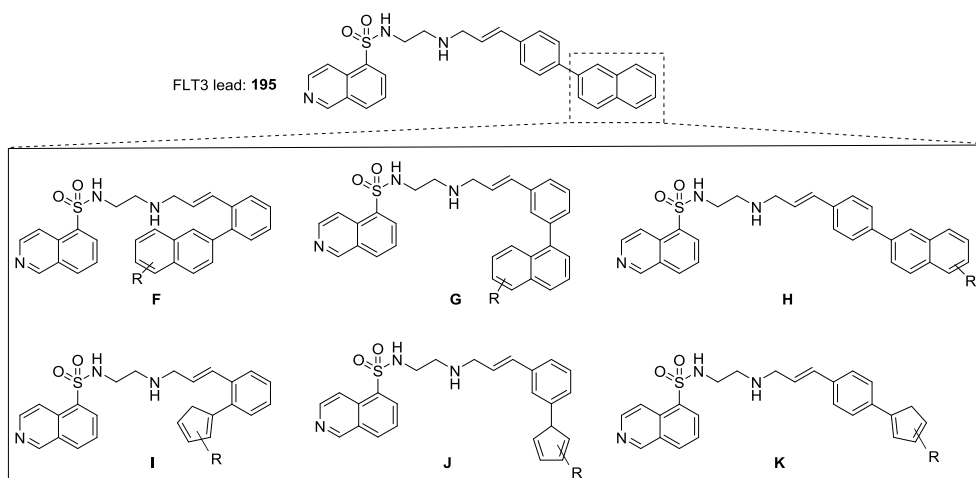


Figure 1. H-89-based libraries. A) H-89 (**3**) was modified by varying the linker length (**A**) or at the styrene moiety (**B – E**). B) FLT3 lead compound **195** was modified at the bulky naphthalene side (**F – H**) or it was displaced by thiophene or pyrrole containing moieties (**I – K**).

Based on the interest in AKT1 inhibitors, FLT3 inhibitors as well as the potential of dual active inhibitors targeting both kinases, a study was initiated in which focused libraries were synthesized based on lead structure **195**. Synthesis details on these compounds are given in the preceding chapter. This chapter describes the inhibitor activities towards PKA, AKT1, AKT2 and FLT3 of the full set of isoquinolinesulfonamide derivatives prepared over the years – both those whose synthesis was described previously and the set of

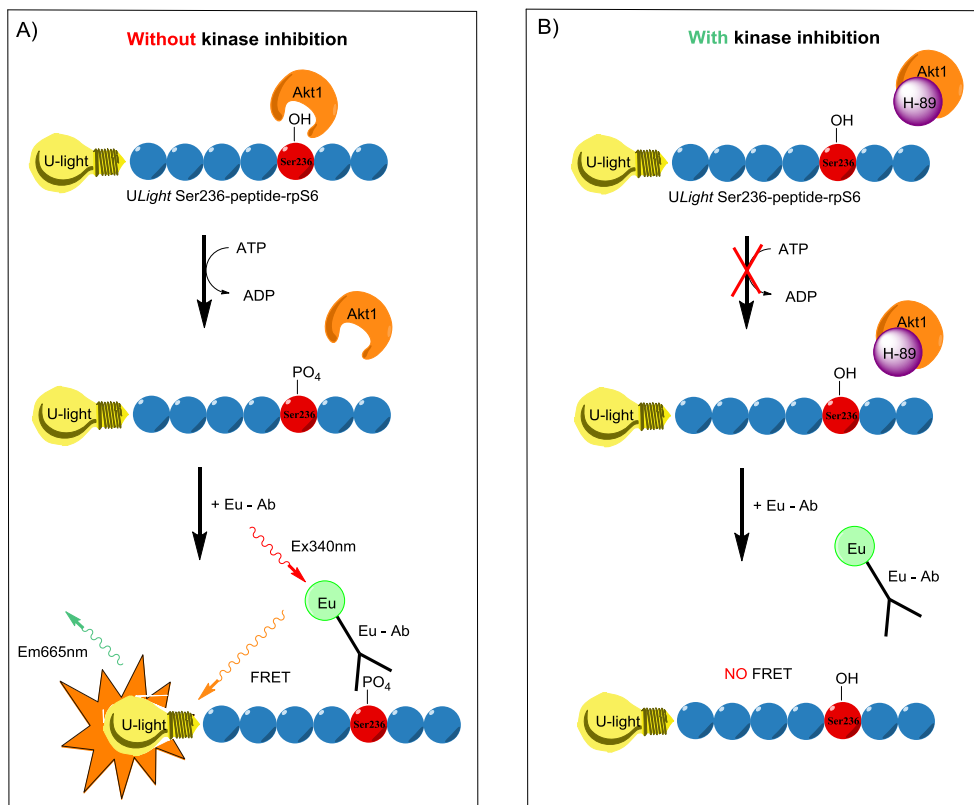


Figure 2. TR-FRET kinase assay. A) In presence of ATP, Ser/Thr kinase AKT1 phosphorylates the acceptor dye-labeled substrate, which is a ULight-labeled peptide containing residues surrounding Ser235 and Ser236 of human 40S ribosomal protein S6 (ULight Ser236 rpS6). The phosphorylated Ser236 will be bound by Eu-chelate donor dye containing rabbit monoclonal antibody. Upon irradiation at 320 nm, a FRET signal will be transferred from the Eu chelate to the ULight fluorophore, which, in turn, generates a light signal at 665 nm. B) In case of addition of an AKT1 inhibitor (e.g. H-89, **3**) to AKT1, phosphorylation of ULight-substrate is (partially) blocked, with (partial) abolishment of the FRET signal as the result.

compounds described in Chapter 2. The inhibitor activities are all determined using a time-resolved fluorescence resonance energy transfer (TR-FRET) kinase activity assay.²⁰

This assay is illustrated in Figure 2, in which AKT1 has been taken as the example kinase. A synthetic ULight-labeled peptide containing residues surrounding Ser235 and Ser236 of human 40S ribosomal protein S6 (ULight Ser236 rpS6) has been used as the acceptor-fluorophore substrate for the Ser/Thr kinases PKA, AKT1 and AKT2. By adding this substrate to a Ser/Thr kinase, the kinase recognizes and in turn phosphorylates amino acid Ser235 in the presence of ATP. Subsequently, the phosphorylated Ser235 will be recognized by the europium chelate donor dye

containing rabbit monoclonal antibody. The binding of this antibody to the *ULight*-labeled substrate brings donor and acceptor dyes into close proximity, which leads to energy transfer for the Eu donor to the *ULight* acceptor after irradiation of the kinase reaction at 320 nm. The generated light at 665 nm is measured and the intensity of the light emission is proportional to the level of *ULight*-substrate phosphorylation, which is a measure of kinase activity (Figure 2A).

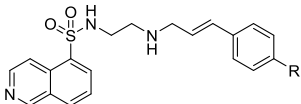
Figure 2B describes the situation wherein an inhibitor (for instance, H-89) is present. In this situation, AKT1 is not able to phosphorylate Ser236 of the *ULight*-containing peptide, which in turn will not be recognized by the Eu-containing antibody. As a result, no FRET signal will be generated. A similar assay was used to determine FLT3 inhibitory activities. However, in that case, a tyrosine containing *ULight* peptide (*ULight*-TK peptide) and an europium-labeled anti-phospho-tyrosine antibody were used instead.

4.2 Results and discussion

In total, the inhibitor activities of 239 isoquinolinesulfonamides were determined. All structures feature the same isoquinoline moiety (left hand part of the structure of the lead compound, H-89) and vary in the nature of the spacer (length, substitution, saturation) and/or the aryl moiety that makes up the right hand part of the molecules (*para*-bromobenzene in H-89). H-89 (**3** in Figure 1) and its 238 analogues were comparatively investigated with respect to their ability to inhibit the Ser/Thr kinases PKA, AKT1 and AKT2 and the Tyr kinase FLT3. In the first instance, relative inhibition percentages of the four kinases were measured at 2 μ M final concentrations of each compound. These numbers are given in Figures 3-11, in which the isoquinoline derivatives are grouped around common themes (linker substitutions, nature and regiochemistry of substituted phenyls, etc.). Following these studies, the most effective AKT1 inhibitors (both in terms of activity and selectivity) were selected and inhibition constants were determined. These numbers are given in Table 1 and the chapter will end with a structure-activity relationship evaluation of the data, with a projection on the use of the most promising compounds as either AKT1 inhibitors or FLT3 inhibitors. All inhibition data were obtained using a TR-FRET kinase activity assay.

Unsubstituted alkene series

The eight analogues of H-89 (**3**), in which the bromide group is substituted with other halogens, alkyl or phenolic groups, were evaluated and compared to **3** in the TR-FRET assay for inhibition of the four kinases PKA, AKT1, AKT2 and FLT3 (Figure 3).



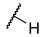
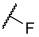
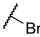
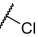
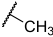
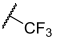
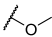
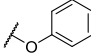
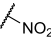
				
1 PKA 89 ± 1	2 PKA 81 ± 1	3 PKA 53 ± 1	4 PKA 68 ± 0	5 PKA 79 ± 1
Akt1 76 ± 5	Akt1 58 ± 1	Akt1 34 ± 1	Akt1 41 ± 1	Akt1 66 ± 1
Akt2 71 ± 9	Akt2 66 ± 7	Akt2 49 ± 8	Akt2 62 ± 3	Akt2 69 ± 5
FLT3 76 ± 5	FLT3 74 ± 6	FLT3 58 ± 4	FLT3 67 ± 4	FLT3 62 ± 5
				
6 PKA 73 ± 18	7 PKA 89 ± 1	8 PKA 94 ± 3	9 PKA 75 ± 2	
Akt1 57 ± 1	Akt1 82 ± 1	Akt1 76 ± 0	Akt1 31 ± 1	
Akt2 63 ± 5	Akt2 79 ± 1	Akt2 74 ± 3	Akt2 50 ± 4	
FLT3 100 ± 54	FLT3 91 ± 1	FLT3 23 ± 0	FLT3 54 ± 3	

Figure 3. Unsubstituted alkene. Relative remaining activity (%) towards PKA, PKB/AKT1, PKB/AKT2 and FLT3 in an *in vitro* kinase reaction in the absence or presence of 2 μ M compound. Relative remaining activity ranges from 0 – 25%, 25 – 50%, 50 – 75%, > 75% are in bold and underlined, bold, italics and normal, respectively. Results are normalized to the activity detected in the absence of any compound, containing DMSO only, from $n = 3$ experiments performed. Negative control: absence of ATP. Positive control: 2 μ M commercial H-89.

Based on the results of Figure 3, substitution of the bromide group with other halogens or other small groups does not improve the relative activity towards all the four different kinases when compared to H-89 (**3**).

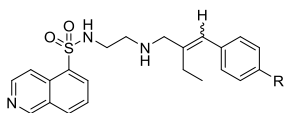
In fact and excepting compound **8** in all cases this substitution led to less potent inhibition. Compound **8** showed to be two times more active against FLT3 than compound **3** and it is slightly more active than its lead compound **195** (Figure 9).

Alkylated alkene series

The relative remaining enzymatic activity towards PKA, AKT1, AKT2 and FLT3 of a set of compounds with methyl (**10** – **24**), ethyl (**25** – **39**) or isopropyl (**40** – **55**) substitution at the double bond and with replacement of the bromide group were determined (Figure 4 – 6 respectively). In the synthesis of these compounds (see the preceding chapter) it was observed that *E/Z* stereoisomers with respect to the alkene configuration could not always be separated. Accordingly, where possible pure *E* and *Z* isomers were evaluated and otherwise *E/Z* mixtures were put to the test.

10 PKA <u>84 ± 2</u> Akt1 <u>70 ± 1</u> Akt2 <u>78 ± 2</u> FLT3 <u>79 ± 4</u>	11 PKA <u>93 ± 2</u> Akt1 <u>84 ± 1</u> Akt2 <u>80 ± 4</u> FLT3 <u>82 ± 3</u>	12 PKA <u>80 ± 3</u> Akt1 <u>54 ± 1</u> Akt2 <u>71 ± 8</u> FLT3 <u>75 ± 5</u>	13 PKA <u>90 ± 3</u> Akt1 <u>65 ± 0</u> Akt2 <u>79 ± 12</u> FLT3 <u>69 ± 3</u>	14 PKA <u>88 ± 2</u> Akt1 <u>62 ± 1</u> Akt2 <u>73 ± 5</u> FLT3 <u>73 ± 4</u>	15 PKA <u>64 ± 2</u> Akt1 <u>43 ± 1</u> Akt2 <u>62 ± 1</u> FLT3 <u>60 ± 7</u>
16 PKA <u>72 ± 2</u> Akt1 <u>48 ± 2</u> Akt2 <u>67 ± 3</u> FLT3 <u>74 ± 5</u>	17 PKA <u>84 ± 2</u> Akt1 <u>69 ± 1</u> Akt2 <u>78 ± 4</u> FLT3 <u>70 ± 5</u>	18 PKA <u>94 ± 3</u> Akt1 <u>79 ± 1</u> Akt2 <u>84 ± 1</u> FLT3 <u>71 ± 10</u>	19 PKA <u>93 ± 2</u> Akt1 <u>68 ± 3</u> Akt2 <u>80 ± 4</u> FLT3 <u>85 ± 5</u>	20 PKA <u>96 ± 3</u> Akt1 <u>66 ± 5</u> Akt2 <u>83 ± 2</u> FLT3 <u>77 ± 13</u>	21 PKA <u>89 ± 3</u> Akt1 <u>81 ± 3</u> Akt2 <u>86 ± 5</u> FLT3 <u>77 ± 6</u>
22 PKA <u>99 ± 1</u> Akt1 <u>82 ± 1</u> Akt2 <u>70 ± 26</u> FLT3 <u>40 ± 5</u>	23 PKA <u>79 ± 1</u> Akt1 <u>31 ± 1</u> Akt2 <u>53 ± 3</u> FLT3 <u>55 ± 3</u>	24 PKA <u>77 ± 2</u> Akt1 <u>28 ± 1</u> Akt2 <u>50 ± 4</u> FLT3 <u>65 ± 3</u>			

Figure 4. Methylated alkene. Relative remaining activity (%) towards PKA, PKB/AKT1, PKB/AKT2 and FLT3 in an *in vitro* kinase reaction in the absence or presence of 2 μ M compound. Relative remaining activity ranges from 0 – 25%, 25 – 50%, 50 – 75%, > 75% are in bold and underlined, bold, italics and normal, respectively. Results are normalized to the activity detected in the absence of any compound, containing DMSO only, from $n = 3$ experiments performed. Negative control: absence of ATP. Positive control: 2 μ M commercial H-89.



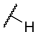
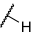
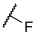
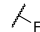
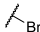
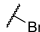
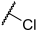
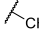
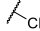
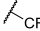
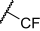
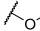
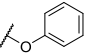
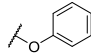
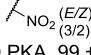
 (E)	 (E/Z) (1/5)	 (E)	 (E/Z) (1/5)	 (Z)	 (E/Z) (5/1)
25 PKA 89 ± 2 Akt1 69 ± 0 Akt2 81 ± 10 FLT3 76 ± 3	26 PKA 90 ± 5 Akt1 78 ± 0 Akt2 79 ± 3 FLT3 80 ± 2	27 PKA 84 ± 2 Akt1 57 ± 1 Akt2 75 ± 1 FLT3 75 ± 8	28 PKA 93 ± 3 Akt1 70 ± 2 Akt2 79 ± 5 FLT3 79 ± 11	29 PKA 84 ± 2 Akt1 <u>48 ± 2</u> Akt2 66 ± 4 FLT3 71 ± 4	30 PKA 82 ± 2 Akt1 <u>50 ± 0</u> Akt2 68 ± 4 FLT3 66 ± 4
 (E)	 (E)	 (E/Z) (1/2)	 (E)	 (Z)	 (E/Z) (5/1)
31 PKA 88 ± 4 Akt1 60 ± 0 Akt2 77 ± 1 FLT3 75 ± 5	32 PKA 88 ± 4 Akt1 69 ± 2 Akt2 78 ± 3 FLT3 71 ± 6	33 PKA 88 ± 1 Akt1 65 ± 1 Akt2 79 ± 3 FLT3 68 ± 8	34 PKA 89 ± 2 Akt1 64 ± 0 Akt2 74 ± 3 FLT3 72 ± 5	35 PKA 90 ± 2 Akt1 66 ± 0 Akt2 79 ± 5 FLT3 70 ± 4	36 PKA 90 ± 3 Akt1 75 ± 1 Akt2 83 ± 1 FLT3 67 ± 2
 (E)	 (Z)	 (E/Z) (3/2)			
37 PKA 100 ± 1 Akt1 83 ± 4 Akt2 92 ± 8 FLT3 <u>39 ± 1</u>	38 PKA 96 ± 2 Akt1 <u>30 ± 2</u> Akt2 58 ± 2 FLT3 <u>39 ± 8</u>	39 PKA 99 ± 5 Akt1 58 ± 2 Akt2 67 ± 9 FLT3 77 ± 8			

Figure 5. Ethylated alkene. Relative remaining activity (%) towards PKA, PKB/AKT1, PKB/AKT2 and FLT3 in an *in vitro* kinase reaction in the absence or presence of 2 μ M compound. Relative remaining activity ranges from 0 – 25%, 25 – 50%, 50 – 75%, > 75% are in bold and underlined, bold, italics and normal, respectively. Results are normalized to the activity detected in the absence of any compound, containing DMSO only, from $n = 3$ experiments performed. Negative control: absence of ATP. Positive control: 2 μ M commercial H-89.

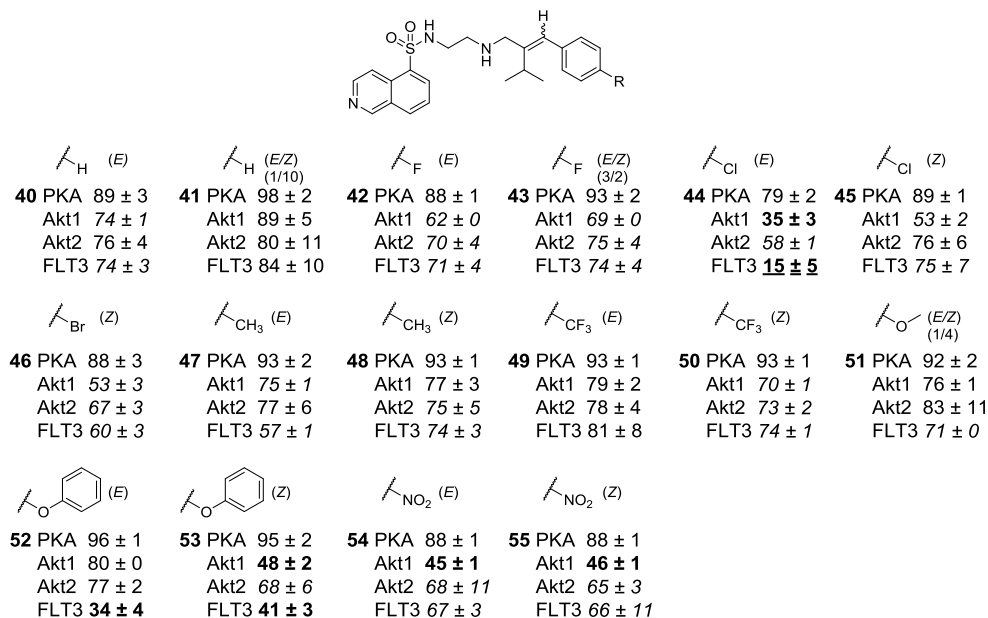
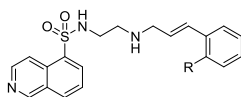


Figure 6. Isopropylated alkene. Relative remaining activity (%) towards PKA, PKB/AKT1, PKB/AKT2 and FLT3 in an *in vitro* kinase reaction in the absence or presence of 2 μ M compound. Relative remaining activity ranges from 0 – 25%, 25 – 50%, 50 – 75%, > 75% are in bold and underlined, bold, italics and normal, respectively. Results are normalized to the activity detected in the absence of any compound, containing DMSO only, from $n = 3$ experiments performed. Negative control: absence of ATP. Positive control: 2 μ M commercial H-89.

The results that are given in Figure 4 – 6 show that addition of an alkyl group to the double bond does not improve the inhibition potency towards PKA, AKT1, AKT2 or FLT3 remarkably. Also the influence of the *E* or *Z* confirmation appeared to be negligible. An exception can be made for compound **44**, which showed to be twice as active against FLT3 as its lead compound **195** and it is remarkable that the *E* compound is five times more active than its corresponding *Z* isomer.

Ortho/meta/para-phenyl sulphonamide series

To obtain more insight into the size and electronics of the pocket that accommodates the distal phenyl ring of H-89 (**3**), this aryl ring has been systematically modified by introducing various large substituents, including bulky aromatic and/or hetero-aromatic groups at the ortho (**56 – 112**), meta (**113 – 169**) and para position (**170 – 229**) (Figure 7 – 9), while keeping the alkene unsubstituted.



56 PKA 98 ± 1 Akt1 41 \pm 0 Akt2 50 \pm 7 FLT3 73 ± 8	57 PKA 100 ± 2 Akt1 59 ± 2 Akt2 64 ± 7 FLT3 72 ± 4	58 PKA 98 ± 1 Akt1 40 \pm 1 Akt2 50 \pm 2 FLT3 76 ± 5	59 PKA 98 ± 2 Akt1 43 \pm 1 Akt2 50 \pm 5 FLT3 74 ± 8	60 PKA 99 ± 3 Akt1 42 \pm 0 Akt2 50 \pm 5 FLT3 60 ± 10	61 PKA 100 ± 2 Akt1 35 \pm 2 Akt2 47 \pm 5 FLT3 63 ± 1
62 PKA 97 ± 1 Akt1 33 \pm 1 Akt2 47 \pm 4 FLT3 76 ± 5	63 PKA 99 ± 3 Akt1 41 \pm 1 Akt2 56 ± 8 FLT3 68 ± 2	64 PKA 100 ± 2 Akt1 45 \pm 0 Akt2 55 ± 2 FLT3 85 ± 4	65 PKA 94 ± 1 Akt1 39 \pm 1 Akt2 52 ± 4 FLT3 76 ± 5	66 PKA 96 ± 3 Akt1 43 \pm 1 Akt2 50 \pm 4 FLT3 62 ± 4	67 PKA 100 ± 5 Akt1 46 \pm 1 Akt2 56 ± 4 FLT3 83 ± 11
68 PKA 100 ± 2 Akt1 36 \pm 1 Akt2 47 \pm 4 FLT3 74 ± 5	69 PKA 100 ± 4 Akt1 62 ± 2 Akt2 64 ± 4 FLT3 87 ± 4	70 PKA 100 ± 3 Akt1 93 ± 0 Akt2 91 ± 4 FLT3 92 ± 2	71 PKA 88 ± 23 Akt1 88 ± 0 Akt2 86 ± 2 FLT3 84 ± 2	72 PKA 100 ± 2 Akt1 45 \pm 1 Akt2 59 ± 7 FLT3 89 ± 7	73 PKA 100 ± 3 Akt1 77 ± 0 Akt2 76 ± 3 FLT3 87 ± 8
74 PKA 88 ± 5 Akt1 59 ± 2 Akt2 79 ± 7 FLT3 78 ± 1	75 PKA 98 ± 9 Akt1 79 ± 1 Akt2 83 ± 8 FLT3 84 ± 2	76 PKA 89 ± 19 Akt1 59 ± 2 Akt2 66 ± 7 FLT3 74 ± 1	77 PKA 96 ± 6 Akt1 65 ± 1 Akt2 93 ± 38 FLT3 77 ± 0	78 PKA 98 ± 5 Akt1 79 ± 1 Akt2 84 ± 5 FLT3 37 \pm 4	79 PKA 97 ± 3 Akt1 88 ± 1 Akt2 85 ± 9 FLT3 78 ± 3
80 PKA 100 ± 1 Akt1 86 ± 1 Akt2 90 ± 13 FLT3 79 ± 5	81 PKA 100 ± 1 Akt1 89 ± 1 Akt2 93 ± 14 FLT3 72 ± 5	82 PKA 100 ± 3 Akt1 99 ± 1 Akt2 100 ± 13 FLT3 84 ± 10	83 PKA 100 ± 3 Akt1 100 ± 1 Akt2 100 ± 13 FLT3 91 ± 3	84 PKA 100 ± 1 Akt1 90 ± 1 Akt2 79 ± 33 FLT3 82 ± 3	85 PKA 99 ± 9 Akt1 100 ± 1 Akt2 100 ± 12 FLT3 84 ± 3
86 PKA 100 ± 1 Akt1 99 ± 2 Akt2 100 ± 19 FLT3 84 ± 2	87 PKA 100 ± 1 Akt1 98 ± 2 Akt2 98 ± 8 FLT3 63 ± 3	88 PKA 100 ± 1 Akt1 100 ± 1 Akt2 96 ± 4 FLT3 92 ± 1	89 PKA 100 ± 1 Akt1 45 \pm 1 Akt2 58 ± 4 FLT3 71 ± 8	90 PKA 100 ± 2 Akt1 48 \pm 3 Akt2 58 ± 4 FLT3 78 ± 3	91 PKA 100 ± 5 Akt1 87 ± 0 Akt2 91 ± 8 FLT3 87 ± 5

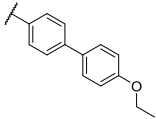
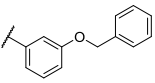
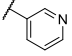
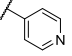
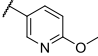
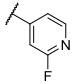
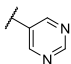
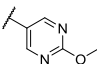
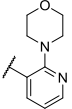
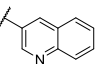
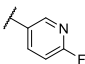
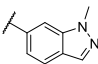
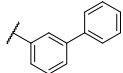
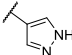
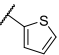
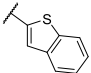
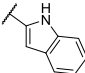
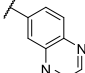
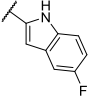
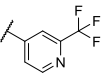
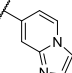
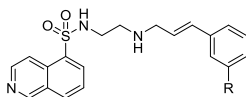
					
92 PKA 100 ± 1 Akt1 100 ± 2 Akt2 99 ± 2 FLT3 89 ± 7	93 PKA 100 ± 4 Akt1 91 ± 2 Akt2 99 ± 19 FLT3 80 ± 4	94 PKA 100 ± 2 Akt1 67 ± 1 Akt2 80 ± 5 FLT3 85 ± 6	95 PKA 100 ± 1 Akt1 70 ± 1 Akt2 81 ± 5 FLT3 86 ± 5	96 PKA 99 ± 5 Akt1 34 ± 1 Akt2 47 ± 5 FLT3 83 ± 8	97 PKA 100 ± 2 Akt1 72 ± 0 Akt2 86 ± 8 FLT3 83 ± 6
					
98 PKA 100 ± 3 Akt1 89 ± 3 Akt2 100 ± 13 FLT3 85 ± 2	99 PKA 100 ± 3 Akt1 82 ± 1 Akt2 98 ± 10 FLT3 88 ± 7	100 PKA 100 ± 3 Akt1 93 ± 1 Akt2 100 ± 8 FLT3 89 ± 9	101 PKA 100 ± 3 Akt1 69 ± 1 Akt2 85 ± 11 FLT3 68 ± 16	102 PKA 100 ± 2 Akt1 94 ± 0 Akt2 97 ± 6 FLT3 90 ± 1	103 PKA 100 ± 2 Akt1 43 ± 1 Akt2 54 ± 1 FLT3 71 ± 4
					
104 PKA 97 ± 11 Akt1 92 ± 1 Akt2 91 ± 6 FLT3 81 ± 5	105 PKA 98 ± 1 Akt1 70 ± 2 Akt2 79 ± 1 FLT3 77 ± 2	106 PKA 100 ± 1 Akt1 52 ± 2 Akt2 62 ± 4 FLT3 75 ± 8	107 PKA 100 ± 2 Akt1 73 ± 0 Akt2 78 ± 2 FLT3 60 ± 5	108 PKA 100 ± 2 Akt1 76 ± 1 Akt2 78 ± 1 FLT3 79 ± 5	109 PKA 100 ± 1 Akt1 66 ± 1 Akt2 71 ± 2 FLT3 67 ± 3
					
110 PKA 100 ± 3 Akt1 86 ± 1 Akt2 77 ± 9 FLT3 82 ± 6	111 PKA 93 ± 3 Akt1 83 ± 2 Akt2 76 ± 10 FLT3 84 ± 10	112 PKA 97 ± 3 Akt1 70 ± 1 Akt2 72 ± 5 FLT3 61 ± 8			

Figure 7. *Ortho*-phenyl sulphonamide inhibitors. Relative remaining activity (%) towards purified PKA, PKB/AKT1, PKB/AKT2 and FLT3 in an *in vitro* kinase reaction in the absence or presence of 2 μ M compound. Relative remaining activity ranges from 0 – 25%, 25 – 50%, 50 – 75%, > 75% are in bold and underlined, bold, italics and normal, respectively. Results are normalized to the activity detected in the absence of any compound, containing DMSO only, from $n = 3$ experiments performed. Negative control: absence of ATP. Positive control: 2 μ M commercial H-89.



113 PKA 100 ± 3 Akt1 85 ± 1 Akt2 90 ± 6 FLT3 55 ± 5	114 PKA 100 ± 2 Akt1 88 ± 0 Akt2 91 ± 9 FLT3 57 ± 3	115 PKA 100 ± 2 Akt1 91 ± 1 Akt2 88 ± 5 FLT3 65 ± 2	116 PKA 100 ± 0 Akt1 84 ± 3 Akt2 85 ± 6 FLT3 60 ± 2	117 PKA 99 ± 2 Akt1 84 ± 1 Akt2 90 ± 10 FLT3 44 ± 2	118 PKA 99 ± 2 Akt1 84 ± 1 Akt2 89 ± 10 FLT3 54 ± 7
119 PKA 96 ± 10 Akt1 85 ± 0 Akt2 86 ± 4 FLT3 38 ± 5	120 PKA 100 ± 1 Akt1 93 ± 1 Akt2 92 ± 5 FLT3 56 ± 5	121 PKA 100 ± 1 Akt1 87 ± 1 Akt2 69 ± 5 FLT3 63 ± 4	122 PKA 100 ± 3 Akt1 95 ± 1 Akt2 95 ± 6 FLT3 72 ± 8	123 PKA 100 ± 5 Akt1 100 ± 2 Akt2 89 ± 10 FLT3 55 ± 3	124 PKA 98 ± 5 Akt1 95 ± 1 Akt2 88 ± 9 FLT3 79 ± 10
125 PKA 98 ± 3 Akt1 89 ± 3 Akt2 85 ± 9 FLT3 58 ± 9	126 PKA 100 ± 2 Akt1 96 ± 1 Akt2 84 ± 8 FLT3 70 ± 3	127 PKA 98 ± 5 Akt1 97 ± 1 Akt2 85 ± 8 FLT3 90 ± 5	128 PKA 100 ± 1 Akt1 97 ± 0 Akt2 87 ± 8 FLT3 77 ± 3	129 PKA 98 ± 3 Akt1 86 ± 0 Akt2 85 ± 4 FLT3 69 ± 7	130 PKA 100 ± 3 Akt1 67 ± 2 Akt2 74 ± 4 FLT3 64 ± 5
131 PKA 87 ± 2 Akt1 67 ± 0 Akt2 76 ± 4 FLT3 69 ± 6	132 PKA 98 ± 3 Akt1 91 ± 2 Akt2 87 ± 4 FLT3 62 ± 7	133 PKA 94 ± 13 Akt1 93 ± 2 Akt2 94 ± 5 FLT3 79 ± 2	134 PKA 99 ± 3 Akt1 96 ± 2 Akt2 90 ± 3 FLT3 53 ± 5	135 PKA 100 ± 2 Akt1 95 ± 0 Akt2 89 ± 3 FLT3 42 ± 1	136 PKA 100 ± 1 Akt1 96 ± 0 Akt2 89 ± 8 FLT3 77 ± 7
137 PKA 97 ± 9 Akt1 97 ± 0 Akt2 87 ± 8 FLT3 72 ± 1	138 PKA 100 ± 0 Akt1 97 ± 2 Akt2 87 ± 13 FLT3 70 ± 2	139 PKA 100 ± 1 Akt1 97 ± 2 Akt2 90 ± 9 FLT3 81 ± 6	140 PKA 100 ± 2 Akt1 97 ± 1 Akt2 93 ± 11 FLT3 88 ± 4	141 PKA 99 ± 1 Akt1 76 ± 1 Akt2 73 ± 9 FLT3 52 ± 3	142 PKA 100 ± 1 Akt1 98 ± 1 Akt2 90 ± 10 FLT3 80 ± 4
143 PKA 100 ± 1 Akt1 98 ± 0 Akt2 91 ± 8 FLT3 91 ± 5	144 PKA 100 ± 0 Akt1 97 ± 1 Akt2 89 ± 8 FLT3 66 ± 1	145 PKA 100 ± 2 Akt1 97 ± 1 Akt2 89 ± 6 FLT3 86 ± 7	146 PKA 99 ± 5 Akt1 88 ± 1 Akt2 85 ± 4 FLT3 44 ± 2	147 PKA 100 ± 3 Akt1 91 ± 1 Akt2 84 ± 4 FLT3 55 ± 2	148 PKA 100 ± 4 Akt1 87 ± 1 Akt2 81 ± 2 FLT3 72 ± 7

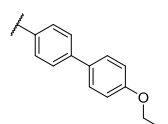
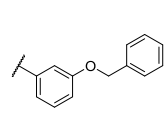
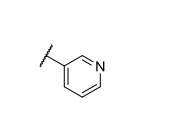
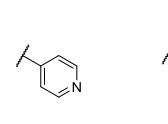
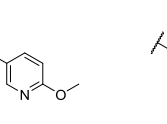

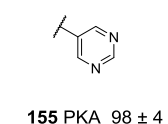
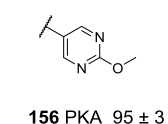
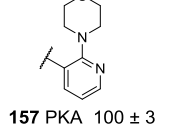
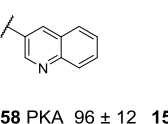
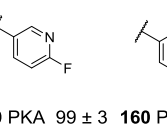
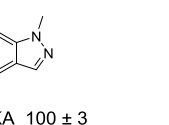
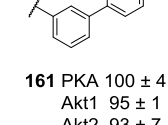
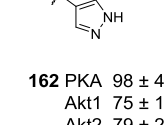
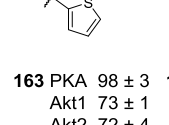
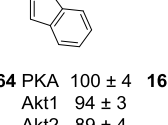
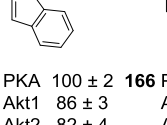
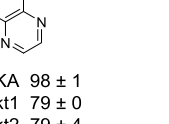
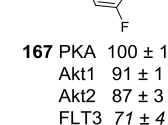
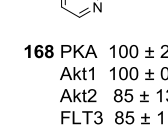
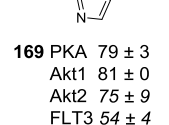
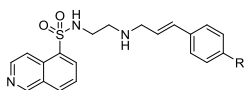
					
149 PKA 99 ± 7 Akt1 96 ± 2 Akt2 90 ± 2 FLT3 81 ± 3	150 PKA 100 ± 2 Akt1 100 ± 2 Akt2 92 ± 2 FLT3 58 ± 2	151 PKA 90 ± 0 Akt1 66 ± 0 Akt2 76 ± 8 FLT3 57 ± 2	152 PKA 98 ± 1 Akt1 90 ± 1 Akt2 91 ± 6 FLT3 80 ± 2	153 PKA 98 ± 2 Akt1 89 ± 3 Akt2 90 ± 6 FLT3 64 ± 5	154 PKA 89 ± 2 Akt1 88 ± 1 Akt2 91 ± 6 FLT3 80 ± 7
					
155 PKA 98 ± 4 Akt1 89 ± 0 Akt2 93 ± 9 FLT3 75 ± 2	156 PKA 95 ± 3 Akt1 89 ± 1 Akt2 94 ± 5 FLT3 75 ± 7	157 PKA 100 ± 3 Akt1 89 ± 1 Akt2 94 ± 10 FLT3 50 ± 2	158 PKA 96 ± 12 Akt1 81 ± 2 Akt2 91 ± 9 FLT3 35 ± 3	159 PKA 99 ± 3 Akt1 91 ± 3 Akt2 91 ± 7 FLT3 73 ± 6	160 PKA 100 ± 3 Akt1 88 ± 3 Akt2 84 ± 5 FLT3 44 ± 1
					
161 PKA 100 ± 4 Akt1 95 ± 1 Akt2 93 ± 7 FLT3 78 ± 2	162 PKA 98 ± 4 Akt1 75 ± 1 Akt2 79 ± 2 FLT3 28 ± 6	163 PKA 98 ± 3 Akt1 73 ± 1 Akt2 72 ± 4 FLT3 56 ± 4	164 PKA 100 ± 4 Akt1 94 ± 3 Akt2 89 ± 4 FLT3 57 ± 3	165 PKA 100 ± 2 Akt1 86 ± 3 Akt2 82 ± 4 FLT3 68 ± 5	166 PKA 98 ± 1 Akt1 79 ± 0 Akt2 79 ± 4 FLT3 35 ± 5
					
167 PKA 100 ± 1 Akt1 91 ± 1 Akt2 87 ± 3 FLT3 71 ± 4	168 PKA 100 ± 2 Akt1 100 ± 0 Akt2 85 ± 13 FLT3 85 ± 1	169 PKA 79 ± 3 Akt1 81 ± 0 Akt2 75 ± 9 FLT3 54 ± 4			

Figure 8. *Meta*-phenyl sulphonamide inhibitors. Relative remaining activity (%) towards PKA, PKB/AKT1, PKB/AKT2 and FLT3 in an *in vitro* kinase reaction in the absence or presence of 2 μ M compound. Relative remaining activity ranges from 0 – 25%, 25 – 50%, 50 – 75%, > 75% are in bold and underlined, bold, italics and normal, respectively. Results are normalized to the activity detected in the absence of any compound, containing DMSO only, from $n = 3$ experiments performed. Negative control: absence of ATP. Positive control: 2 μ M commercial H-89.



170 PKA 99 ± 2
Akt1 84 ± 1
Akt2 88 ± 0
FLT3 36 ± 1



171 PKA 98 ± 0
Akt1 88 ± 1
Akt2 88 ± 3
FLT3 43 ± 7



172 PKA 100 ± 2
Akt1 92 ± 1
Akt2 92 ± 5
FLT3 31 ± 3



173 PKA 100 ± 2
Akt1 88 ± 1
Akt2 96 ± 6
FLT3 58 ± 6



174 PKA 100 ± 3
Akt1 100 ± 4
Akt2 100 ± 3
FLT3 92 ± 6



175 PKA 100 ± 2
Akt1 98 ± 2
Akt2 98 ± 6
FLT3 45 ± 2



176 PKA 100 ± 1
Akt1 93 ± 0
Akt2 94 ± 5
FLT3 43 ± 3



177 PKA 100 ± 2
Akt1 93 ± 1
Akt2 99 ± 15
FLT3 40 ± 6



178 PKA 99 ± 2
Akt1 89 ± 1
Akt2 95 ± 4
FLT3 41 ± 7



179 PKA 98 ± 2
Akt1 85 ± 1
Akt2 90 ± 8
FLT3 56 ± 1



180 PKA 99 ± 4
Akt1 88 ± 2
Akt2 88 ± 6
FLT3 51 ± 1



181 PKA 97 ± 2
Akt1 82 ± 2
Akt2 89 ± 6
FLT3 34 ± 4



182 PKA 99 ± 0
Akt1 88 ± 1
Akt2 89 ± 7
FLT3 47 ± 3



183 PKA 99 ± 0
Akt1 87 ± 1
Akt2 100 ± 21
FLT3 62 ± 29



184 PKA 98 ± 1
Akt1 83 ± 2
Akt2 90 ± 2
FLT3 36 ± 5



185 PKA 96 ± 6
Akt1 93 ± 0
Akt2 91 ± 4
FLT3 78 ± 7



186 PKA 99 ± 2
Akt1 94 ± 2
Akt2 87 ± 3
FLT3 100 ± 4



187 PKA 100 ± 2
Akt1 91 ± 1
Akt2 91 ± 4
FLT3 49 ± 4



188 PKA 100 ± 0
Akt1 97 ± 2
Akt2 87 ± 4
FLT3 71 ± 4



189 PKA 98 ± 1
Akt1 86 ± 0
Akt2 85 ± 4
FLT3 52 ± 7



190 PKA 100 ± 1
Akt1 67 ± 1
Akt2 74 ± 4
FLT3 35 ± 8



191 PKA 87 ± 2
Akt1 67 ± 2
Akt2 76 ± 5
FLT3 64 ± 1



192 PKA 98 ± 4
Akt1 91 ± 5
Akt2 87 ± 5
FLT3 41 ± 3



193 PKA 94 ± 2
Akt1 93 ± 3
Akt2 94 ± 5
FLT3 49 ± 5



194 PKA 99 ± 1
Akt1 96 ± 3
Akt2 90 ± 5
FLT3 35 ± 16



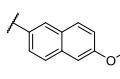
195 PKA 100 ± 3
Akt1 95 ± 5
Akt2 89 ± 14
FLT3 36 ± 4



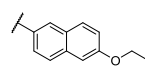
196 PKA 100 ± 4
Akt1 100 ± 1
Akt2 86 ± 10
FLT3 85 ± 13



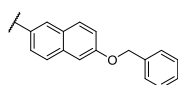
197 PKA 97 ± 8
Akt1 99 ± 4
Akt2 89 ± 10
FLT3 72 ± 7



198 PKA 100 ± 7
Akt1 100 ± 3
Akt2 95 ± 15
FLT3 169 ± 15



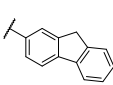
199 PKA 100 ± 5
Akt1 152 ± 3
Akt2 183 ± 20
FLT3 50 ± 3



200 PKA 100 ± 3
Akt1 100 ± 2
Akt2 99 ± 12
FLT3 90 ± 6



201 PKA 100 ± 4
Akt1 100 ± 3
Akt2 100 ± 10
FLT3 57 ± 8



202 PKA 100 ± 4
Akt1 98 ± 1
Akt2 100 ± 16
FLT3 272 ± 49



203 PKA 100 ± 0
Akt1 100 ± 1
Akt2 100 ± 9
FLT3 74 ± 2



204 PKA 100 ± 4
Akt1 100 ± 2
Akt2 100 ± 6
FLT3 28 ± 4



205 PKA 100 ± 3
Akt1 100 ± 1
Akt2 100 ± 10
FLT3 100 ± 4

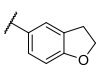
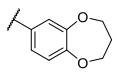
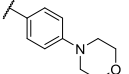
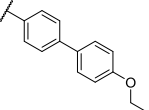
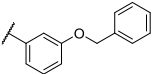
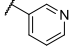
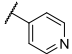
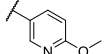
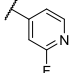
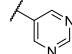
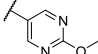
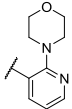
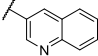
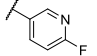
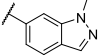
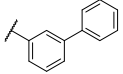
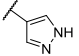
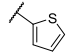
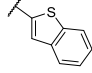
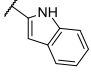
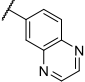
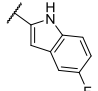
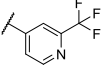
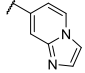
					
206 PKA 100 ± 3 Akt1 100 ± 3 Akt2 100 ± 8 FLT3 38 ± 4	207 PKA 100 ± 2 Akt1 100 ± 1 Akt2 100 ± 5 FLT3 55 ± 5	208 PKA 87 ± 1 Akt1 62 ± 2 Akt2 70 ± 4 FLT3 288 ± 21	209 PKA 99 ± 1 Akt1 100 ± 2 Akt2 54 ± 6 FLT3 116 ± 3	210 PKA 100 ± 3 Akt1 98 ± 2 Akt2 95 ± 1 FLT3 46 ± 2	211 PKA 100 ± 5 Akt1 87 ± 2 Akt2 92 ± 4 FLT3 13 ± 5
					
212 PKA 100 ± 3 Akt1 99 ± 5 Akt2 100 ± 3 FLT3 72 ± 7	213 PKA 100 ± 5 Akt1 95 ± 1 Akt2 99 ± 7 FLT3 30 ± 2	214 PKA 100 ± 3 Akt1 96 ± 1 Akt2 92 ± 13 FLT3 55 ± 6	215 PKA 100 ± 5 Akt1 91 ± 1 Akt2 98 ± 7 FLT3 13 ± 2	216 PKA 96 ± 10 Akt1 94 ± 1 Akt2 100 ± 10 FLT3 18 ± 2	217 PKA 100 ± 5 Akt1 95 ± 0 Akt2 100 ± 9 FLT3 79 ± 6
					
218 PKA 100 ± 6 Akt1 95 ± 0 Akt2 100 ± 12 FLT3 9 ± 5	219 PKA 100 ± 3 Akt1 93 ± 1 Akt2 100 ± 5 FLT3 27 ± 4	220 PKA 100 ± 2 Akt1 91 ± 1 Akt2 100 ± 13 FLT3 36 ± 3	221 PKA 100 ± 3 Akt1 100 ± 1 Akt2 100 ± 6 FLT3 91 ± 1	222 PKA 91 ± 6 Akt1 82 ± 1 Akt2 99 ± 3 FLT3 14 ± 1	223 PKA 100 ± 2 Akt1 84 ± 3 Akt2 92 ± 3 FLT3 31 ± 4
					
224 PKA 83 ± 1 Akt1 70 ± 1 Akt2 95 ± 3 FLT3 356 ± 8	225 PKA 100 ± 7 Akt1 95 ± 4 Akt2 100 ± 19 FLT3 36 ± 2	226 PKA 100 ± 3 Akt1 84 ± 3 Akt2 93 ± 3 FLT3 19 ± 3	227 PKA 100 ± 2 Akt1 91 ± 8 Akt2 81 ± 11 FLT3 49 ± 2	228 PKA 98 ± 6 Akt1 93 ± 1 Akt2 88 ± 14 FLT3 60 ± 6	229 PKA 95 ± 7 Akt1 75 ± 1 Akt2 77 ± 10 FLT3 27 ± 3

Figure 9. Para-phenyl sulphonamide inhibitors of first (A) and second (B) generation library. Relative remaining activity (%) towards PKA, PKB/AKT1, PKB/AKT2 and FLT3 in an *in vitro* kinase reaction in the absence or presence of 2 μ M compound. Relative remaining activity ranges from 0 – 25%, 25 – 50%, 50 – 75%, > 75% are in bold and underlined, bold, italics and normal, respectively. Results are normalized to the activity detected in the absence of any compound, containing DMSO only, from $n = 3$ experiments performed. Negative control: absence of ATP. Positive control: 2 μ M commercial H-89.

It can be seen from Figure 7 - 9 that the compounds having a functional group at the meta position have the least activity against the kinases PKA, AKT1, and AKT2 when compared to its corresponding ortho and para analogues. Analogues having an aromatic group at the ortho position appear to have the most activity for AKT1 and AKT2. Of note, all compounds are poor PKA inhibitors. This indicates that substitution of the bromide in H-89 (**3**) for an aromatic moiety is detrimental for PKA/AKT1/AKT2 inhibition. In addition, bulky aromatic groups at the para position result in active inhibitors against FLT3. Compounds with nitrogen-containing aromatic rings at the para position are amongst the most active FLT3 inhibitors.

Introduction of functional groups at the ortho position seems to be least favourable for gaining active FLT3 inhibitors. Finally, a few activators for FLT3 has been observed, namely compounds **198**, **202**, **208**, **209** and **224**.

Linker length alteration

The linker length has been altered and the double bond has been excluded in compounds **230** – **236** (Figure 10). This will give information about the importance of the double bond and the influence of the linker length on the activity.

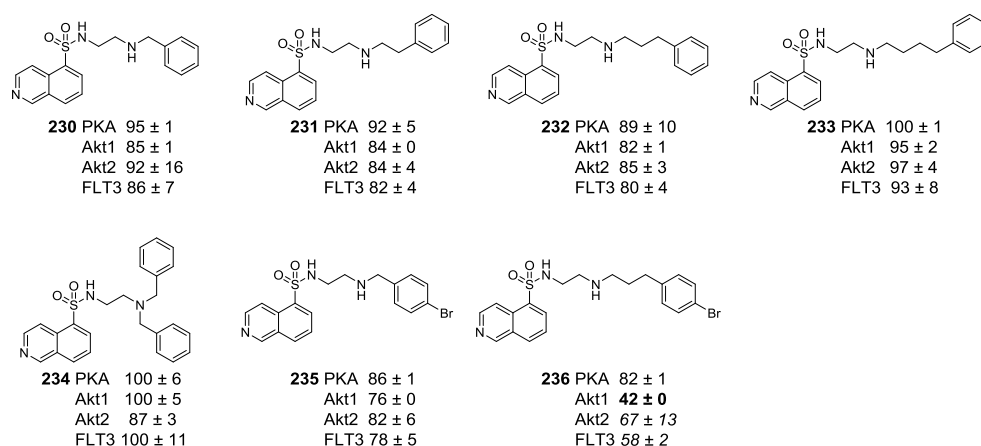


Figure 10. Variation in linker length. Relative remaining activity (%) towards PKA, PKB/AKT1, PKB/AKT2 and FLT3 in an *in vitro* kinase reaction in the absence or presence of 2 μ M compound. Relative remaining activity ranges from 0 – 25%, 25 – 50%, 50 – 75%, > 75% are in bold and underlined, bold, italics and normal, respectively. Results are normalized to the activity detected in the absence of any compound, containing DMSO only, from $n = 3$ experiments performed. Negative control: absence of ATP. Positive control: 2 μ M commercial H-89.

Figure 10 shows that changes in linker length and double bond have drastic influence on the activity towards the four different kinases. The linker length in H-89 (**3**) appears to be optimal and the double bond, which leads to rigidity in the molecule, appears to be important for activity.

Boc protected analogues

The amine group in compounds **237** – **239** have been protected by a Boc group (Figure 11). According to the relative activities given in Figure 11, it seems that the amine functionality needs to be unprotected and or the bulky Boc-group seems to give steric hindrance with the active site. Thus a free amine contributes to the inhibition towards PKA, AKT1, AKT2 and FLT3.

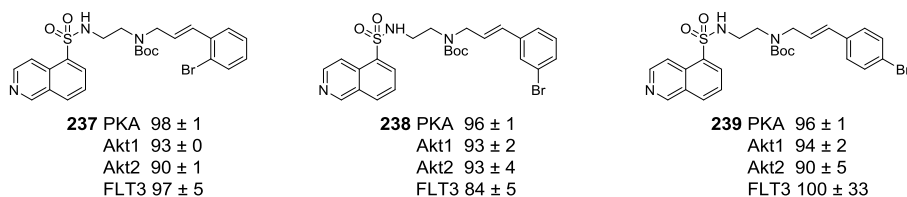


Figure 11. Boc protected isoquinoline sulfonamide analogues. Relative remaining activity (%) towards PKA, PKB/AKT1, PKB/AKT2 and FLT3 in an *in vitro* kinase reaction in the absence or presence of 2 μ M compound. Relative remaining activity ranges from 0 – 25%, 25 – 50%, 50 – 75%, > 75% are in bold and underlined, bold, italics and normal, respectively. Results are normalized to the activity detected in the absence of any compound, containing DMSO only, from $n = 3$ experiments performed. Negative control: absence of ATP. Positive control: 2 μ M commercial H-89.

K_i and IC_{50} values of selected compounds

An estimation of the activities of the 239 inhibitors has been made by determining the relative activities towards PKA, AKT1, AKT2 and FLT3. However, to compare the activity and the selectivity between these compounds, it is necessary to determine their K_i values. K_i values were only determined for potential active and selective compounds, that is to say, only compounds showing > 50% inhibitory activity towards PKA, AKT1 or AKT2 (Table 1).

Table 1. Inhibition constant (K_i) values in μM of H-89 analogues. The mean K_i values are calculated using the Cheng-Prusoff equation from the IC_{50} values from $n = 3$ experiments performed. The conditions are: $K_M = 10.35$, 207.8 and 0.82 μM for AKT1, AKT2 and PKA respectively and [ATP] was 100 μM .

Compound	AKT1	AKT2	PKA
24	0.06 ± 0.01	1.40 ± 0.26	0.04 ± 0.01
9	0.08 ± 0.01	1.28 ± 0.21	0.05 ± 0.01
38	0.09 ± 0.02	2.17 ± 0.55	0.46 ± 0.30
23	0.10 ± 0.03	1.76 ± 0.48	0.07 ± 0.01
68	0.09 ± 0.01	1.30 ± 0.21	0.28 ± 0.12
62	0.08 ± 0.02	1.19 ± 0.33	> 0.16
3	0.11 ± 0.02	2.25 ± 0.37	0.02 ± 0.00
96	0.07 ± 0.01	0.78 ± 0.16	0.20 ± 0.09
61	0.07 ± 0.02	1.34 ± 0.30	> 0.16
65	0.10 ± 0.01	1.86 ± 0.30	0.17 ± 0.06
56	0.17 ± 0.05	2.63 ± 0.63	0.20 ± 0.09
4	0.17 ± 0.04	3.40 ± 0.87	-
60	0.19 ± 0.03	2.87 ± 0.59	-
58	0.14 ± 0.03	2.16 ± 0.26	-
3 (H-89)	0.09 ± 0.01	1.67 ± 0.26	0.02 ± 0.01
236	0.13 ± 0.02	2.22 ± 0.34	0.02 ± 0.01
59	0.12 ± 0.02	1.74 ± 0.40	-
191	0.10 ± 0.01	1.64 ± 0.33	0.02 ± 0.01
218	0.08 ± 0.01	1.22 ± 0.19	0.01 ± 0.00
66	0.14 ± 0.03	1.76 ± 0.30	-
64	0.13 ± 0.02	2.12 ± 0.41	-
63	0.08 ± 0.02	1.17 ± 0.21	0.18 ± 0.04
103	0.06 ± 0.01	1.13 ± 0.19	0.36 ± 0.20
15	0.08 ± 0.01	2.22 ± 0.36	0.03 ± 0.01
89	0.05 ± 0.01	1.12 ± 0.23	> 0.16
54	0.19 ± 0.05	5.34 ± 0.96	0.10 ± 0.02
72	0.09 ± 0.01	1.51 ± 0.42	0.26 ± 0.14
67	0.11 ± 0.02	2.12 ± 0.35	-
55	0.13 ± 0.02	3.88 ± 0.65	-
29	0.09 ± 0.01	2.63 ± 0.37	-
16	0.09 ± 0.01	2.19 ± 0.23	0.04 ± 0.02
53	0.16 ± 0.02	3.74 ± 0.83	-
30	0.16 ± 0.04	4.42 ± 1.30	
45	0.08 ± 0.01	2.32 ± 0.36	0.04 ± 0.01

106	0.13 ± 0.01	1.64 ± 0.29	-
46	0.09 ± 0.02	2.13 ± 0.39	-
12	0.13 ± 0.01	6.15 ± 4.18	-
101	0.17 ± 0.03	2.76 ± 0.49	-
6	0.12 ± 0.02	1.91 ± 0.26	-
90	0.10 ± 0.01	1.72 ± 0.22	-
34	0.14 ± 0.02	3.11 ± 0.54	-
74	0.35 ± 0.10	7.93 ± 2.52	0.08 ± 0.02
39	0.15 ± 0.03	2.97 ± 1.34	-
2	0.14 ± 0.05	6.41 ± 1.77	-
27	0.33 ± 0.07	6.34 ± 1.43	-
31	0.22 ± 0.06	5.55 ± 1.54	-
45	0.47 ± 0.18	9.25 ± 2.55	-
57	0.41 ± 0.13	7.05 ± 2.49	-
76	0.36 ± 0.10	6.74 ± 2.31	-
190	0.10 ± 0.04	0.97 ± 0.13	0.04 ± 0.01
99	0.55 ± 0.30	-	-
224	0.42 ± 0.07	1.71 ± 0.43	0.05 ± 0.01
13	0.24 ± 0.10	20.42 ± 12.91	-
97	0.69 ± 0.22	12.25 ± 2.63	-
77	0.95 ± 0.27	14.97 ± 7.08	-
69	0.74 ± 0.24	8.47 ± 2.04	-
109	0.38 ± 0.06	5.04 ± 1.46	-
95	0.25 ± 0.04	5.37 ± 1.47	-
94	0.23 ± 0.03	3.03 ± 0.73	-
130	0.73 ± 0.08	6.61 ± 1.56	-
209	0.72 ± 0.18	1.47 ± 0.29	0.05 ± 0.01
199	3.10 ± 2.04	-	-
44	0.10 ± 0.02	1.92 ± 0.39	-

Based on the results shown in Table 1, a selection of most active AKT1 inhibitors has been made (Figure 12). These compounds (**24**, **61**, **89**, **96** and **103**) showed to have a significantly lower K_i value, which varies between 1.3 – 1.8 times more activity, than the lead compound H-89 (**3**).

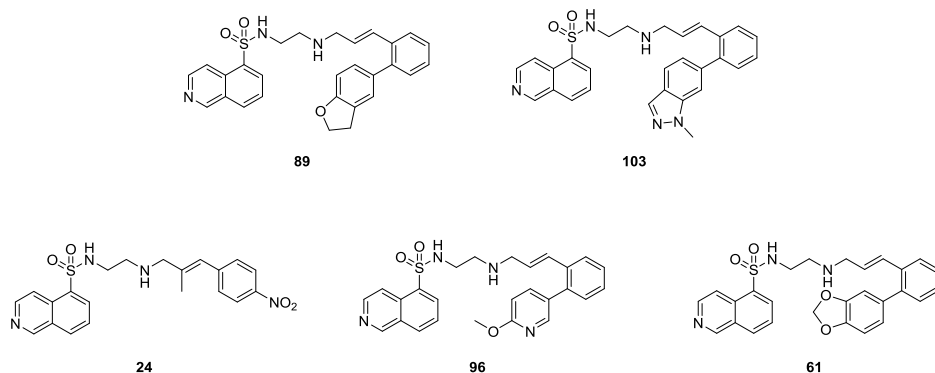


Figure 12. Selection of AKT1 inhibitors, which are more active than lead compound H-89 (**3**) based on their K_i values.

The ortho-phenyl substituted compounds are the most active inhibitors towards AKT1 in this library (Figure 10). It appears that bulky and electron-donating groups are favoured in the active site of AKT1. In addition, methyl-alkene derivatives appear to be more active AKT1 inhibitors compared to their non-substituted (at the alkene) counterparts. In general, the *E* configuration is preferred over the *Z* configuration.

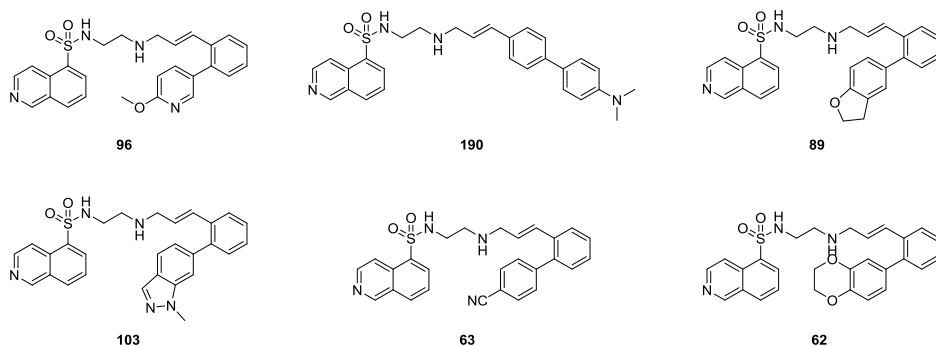


Figure 13. Selection of AKT2 inhibitors, which are more active than lead compound H-89 (**3**) based on their K_i values.

The six compounds (**62**, **63**, **89**, **96**, **103** and **190**) that are shown in Figure 13 are the most active AKT2 inhibitors found in this library. They are all significant more active than H-89 (**3**) showing an increase varying from 1.5 – 2.1 times. Based on these structures it can be seen that bulky, electron negative containing phenyl groups which are on the ortho position are preferred in the active site of AKT2. Compound

190 is the only compound in the top six having an aromatic group on the para position. The high activity is likely due to the dimethylamine group.

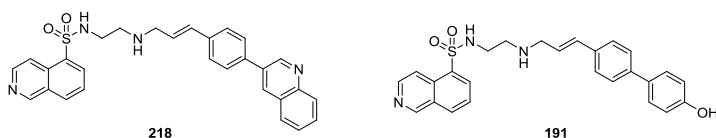


Figure 14. Selection of PKA inhibitors, which are more active than lead compound H-89 (**3**) based on their K_i values.

The lead compound H-89 (**3**) is already a potent PKA inhibitor, and it is therefore not surprising (also given that optimization was conducted towards AKT1, and not PKA) that stronger PKA inhibitors are scarce in the evaluated series of compounds. In fact, only compound **218** (Figure 14) showed a significant lower K_i value than lead compound H-89 (**3**). According to the results presented in Table 1, the most active PKA inhibitors are all containing a functional group at the para position, for instance, compound **191** (Figure 14). This is perhaps not surprising since the lead compound H-89 (**3**), which is a PKA inhibitor, contains a bromide on the para position.

Both AKT1 and AKT2 prefer roughly the same compounds (compounds **89**, **96** and **103**). Since inhibition of AKT2 is lethal in mice, it is important to find active and selective compounds towards AKT1. In Figure 15 the three most selective AKT1 over AKT2 compounds are shown.

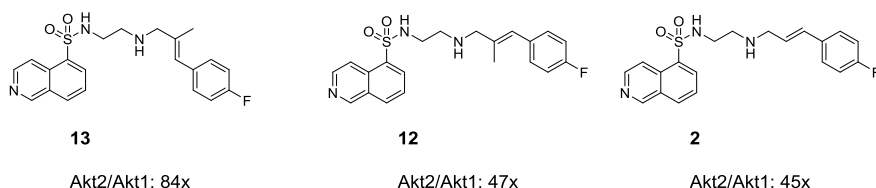


Figure 15. Most selective AKT1 over AKT2 inhibitors based on their K_i values difference.

It appears that a methyl substituent at the linker alkene contributes to AKT1 selectivity over AKT2. Next to this, introduction of a para-halogen at the phenyl ring appears to improve the selectivity of AKT1 over AKT2. Compared to the selectivity of the lead compound H-89 (**3**), which is 18 times more selective for AKT1 over AKT2, these compounds showed to have at least twice as selective as their lead compound. As can be seen in Figure 16, the most selective AKT1 over PKA inhibitors prefer to contain aromatic groups having oxygen or nitrogen groups at an ortho position.

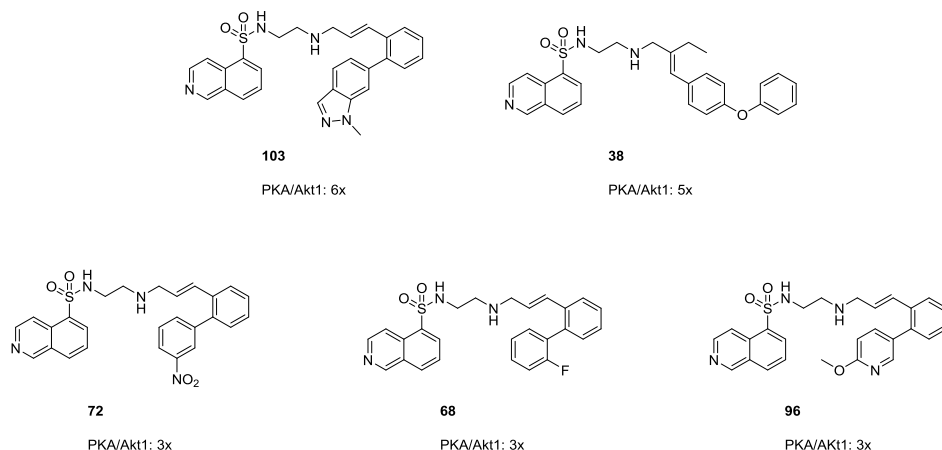


Figure 16. The most selective AKT1 over PKA inhibitors based on their K_i values difference.

Since FLT3 plays a role in the same pathway as AKT1, IC_{50} values of a few compounds showing a lower relative activity value than the FLT3 lead compound **195** and other relevant compounds have been determined (Table 2). This Table shows the importance of the position at which the aryl side is substituted. When comparing compounds **101**, **158** and **218**, which all contain an isoquinoline group at the ortho, meta or para position respectively, it becomes evident that the compound having a *para*-isoquinoline group (**218**) is more than 40 times more active than the ortho and meta analogues (**101** and **158**).

Table 2. IC_{50} values of selected isoquinolinesulfonamide compounds for FLT3.

Compound	IC_{50} (nM)	Compound	IC_{50} (nM)
101	3500 ± 3043	215	42.5 ± 15.3
158	715.5 ± 66.1	216	202.8 ± 73.6
195	290.7 ± 92.2	218	15.4 ± 1.4
211	17.8 ± 7.2	222	28.0 ± 10.3

Figure 17 shows the structures of the most active FLT3 compounds based on their IC_{50} values. These compounds are 5x or more active than **195** and it seemed that bulky, nitrogen containing aromatic groups at the para position leads to more inhibition of FLT3.

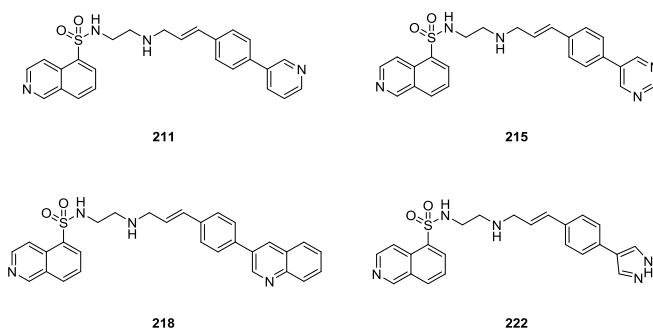


Figure 17. Selection of FLT3 inhibitors, which are more active than lead compound **195** based on their IC_{50} values.

4.3 Conclusion

This chapter describes the biological evaluation of 239 H-89-based compounds **1** – **239**. Evaluation of these compounds reveal that the structure-activity relationship (SAR) of AKT1 inhibition favours a hetero-aromatic group at the ortho position, which gives a more active AKT1 inhibitor and a more selective AKT1 over PKA inhibitor. The most active AKT1 inhibitor in this study is compound **89**, which has a benzofuran group at the ortho position, and the most selective AKT1 over PKA inhibitor is compound **103**, which has a methyl indazole group at the ortho position. Substitution of the double bond with a methyl or isopropyl group gives a more selective AKT1 over AKT2 inhibitor. This finding is applicable on the most selective AKT1 over AKT2 inhibitor **13**, which has a methyl group at the double bond. These results indicate that the ATP binding pocket of AKT1, in contrast with AKT2, does contain an additional cavity that can be occupied by a bulkier apolar group.

Furthermore, the SAR of FLT3 inhibition prefers bulky hetero-aromatic groups at the para position, especially nitrogen-containing aromatic groups are favourable. In this study, the most active FLT3 inhibitor is compound **218**.

In summary, thus far the two kinases AKT1 and FLT3, which act in the same biological pathway, cannot be inhibited by the same compound having this isoquinolinesulfonamide scaffold, since one prefers substitution at the para position and the other the ortho position, respectively. Therefore, new scaffolds need to be developed to cope this.

Experimental

Synthesis

Compounds 1 – 76, 113 – 133, 170 – 193 and 230 – 239: see thesis “Synthetic studies on kinase inhibitors and cyclic peptides: strategies towards new antibiotics”, Adriaan W. Tuin, 2008, https://openaccess.leidenuniv.nl/bitstream/handle/1887/13365/Proefschrift%2BAW_Tuin%2Balles.pdf?sequence=7.

Compounds 77 – 112, 134 – 169 and 194 - 229: see Chapter 3.

Biochemistry

Kinase assay: Determination of the relative activity, IC_{50} and K_i of inhibitors 1 – 239 at 2 μ M final concentration towards PKA, AKT1 and AKT2

A solution of 2 μ M of inhibitor, 10 nM *ULight*-rpS6 (pSer235/Ser236) peptide (Perkin-Elmer, human 40S ribosomal protein), 2 nM Eu-labeled anti-phospho-rpS6 antibody (Perkin-Elmer, Europium-labeled rabbit monoclonal antibody) and 100 μ M ATP in 50 mM HEPES buffer pH 7.5 was incubated with 0.5 nM/min AKT1, AKT2 or 0.05 nM/min of PKA (SignalChem) for 6 h at RT. During these 6 h of incubation, the intensity of the light emission was measured with intervals of 30 min on a PE Envision reader using the Lance Ultra kinase assay settings (λ_{ex} 320 nm; λ_{em} 665 nm) and a secondary control emission was measured at 615 nm. In control experiments, no ATP was added into the buffer (negative control) or DMSO was added to the reaction instead of an inhibitor (background control). Alternatively, the kinases were incubated with 2 μ M commercial H-89 (CalBiochem) (positive control).

To determine the K_M for the kinases, the same assay was performed using 0, 0.1, 0.2, 0.5, 1, 2, 5, 10, 20, 50, 100, 200, 500, 1000 μ M ATP. K_M values were calculated using GraphPad Prism 5 (GraphPad software, La Jolla, USA).

To determine K_i values for inhibitors **1 - 239**, they were tested at a concentration ranging from 0.05 to 20 μ M. Data was analyzed using GraphPad Prism 5 (GraphPad software, La Jolla, USA).

K_i values were calculated via equation 3.1:

$$K_i = IC_{50} / (1 + ([S]/K_M)) \quad (3.1)$$

where K_i is the inhibition constant, IC_{50} is the half maximal inhibitory concentration, S is the concentration of substrate and K_M is the Michaelis-Menten constant, which is the substrate concentration at which the reaction rate is half maximum. All experiments were conducted in triplicate and curves were corrected for background fluorescent of the solvent.

Kinase assays for FLT3

A solution of 2 μ M of inhibitors **101, 158, 195, 211, 215, 216, 218 or 222**, 10 nM *ULight*-TK peptide (Perkin-Elmer, phosphorylated tyrosine residues), 2 nM Eu-labeled anti-phospho-tyrosine antibody (Perkin-Elmer, Europium-labeled rabbit monoclonal antibody) and 100 μ M ATP in 50 mM HEPES buffer pH 7.5 was incubated with 0.05 nM/min FLT3 (SignalChem) for 6 h at RT. During these 6 h of incubation, the intensity of the light emission was

measured with intervals of 30 min similar to as for AKT1. In control experiments, no ATP was added into the buffer (negative control) or DMSO was added to the reaction instead of an inhibitor (background control). Alternatively, the kinases were incubated with 2 μ M H-89 (CalBiochem) (positive control). To determine the IC₅₀ values, inhibitors were tested at a concentration range from 0.3 to 10000 nM. All experiments were conducted in triplicate. Data was analyzed using GraphPad Prism 5 and curves were corrected for background fluorescent of the solvent.

References

- ¹ J. D. Carpten, A. L. Faber, C. Horn, G. P. Donoho, S. L. Briggs, C. M. Robbins, G. Hostetter, S. Boguslawski, T. Y. Moses, S. Savage, M. Uhlik, A. Lin, J. Du, Y. Qian, D. J. Zeckner, G. Tucker-Kellogg, J. Touchman, K. Patel, S. Mousses, M. Bittner, R. Schevitz, M. T. Lai, K. L. Blanchard and J. E. Thomas, *Nature*, 2007, **448**, 439.
- ² V. Jendrossek, M. Henkel, J. Hennenlotter, U. Vogel, U. Ganswindt, I. Muller, R. Handrick, A. G. Anastasiadis, M. Kuczyk, A. Stenzl and C. Belka, *BJUI*, 2008, **102**, 371.
- ³ L. Logie, A. J. Ruiz-Alcaraz, M. Keane, Y. L. Woods, J. Bain, R. Marquez, D. R. Alessi and C. Sutherland, *Diabetes*, 2007, **56**, 2218.
- ⁴ C. Kuijl, N. D. L. Savage, M. Marsman, A. W. Tuin, L. Janssen, D. A. Egan, M. Ketema, R. van den Nieuwendijk, S. J. F. van den Eeden, A. Geluk, A. Poot, G. van der Marel, R. L. Beijersbergen, H. S. Overkleeft, T. H. M. Ottenhof and J. Neefjes, *Nature*, 2007, **450**, 725.
- ⁵ C. C. Kumar, R. Diao, Z. Yin, Y-H. Liu, A. A. Samatar, V. Madison, L. Xiao, *Biochim. Biophys. Acta*, 2001, **1526**, 257.
- ⁶ a) Z. Z. Yang, O. Tschopp, A. Baudry, B. Dummler, D. Hynx, B. A. Hemmings, *Biochem. Soc. Trans.*, 2004, **32**, 350.
b) B. Dummler, B. A. Hemmings, *Biochem. Soc. Trans.*, 2007, **35**, 231.
- ⁷ Q. Li, *Exp. Op. Ther. Pat.*, 2007, **17**, 1077.
- ⁸ H. Hidaka and R. Kobayashi, *Annu. Rev. Pharmacol. Toxicol.*, 1992, **32**, 377.
- ⁹ C. Kuijl, A. W. Tuin, H. S. Overkleeft and J. Neefjes, *Nature*, 2008, **4**, 1001.
- ¹⁰ Compounds **1 – 76**, **113 – 133**, **170 – 193** and **230 – 239**: Thesis A. W. Tuin, *Synthetic Studies on Kinase Inhibitors and Cyclic Peptides: Strategies Towards New Antibiotics*, 2008.
- ¹¹ H. Reuveni, N. Livnah, T. Geiger, S. Klein, O. Ohne, I. Cohen, M. Benhar, G. Gellerman and A. Levitzki, *Biochem.*, 2002, **41**, 10304.
- ¹² I. Collins, J. Caldwell, T. Fonseca, A. Donald, V. Bavetsis, L-J. K. Hunter, M. D. Garrett, M. G. Rowlands, g. W. Aherne, T. G. Davies, V. Berdini, S. J. Woodhead, D. Davis, L. C. A. Seavers, P. G. Wyatt, P. Workman and E. McDonald, *Bioorg. Med. Chem.*, 2006, **14**, 1255.
- ¹³ T. G. Davies, M. L. Verdonk, B. Graham, S. Saaulau-Bethell, c. C. F. Hamlett, T. McHardy, I. Collins, M. D. Garrett, P. Workman, S. J. Woodhead, H. Jhoti and D. Barford, *J. Mol. Biol.*, 2007, **367**, 882.
- ¹⁴ Company DiscoverX Corporation, United States.
- ¹⁵ D. L. Stirewalt and J. P. Radlich, *Nat. Rev.*, 2003, **3**, 650.
- ¹⁶ B. Scheijen, H. T. Ngo, H. Kang and J. D. Griffin, *Onc.*, 2004, **23**, 3338.
- ¹⁷ M. Jonsson, M. Engstrom and J-I. Jonsson, *Biochem. and Biophys Res. Comm.*, 2004, **318**, 899.

Chapter 4

¹⁸ a) N. N. Kabir, L. Ronnstrand and J. U. Kazi, *Med. Oncol.*, 2013, **30**, 462. b) C. A. Portell and A. S. Advani, *Leukemia & Lymphoma*, 2014, **55**, 737.

¹⁹ M. R Grunwald and M. J. Levis, *Int. J. Hematol.*, 2013, **97**, 683.

²⁰ D. J. Moshinsky, L. Ruslim, R. A. Blake and F. Tang, *J. Biomol. Screen.*, 2003, **8**, 447.

5

Direct and two-step bioorthogonal probes for Bruton's tyrosine kinase based on ibrutinib: a comparative study

N. Liu, S. Hoogendoorn, B. van der Kar, A. Kaptein, T. Barf, C. Driessen, D. V. Filipov, G. A. van der Marel, M. van der Stelt, H. S. Overkleeft, *Organic and Biomolecular Chemistry*, 2015, **13**, 5147.

5.1 Introduction

Bruton's tyrosine kinase (BTK), a nonreceptor tyrosine kinase member of the Tec kinase family, is involved in B cell receptor (BCR) signaling and governs B-lymphocyte development, differentiation, signaling and survival.^{1,2,3} Aberrant BTK activity is a fundamental feature of the human B-cell malignancies; chronic lymphocytic leukemia (CLL), mantle cell lymphoma (MCL), follicular lymphoma (FL), diffuse large B-cell lymphoma (DLBCL), and Waldenström's macroglobulinemia (WM).^{4,5,6,7}

The First-in-Class BTK-inhibitor ibrutinib (Imbruvica®, PCI-32765, **1**, Figure 1) has recently been approved for the treatment of WM, MCL and CLL by the FDA.^{8,9,10,11} Apart from its clinical efficacy, ibrutinib is of interest because of its mechanism of action. Ibrutinib irreversibly blocks BTK activity through covalent modification of Cys481 within the enzyme ATP-binding pocket following conjugate addition of the cysteine thiol to the acrylamide moiety in **1** (Figure 1), an event that prevents phosphorylation of Tyr223, an essential step for BTK activation. At present, numerous covalent kinase inactivators are pursued for a range of human malignancies.¹² Besides the clinical relevance of mechanism-based inhibitors (long residence time, lasting inhibitory effect which is only dependent on de novo synthesis of the protein target), covalent and irreversible enzyme inhibitors are highly useful starting points for the development of activity-based protein profiling (ABPP) probes.^{13,14,15} Such probes, also termed activity-based probes (ABPs), are composed of a mechanism-based enzyme inhibitor modified to contain an identification tag, which can be a biotin (for visualisation and/or enrichment), a fluorophore (for visualisation), or a bioorthogonal tag (to install a fluorophore or affinity tag following enzyme labeling).

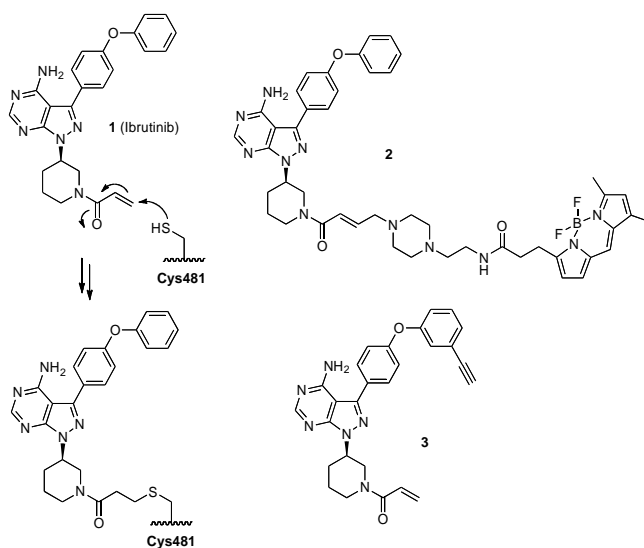


Figure 1. Mechanism-based inactivation of Bruton's tyrosine kinase (BTK) by ibrutinib (**1**) (left) and the direct (**2**) and two-step (**3**) BTK activity-based probes reported to date (right).

In the recent literature both direct and two-step bioorthogonal ibrutinib-based ABPs have been described. Honigberg and co-workers reported on the development of BODIPY-FL-ibrutinib **2** and its application in detection of BTK in

BTK-positive tumor cells and mouse models of autoimmune disease.¹⁰ Cravatt and co-workers in turn described ibrutinib-alkyne **3** as part of a series of alkyne-modified covalent kinase inhibitors in a broad-spectrum Huisgen [2+3]-cycloaddition 'click'-based two-step ABPP study on kinase activities in a variety of tumor tissues.¹⁶ Recently, a near infra-red (IR) fluorescent agent has been developed that can be used for spatial profiling of BTK expression in malignancies or other inflammatory tissues and pharmacokinetic and pharmacodynamic studies at the single cell level.¹⁷

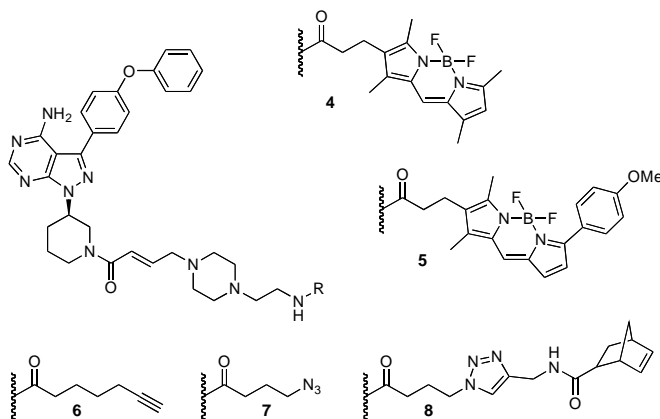


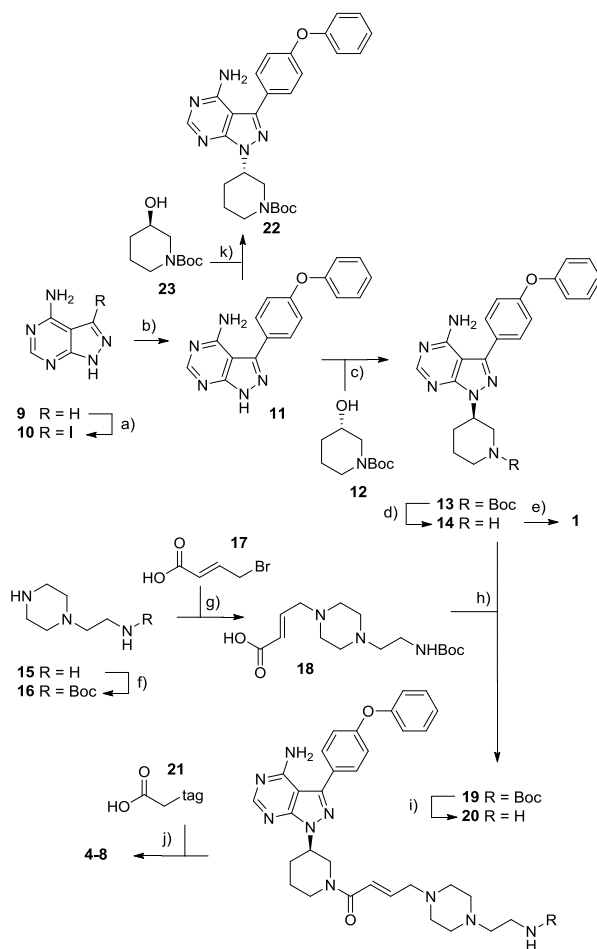
Figure 2. Direct (**4** and **5**) and two-step bioorthogonal (**6-8**) BTK activity-based probes that are subject of the here presented study.

The ABPP research in this chapter describes a head-to-head comparison of direct and two-step bioorthogonal ABPP methodologies.¹⁸ In these studies, assessment of the relative efficiency of Cu(I)-catalyzed and strain-promoted azide-alkyne [2+3] cycloaddition, Staudinger-Bertozzi ligation and inverse-electron demand Diels-Alder ligation have been included. Previously it has been shown that with the exception of strain-promoted alkyne-azide cycloadditions all of the above are effective bioorthogonal chemistries in the two-step ABPP modification of the catalytic activities of mammalian proteasomes and moreover that these reactions can be executed consecutively in a multiplexing fashion in a single biological sample.¹⁹ This chapter describes a comparative study in which BTK-positive Ramos cells have been probed for catalytically active BTK levels with direct ABPs **4** and **5** (Figure 2) as well as with two-step ABPs **6** and **7** (Cu(I)-catalyzed azide-alkyne [2+3] cycloaddition) and **8** (inverse-electron demand Diels-Alder).

5.2 Results and discussion

Synthesis of ibrutinib and ibrutinib-based ABPs

Perusal of the literature on structure-activity relationship studies on ibrutinib revealed that analogues featuring a piperazinyl extension at the acrylamide side of the parent compound are well tolerated by the target enzyme, BTK. Weissleder and co-workers used this finding in their design of direct BTK ABP **2** (Figure 1).^{20,21}



Scheme 1. Reagents and conditions: a) *N*-iodosuccinimide, DMF, 80 °C, 87%; b) K_3PO_4 , 4-phenoxybenzoic acid, $Pd(PPh_3)_4$, dioxane, 180 °C, 79%; c) **12**, PPh_3 polymer-bound, DIAD, THF, 56%; d) 4.0 M HCl in dioxane, 100%; e) acryloyl chloride, TEA, DCM, 46%; f) i) benzaldehyde, Cbz-Cl, toluene, 38%; ii) Boc_2O , THF, 79%; iii) Pd/C , H_2 , MeOH, 94%; g) **17**, TEA, THF; h) **14**, HATU, TEA, DMF, 87%; i) 4.0 M HCl in dioxane, 100%; j) HATU, DiPEA, DMF, **21**, **4**: 17%, **5**: 10%, **6**: 36%, **7**: 22%, **8**: 10%; k) **23**, PPh_3 polymer-bound, DIAD, THF, 61%.

Based on these literature findings ibrutinib derivative **20** (Scheme 1) has been used as common core onto which the BODIPY fluorophores and two-step bioorthogonal ligation handles as depicted in Figure 2 are grafted. Thus the first research objective was to synthesise amine **20** (Scheme 1).

Iodide **10** was prepared from commercially available aminopyrazolopyrimidine **9** in an electrophilic aromatic substitution using *N*-iodosuccinimide as the iodinating agent. Ensuing Suzuki coupling with 4-phenoxybenzene boronic acid according to the literature procedure provided diphenyl ether **11**, which was reacted with enantiopure (S)-*N*-Boc-3-hydroxypiperidine **12** under Mitsunobu conditions to give intermediate **13** with full inversion of stereochemistry.^{22, 23, 24} To prove that the Mitsunobu reaction gives enantiopure product, chiral HPLC was used to analyze and separate R-enantiomer **13** from S-enantiomer **22**, which was obtained in the same way as compound **13** except that enantiopure (R)-*N*-Boc-3-hydroxypiperidine **23** was used as the starting material (scheme 1). Figure 3 shows that the different chiral products **13** and **22** can be separated using chiral HPLC and that the used Mitsunobu reaction conditions give full inversion of stereochemistry in both situations.

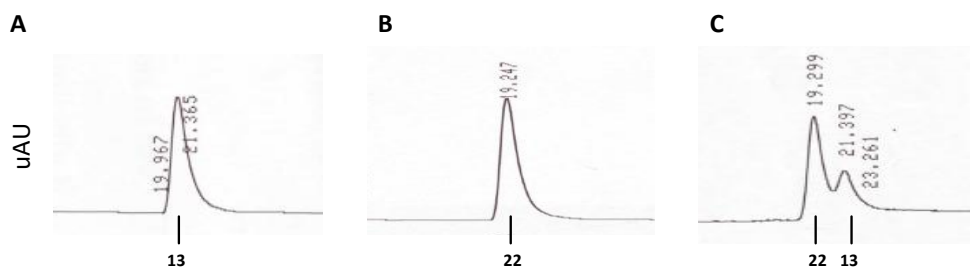


Figure 3. Chiral HPLC analysis of R-enantiomer **13** (A), S-enantiomer **22** (B), and a mixture of compound **13** and **22** (C).

The Boc protective group of the enantiopure R-enantiomer **13** was removed under acidic conditions. Subsequently, condensation of the thus liberated secondary amine with acryloyl chloride gave ibrutinib **1**, the analytical and spectral data of which were in full agreement with those reported in the literature.^{25,26} The synthesis of ABPs **4-8** requires access to piperazine-functionalised acrylate **18**, for which a synthesis scheme adapted from the patent literature by Astrazeneca was used.²⁷ In the first instance, it was attempted to prepare the precursor, single Boc-protected aminoethylpiperazine **16**, as described by treatment of aminoethylpiperazine with di-*tert*-butyldicarbonate in the presence of benzyl aldehyde. However, this one-step procedure, not unexpectedly,²⁸ failed. In this procedure, the secondary amine was protected as the benzyloxycarbamate, since

the primary amine reacted with benzaldehyde to form a benzylimine *in situ*. Therefore, the following three-step procedure has been used as depicted in scheme 1.²⁹ Thus, *in situ* formation of the primary benzylimine, ensuing Cbz protection of the secondary amine and liberation of the primary amine yielded mono-Cbz-aminoethylpiperazine, with the secondary amine temporarily protected as the benzyloxycarbamate. Introduction of the Boc protective group at this stage followed by hydrogenolysis of the Cbz group afforded compound **16**, which was *N*-alkylated with *E*-bromobutenoic acid **17**³⁰ to yield compound **18**. Condensation of **14** and **18** under the agency of HATU and triethylamine followed by acidic removal of the Boc group afforded ibrutinib derivative **20**. Condensation (HATU, DiPEA) with the appropriately modified tags **21** (see for the used tags the experimental section) afforded target direct ABPs **4** and **5** as well as the two-step bioorthogonal ABPs (**6-8**) in moderate yield but good purity after HPLC purification.

Evaluation of the inhibitory potency and labeling efficiency

In the first instance, the ability of the potential ABPs **4-8** to inhibit BTK was established. Non-fluorescent derivatives **6-8** were measured in an immobilized metal ion affinity-based fluorescence polarization (IMAP) assay using recombinantly expressed human BTK with ibrutinib **1** included as benchmark. Fluorescent, direct ABPs **4** and **5** were added to Ramos cell extract, which contains endogenously expressed BTK, after which the protein content was denatured and resolved on SDS-PAGE.

Direct and two-step bioorthogonal probes for Bruton's tyrosine kinase based on ibrutinib: a comparative study

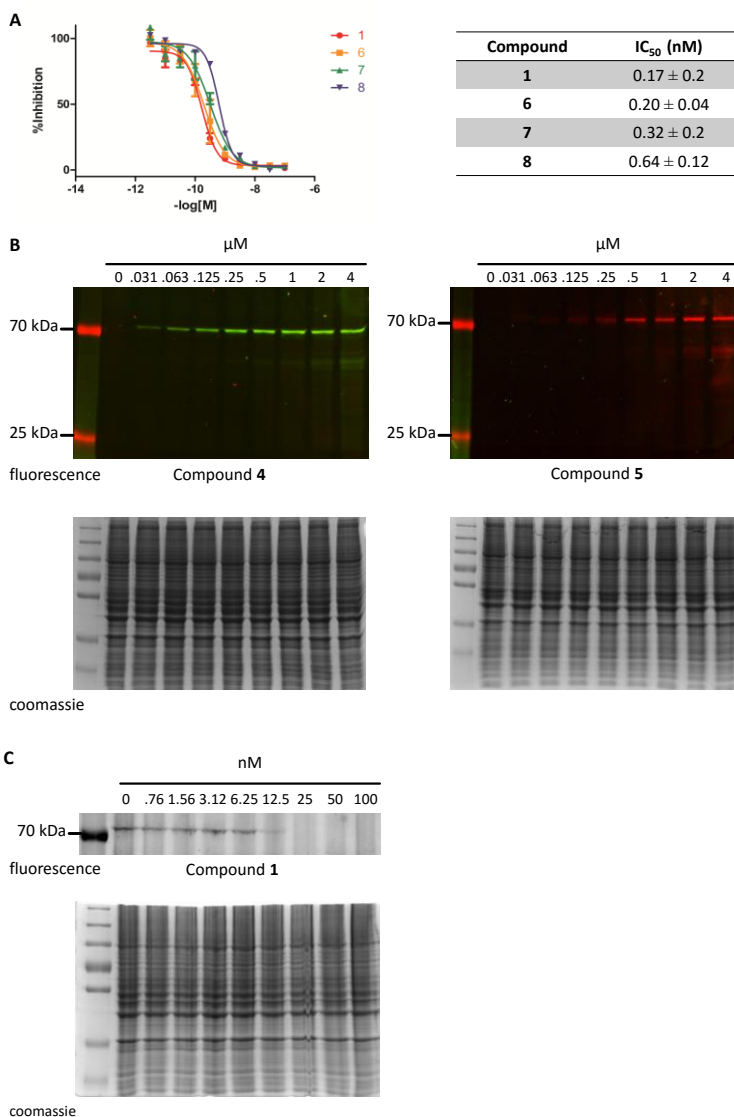


Figure 4. A) BTK inhibitory potency (IC₅₀) of ibrutinib **1** and two-step bioorthogonal ABPs **6-8**. The mean IC₅₀ values are calculated from two independent experiments performed in duplicate. B) BTK labeling efficiency of direct ABPs **4** and **5** in Ramos cell extract. Ramos cell extracts were exposed for 1 hr at room temperature to the indicated concentrations of ABP **4** or **5**. Three independent experiments were performed. C) Competition experiments of ibrutinib **1** versus fluorescent ABP **4** in Ramos cell lysates. Three independent experiments were performed. Ramos cell extracts were exposed to the indicated concentrations of ibrutinib **1** for 1 hr at room temperature and then incubated with ABP **4** (1 μM) for 1 hr at room temperature. Proteins were analysed by SDS-PAGE using detection by in-gel fluorescent readout. Coomassie staining was used as a loading control. Lane 1: Dual Color protein standard.

As can be seen from Figure 4A, ibrutinib analogues **6-8** inhibit recombinant, purified BTK with IC_{50} values in the same range as ibrutinib **1**. The fluorescent analogues **4** and **5** are not compatible with the IMAP assay and thus in an activity-based protein profiling setting, it was established whether these compounds would be able to detect ibrutinib. As can be seen (Figure 4B) both compounds label a single band with an apparent molecular weight corresponding to that of BTK. Of note, labeling of this protein could be prevented in a dose-dependent manner by pre-incubation with ibrutinib, strongly suggesting BTK specificity of these probes in live cells (Figure 4C).

Next, the ability of compounds **4-8** to target BTK in living cells was evaluated. Figure 5A shows that both green (**4**) and red (**5**) fluorescent probes readily and selectively modify BTK in a concentration-dependent manner. They do so at concentrations as low as 100 nM (for ABP **4**). Thus both direct ABPs behave as expected, given the literature precedent.³¹ This makes the probes also useful for the assessment of the inhibitory potency and cell permeability of putative BTK inhibitors in a competitive ABPP setting. To establish whether putative two-step ABPs **6-8** are able to reach and modify BTK in living cells, living Ramos cells were treated in culture with varying concentration of these compounds, prior to treatment with BODIPY-FL-ibrutinib **4**, cell lysis and SDS-PAGE. As is evident from Figure 5B, the three compounds abolish labeling at the lowest concentration (4 μ M; approximately 6000x IC_{50} value for all compounds, see Figure 4A) applied and it can thus be concluded that all 5 compounds – direct and two-step ABPs – are able to modify BTK in live cells.

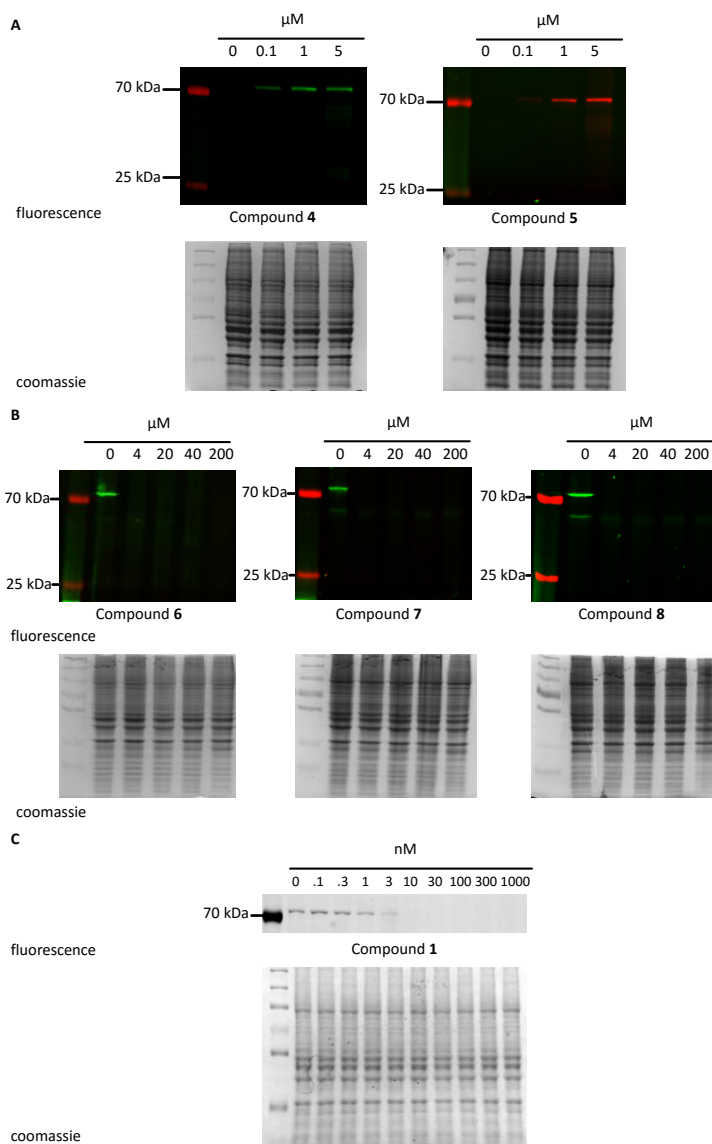


Figure 5. A) *In situ* labeling of BTK in Ramos cells by **4** and **5**. Ramos cells were exposed to the indicated concentrations of **4** or **5** for 4 hrs at 37° C. Proteins were analysed by SDS-PAGE using detection by in-gel fluorescent readout. Three independent experiments were performed. B) Competition experiments of BODIPY-FL-ibrutinib **4** versus compounds **6-8** in Ramos cells. Ramos cells were exposed to the indicated concentrations of ABP **6**, **7**, or **8** for 3 hrs at 37° C and then lysed. The cell lysates were exposed to 1 μM of BODIPY-FL-ibrutinib **4** for 1 hr at room temperature. Two independent experiments were performed. Labeled proteins were analyzed by SDS-PAGE and detected by in-gel fluorescent read-out. Coomassie staining was used as a loading control. Lane 1: Dual Color protein standard.

The efficiency and selectivity of the two-step ABPs **6-8** to modify BTK in living Ramos cells was assessed next. Figure 6 depicts the complementary reagents used in these experiments, that is, BODIPY-FL-modified bioorthogonal reagent **22**³² (for copper(I)-catalyzed alkyne-azide [2+3] cycloaddition (CuAAC) ligation to alkyne-modified ibrutinib **6**), BODIPY-green-alkyne **23**³³ (for copper(I)-catalyzed click ligation to azide-modified ibrutinib **7**) and BODIPY-FL-tetrazine **24**³² (for inverse-electron demand Diels-Alder ligation to norbornene-modified ibrutinib **8**).

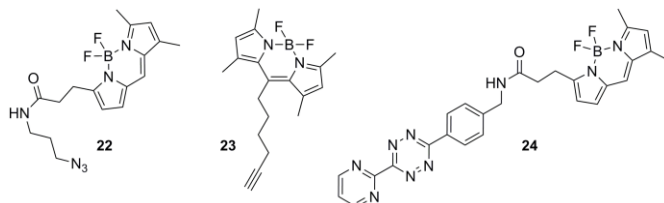


Figure 6. Ligation reagents used in the study described in this Chapter.

Ramos cell lysates were treated with ibrutinib-alkyne **6**, ibrutinib-azide **7** or ibrutinib-norbornene **8** at 4 micromolar final concentrations for one hour at room temperature. Next the samples were treated with the complementary bioorthogonal ligation handles **22-24** at various final concentrations for one hour. The proteins were resolved on SDS-PAGE and the wet gel slabs were analyzed by fluorescence read-out. As can be seen (Figure 7A) both copper(I)-catalyzed click reactions give BTK labeling in a concentration-dependent manner, as does the inverse-electron demand Diels-Alder (IEDDA) ligation. Though the two click ligation steps appear about equally effective in terms of activity, differences are apparent when considering aspecific reaction of the (click/tetrazine) ligation handles, with alkyne-azide click ligation giving the optimal result. The IEDDA ligation appears to proceed equally selective though the labeling intensity appears somewhat lower.

As a final set of experiments the ability of the two-step BTK ABPs to modify BTK *in situ* in living Ramos cells has been explored (Figure 7D). For this purpose, Ramos cells were treated with 4 micromolar **6-8** for 1 hour at 37 °C. For the purpose of the two CuAAC click ligations the cells were lysed, whereas IEDDA ligation (addition of norbornene **24**) was performed *in situ* and *in vitro*. As can be seen (Figure 7D) also these partial or complete *in situ* ligations proved successful, with here the two CuAAC ligations more selective compared to the IEDDA ligation.

Direct and two-step bioorthogonal probes for Bruton's tyrosine kinase based on ibrutinib: a comparative study

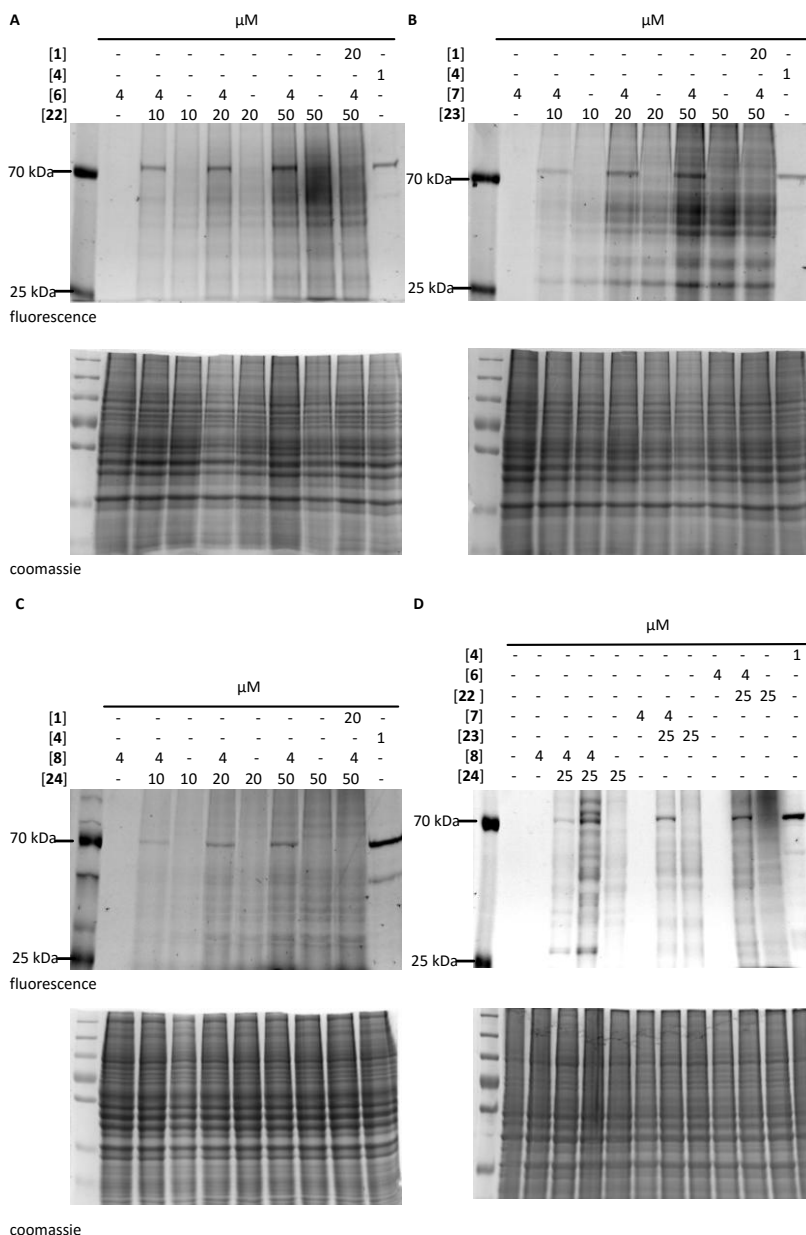


Figure 7. A-C) *In vitro* two-step bioorthogonal labeling of BTK in Ramos cell extract using reagent pairs (6/22), (7/23) and (8/24). Ramos cell lysates were exposed to ABP 6 or 7 for 1 hr at room temperature and then reacted with the indicated concentrations of BODIPY-azide 22 or BODIPY-alkyne 23 for 1 hr at room temperature. Copper-catalyzed click reactions were performed in the presence of CuSO_4 (6.5 mM), Tris(3-hydroxypropyltriazolylmethyl) amine (THPTA, 6.5 mM) and sodium L-ascorbate (6.5 mM). Alternatively, ABP 8 (4 μM) was used for ligation with tetrazine 24. In control experiments different

ligation strategies were performed in the absence of ABP **6-8** or after competition by an excess of ibrutinib **1**. As a positive control, extracts were labelled with fluorescent ABP **4** (1 μ M). Three independent experiments were performed. D) Two-step bioorthogonal profiling of BTK activity by different ligation strategies. Ramos cells were exposed to ABP **6-8** (4 μ M) for 3 hrs at 37 °C, washed, lysed, and then reacted with their corresponding ligation reagent **22-24** (25 μ M) for 1 hr at room temperature. Alternatively, cells were consecutively exposed to ABP **8** and ligation reagent **24** *in situ* (lane 5). In control experiments different ligation strategies were performed in the absence of ABP **6-8** and/or ligation reagent. As a positive control, cells were labelled with fluorescent ABP **4** (1 μ M). Three independent experiments were performed. Proteins were analysed by SDS-PAGE using detection by in-gel fluorescent readout. Coomassie staining was used as a loading control. Lane 1: Dual Color protein standard.

5.3 Conclusion

The BTK activity-based probe set has been expanded by the development of two direct ABPs **4** and **5** equipped with BODIPY fluorophores that emit at two distinct wavelengths, as well as three bioorthogonal two-step ABPs that can be addressed through either CuAAC or IEDDA bioorthogonal chemistry. As such this BTK imaging toolset adds to the existing BTK probes – both direct and two-step – for measuring catalytically active BTK in various settings. Though direct imaging with BODIPY-ibrutinib derivatives **4** and **5** appears most effective in live cells, the situation may differ in case live animals are to be subject of study and for this purpose the IEDDA bioorthogonal ABP pair **8/24** may be most effective – even though labeling efficiency appears the lowest. In an alternative setting, BTK occupancy may be monitored in conjunction with other enzymatic activities in a multiplexing setting, using either the direct probes in conjunction with ABPs targeting other enzymes and equipped with complementary fluorophores, or by making use of a number of mutually exclusive bioorthogonal ligations.

Experimental

General: Tetrahydrofuran (THF) was distilled over LiAlH₄ before use. Acetonitrile (ACN), dichloromethane (DCM), *N,N*-dimethylformamide (DMF), methanol (MeOH) and trifluoroacetic acid (TFA) were of peptide synthesis grade, purchased at Biosolve, and used as received. All general chemicals (Fluka, Acros, Merck, Aldrich, Sigma) were used as received. Traces of water were removed from reagents used in reactions that require anhydrous conditions by coevaporation with toluene. Solvents that were used in reactions were stored over 4Å molecular sieves, except methanol and acetonitrile, which were stored over 3Å molecular sieves. Molecular sieves were flame dried before use. Unless noted otherwise all reactions were performed under an argon atmosphere. Column chromatography was performed on Silicycle Silia-P Flash Silica Gel, with a particle size of 40 – 63 μ m. The

Direct and two-step bioorthogonal probes for Bruton's tyrosine kinase based on ibrutinib: a comparative study

eluent toluene and ethyl acetate were distilled prior to use. TLC analysis was conducted on Merck aluminium sheets (Silica gel 60 F254). Compounds were visualized by UV absorption (254 nm), by spraying with a solution of $(\text{NH}_4)_6\text{Mo}_7\text{O}_{24}\cdot 4\text{H}_2\text{O}$ (25 g/L) and $(\text{NH}_4)_4\text{Ce}(\text{SO}_4)_4\cdot 2\text{H}_2\text{O}$ (10 g/L) in 10% sulphuric acid, a solution of KMnO_4 (20 g/L) and K_2CO_3 (10 g/L) in water, or ninhydrin (0.75 g/L) and acetic acid (12.5 mL/L) in ethanol, where appropriate, followed by charring at ca. 150 °C. ^1H - and ^{13}C -NMR spectra were recorded on a Bruker DMX-400 (400 MHz) or a Bruker DMX-600 (600 MHz) spectrometer. Chemical shifts are given in ppm (δ) relative to tetramethylsilane (^1H -NMR) or CDCl_3 (^{13}C -NMR) as internal standard. Mass spectra were recorded on a PE/Sciex API 165 instrument equipped with an Electrospray Interface (ESI) (Perkin-Elmer). High-resolution MS (HRMS) spectra were recorded with a Finnigan LTQ-FT (Thermo Electron). IR spectra were recorded on a Shimadzu FTIR-8300 and absorptions are given in cm^{-1} . Optical rotations $[\alpha]_D^{23}$ were recorded on a Propol automatic polarimeter at room temperature. LC-MS analysis was performed on a Jasco HPLC system with a Phenomenex Gemini 3 μm C18 50 x 4.6 mm column (detection simultaneously at 214 and 254 nm), coupled to a PE Sciex API 165 mass spectrometer with ESI. HPLC gradients were 10 \rightarrow 90%, 0 \rightarrow 50% or 10 \rightarrow 50% ACN in 0.1% TFA/ H_2O . Chiral HPLC analysis was performed on a Spectroflow 757 system (ABI Analytical Kratos Division, detection at 254 nm) equipped with a Chiralcel OD column (150 x 4.6 mm). The compounds were purified on a Gilson HPLC system coupled to a Phenomenex Gemini 5 μm 250 x 10 mm column and a GX281 fraction collector. The used gradients were either 0 \rightarrow 30% or 10 \rightarrow 40% ACN in 0.1% TFA/water, depending on the lipophilicity of the product. Appropriate fractions were pooled, and concentrated in a Christ rotary vacuum concentrator overnight at room temperature at 0.1 mbar.

3-Iodo-1H-pyrazolo[3,4-d]pyrimidin-4-amine (10)

To a solution of 4-aminopyrazolo[3,4-d]pyrimidine (**9**, 2.50 g, 18.5 mmol) in DMF (43 mL) was added *N*-iodosuccinimide (1.5 eq., 6.24 g, 27.7 mmol) and the mixture was heated to 80 °C overnight, before being cooled to 0 °C. H_2O (110 mL) was added and the mixture was allowed to stand at 0 °C for 30 min followed by filtration of the solid. The residue was washed with ice-cold EtOH, Et₂O and EtOAc and dried *in vacuo*. The title compound was obtained without further purification as a pale yellow solid (yield: 4.22 g, 16.17 mmol, 87%). R_f = 0.30 (10% MeOH/DCM). ^1H NMR (400 MHz, DMSO- d_6) δ 13.84 (s, 1H, NH), 8.17 (s, 1H, CH). ^{13}C NMR (101 MHz, DMSO- d_6) δ 157.50, 155.90, 155.0, 102.51, 89.88.

3-(4-Phenoxyphenyl)-1H-pyrazolo[3,4-d]pyrimidin-4-amine (11)

Compound **10** (0.20 g, 0.77 mmol), K_3PO_4 (3 eq., 0.49 g, 2.30 mmol), 4-phenoxybenzene boronic acid (3 eq., 0.49 g, 2.29 mmol) and $\text{Pd}(\text{PPh}_3)_4$ (0.14 eq., 0.12 g, 0.11 mmol) were dissolved in sonicated dioxane (2.5 mL) in a microwave vial. The resulting mixture was heated to 180 °C for 10 min under microwave irradiation. EtOAc (10 mL) was added and the mixture was washed with H_2O and brine before being dried over MgSO_4 , filtered and concentrated under reduced pressure. The title compound was obtained after purification by column chromatography (100% DCM \rightarrow 4% MeOH/DCM) as a white solid (yield: 0.18 g, 0.61 mmol, 79%). R_f = 0.19 (5% MeOH/DCM). ^1H NMR (400 MHz, DMSO- d_6) δ 13.58 (s, 1H, NH), 8.22 (s, 1H, CH), 7.67 (d, J = 8.8 Hz, 2H, 2xCH), 7.43 (t, J = 8.0 Hz, 2H, 2xCH), 7.20 – 7.11 (m, 5H, 5xCH). ^{13}C NMR (101 MHz, DMSO- d_6) δ 158.11, 157.04, 156.33,

155.82, 143.99, 130.17, 128.48, 123.82, 119.05, 96.95. LC-MS analysis: Rt 5.63 min (linear gradient 10-90% acetonitrile in H₂O, 0.1% TFA, 15 min). ESI-MS (*m/z*): 304.07 [M+H⁺].

***Tert*-butyl(R)-3-(4-amino-3-(4-phenoxyphenyl)-1H-pyrazolo[3,4-d]pyrimidin-1-yl)piperidine-1-carboxylate (13)**

To a suspension of (S)-1-Boc-3-hydroxypiperidine **12** (2 eq., 1.24 g, 6.2 mmol) and polymer-bound triphenylphosphine (3 eq., 3.08 g, 9.2 mmol) in THF (20 mL) was added dropwise diisopropyl diazodicarboxylate (2 eq., 1.21 mL, 6.1 mmol) and the reaction mixture was stirred for 5 min. Compound **11** (0.93 g, 3.08 mmol) was added and the resulting mixture was heated with a heatgun for 5 min. The suspension was stirred overnight before being filtered over Celite to remove the resins and the resins were washed with MeOH and DCM. The filtrate was concentrated and the target compound was obtained by column chromatography (40% → 55% EtOAc/Pentane) as a yellow solid (yield: 0.84 g, 1.72 mmol, 56%). *R*_f = 0.50 (90% EtOAc/Pentane). ¹H NMR (400 MHz, CDCl₃) δ 8.31 (s, 1H, CH), 7.65 (d, *J* = 8.4 Hz, 2H, 2xCH), 7.35 (t, *J* = 8.0 Hz, 2H, 2xCH), 7.15 – 7.12 (m, 3H, 3xCH), 7.06 (d, *J* = 8.0 Hz, 2H, 2xCH), 4.90 – 4.81 (m, 1H, CH), 4.36 – 4.19 (m, 1H), 4.12 – 4.06 (m, 1H), 3.50 – 3.34 (m, 1H), 2.86 (t, *J* = 10.8 Hz, 1H), 2.31 – 2.16 (m, 2H), 1.93 – 1.88 (m, 1H), 1.72 – 1.67 (m, 1H), 1.44 (s, 9H). ¹³C NMR (101 MHz, CDCl₃) δ 158.10, 157.97, 156.02, 154.87, 154.30, 143.63, 130.60, 128.50, 124.44, 119.37, 98.09, 79.51, 52.51, 48.20, 44.05, 29.90, 28.95, 24.51. LC-MS analysis: Rt 8.26 min (linear gradient 10-90% acetonitrile in H₂O, 0.1% TFA, 15 min). ESI-MS (*m/z*): 487.13 [M+H⁺].

(R)-3-(4-phenoxyphenyl)-1-(piperidin-3-yl)-1H-pyrazolo[3,4-d]pyrimidin-4-amine (14)

Compound **13** (0.05 g, 0.1 mmol) was stirred in 4.0 M HCl in dioxane (1 mL) for 2 hrs. The reaction mixture was concentrated *in vacuo* and the residue was suspended in EtOAc before being filtered. The residue was washed with EtOAc and dried under reduced pressure. The title compound was obtained without further purification as a white solid (yield: 0.042 g, 0.1 mmol, 100%). *R*_f = 0.05 (90% EtOAc/Pentane). LC-MS analysis: Rt 5.34 min (linear gradient 10-90% acetonitrile in H₂O, 0.1% TFA, 15 min). ESI-MS (*m/z*): 387.01 [M+H⁺].

Ibrutinib (1)

To a solution of crude amine **14** (0.20 mmol) in DCM (1 mL) were added TEA (3.0 eq., 84 μL, 0.6 mmol) and acryloyl chloride (1.3 eq., 20 μL, 0.26 mmol). The resulting mixture was stirred overnight prior to washing with aqueous solution of citric acid (5%, 5 mL) and brine. The title compound was obtained after RP-HPLC purification (linear gradient 40% → 60% ACN in H₂O, 0.1% TFA, 15 min) as a white solid (yield: 12.0 g, 92.0 μmol, 46%). ¹H NMR (600 MHz, DMSO-*d*₆) δ 8.42 (s, 1H), 7.67 (d, *J* = 7.2 Hz, 2H), 7.44 (t, *J* = 7.2 Hz, 2H), 7.19 (t, *J* = 7.2 Hz, 1H), 7.16 (d, *J* = 9.0 Hz, 2H), 7.13 (d, *J* = 9.0 Hz, 2H), 6.85 (t, *J* = 13.2, 0.5 H), 6.69 (t, *J* = 15.6 Hz, 0.5 H), 6.13 (d, *J* = 16.2 Hz, 0.5H), 6.06 (d, *J* = 16.8 Hz, 0.5H), 5.70 (d, *J* = 10.2 Hz, 0.5H), 5.59 (d, *J* = 9.6 Hz, 0.5H), 4.79 – 4.71 (m, 1H), 4.56 (d, *J* = 10.8 Hz, 1H), 4.19 (br s, 1H), 4.06 (d, *J* = 13.2 Hz, 0.5H), 3.71 (t, *J* = 10.8 Hz, 0.5H), 3.26 – 3.19 (m, 1H), 3.04 (t, *J* = 12.0 Hz, 0.5H), 2.30 – 2.23 (m, 1H), 2.15 – 2.13 (m, 1H), 1.95 – 1.92 (m, 1H), 1.66 – 1.54 (m, 1H). ¹³C NMR (150 MHz, DMSO-*d*₆) δ 164.64, 157.48, 156.15, 152.66, 144.73, 130.11, 128.28, 127.49, 127.21, 126.95, 126.12, 123.86, 119.02, 115.76, 97.06, 53.03, 52.41, 49.220, 45.65, 45.12, 41.54, 29.49, 29.27, 24.74, 23.13. IR film (cm⁻¹): 2936.8, 1688.8, 1609.7, 1586.58, 1516.1, 1489.1, 1436.1, 1233.5, 1197.9, 1134.2, 856.9, 801.6, 759.6, 725.3, 698.6. HRMS: calculated for C₂₅H₂₄N₆O₂ [M+H⁺]: 441.20335; found: 441.20315.

***Tert*-butyl 2-(piperazin-1-yl)ethyl)carbamate (16)**

1-(2-Aminoethyl)piperazine (**15**, 32.8 mL, 250 mmol) and benzaldehyde (1 eq., 25.5 mL, 250 mmol) were dissolved in toluene (200 mL) and the reaction mixture was refluxed over a Dean-Stark apparatus in 3 hrs, cooled to 0 °C, and treated with dropwise addition of benzylchloroformate (1 eq., 38 mL, 250 mmol). The resulting mixture was stirred overnight before being concentrated. The residue was dissolved in MeOH (500 mL), cooled to 0 °C and treated with 2 N HCl (125 mL). The resulting mixture (pH 1-2) was allowed to warm up to RT and concentrated under reduced pressure. The aqueous layer was washed with DCM before being made basic with NH₄OH (pH = 10) and extracted with DCM (3x), washed with brine, dried, filtered and evaporated. The residue was applied to silica column chromatography (4% → 6% MeOH/DCM + 1% TEA) to afford benzyl 4-(2-aminoethyl)piperazine-1-carboxylate as a yellowish oil (yield: 25.15 g, 95.5 mmol, 38%). R_f = 0.20 (20% MeOH/DCM). ¹H NMR (400 MHz, CDCl₃) δ 7.36 – 7.28 (m, 5H, CH_{ar}), 5.12 (s, 2H, CH₂), 3.51 (t, J = 4.8 Hz, 4H, 2xCH₂), 2.79 (t, J = 6.0 Hz, 2H, CH₂), 2.44 (t, J = 6.0 Hz, 2H, CH₂), 2.40 (br s, 4H, 2xCH₂), 2.30 (s, 2H, NH₂). ¹³C NMR (101 MHz, CDCl₃) δ 154.76, 136.32, 128.09, 127.59, 127.44, 67.10, 60.06, 52.48, 43.42, 38.03. After the solution of the carboxylate product (12.58 g, 47.75 mmol) in THF (200 mL) was cooled to 0 °C, Boc₂O (1.2 eq., 12.51 g, 57.30 mmol) was added portion wise and the reaction mixture was allowed to warm up to RT overnight before being concentrated. The residue was further purified by silica column chromatography (20% → 30% EtOAc/Pentane) to afford benzyl 4-(2-((tert-butoxycarbonyl)amino)ethyl)piperazine-1-carboxylate as a yellowish oil (13.71 g, 37.72 mmol, 79%). R_f = 0.30 (80% EtOAc/Pentane). ¹H NMR (400 MHz, CDCl₃) δ 7.37 - 7.30 (m, 5H, CH_{ar}), 5.13 (s, 2H, CH₂), 4.98 (br s, 1H, NH), 3.51 (t, J = 5.2 Hz, 4H, 2xCH₂), 3.25 – 3.21 (m, 2H, CH₂), 2.46 (t, J = 6.0 Hz, 2H, CH₂), 2.41 (br s, 4H, 2xCH₂). ¹³C NMR (101 MHz, CDCl₃) δ 155.85, 155.11, 136.59, 128.42, 127.96, 127.82, 79.17, 67.05, 57.14, 52.53, 43.67, 36.93, 28.35. HRMS: calculated for C₁₉H₂₉N₃O₄ [M+H]⁺: 364.21581; found: 364.20315.

To a solution of 4-(2-((tert-butoxycarbonyl)amino)ethyl)piperazine-1-carboxylate (1.82 g, 5.0 mmol) in MeOH (20 mL) Pd/C (10% w/w, 150 mg) was added. Hydrogen gas was then bubbled through the mixture overnight. The reaction mixture was filtered over Celite and concentrated to obtain the target compound as a yellowish oil (yield: 1.08 g, 4.71 mmol, 94%). The target compound was used without further purification. R_f = 0.29 (1/1/1 v/v/v H₂O/ACN/*t*BuOH). ¹H NMR (400 MHz, MeOD) δ 3.80 - 3.65 (m, 6H, 3xCH₂), 3.57 – 3.51 (m, 4H, 2xCH₂), 3.38 (t, J = 7.6 Hz, 2H, CH₂), 1.46 (s, 9H, 3xCH₃). ¹³C NMR (101 MHz, MeOD) δ 158.03, 80.43, 57.74, 54.59, 53.30, 49.87, 41.93, 36.11, 35.09, 28.67. HRMS: calculated for C₁₁H₂₃N₃O₂ [M+H]⁺: 230.17903; found: 230.17907.

(*E*)-4-bromobut-2-enoic acid (17)

To a solution of commercially available crotonic acid (10 g, 116 mmol) in benzene (150 mL) was added *N*-bromosuccinimide (1.1 eq., 22.74 g, 120 mmol) and benzoyl peroxide (0.01 eq, 0.45 g, 1.4 mmol) and the resulting mixture was refluxed for 4 hrs. The reaction mixture was then allowed to cool to 0 °C, which resulted in precipitation of succinimide crystals. The crystals were filtered over Celite and washed with toluene. The filtrate was concentrated and the residue was recrystallized from hexanes yielding the title compound as a pale yellow solid (yield: 9.55 g, 57.9 mmol, 50%). R_f = 0.79 (1/1/1 v/v/v H₂O/ACN/*t*BuOH). ¹H NMR (400 MHz, CDCl₃) δ 9.04 (bs, 1H), 7.12 (m, 1H), 6.05 (d, J = 15.2 Hz, 1H), 4.04 (dd, J_1 = 1.2 Hz, J_2 = 7.2 Hz, 2H). ¹³C NMR (101 MHz, CDCl₃) δ 170.41, 144.20, 123.79, 28.72.

(E)-4-(4-(2-((tert-butoxycarbonyl)amino)ethyl)piperazin-1-yl)but-2-enoic acid (18)

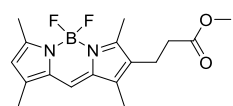
Compound **17** (1 eq., 0.22 g, 1 mmol) was dissolved in THF (5 mL). A solution of compound **16** (0.27 g, 1 mmol) and TEA (3 eq., 0.42 mL, 3.0 mmol) in THF (2 mL) was added and the mixture was stirred overnight and concentrated under reduced pressure. The title compound was used without further purification. $R_f = 0.29$ (1/1/1 v/v/v H₂O/ACN/*t*BuOH). LC-MS analysis: Rt 5.69 min (linear gradient 0-50% acetonitrile in H₂O, 0.1% TFA, 15 min). ESI-MS (m/z): 313.93 [$M+H^+$].

Tert-butyl (R,E)-2-(4-(4-(3-(4-amino-3-(4-phenoxyphenyl)-1H-pyrazolo[3,4-d]pyrimidin-1-yl)piperidin-1-yl)-4-oxobut-2-en-1-yl)piperazin-1-yl)ethyl)carbamate (19)

HATU (2.2 eq., 1.25 g, 3.3 mmol) was added to a solution of compound **18** (4 eq., 1.88 g, 6.0 mmol) and TEA (7 eq., 1.46 mL, 10.5 mmol) in DMF (5 mL) and the reaction mixture was allowed to stir for 1 min. A solution of amine **14** (0.63 g, 1.5 mmol) in DMF (2 mL) was added and the resulting mixture was stirred overnight. EtOAc (25 mL) was added and the organic layer was washed with sat. aq. NaHCO₃ and brine, dried over MgSO₄, filtered and concentrated *in vacuo*. The title compound was obtained after column chromatography (4% → 8% MeOH/DCM) as a brown solid (yield: 0.89 g, 1.31 mmol, 87%). $R_f = 0.55$ (10% MeOH/DCM). ¹H NMR (400 MHz, DMSO-*d*₆) δ 8.26 (s, 1H), 7.68 (d, *J* = 8.8 Hz, 2H), 7.42 (t, *J* = 7.6 Hz, 2H), 7.20 – 7.11 (m, 5H), 6.52 (t, *J* = 9.8 Hz, 1H), 6.48 – 6.42 (m, 2H), 5.88 (br s, 1H), 4.78 – 4.72 (m, 1H), 4.33 (d, *J* = 12.0 Hz, 1H), 4.01 (dt, *J* = 16, 8 Hz, 1H), 3.60 – 3.57 (m, 1H), 3.51 (t, *J* = 12 Hz, 1H), 3.27 – 3.18 (m, 1H), 3.10 – 3.04 (m, 6H), 2.42 – 2.37 (m, 6H), 2.21 – 2.17 (m, 1H), 2.03 – 1.96 (m, 1H), 1.70 – 1.59 (m, 1H), 1.41 (s, 9H). ¹³C NMR (101 MHz, DMSO-*d*₆) δ 164.36, 157.69, 156.91, 154.96, 153.82, 142.61, 139.95, 129.39, 127.66, 123.12, 122.37, 118.42, 97.38, 77.08, 57.99, 56.64, 52.32, 52.07, 47.51, 42.81, 37.39, 28.57, 27.73, 23.18. HRMS: calculated for C₃₇H₄₇N₉O₄ [$M+H^+$]: 682.37510; found: 682.37513. LC-MS analysis: Rt 6.05 min (linear gradient 10-90% acetonitrile in H₂O, 0.1% TFA, 15 min). ESI-MS (m/z): 682.13 [$M+H^+$].

(R,E)-1-(3-(4-(3-(4-amino-3-(4-phenoxyphenyl)-1H-pyrazolo[3,4-d]pyrimidin-1-yl)piperidin-1-yl)-4-(2-aminoethyl)piperazin-1-yl)but-2-en-1-one (20)

Compound **19** (0.015 g, 0.022 mmol) was stirred in 4.0 M HCl in dioxane (2 mL) for 2 hrs. The reaction mixture was concentrated *in vacuo* and the residue was suspended in EtOAc before being filtered. The residue was washed with EtOAc and dried under reduced pressure. The title compound was obtained without further purification as a white solid (yield: 0.013 g, 0.022 mmol, 100%). $R_f = 0.05$ (90% EtOAc/Pentane). LC-MS analysis: Rt 5.26 min (linear gradient 10-90% acetonitrile in H₂O, 0.1% TFA, 15 min). ESI-MS (m/z): 587.27 [$M+H^+$].

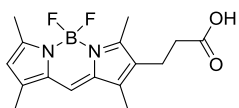
(R,E)-N-(2-(4-(4-(3-(4-amino-3-(4-phenoxyphenyl)-1H-pyrazolo[3,4-d]pyrimidin-1-yl)piperidin-1-yl)-4-oxobut-2-en-1-yl)piperazin-1-yl)ethyl)-3-(5,5-difluoro-1,3,7,9-tetramethyl-5H-5i4,6i4-dipyrrolo[1,2-*c*:2',1'-f][1,3,2]diazaborinin-2-yl)propanamide (4)

Carboxaldehyde pyrrole³⁴ (90 mg, 0.43 mmol, 1 eq) was dissolved in MeOH (5 mL) and 2,4-dimethylpyrrole (41 mg, 44 μL, 0.43 mmol, 1 eq) was added. The resulting mixture was cooled to 0°C, and hydrobromic acid, 48% solution in water (0.072 mL, 0.64 mmol, 1.5 eq) was added. After 2 h of stirring a yellowish precipitate formed

and TLC analysis showed complete consumption of the starting materials. The crude dipyrrole HBr salt was

Direct and two-step bioorthogonal probes for Bruton's tyrosine kinase based on ibrutinib: a comparative study

concentrated and coevaporated with DCE (3x) and dissolved in DCE (10 mL) under an argon atmosphere. Triethylamine (0.178 mL, 1.29 mmol, 3 eq) and $\text{BF}_3 \cdot \text{Et}_2\text{O}$ (0.57 mL, 2.15 mmol, 5 eq) were added, and the reaction was subsequently stirred at room temperature until TLC showed completion of the reaction. The solution was concentrated and the product purified by silica gel column chromatography (0% \rightarrow 2% EtOAc in toluene) which gave 4,4-Difluoro-1,3,7,9-tetramethyl-2-(2-(ethoxycarbonylmethyl))-4-bora-3a,4a-diaza-s-indacene (106 mg, 0.32 mmol, 74%). $R_f = 0.4$ (6:1 toluene:EtOAc). $^1\text{H-NMR}$ (400 MHz, CDCl_3) δ 6.99 (s, 1H), 6.00 (s, 1H), 3.66 (s, 3H), 2.70 (t, $J = 7.8$ Hz, 2H), 2.50 (s, 6H), 2.43 (t, $J = 7.8$, 2H), 2.18 (d, $J = 15.4$, 6H). $^{13}\text{C-NMR}$ (101 MHz, CDCl_3) δ 173.41, 156.51, 155.86, 141.20, 138.54, 133.59, 133.07, 128.61, 120.05, 119.08, 77.80, 77.48, 77.16, 52.04, 34.45, 19.86, 14.96, 13.03, 11.56, 9.87. LC-MS analysis (10% \rightarrow 90% ACN) Rt: 9.18 min, ESI-MS (m/z): $[\text{M}+\text{H}]^+$: 335.0; $[\text{M}-\text{F}]^+$: 315.2.



4,4-Difluoro-1,3,7,9-tetramethyl-2-(2-(ethoxycarbonylmethyl))-4-bora-3a,4a-diaza-s-indacene (106 mg, 0.32 mmol) was dissolved in MeOH (20 mL) and aq. NaOH (3.68 mL, 0.1 M, 1.15 eq, 0.37 mmol) was added. The mixture was heated to reflux for 1.5 h, after which by-product formation started to occur. The reaction was

quenched by the addition of aq. HCl (3.68 mL, 0.1 M, 1.15 eq), followed by extraction with EtOAc (3x). The organic layers were dried (MgSO_4), concentrated and 4,4-Difluoro-1,3,7,9-tetramethyl-2-(2-(carboxyethyl))-4-bora-3a,4a-diaza-s-indacene was obtained by silica column chromatography (0 \rightarrow 1% EtOAc in toluene (starting material) \rightarrow 1% EtOAc in toluene + 1% AcOH (product)) as a red powder (65 mg, 0.2 mmol, 64% (74% based on recovered starting material)). $R_f = 0.2$ (6:1 toluene:EtOAc + AcOH). λ_{abs} 514 nm/ λ_{em} 523 nm (MeOH). $^1\text{H-NMR}$ (400 MHz, CDCl_3) δ 7.01 (s, 1H), 6.02 (s, 1H), 2.72 (t, $J = 7.7$ Hz, 2H), 2.56 – 2.40 (m, 8H), 2.21 (d, $J = 14.7$ Hz, 6H). $^{13}\text{C-NMR}$ (101 MHz, CDCl_3) δ 178.68, 156.57, 155.48, 141.10, 138.22, 133.42, 132.77, 127.97, 119.84, 118.95, 34.16, 19.37, 14.76, 12.81, 11.36, 9.69. LC-MS analysis (10% \rightarrow 90% ACN) Rt: 7.94 min, ESI-MS (m/z): $[\text{M}+\text{H}]^+$: 320.93; $[\text{M}-\text{F}]^+$: 301.13.

HATU (1.3 eq., 49 mg, 0.13 mmol) was added to a solution of compound 4,4-Difluoro-1,3,7,9-tetramethyl-2-(2-(carboxyethyl))-4-bora-3a,4a-diaza-s-indacene (2 eq., 64 mg, 0.20 mmol) and TEA (5 eq., 70 μL , 0.5 mmol) in DMF (0.4 mL) and the reaction mixture was allowed to stir for 1 min. A solution of amine **20** (42 mg, 0.1 mmol) in DMF (0.3 mL) was added and the resulting mixture was stirred overnight. EtOAc (10 mL) was added and the organic layer was washed with sat. aq. NaHCO_3 and brine, dried over MgSO_4 , filtered and concentrated under reduced pressure. The title compound was obtained after RP-HPLC purification (linear gradient 40% \rightarrow 60% ACN in H_2O , 0.1% TFA, 15 min) as a red/brown solid (yield: 15.60 mg, 16.51 μmol , 16.5%). $R_f = 0.05$ (90% EtOAc/Pentane). $^1\text{H-NMR}$ (600 MHz, $\text{DMSO}-d_6$): δ 8.38 (s, 1H), 8.10 (br s, 1H), 7.66 (t, $J = 7.8$ Hz, 2H), 7.61 (s, 1H), 7.44 (t, $J = 7.2$ Hz, 2H), 7.19 (t, $J = 7.2$ Hz, 1H), 7.17 (d, $J = 8.4$ Hz, 2H), 7.13 (d, $J = 7.8$ Hz, 2H), 6.84 (d, $J = 15.0$ Hz, 0.5H), 6.69 (d, $J = 15.0$ Hz), 6.62 – 6.58 (m, 0.5H), 6.55 – 6.52 (m, 0.5H), 6.15 (s, 1H), 4.76 – 4.66 (m, 1H), 4.57 (d, $J = 11.4$ Hz, 1H), 4.20 – 4.19 (m, 2H), 4.06 (d, $J = 12.6$ Hz, 1H), 3.77 (t, $J = 12$ Hz, 1H), 3.53 (br s, 1H), 3.40 (br s, 1H), 3.37 – 3.32 (m, 4H), 3.24 – 3.21 (m, 2H), 3.04 (m, 1H), 2.98 – 2.88 (m, 4H), 2.61 – 2.60 (m, 2H), 2.42 (s, 3H), 2.40 (s, 1H), 2.25 (s, 6H), 2.22 (s, 3H), 2.14 – 2.12 (m, 1H), 1.95 – 1.93 (m, 1H), 1.63 – 1.56 (m, 1H). $^{13}\text{C-NMR}$ (150 MHz, $\text{DMSO}-d_6$): δ 172.0, 163.79, 158.79, 158.56, 157.40, 156.76, 156.24, 155.70, 154.55, 153.38, 153.07, 144.43, 144.03, 140.94, 139.24, 132.43, 130.09, 129.22, 127.24, 126.87, 123.90, 121.47, 119.04, 118.45, 117.45, 97.22, 56.69, 55.02, 52.96, 52.32, 50.16, 49.32, 45.77, 45.21, 41.63, 35.16, 34.13, 29.47, 24.88, 23.25, 19.57, 14.21, 12.51, 10.96,

9.25. IR film (cm^{-1}): 1670.4, 1603.9, 1517.1, 1471.8, 1436.1, 1227.7, 1199.8, 1131.3, 974.1, 832.3, 799.5, 720.4, 666.4. HRMS: calculated for $\text{C}_{48}\text{H}_{56}\text{BF}_2\text{N}_{11}\text{O}_3$ [$\text{M}+2\text{H}^{2+}$]: 442.73912; found: 442.73849.

Ibrutinib-BODIPY-TMR (5)

DiPEA (3.5 eq., 60 μL , 0.35 mmol) and BODIPY-TMR-OSu³⁵ (2.2 eq., 0.11 g, 0.22 mmol) were added to a solution of crude amine **20** (42 mg, 0.1 mmol) in DMF (0.5 mL). The reaction mixture was stirred overnight before being evaporated. The title compound was obtained after RP-HPLC purification (linear gradient 40% \rightarrow 60% ACN in H_2O , 0.1% TFA, 15 min) as a purple solid (yield: 12.19 mg, 10.25 μmol , 10.3%). R_f = 0.05 (90% EtOAc/Pentane). ^1H NMR (600 MHz, $\text{DMSO}-d_6$): δ 8.26 (s, 1H), 7.85 (d, J = 6.6 Hz, 2H), 7.66 (d, J = 7.8 Hz, 3H), 7.43 (t, J = 10.8 Hz, 2H), 7.19 (t, J = 7.2 Hz, 1H), 7.16 – 7.11 (m, 5H), 7.02 (d, J = 7.8 Hz, 2H), 6.69 (br s, 1H), 6.61 – 6.58 (m, 1H), 6.5 (br s, 1H), 4.73 – 4.67 (m, 1H), 4.54 (d, J = 11.4 Hz, 1H), 4.14 (d, J = 10.2 Hz, 1H), 4.03 (d, J = 11.4 Hz, 1H), 3.82 (s, 3H), 3.76 – 3.72 (m, 1H), 3.24 – 3.19 (m, 3H), 3.09 (q, J = 7.8 Hz, J = 15.0 Hz, 4H), 2.66 – 2.61 (m, 3H), 2.55 – 2.54 (m, 2H), 2.49 (s, 3H), 2.26 (d, J = 6.6 Hz, 3H), 2.22 (s, 3H), 2.12 (d, J = 10.2 Hz, 1H), 1.96 – 1.89 (m, 1H), 1.63 – 1.52 (m, 1H), 1.18 (t, J = 7.2 Hz, 4H). ^{13}C NMR (150 MHz, $\text{DMSO}-d_6$): δ 159.97, 158.18, 157.14, 156.28, 155.66, 153.96, 143.34, 143.20, 140.58, 134.68, 133.92, 131.07, 130.39, 130.12, 128.30, 127.89, 124.90, 124.19, 123.80, 118.97, 117.98, 113.78, 97.39, 55.71, 45.76, 40.06, 34.93, 19.80, 12.90, 9.25, 8.59. IR film (cm^{-1}): 1672.3, 1604.8, 1523.8, 1464.0, 1234.4, 1201.7, 1180.4, 1139.9, 1045.4. HRMS: calculated for $\text{C}_{53}\text{H}_{58}\text{BF}_2\text{N}_{11}\text{O}_4$ [$\text{M}+2\text{H}^{2+}$]: 481.7444; found: 481.74402.

Ibrutinib-alkyne (6)

DiPEA (4.0 eq., 70 μL , 0.4 mmol) and 6-heptynoic-OSu³⁶ (2.2 eq., 4.9 mg, 0.25 mmol) were added to a solution of crude amine **20** (42 mg, 0.1 mmol) in DMF (0.5 mL). The reaction mixture was stirred overnight before being evaporated. The title compound was obtained after RP-HPLC purification (linear gradient 40% \rightarrow 60% ACN in H_2O , 0.1% TFA, 15 min) as a white solid (yield: 32.92 mg, 35.87 μmol , 35.9%). R_f = 0.05 (90% EtOAc/Pentane). ^1H NMR (600 MHz, $\text{DMSO}-d_6$): δ 8.39 (s, 1H), 8.03 (br s, 1H), 7.67 – 7.66 (m, 2H), 7.44 (t, J = 7.2 Hz, 2H), 7.19 (t, J = 7.2 Hz, 1H), 7.16 (d, J = 9.0 Hz, 2H), 7.13 (d, J = 8.4 Hz, 2H), 6.85 (d, J = 15.0 Hz, 0.5H), 6.70 (d, J = 15.0 Hz, 0.5H), 6.63 – 6.61 (m, 0.5H), 6.56 – 6.54 (m, 0.5H), 4.77 – 4.71 (m, 2H), 4.57 (d, J = 12 Hz, 1H), 4.19 (d, J = 12.0 Hz, 2H), 4.06 (d, J = 12.6 Hz, 1H), 3.75 (t, J = 11.4 Hz, 1H), 3.58 (s, 1H), 3.44 (s, 1H), 3.35 (br s, 3H), 3.23 (q, J = 11.4 Hz, J = 22.2 Hz, 3H), 3.07 – 2.93 (m, 4H), 2.73 (s, 1H), 2.28 – 2.24 (m, 1H), 2.20 (br s, 3H), 2.12 – 2.11 (m, 2H), 1.95 – 1.93 (m, 1H), 1.63 – 1.58 (m, 3H), 1.47 – 1.44 (m, 2H). ^{13}C NMR (150 MHz, $\text{DMSO}-d_6$): δ 174.26, 163.81, 157.40, 156.58, 156.18, 152.98, 144.44, 130.12, 127.16, 126.12, 123.63, 119.00, 115.78, 97.15, 85.35, 71.18, 62.04, 61.17, 52.95, 52.33, 50.06, 19.23, 45.70, 45.19, 41.60, 34.66, 34.35, 29.53, 27.51, 24.80, 24.51, 23.48, 17.43. IR film (cm^{-1}): 3290.7, 2940.0, 1663.7, 1614.5, 1520.9, 1490.1, 1455.4, 1235.5, 1198.8, 1131.3, 831.4, 711.2. HRMS: calculated for $\text{C}_{39}\text{H}_{47}\text{N}_9\text{O}_3$ [$\text{M}+2\text{H}^{2+}$]: 345.69737; found: 345.69732.

Ibrutinib- N_3 (7)

DiPEA (4.0 eq., 70 μL , 0.4 mmol) and azido-PNP ester³⁷ (2.5 eq., 63 mg, 0.25 mmol) were added to a solution of crude amine **20** (42 mg, 0.1 mmol) in DMF (0.5 mL). The reaction mixture was stirred overnight before being evaporated. The title compound was obtained after RP-HPLC purification (linear gradient 40% \rightarrow 60% ACN in

Direct and two-step bioorthogonal probes for Bruton's tyrosine kinase based on ibrutinib: a comparative study

H₂O, 0.1% TFA, 15 min) as a white solid (yield: 20.39 mg, 22.14 μ mol, 22.1%). ¹H NMR (600 MHz, DMSO-d₆): δ 8.37 (s, 1H), 8.08 (br s, 1H), 7.66 (br s, 2H), 7.44 (t, J = 8.4 Hz, 2H), 7.20 (t, J = 7.2 Hz, 1H), 7.16 (d, J = 9.0 Hz, 2H), 7.13 (d, J = 8.4 Hz, 2H), 6.84 (d, J = 15.0 Hz, 0.5H), 6.70 (d, J = 14.4 Hz, 0.5H), 6.63 – 6.60 (m, 0.5H), 6.56 – 6.52 (m, 0.5H), 4.76 – 4.71 (m, 1H), 4.56 (d, J = 12.0 Hz, 0.5H), 4.19 (d, J = 12.0 Hz, 0.5H), 4.06 (d, J = 12.6 Hz, 0.5H), 3.75 (t, J = 10.2 Hz, 0.5H), 3.37 – 3.33 (m, 4H), 3.23 – 3.20 (m, 2H), 3.07 – 2.97 (m, 4H), 2.31 – 2.24 (m, 2H), 2.19 – 2.13 (m, 6H), 1.95 – 1.93 (m, 2H), 1.77 – 1.75 (m, 4H), 1.63 – 1.53 (m, 2H). ¹³C NMR (150 MHz, DMSO-d₆): δ 171.95, 163.81, 157.37, 156.19, 153.07, 152.79, 144.31, 143.91, 130.12, 127.25, 126.13, 123.85, 119.00, 115.78, 97.17, 56.67, 55.04, 52.92, 52.30, 50.16, 49.30, 45.71, 45.19, 41.60, 34.07, 32.12, 29.54, 29.38, 24.81, 24.29, 23.18, 22.94. IR film (cm⁻¹): 3317.7, 2097.7, 1671.4, 1587.5, 1520.9, 1490.1, 1437.0, 1236.4, 1201.7, 1131.3, 760.3, 613.4. HRMS: calculated for C₃₆H₄₄N₁₂O₃ [M+2H²⁺]: 347.19024; found: 347.19022.

Ibrutinib-norbornene (8)

Azido-ibrutinib **7** (69 mg, 0.1 mmol) and N-(2-propynyl)-5-norbornene-2-carboxamide³² (1.5 eq., 26.3 mg, 0.15 mmol) were dissolved in DMF (0.5 mL). The reaction mixture was stirred overnight after addition of CuSO₄·5 H₂O (0.2 eq., 20 μ L 1 M in H₂O, 20 μ mol) and sodium ascorbate (0.4 eq., 40 μ L 1 M in H₂O, 40 μ mol). The mixture was then concentrated and purified by RP-HPLC (linear gradient 40% \rightarrow 60% ACN in H₂O, 0.1% TFA, 15 min) to yield the title compound as a white solid (yield: 10.75 mg, 9.81 μ mol, 10.2%). ¹H NMR (600 MHz, DMSO-d₆): δ 8.34 (s, 1H), 8.09 (br s, 1H), 8.00 (br s, 1H), 7.08 (s, 1H), 7.67 – 7.66 (m, 2H), 7.45 (t, J = 7.2 Hz, 2H), 7.19 (t, J = 7.2 Hz, 1H), 7.16 (d, J = 9.0 Hz, 2H), 7.13 (d, J = 8.4 Hz, 2H), 6.84 (d, J = 14.4 Hz, 0.5H), 6.69 (d, J = 14.4 Hz, 0.5H), 6.63 – 6.61 (m, 0.5H), 6.56 – 6.53 (m, 0.5H), 6.10 – 6.08 (m, 1H), 5.80 – 5.78 (m, 1H), 4.75 – 4.70 (m, 1H), 4.56 (br s, 1H), 4.33 (br s, 2H), 4.23 (br s, 2H), 4.08 – 4.05 (m, 1H), 3.78 (dd, J = 2.4 Hz, J = 5.4 Hz, 2H), 3.34 (br s, 2H), 3.25 – 3.21 (m, 1H), 3.17 (br s, 1H), 3.14 (br s, 1H), 2.97 – 2.92 (br s, 2H), 2.82 – 2.79 (m, 2H), 2.28 – 2.23 (m, 1H), 2.16 – 2.14 (m, 1H), 2.12 – 2.09 (m, 4H), 2.07 (s, 1H), 2.11 (br s, 2H), 2.00 – 1.93 (m, 1H), 1.78 – 1.72 (m, 3H), 1.68 – 1.54 (m, 2H), 1.33 – 1.22 (m, 9H). ¹³C NMR (150 MHz, DMSO-d₆): δ 172.87, 172.66, 171.70, 163.80, 158.32, 158.10, 157.32, 156.19, 153.20, 147.73, 145.42, 136.83, 132.21, 132.02, 130.12, 127.73, 127.47, 126.59, 123.84, 122.51, 118.99, 97.23, 81.61, 72.37, 69.75, 55.08, 54.03, 49.34, 48.71, 47.37, 46.64, 45.48, 43.23, 42.07, 34.33, 31.85, 28.41, 27.83, 25.72. IR film (cm⁻¹): 3337.0, 2945.4, 1663.7, 1518.0, 1490.1, 1446.7, 1418.7, 1235.5, 1199.8, 1185.3, 839.1, 799.5, 720.4. HRMS: calculated for C₄₇H₅₇N₁₃O₄ [M+2H²⁺]: 434.74010; found: 434.74012.

Experimental procedures: biochemistry

General

Ramos cells, a Burkitt's lymphoma B lymphocyte cell line, were cultured on Dulbecco's Modified Eagle Medium: Nutrient Mixture F-12 (DMEM/F-12) supplemented with 10% Fetal Bovine Serum, 0.1 mg/mL penicillin, 0.1 mg/mL streptomycin in a 5% CO₂ humidified incubator at 37° C. Cell lysates were prepared from cell pellets by resuspension in cold digitonin lysis buffer (50 mM Tris pH 7=0, 250 mM sucrose, 5 mM MgCl₂, 1 mM DTT, 0.025% digitonin; 3x pellet volume), incubation on ice for 30 min and centrifugation for 15 min at 16, 000 g (4° C), after which the supernatants containing the cytosolic fractions were collected and the protein concentration was determined by Qubit[®] Protein Assay kit. Precipitations of proteins was done using a chloroform/methanol (c/m)

precipitation protocol.³⁸ SDS-PAGE analysis: in-gel fluorescence was measured on a ChemiDoc MP system (Cy2 settings, 530/30 filter and Cy3 settings, 605/50 filter) and analysed using Image Lab 4.1. As a loading control gels were stained with Coomassie Blue. Protein standard is Dual Color protein standard (DC, Bio-Rad).

IMAP Reaction Buffer (10 mM Tris-HCl, 10 mM MgCl₂, 0.01% Tween-20, 0.05% NaN₃ pH 7.2) and the IMAP Progressive Binding System (IMAP Progressive Binding Buffer A, IMAP Progressive Binding Buffer B, and IMAP Progressive binding Reagent), were all from Molecular Devices.

IMAP FP assay

Compounds **1**, **6**, **7** and **8** (5 μ L 10x solution in DMSO/kinase reaction (KR)-buffer, such that the final concentration of DMSO was 4%) and 100 mU/mL BTK (5 μ L 100 mU/mL in KR-buffer) were incubated for 60 min at room temperature. Next, 50 nM of Fluorescein labeled Blk/Lyntide substrate (5FAM-EFPIYDFLPAKKK-NH₂, 5 μ L 200 nM in KR-buffer) and 5 μ M ATP (5 μ L 20 μ M in KR-buffer) were added to the mixture and incubated for 120 min at room temperature. The reaction was stopped after 120 min by a 40 μ L addition of IMAP binding reagent in binding buffer and read on the Envision 2102 Multilabel Reader, Dichroic mirror D505FP/D535, excitation filter: 480 nm cwl. Parallel and perpendicular filters 535 nm cwl. For every measurement 18 wells were used as minimum wells (wells with ATP, 0% effect), 18 wells were used as maximum wells (wells without ATP, 100% effect). 16 wells were used to measure the background signal, which contained no substrate. Enzyme, substrate, and ATP were prepared in kinase reaction buffer containing 1 mM DTT. The IMAP binding reagent was 2000x diluted in the binding buffer.

***In vitro* labeling of BTK in Ramos cells (ABPs 4 and 5)**

Ramos cell lysates (30 μ g total protein per experiment) in lysis buffer (9 μ L) were exposed to the indicated concentrations of the ABP (1 μ L 10x solution in DMSO) for 1 hr at room temperature. The reaction mixtures were then boiled for 5 min at 95° C with 3.3 μ L 4x Laemmli's sample buffer containing 2-mercaptoethanol and resolved on 10% SDS-PAGE, followed by fluorescence scanning (Cy2 or Cy3 settings) and CBB staining.

***In situ* labeling of BTK in Ramos cells (ABPs 4 and 5)**

Ramos cells ($\pm 1 \times 10^7$ cells per experiment) were exposed to the indicated concentrations of the ABP (1 μ L 10000x solution in DMSO) in 10 mL fresh medium for 4 hrs at 37° C, before being centrifuged for 5 min at 1200 rpm, and washed with PBS (3x). The cell pellets were then flash frozen in liquid nitrogen and lysed in 30 μ L lysis buffer. The lysates (30 μ g total protein per experiment) in lysis buffer (10 μ L) were boiled for 5 min at 95° C with 3.3 μ L 4x Laemmli's sample buffer containing 2-mercaptoethanol and resolved on 10% SDS-PAGE. In-gel visualization of the fluorescent labeling was performed in the wet gel slabs directly using Cy2 or Cy3 settings.

Competition experiments of ABP 4 versus ABPs 6-8: *in situ* modification of BTK by ABP 4 and *in vitro* competition by ABPs 6-8 .

Ramos cells ($\pm 5 \times 10^6$ cells per experiment) were seeded in 6 cm petri dishes and grown 2 hrs at 37° C, before being exposed to the indicated concentrations of ABP (2 μ L 1000x solution in DMSO) in 2 mL fresh medium for 3 hrs at 37° C. Next, the cells were centrifuged for 5 min at 1200 rpm, and washed with PBS (3x), before flash

Direct and two-step bioorthogonal probes for Bruton's tyrosine kinase based on ibrutinib: a comparative study

freezing the cell pellets in liquid nitrogen and cell lysis in 15 μ L lysis buffer. The lysates (30 μ g total protein per experiment) in lysis buffer (10 μ L) were exposed to 1 μ M ABP **4** (1.11 μ L 10x solution in DMSO) for 1 hr at room temperature, boiled for 5 min at 95° C with 3.7 μ L 4x Laemmli's sample buffer containing 2-mercaptoethanol and resolved on 10% SDS-PAGE. In-gel visualization of the fluorescent labeling was directly performed in the wet gel slabs using Cy2 or Cy3 settings.

In vitro tetrazine ligation

Ramos lysates (50 μ g total protein per experiment) in lysis buffer (9 μ L) were exposed to 4 μ M ABP **8** (1 μ L 40 μ M in DMSO) for 1 hr at room temperature, followed by addition of 1% SDS (1.11 μ L 10% SDS in H₂O) and boiling for 5 min at 95° C. Hereafter, the lysates were exposed for 1 hr at room temperature to the indicated concentrations of tetrazine **24** (1.23 μ L 10x solution in DMSO). In control experiments, lysates were treated with ABP **4** (1 μ M) (positive control) or subjected to tetrazine labeling in the absence of ABP **8** (background control). As a negative control, tetrazine ligation was performed on lysates pretreated with 20 μ M ibrutinib (**1**). After the ligation reaction proteins were precipitated by c/m precipitation and taken up in 10 μ L 8 M urea and 3.5 μ L 4x Laemmli's sample buffer containing 2-mercaptoethanol, boiled for 5 min at 95° C and resolved on 10% SDS-PAGE. In-gel visualization of the fluorescent labeling was performed in the wet gel slabs directly using Cy2 settings.

In situ and post-lysis tetrazine ligation

Ramos cells ($\pm 5 \times 10^6$ cells per experiment) were seeded in 6 cm petri dishes and grown 2 hrs at 37° C, before being exposed to 4 μ M ABP **8** (2 μ L 1000x solution in DMSO) in 2 mL fresh medium for 3 hrs at 37° C. After centrifugation of the cells for 5 min at 1200 rpm, the cells were washed with fresh medium for 5 min at 37° C (3x), and then exposed to 25 μ M of tetrazine **24** (4 μ L 10x solution in DMSO) in 4 mL fresh medium for 1 hr at 37° C. As a positive control, cells were exposed to ABP **4** (1 μ M) for 3 hrs at 37° C. As a background control, cells were lysed and subjected to tetrazine labeling in the absence of ABP **8**. Next, cells were harvested in PBS, centrifuged for 5 min at 1200 rpm, and washed with PBS (3x), before flash freezing the cell pellets in liquid nitrogen and cell lysis in 15 μ L lysis buffer. The lysates (50 μ g total protein per experiment) in lysis buffer (10 μ L) were precipitated by c/m precipitation and taken up in 10 μ L 8 M urea and 3.5 μ L 4x Laemmli's sample buffer containing 2-mercaptoethanol, boiled for 5 min at 95° C. the proteins were resolved on 10% SDS-PAGE. Fluorescence was measured in the wet gel slabs using Cy2 settings.

For post-lysis ligation experiments, cells were harvested directly after treatment with ABP **8** and lysed. The lysates (50 μ g total protein per experiment) in lysis buffer (10 μ L) were boiled for 5 min at 95° C after addition of 1% SDS (1.11 μ L 10% SDS in H₂O) and boiling for 5 min at 95° C. Next, the lysates were exposed for 1 hr at room temperature to 25 μ M of tetrazine **24** (1.23 μ L 10x solution in DMSO). After the ligation reaction proteins were precipitated by c/m precipitation and taken up in 10 μ L 8 M urea and 3.5 μ L 4x Laemmli's sample buffer containing 2-mercaptoethanol, boiled for 5 min at 95° C and resolved on 10% SDS-PAGE. In-gel visualization of the fluorescent labeling was performed in the wet gel slabs directly using Cy2 settings.

Copper(I)-catalyzed click ligation *in vitro*

Ramos lysates (50 µg total protein per experiment) in lysis buffer (9 µL) were exposed to 4 µM ABP **6** or **7** (1 µL 40 µM in DMSO) for 1 hr at room temperature. The reaction mixtures were subsequently diluted with an additional 9 µL buffer containing 6.5 mM CuSO₄ (0.58 µL 100 mM in H₂O), 6.5 mM THPTA (0.58 µL 100 mM in H₂O), 6.5 mM sodium L-ascorbate (0.58 µL 100 mM in H₂O) and exposed for 1 hr at room temperature to the indicated concentrations of azide **22** (reaction with **6**) or alkyne **23** (reaction with **7**) (1 µL 20x solution in DMSO). In control experiments, lysates were treated with ABP **4** (1 µM) (positive control) or subjected to azide or alkyne labeling in the absence of an ABP (background control). Alternatively, click ligation was performed on lysates pretreated with 20 µM ibrutinib (**1**) (negative control). Next, proteins were precipitated by c/m precipitation and taken up in 10 µL 8 M urea and 3.5 µL 4x Laemmli's sample buffer containing 2-mercaptoethanol, boiled for 5 min at 95° C and resolved on 10% SDS-PAGE. In-gel visualization of the fluorescent labeling was performed in the wet gel slabs directly using Cy2 settings.

In situ modification of BTK by ABPs **6** or **7** followed by *in vitro* copper(I)-catalyzed click ligation

Ramos cells ($\pm 5 \times 10^6$ cells per experiment) were seeded in 6 cm petri dishes and grown 2 hrs at 37° C, before being exposed to 4 µM ABP **6** or **7** (2 µL 1000x solution in DMSO) in 2 mL fresh medium for 3 hrs at 37° C. As a positive control, cells were exposed to ABP **4** (1 µM) for 3 hrs at 37° C. As a background control, cells were lysed and subjected to click labeling in the absence of ABP **6** or **7**. Next, the cells were centrifuged for 5 min at 1200 rpm, and washed with PBS (3x), before flash freezing the cell pellets in liquid nitrogen and cell lysis in 15 µL lysis buffer. The lysates (50 µg total protein per experiment) in lysis buffer (10 µL) were diluted with an additional 9 µL buffer containing 6.5 mM CuSO₄ (0.58 µL 100 mM in H₂O), 6.5 mM THPTA (0.58 µL 100 mM in H₂O), 6.5 mM sodium L-ascorbate (0.58 µL 100 mM in H₂O) and exposed for 1 hr at room temperature to 25 µM of azide **22** (reaction with **6**) or alkyne **23** (reaction with **7**) (1 µL 20x solution in DMSO). Next, proteins were precipitated by c/m precipitation and taken up in 10 µL 8 M urea and 3.5 µL 4x Laemmli's sample buffer containing 2-mercaptoethanol, boiled for 5 min at 95° C and resolved on 10% SDS-PAGE. In-gel visualization of the fluorescent labeling was performed in the wet gel slabs directly using Cy2 settings.

References

¹ C. M. Lewis, C. Broussard, M. J. Czar and P. L. Schwartzberg, *Curr. Opin. Immunol.*, 2001, **13**, 317.

² A. B. Satterthwaite and O. N. Witte, *Immunol. Rev.*, 2000, **175**, 120.

³ W. N. Khan, *Immunol. Res.*, 2001, **23**, 147.

⁴ R. E. Davis, V. N. Ngo, G. Lenz, P. Tolar, R. M. Young, P. B. Romesser, H. Kohlhammer, L. Lamy, H. Zhao, Y. Yang, W. Xu, A. L. Shaffer, G. Wright, W. Xiao, J. Powell, J. Jiang, C. J. Thomas, A. Rosenwald, G. Ott, H. K. Muller-Hermelink, R. D. Gascoyne, J. M. Connors, N. A. Johnson, L. M. Rimsza, E. Campo, E. S. Jaffe, W. H. Wilson, J. Delabie, E. B. Smeland, R. I. Fisher, R. M. Braziel, R. R. Tubbs, J. R. Cook, D. D. Weisenburger, W. C. Chan, S. K. Pierce and L. M. Staudt, *Nature*, 2010, **463**, 88.

⁵ M. Cinar, F. Hamedani, Z. Mo, B. Cinar, H. M. Amin, S. Alkan, *Leuk. Res.*, 2013, **37**, 1271.

- ⁶ M. F. M. De Rooij, A. Kuil, C. R. Geest, E. Eldering, B. Y. Chang, J. J. Buggy, S. T. Pals and M. Spaargaren, *Blood*, 2012, **119**, 2590.
- ⁷ G. Yang, Y. Zhou, X. Liu, L. Xu, Y. Cao, R. J. Manning, C. J. Patterson, S. J. Buhrlage, N. Gray, Y.-T. Tai, K. C. Anderson, Z. R. Hunter and S. P. Treon, *Blood*, 2013, **122**, 1222.
- ⁸ F. Cameron and M. Sanford, *Drugs*, 2014, **74**, 263.
- ⁹ US Food and Drug Administration, Imbruvica, 2013, (Accessed 9 December 2013).
- ¹⁰ L. A. Honigberg, A. M. Smith, M. Sirisawas, E. Verner, D. Loury, B. Chang, S. Li, Z. Pan, D. H. Thamm, R. A. Miller and J. J. Buggy, *PNAS*, 2010, **107**, 13075 – 13080.
- ¹¹ Z. Pan, H. Scheerens, S.-J. Li, B. E. Schultz, P. A. Sprengeler, L. C. Burrill, R. V. Mendonca, M. D. Seeney, K. C. K. Scott, P. G. Grothaus, D. A. Jeffery, J. M. Spoerke, L. A. Honigberg, P. R. Young, S. A. Dalrymple and J. T. Palmer, *Chem. Med. Chem.*, 2007, **2**, 58.
- ¹² T. Barf and A. Kaptein, *J. Med. Chem.*, 2012, **55**, 6243.
- ¹³ Y. Liu, M. P. Patricelli and B. F. Cravatt, *PNAS*, 1999, **96**, 14694.
- ¹⁴ B. F. Cravatt, A. T. Wright and J. W. Kozarich, *Annu. Rev. Biochem.*, 2008, **77**, 383.
- ¹⁵ M. J. Niphakis and B. F. Cravatt, *Annu. Rev. Biochem.*, 2014, **83**, 341.
- ¹⁶ B. R. Lanning, L. R. Whitby, M. M. Dix, J. Douhan, A. M. Gilbert, E. C. Hett, T. O. Johnson, C. Joslyn, J. C. Kath, S. Niessen, L. R. Roberts, M. E. Schnute, C. Wang, J. J. Hulce, B. Wei, L. O. Whiteley, M. M. Hayward and B. F. Cravatt, *Nat. Chem. Biol.*, 2014, **10**, 760.
- ¹⁷ E. Kim, K. S. Yang, R. H. Kohler, J. M. Dubach, H. Mikula and R. Weissleder, *Bioconj. Chem.*, 2015, **26**, 1513.
- ¹⁸ L. I. Willems, W. A. van der Linden, N. Li, K.-Y. Li, N. Liu, S. Hoogendoorn, G. A. van der Marel, B. I. Florea, H. S. Overkleeft, *Acc. Chem. Res.*, 2011, **44**, 718.
- ¹⁹ L. I. Willems, N. Li, B. I. Florea, M. Ruben, G. A. van der Marel and H. S. Overkleeft, *Angew. Chem. Int. Ed.*, 2012, **51**, 4431.
- ²⁰ A. Turetsky, E. Kim, R. H. Kohler, M. A. Miller and R. Weissleder, *Sci. Rep.*, 2014, **4**, 4782.
- ²¹ Z. Pan, S. J. Li, H. Scheerens, L. Honigberg, E. verner, *US Pat.*, US 2008/0214501 A1, 2008.
- ²² A. Turetsky, E. Kim, R. H. Kohler, M. A. Miller and R. Weissleder, *Sci. Rep.*, 2014, **4**, 4782.
- ²³ L. Honigberg, E. Verner, Z. Pan, *US Pat.*, US 2008/0076921 A1, 2008.
- ²⁴ Z. Pan, S. J. Li, H. Scheerens, L. Honigberg, E. verner, *US Pat.*, US 2008/0214501 A1, 2008.
- ²⁵ L. Honigberg, E. Verner, Z. Pan, *US Pat.*, US 2008/0076921 A1, 2008.
- ²⁶ The Walter and Eliza Hall institute of medical research, *WO* 2012 003544 A1, 2012.
- ²⁷ Astrazeneca AB, *US Pat.*, US6518286 B1, 2003.
- ²⁸ M. Han, Y. Han, C. Song and H.-G. Hahn, *Bull. Korean Chem. Soc.*, 2012, **33**, 2597.
- ²⁹ H. D. H. Showalter, J. L. Johnson, J. M. Hoftiezer, W. R. Turner, L. M. Werbel, W. R. Leopold, J. L. Shillis, R. C. Jackson and E. F. Elslager, *J. Med. Chem.*, 1987, **30**, 121.
- ³⁰ N. J. Matovic, P. Y. Hayes, K. Penman, R. P. Lehmann and J. J. de Voss, *J. Org. Chem.*, 2011, **76**, 4467.
- ³¹ L. A. Honigberg, A. M. Smith, M. Sirisawas, E. Verner, D. Loury, B. Chang, S. Li, Z. Pan, D. H. Thamm, R. A. Miller and J. J. Buggy, *PNAS*, 2010, **107**, 13075.

³² L. I. Willems, N. Li, B. I. Florea, M. Ruben, G. A. van der Marel and H. S. Overkleeft, *Angew. Chem. Int. Ed.*, 2012, **51**, 4431.

³³ M. Verdoes, U. Hillaert, B. I. Florea, M. Sae-Heng, M. D. P. Risseuw, D. V. Filippov, G. A. van der Marel and H. S. Overkleeft, *Bioorg. Med. Chem. Lett.*, 2007, **17**, 6169.

³⁴ S. E. Boiadjev and D. A. Lightner, *J. Heterocycl. Chem.*, 2003, **40**, 181.

³⁵ M. Verdoes, B. I. Florea, V. Menendez-Benito, C. J. Maynard, M. D. Witte, W. A. Van der Linden, A. M. C. H. van den Nieuwendijk, T. Hofmann, C. R. Berkers, F. W. van Leeuwen, T. A. Groothuis, M. A. Leeuwenburgh, H. Ovaa, J. J. Neefjes, D. V. Filippov, G. A. van der Marel, N. P. Dantuma, H. S. Overkleeft, *Chem. Biol.*, 2006, **13**, 1217.

³⁶ A. E. Speers, G. C. Adam, B. F. Cravatt, *J. Am. Chem. Soc.*, 2003, **125**, 1217.

³⁷ U. Hillaert, M. Verdoes, B. I. Florea, A. Saragliadis, K. L. L. Habets, J. Kuiper, S. van Calenbergh, F. Ossendorp, G. A. van der Marel, C. Driessen, H. S. Overkleeft, *Angew. Chem. Int. Ed.*, 2009, **48**, 1629.

³⁸ D. Wessel and U. I. Flügge, *Anal. Biochem.*, 1984, **138**, 141.

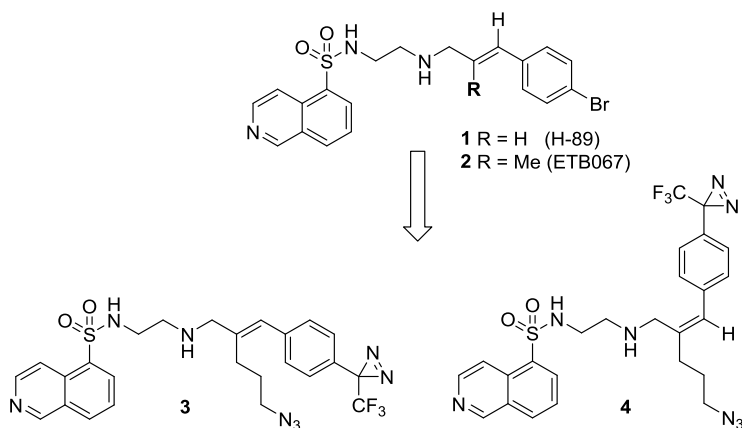
6

Probing for PKA and AKT1 using photoaffinity probes

N. Liu*, S. C. Stolze*, R. H. Wijdeven, A. W. Tuin, A. M. C. H. van den Nieuwendijk, B. I. Florea, M. van der Stelt, G. A. van der Marel, J. J. Neeffjes, H. S. Overkleeft, *Molecular Biosystems*, 2016, **12**, 1809.

6.1 Introduction

The isoquinolinesulfonamide-based kinase inhibitor H-89 (**1**, Scheme 1) was originally identified as a selective and potent inhibitor of protein kinase A (PKA)¹ and has been used to study the role of PKA in various physiological processes.² H-89 inhibits PKA in an ATP-competitive manner with the bromocinnamoyl side chain being a crucial factor for the potency and selectivity over other kinases.³ Though initially presented as a selective PKA inhibitor, H-89 also inhibits a number of other kinases, which is not surprising taking into account that the ATP binding site is



Scheme 1. Structures of the lead compounds: H-89 (**1**) and ETB067 (**2**) and structures of target compounds: diazerine-functionalized photocrosslinking probes **3** (E) and **4** (Z).

conserved in all kinases.^{2,4} PKB α , also referred to as AKT1, is a prominent target of H-89 because of its importance in cancer therapy research. The PI3K/AKT signaling pathway, hyper-activated in many cancer types⁵, has effects on vital cellular processes such as survival, metabolism, growth and proliferation.⁶ AKT signaling also influences angiogenesis and is involved in metastasis formation via the isoform AKT2. In addition, the PI3K/AKT pathway connects to another critical cell signaling pathway: the Ras/Raf/MEK/ERK signaling cascade.⁷ Aside from its involvement in cancer, AKT1 has also been shown to be a key player in bacterial infections by regulation of a network of enzymes essential for the survival of pathogens in phagosomes of host cells. In this context, H-89 and its derivative ETB067 (Scheme 1) were used to distinguish AKT1 from PKA as the crucial enzyme in the control of intracellular bacteria such as *Salmonella typhimurium* and *M. tuberculosis*.⁸ AKT1 inhibitors are the first lead antibiotics described that target host proteins rather than bacterial processes.

In the last years, a number of techniques to profile kinases have emerged, such as the kinobead approach that has recently been used to cluster the activity of well-known inhibitors in a kinome-wide screen.⁹ Another important technique is capture compound mass spectrometry (CCMS), which is based on combining photo-affinity labeling with biotin-based capture techniques in order to pull-down proteins that bind to an inhibitor and have been covalently captured following photo-affinity labeling. This approach has been used to identify targets of dasatinib, imatinib and staurosporine by converting the inhibitors into capture compounds.¹⁰ The staurosporine capture compound could also be used in comprehensive kinase profiling due to the broad binding profile of staurosporine.¹¹

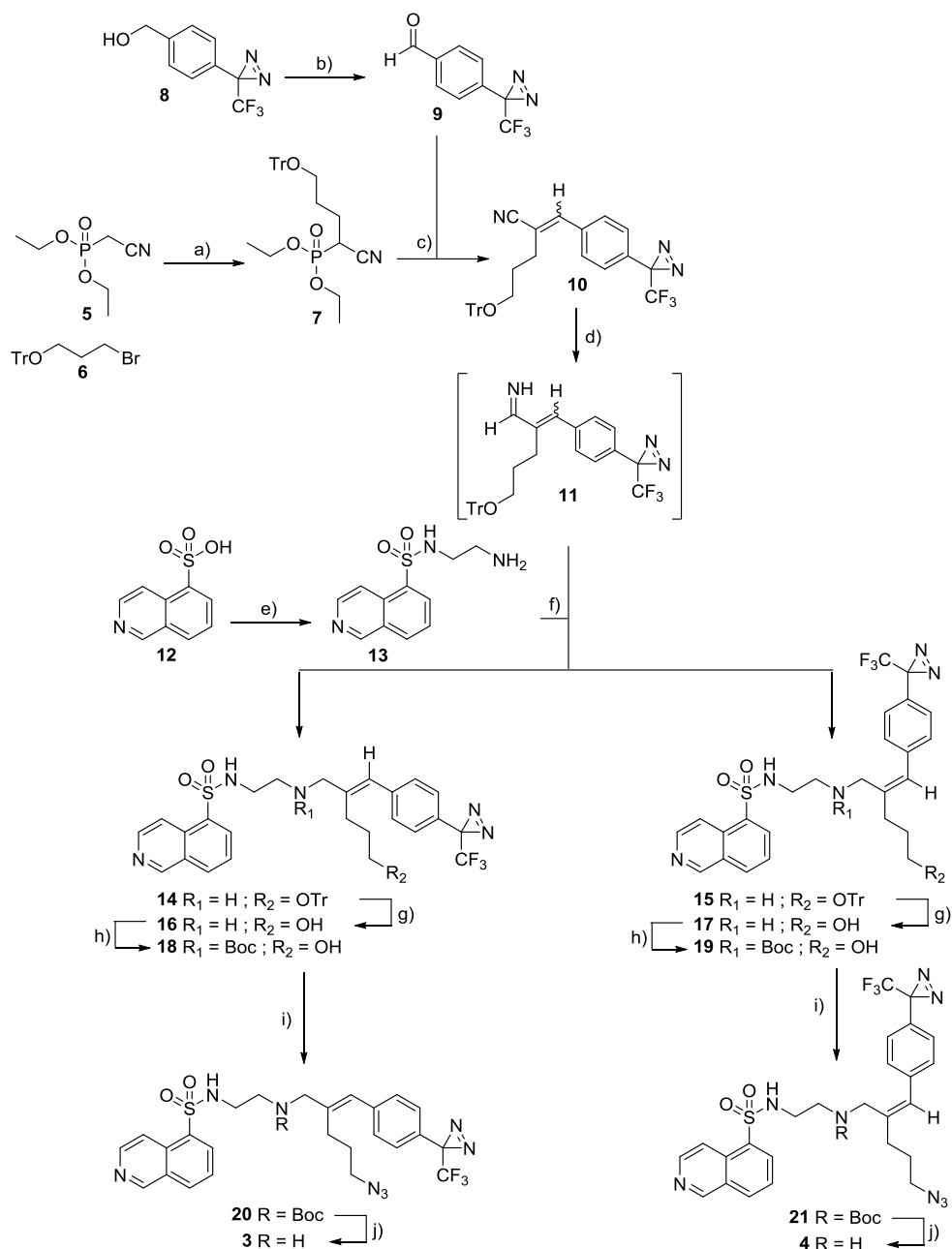
Finally, covalent irreversible kinase inhibitors have received increasing attention both in drug discovery programs and as starting points for kinase bait design. Most of these mechanism-based inhibitors rely on a cysteine thiol in proximity of the binding site that is covalently modified upon binding of the inhibitor.¹² This approach was recently used to target Bruton's tyrosine kinase with Ibrutinib-derived mechanism-based probes.¹³ However, not all kinases possess cysteines near the active site, and this holds true as well for PKA and AKT1.¹²

This study aimed at developing a probe derived from H-89 that a) binds efficiently to the target kinases PKA and AKT1; b) contains a photo-activatable group enabling a covalent modification of a captured kinase and c) carries a conjugation handle to attach a reporter moiety such as a fluorophore or biotin using copper-catalysed click chemistry. The studies on H-89 clearly show that the cinnamoyl side chain has an effect on potency and selectivity,³ so this moiety in the design was kept and the aromatic part of the side chain was modified into an aryl trifluoromethyldiazirine (Scheme 1). Based on the previous studies on ETB067, modification on the double bond of the cinnamoyl system should not have a major influence on activity and therefore a short alkyl chain bearing an azide moiety to enable click labeling has been placed.

6.2 Results and discussion

Synthesis of H-89-based kinase photo-affinity based probes

The synthetic route towards H-89-based photo-affinity based probes **3** and **4** is depicted in Scheme 2. The synthesis commenced from commercially available diethyl cyanomethylphosphonate **5**, which was reacted with trityl-protected bromopropanol **6**¹⁴ to obtain monoalkylated cyanomethylphosphonate **7** in 53% yield. The yield is affected by the fact that dialkylation also occurred, and separation of the two products by column chromatography appeared cumbersome. Before installing the photo-affinity moiety into the probes, trifluoromethylphenyldiazirine functionalised alcohol **8**, which was synthesized by applying a seven step literature procedure¹⁵, was converted into its corresponding aldehyde **9** by Swern oxidation. Next, a Horner-Wadsworth-Emmons (HWE) reaction between *p*-substituted benzaldehyde **9** and phosphonate **7** resulted in α -substituted cinnamitrile **10** as a 3/2 mixture of *E/Z* isomers in 79% yield. Since separation of the isomers in the nitrile-stage was partially successful, and the nitriles were observed to isomerise during the ensuing transimination, the nitriles were used in the following reaction as an *E/Z* mixture. Subsequently, *E/Z* cinnamitrile mixture **10** was used in the four-step-one-pot trans-imation



procedure according to Brussee *et al.*¹⁶, which started with the reduction of nitrile **10** with DiBALH to form its corresponding aluminated iminium salt intermediate. Excess reagent was then quenched at -100 °C with methanol to obtain the primary imine **11**. The latter was reacted with amine **13**, which was obtained by activating isoquinoline sulfonic amine **12** with thionyl chloride and reacting with ethylenediamine. Next, the resulting secondary imine was reduced by NaBH₄ and the crude trityl-protected isoquinolinesulfonamide mixture of **14** and **15** was deprotected under acidic conditions to obtain a crude mixture of **16** and **17** before instalment of the Boc-group to yield isoquinolinesulfonamide **18** and **19** as crude *E/Z* mixture. HPLC purification allowed separation and isolation of both isomers. Both alcohols **18** and **19** were tosylated followed by substitution using NaN₃ to obtain compounds **20** and **21**. At last, deprotection of the Boc-group furnished the photo-affinity based probes **3** and **4** in 14% yield after HPLC purification.

Evaluation of the inhibitory potency and labeling efficiency

With probes **3** and **4** in hand, their biological activity was evaluated. First, the capability of these probes to label a panel of 111 human kinases was examined, which was performed by the company LeadHunter discovery services using a single point kinase active site-directed competition binding KinomescanTM assay (see Chapter 2 for a detailed description)¹⁷. Briefly, purified recombinant kinases (111 in total) tagged with DNA for qPCR detection are incubated with 10 µM of test compound (here: probe **3** or **4**) and subsequently the mixture of kinases and test compound is transferred to an immobilized ligand that competes with probes for binding to kinases. The results for binding interactions are reported as relative activity percentage, where lower numbers indicate stronger hits in the matrix (Table 1). From Table 1, it can be concluded that the probes **3** and **4** have a preference to inhibit Ser/Thr kinases, since the top ten hits all belong to this family. As expected probe **3**, of which the structure and conformation is most similar to PKA inhibitor H-89 (**1**), inhibits PKA and AKT1 more than its *Z*-analogue **4**. Both probes also inhibited the related kinases AKT2 and AKT3, however at a much lower activity, as also observed for the H-89-derived ETB067 inhibitor.⁸

Table 1. Relative kinase activity compared to control sample (%) after inhibition by compounds **3** and **4** (10 μ M).^a

Kinase	3	4	Kinase	3	4
PKAc- α	1.5	3.4	TAOK1	72	52
AKT1	2.6	18	MEK2	73	72
ROCK2	3	1.7	FAK	74	100
AKT3	3.4	25	VEGFR2	75	85
PRKCH	5	2.8	CLK2	76	72
PRKCE	20	10	JNK1	78	82
PRKCD	23	14	TYK2	78	97
SNARK	23	24	TRKA	79	82
SGK3	31	32	AURKB	80	79
CDK11	35	78	GSK3B	80	74
PRKCI	35	35	PCTK1	80	84
CSNK1D	39	38	JNK3	81	89
MARK3	40	53	FGFR3	82	84
CDK7	43	48	PIK3CG	82	78
DYRK1B	45	74	PLK1	82	83
ALK	50	62	YANK3	82	88
FLT3	50	60	MAPKAPK2	83	95
MLCK	50	76	PIM1	83	81
CSF1R	51	96	ULK2	83	65
TSSK1B	53	56	ZAP70	83	94
AXL	54	74	DYRK1A	84	85
CHEK1	56	72	ERBB4	84	90
SRPK3	57	86	ERN1	85	57
CDK9	58	70	LKB1	85	94
PDGFRB	58	57	PAK4	86	98
PIP5K1A	58	37	ACVR1B	87	100
PDPK1	59	69	p38-beta	87	100
PLK4	59	57	CSNK1G3	89	91
RET	59	76	ERBB2	89	64
FGFR2	60	67	INSR	89	81
KIT	61	70	PAK2	89	96
AMPK- α 2	63	83	TGFBR1	89	88
DCAMKL1	63	86	PIM3	90	94
PRKCQ	63	46	AURKA	91	69
EPHA2	65	66	JAK3	91	84
MAP3K4	65	68	PDGFRA	91	98

Probing for PKA and AKT1 using photoaffinity probes

AKT2	66	91	RAF1	91	78
CDK2	66	92	BMPR2	92	89
CDK3	66	78	PIK3CA	93	94
ABL1-p	67	81	CSNK1G2	94	80
JAK2	67	90	MEK1	95	83
MET	67	55	PAK1	95	95
RSK2	67	72	BTK	96	92
TIE2	68	86	p38- α	96	94
ERK1	69	70	HIPK2	97	95
JNK2	69	86	EGFR	98	100
PLK3	69	73	PIK3C2B	98	94
PIM2	70	62	IKK-beta	99	80
SRC	70	70	MKNK1	99	92
ADCK3	71	96	PIK4CB	99	97
MKNK2	71	71	BRAF	100	93
MST2	71	73	IKK-alpha	100	86
FLT1	72	69	MTOR	100	100
IGF1R	72	63	MYO3A	100	100
MLK1	72	69	RIOK2	100	88
MUSK	72	77			

To further establish the potency of the probes and lead compound H-89 (**1**) for the kinases, PKA, AKT1 and AKT2, their IC_{50} values were determined in a FRET-based assay and their corresponding K_i values were calculated. The results are presented in Table 2.

Table 2. Inhibitory activities of compounds H-89, **3** and **4** against PKA, AKT1 and AKT2 (IC_{50} and K_i values in μM).

		PKA	AKT1	AKT2
H89	IC_{50}	1.88 ± 0.64	0.97 ± 0.12	2.47 ± 0.38
	K_i	0.02 ± 0.01	0.09 ± 0.01	1.67 ± 0.26
Probe 3	IC_{50}	75.5 ± 12.54	3.2 ± 1.13	23.1 ± 1.06
	K_i	0.61 ± 0.10	0.02 ± 0.00	0.19 ± 0.09
Probe 4	IC_{50}	74.7 ± 23.12	10.5 ± 4.58	34.4 ± 2.38
	K_i	0.60 ± 0.10	0.04 ± 0.01	0.23 ± 0.03

This kinase assay revealed that probes **3** and **4** are highly potent inhibitors of AKT1 having K_i values varying from 0.02 to 0.04 μM , which are significantly lower than the ones observed for PKA. The trend observed in the Kinomescan for AKT1 is however

preserved with probe **4** being the less potent of the two. A possible explanation for the discrepancy between the assays might be the use of the natural substrate ATP as a competitor to the probes in the FRET-based assay. By comparing the IC_{50} and K_i values of probes **3** and **4** with the lead compound H-89 (**1**), both probes show less activity against PKA, AKT1 and AKT2, but have higher selectivity. Having confirmed the activity of the two probes, a protocol for the photo-labeling of the kinases PKA and AKT1 was designed to validate these compounds as potential photo-affinity based probes.

Using recombinant PKA and AKT1 a robust protocol for the labeling of the kinases with the respective probe was first elucidated, followed by photo-crosslinking at 350 nm, performed in the CaproBoxTM system¹⁸ (Caprotec Bioanalytics GmbH, Berlin) and a final click reaction with an alkyne-modified Cy5 reporter for in-gel analysis. Using different concentrations of probe the amounts of probe equivalents required to label the respective kinases was determined. For both PKA and AKT1 5 equivalents of probe (390 nM, PKA; 295 nM AKT1) with respect to the molar amount of kinase were sufficient to label and detect the kinases by in-gel fluorescence (Figure 1, lane 3). Already in these initial experiments it became apparent that probe **3** labels both kinases with a higher affinity than probe **4**, especially in the case of AKT1. The overall stronger labeling of PKA compared to AKT1 can be explained with a higher specific activity of the commercially obtained kinase. The differences in AKT1 labeling are in accordance with the kinetics data. Taking these first results into account, a focus was set on the evaluation of probe **3** in the following experiments.

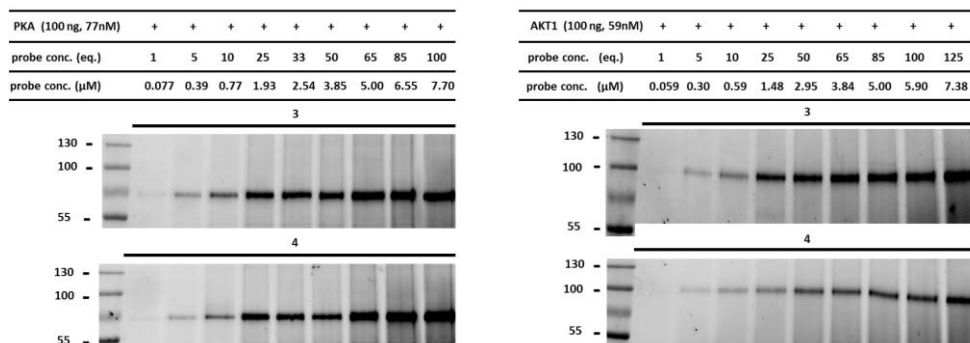


Figure 1. Initial photo-labeling experiments on recombinant kinases using different probe concentrations. Left panel: photolabeling of recombinant PKA using probes **3** and **4**. Right panel: photo-labeling of recombinant AKT1 using probes **3** and **4**.

Subsequently, to prove that the labeling that had been observed in the initial experiments is truly based on affinity to the target kinases and requires active kinases, a number of control experiments have been conducted. First, in order to establish if the labeling is affinity-based, the kinases were mixed with increasing amounts (w/w) of a control protein of similar size and incubated with 5 eq. of **3** (Figure 2, lanes 5-10). The 1:1 controls were also used for further control experiments: one sample was incubated with DMSO and the click mixture to visualize background from association of the proteins with the Cy5 dye (Figure 2, lane 2). A second sample was not irradiated after incubation with the probe, to establish that the UV activation is necessary for labeling (Figure 2, lane 3). Finally, a third sample was denatured by the addition of SDS and subsequent boiling and then treated with the probe to prove that an active enzyme is required for the labeling (Figure 2, lane 4). For both PKA and AKT1 the co-incubation experiment with equivalent amounts of a control protein reveals that the labeling of the targeted kinases with our probes is based on the affinity of the probe towards the target. At higher concentrations of control protein an unspecific reaction of the

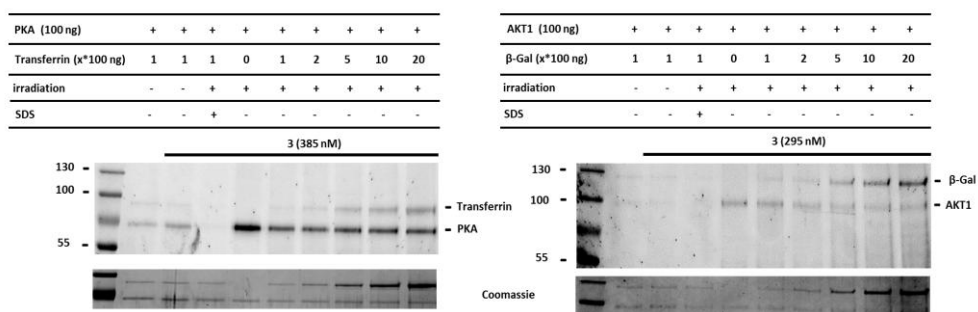


Figure 2. Control experiments using increasing concentrations of Transferrin (PKA, left panel) and β -Galactosidase (AKT1, right panel) as control proteins to determine probe specificity (lanes 5-10). Further controls with 1:1 (w/w) mixtures of kinase and control protein were used to check for background labeling (lane 2), requirement of UV activation (lane 3) and requirement of an active kinase (lane 4).

probe with the control protein and a partial loss of signal for the kinase is observed, especially in the case of AKT1. It has to be noted, that throughout all experiments the labeling of AKT1 was less intense than the labeling of PKA. Since the IC_{50} values that have been determined for both kinases are in the same range for probe **3**, this observation could be explained with different specific activities of the recombinant kinases used in the experiments.

The additional control experiments proved that an active enzyme is indeed required to achieve labeling proven by the disappearance of the labeled kinase when denaturing the sample before incubation with the probe. Also, the labeling relies on UV irradiation proven by the absence of bands in the non-irradiated samples.

In the next set of experiments, competition between **3** and the well-known broad-spectrum kinase inhibitor staurosporine¹⁷ and the parent inhibitors to our probes, H-89 (**1**) and ETB067 (**2**), were visualized. For PKA a very clear competition when pre-incubating with staurosporine was observed, already at 0.5 equivalents to probe **3** (Figure 3, upper panel). For AKT1 a competition is observed as well, however, higher concentrations of staurosporine would be required to achieve full competition (Figure 3, middle panel). Furthermore, the already mentioned lower intensity of labeling for AKT1 not only hampers the visual detection of the competition, it also hinders an accurate quantification by fluorescent densitometry of the bands due to their low intensity (Figure 3, lower panel).

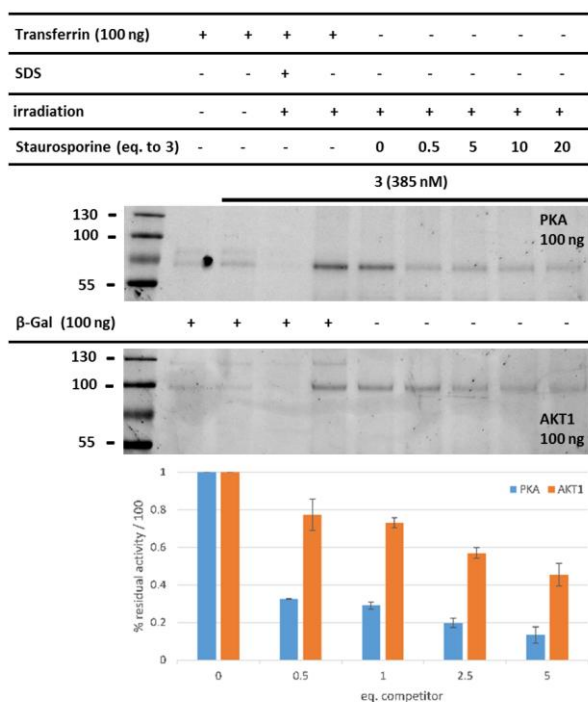


Figure 3 Competition experiments on PKA (upper panel) and AKT1 (middle panel) using Staurosporine as competitor to probe **3**. Quantification of residual activity (lower panel) by fluorescent densitometry from n=3 experiments.

In the competition experiments with H-89 and ETB067, H-89 showed a higher inhibition than ETB067 for both kinases, which is in accordance with previously reported IC_{50} data (Figure 4).⁸ For PKA (Figure 4, left panel) a distinct inhibition profile for increasing concentrations of the competitors both in the visual detection of the bands as well as in the quantification of the detected bands was observed. The apparent poorer inhibition of AKT1 can again be explained with the lower signal intensity.

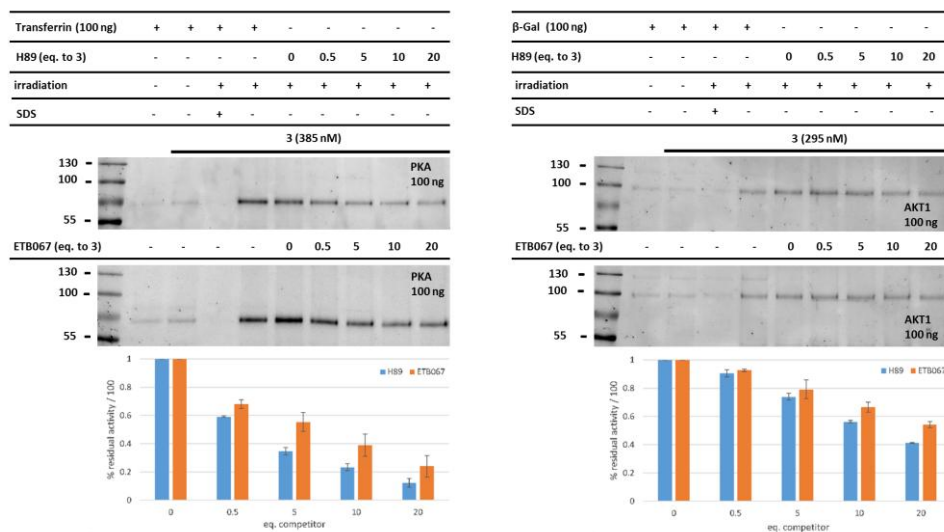


Figure 4 Competition experiments on PKA (left panel) and AKT1 (right panel) using H-89 and ETB067 as competitors to probe **3**. Quantification of residual activity (lower panel) by fluorescent densitometry from n=3 experiments

6.3 Conclusion

Two photo-affinity probes based on the well-known kinase inhibitor H-89 (**1**) have been designed and synthesized. The probes were tested on a panel of kinases and proved to be inhibitors of both PKA and AKT1. Probe **3** has the same double bond geometry as the parent inhibitor H-89 (**1**) and inhibits both PKA and AKT1 with a high potency. A change of the double bond configuration to (*Z*) does not have significant influence on the inhibition of PKA but for AKT1 a partial loss of potency was observed. This indicates a difference in the periphery of the two kinases and offers a possibility to improve selectivity towards AKT1. Furthermore, the efficacy of both probes in the photolabeling of the clinically relevant kinases PKA and AKT1 is shown. The performed experiments however also show that photolabeling conditions need to be adjusted for every new target enzyme. In this study, the

recombinant kinases in pure form as well as in mixtures with control proteins could be labelled; additionally a variety of control experiments reveal that the probes act in an affinity-based manner on active enzymes and that UV activation is required for labeling have been performed. Furthermore, competition experiments with different kinase inhibitors have been performed.

Generating photo-affinity labelled kinase inhibitors is an attractive way to identify other kinase inhibitors and – when used in cell lysates in combination with a conjugation handle – to identify novel inhibitor-novel kinase targets in a relatively unbiased manner. The isolation and identification then have to be improved for reliable detection of targets. This may be achieved by optimizing the probes with *in silico* methods for an optimal placement of the photo-affinity group and the isolation handle. Furthermore, alternative bioconjugation handles could improve the isolation of the targeted kinases.

Experimental

Chemistry

General materials and methods

Tetrahydrofuran (THF) was distilled over LiAlH₄ before use. Acetonitrile (ACN), dichloromethane (DCM), *N,N*-dimethylformamide (DMF), methanol (MeOH) and trifluoroacetic acid (TFA) were of peptide synthesis grade, obtained from Biosolve, and were used as received. All general chemicals (Fluka, Acros, Merck, Aldrich, Sigma) were used as received. Traces of water were removed from reagents used in reactions that require anhydrous conditions by co-evaporation with toluene. Solvents that were used in reactions were stored over activated 4 Å molecular sieves, with the exception of methanol and acetonitrile which were stored over activated 3 Å molecular sieves. Unless noted otherwise all reactions were performed under an argon atmosphere. Column chromatography was performed on Silicycle Silia-P Flash Silica Gel, with a particle size of 40 – 63 µm. The eluents toluene and ethyl acetate were distilled prior to use. TLC analysis was conducted on Merck aluminium sheets (Silica gel 60 F254). Compounds were visualized by UV absorption (254 nm), by spraying with a solution of (NH₄)₆Mo₇O₂₄·4H₂O (25 g/L) and (NH₄)₄Ce(SO₄)₄·2H₂O (10 g/L) in 10% sulphuric acid, a solution of KMnO₄ (20 g/L) and K₂CO₃ (10 g/L) in water, or ninhydrin (0.75 g/L) and acetic acid (12.5 mL/L) in ethanol, where appropriate, followed by charring at ca. 150 °C. ¹H- and ¹³C-NMR spectra were recorded on a Bruker DMX-400 (400 MHz) or a Bruker DMX-600 (600 MHz) spectrometer. Chemical shifts are given in ppm (δ) relative to tetramethylsilane (¹H-NMR) or CDCl₃ (¹³C-NMR) as internal standard. Mass spectra were recorded on a PE/Sciex API 165 instrument equipped with an Electrospray Interface (ESI) (Perkin-Elmer). High-resolution MS (HRMS) spectra were recorded with a Finnigan LTQ-FT (Thermo Electron). IR spectra were recorded on a Shimadzu FTIR-8300 and absorptions are given in cm⁻¹. Optical rotations [α]_D²³ were recorded on a Propol automatic polarimeter at room temperature. LC-MS analysis was performed on a

Jasco HPLC system with a Phenomenex Gemini 3 μ m C18 50 x 4.6 mm column (detection simultaneously at 214 and 254 nm), coupled to a PE Sciex API 165 mass spectrometer with ESI. HPLC gradients were 10 \rightarrow 90%, 0 \rightarrow 50% or 10 \rightarrow 50% ACN in 0.1% TFA/H₂O. Chiral HPLC analysis was performed on a Spectroflow 757 system (ABI Analytical Kratos Division, detection at 254 nm) equipped with a Chiralcel OD column (150 x 4.6 mm). The compounds were purified on a Gilson HPLC system coupled to a Phenomenex Gemini 5 μ m 250 x 10 mm column and a GX281 fraction collector. The used gradients were either 0 \rightarrow 30% or 10 \rightarrow 40% ACN in 0.1% TFA/water, depending on the lipophilicity of the product. Appropriate fractions were pooled, and concentrated in a Christ rotary vacuum concentrator overnight at room temperature at 0.1 mbar.

Diethyl (1-cyano-4-(trityloxy)butyl)phosphonate (7)

To an ice-cold solution of NaH (1 eq., 0.20 g, 5.1 mmol, 60% mineral oil) in DMF (15 mL) diethyl cyanomethylphosphonate **5** (0.89 g, 5.0 mmol) was added slowly and allowed to stir for 30 min before addition of ((3-bromopropoxy)methanetrityl) tribenzene **6** (1 eq., 1.94 g, 5.1 mmol). The reaction mixture was allowed to warm to RT and then stirred overnight. The mixture was diluted with H₂O (75 mL) and Et₂O (25 mL), the layers were separated, the aqueous phase extracted with Et₂O (3 x 25 mL) and the combined organic phases were washed with sat. aq. NaHCO₃ and brine, dried over MgSO₄, filtered and concentrated *in vacuo*. The residue was further purified by silica column chromatography (10% \rightarrow 50% EtOAc/PE) to afford the title compound as pale yellow oil (yield: 1.27 g, 2.7 mmol, 53%). *R*_F = 0.3 (50% EtOAc/PE). ¹H-NMR (400 MHz, CDCl₃, Me₄Si) δ 7.42 (6H, d, *J* = 7.2 Hz, 6 x CH_{ar}), 7.29 (6H, t, *J* = 6.8 Hz, 6 x CH_{ar}), 7.22 (3H, t, *J* = 7.2 Hz, 3 x CH_{ar}), 4.26 – 4.15 (4H, m, 2 x CH₂CH₃), 3.14 (2H, t, *J* = 5.6 Hz, CH₂OCPH₃), 2.95 (1H, ddd, *J*₁ = 4.8, *J*₂ = 10.4 Hz, *J*₃ = 23.2 Hz, CH), 2.12 – 2.00 (1H, m, CH₂-H^a), 1.98 – 1.90 (2H, m, CH₂), 1.84 – 1.75 (1H, m, CH₂-H^b), 1.35 (6H, m, 2 x CH₃). ¹³C-NMR (101 MHz, CDCl₃) δ 143.82, 128.40, 127.66, 126.86, 116.12, 86.47, 63.84, 63.46, 61.91, 30.18, 28.76, 27.74, 24.22, 16.23. HRMS: calculated for C₂₈H₃₂NO₄P [M+H]⁺ 478.20690; found 478.20372.

4-(3-(Trifluoromethyl)-3H-diazirin-3-yl)benzaldehyde (9)

A solution of DMSO (2.5 eq., 3.22 mL, 45.4 mmol) was cooled to -78 °C and oxalyl chloride (1.3 eq., 2.06 mL, 24.0 mmol) was added dropwise, the reaction mixture was stirred for 30 min at -78 °C. Next, a solution of alcohol **8** (3.93 g, 18.2 mmol) in DCM (10 mL) was added slowly. The reaction was stirred for 1 h at -78 °C before TEA (5 eq., 12.6 mL, 90.8 mmol) was slowly added at -78 °C. The reaction mixture was allowed to warm to 0 °C and was subsequently stirred for 3h. A cold aqueous solution of 20% KH₂PO₄ (50 mL) and cold H₂O (200 mL) was added and the resulting mixture was stirred for 15 min at RT. The mixture was diluted with Et₂O (200 mL) and the layers were separated. The organic layer was washed with a cold aqueous solution of 10% KH₂PO₄ (3 x 50 mL) and brine, dried over MgSO₄, filtered and evaporated *in vacuo*. The obtained material was purified by column chromatography (1% EtOAc/PE \rightarrow 5% EtOAc/PE) and the product was obtained as pale yellow oil (yield: 3.45 g, 16.12 mmol, 89%). ¹H-NMR (400 MHz, CDCl₃, Me₄Si) δ 10.05 (1H, s, CHO), 7.91 (2H, d, *J* = 8.4 Hz, 2 x CH_{ar}), 7.34 (2H, d, *J* = 8.0

Hz, 2 x CH_{ar}). ¹³C-NMR (101 MHz, CDCl₃) δ 190.85, 136.73, 134.99, 129.65, 126.77, 121.69 (q, *J* = 275.73 Hz), 28.31 (q, *J* = 41.41 Hz). HRMS: calculated for C₉H₅F₃N₂O [M+H]⁺ 215.03540; found 215.03549.

(*E/Z*)-2-(4-(3-(trifluoromethyl)-3*H*-diazirin-3-yl)benzylidene)-5-(trityloxy)pentanenitrile (10)

To an ice-cold suspension of NaH (1.1 eq., 0.64 g, 15.9 mmol, 60% mineral oil) in THF (75 mL) a solution of phosphonate **7** (6.91 g, 14.5 mmol) in THF (25 mL) was added dropwise and stirred for 30 min. Next, a solution of aldehyde **9** (1.1 eq., 3.45 g, 16.6 mmol) in THF (10 mL) was added and the reaction mixture was allowed to warm to RT and stirred overnight. The solution was quenched by addition of freshly prepared sat. aq. Na₂HSO₃ (60 mL) and diluted with H₂O (200 mL) and Et₂O (100 mL). The layers were separated and the aqueous phase was extracted with Et₂O (3 x 100 mL). The combined organic layers were washed with sat. aq. NaHCO₃ and brine, dried over MgSO₄, filtered and evaporated. The residue was further purified by silica column chromatography (10% → 80% toluene/pentane) to afford the title compound as a white solid with an *E/Z* ratio of 3/2 (yield: 6.16 g, 11.5 mmol, 79%). ¹H-NMR (400 MHz, CDCl₃, Me₄Si) δ 7.62 (2H, d, *J* = 8.4, 2 x CH_{ar}), 7.42 (6H, d, *J* = 7.2 Hz, 6 x CH_{ar}), 7.27 – 7.15 (11H, m, 11 x CH_{ar}), 6.82 (1H, s, CH), 3.14 (2H, t, *J* = 5.6 Hz, CH₂), 2.55 (2H, t, *J* = 7.2 Hz, CH₂), 1.98 – 1.91 (2H, m, CH₂). ¹³C-NMR (101 MHz, CDCl₃) δ 144.02, 142.03, 134.84, 130.34, 128.71, 128.51, 128.16, 126.94, 126.57, 121.91 (q, 198.97 Hz), 125.24, 118.16, 112.96, 86.46, 61.51, 33.51, 28.23. HRMS: calculated for C₃₃H₂₆F₃N₃O [M+H]⁺ 538.20280; found 538.20293.

***N*-(2-aminoethyl)isoquinoline-5-sulfonamide (13)**

Isoquinoline-5-sulfonic acid **12** (20.92 g, 100 mmol) was treated with thionylchloride (13 eq., 91.5 mL, 1300 mmol) and a catalytic amount of DMF for 2 h at reflux. The reaction mixture was concentrated and the residue was thoroughly washed with DCM before being re-suspended in H₂O (300 mL) at 0 °C. NaHCO₃ (1 eq., 8.42 g, 100.2 mmol) was added portion-wise. Next, the mixture was extracted with DCM (3x 500 mL) and dried over MgSO₄. The filtrate was added dropwise to a cooled solution of ethylene diamine (5 eq., 33.4 mL, 500 mmol) in DCM (250 mL) and the reaction mixture was allowed to warm to RT and stirred for 1 h. The mixture was then concentrated before being washed with brine (50 mL). The aqueous layer was extracted with DCM (10 x 50 mL) and the combined organic layers were washed with brine (50 mL), dried over MgSO₄, filtered and concentrated. The title compound was obtained as a thick yellow oil (yield: 17.3 g, 69 mmol, 69%) and was used without further purification. ¹H-NMR (400 MHz, CDCl₃, Me₄Si) δ 9.36 (1H, s, CH_{ar}), 8.67 (1H, d, *J* = 8.4 Hz, CH_{ar}), 8.47 – 8.43 (2H, m, 2 x CH_{ar}), 8.21 (1H, d, *J* = 11.2 Hz, CH_{ar}), 7.71, (1H, t, *J* = 10.0 Hz, CH_{ar}), 3.45 (3H, bs, NH₂ and NH), 3.00 (2H, t, *J* = 5.2 Hz, CH₂), 2.76 (2H, t, *J* = 6.0 Hz, CH₂). ¹³C-NMR (101 MHz, CDCl₃) δ 153.26, 145.06, 133.46, 133.19, 131.23, 129.01, 125.91, 117.22, 45.12, 40.76.

***Tert*-butyl(*E*)-[5-hydroxy-2-(4-(3-(trifluoromethyl)-3*H*-diazirin-3-yl)benzylidene)pentyl](2-(isoquinoline-5-sulfonamido)ethyl)-carbamate (18)**

A solution of nitrile **10** (3.34 g, 6.2 mmol) in anhydrous Et₂O (20 mL) and DCM (20 mL) was cooled to -78 °C. DiBAL-H (2 eq., 12.4 mL, 12.4 mmol, 1M solution in hexanes) was added dropwise and the reaction

mixture was allowed to warm to 0 °C and stirred for 2h, after which TLC analysis showed complete consumption of the starting material. Next, the mixture was cooled to -100 °C followed by rapid addition of MeOH (13 mL). After 5 min a solution of isoquinoline amine **13** (2.5 eq., 3.90 g, 15.5 mmol) in MeOH (10 mL) was added dropwise and the reaction mixture was allowed to stir at RT overnight. Hereafter, the reaction was cooled to -10 °C and NaBH₄ (2 eq., 0.47 g, 12.4 mmol) was added and the mixture was allowed to stir for 4h at RT. The reaction mixture was diluted with 0.5 M aq. NaOH (100 mL) and the layers were separated. The aqueous layer was extracted with DCM (3 x 50 mL) and the combined organic phases were washed with H₂O (3 x 50 mL) and brine, dried over MgSO₄, filtered and evaporated. The crude product was subjected to the next step without further purification.

The crude product was dissolved in DCM (20 mL) and TFA (20 mL) was added dropwise. The reaction mixture was stirred for 30 min at RT before addition of H₂O (40 mL), the resulting mixture was stirred for 1h at RT. Hereafter, the mixture was co-evaporated with toluene dissolved in DCM (70 mL) and cooled in an ice bath. To the mixture Boc₂O (1.1 eq., 1.49 g, 6.8 mmol) and TEA (4 eq., 3.4 mL, 24.8 mmol) were added and the reaction was allowed to warm to RT and stirred overnight. The reaction mixture was concentrated under reduced pressure and re-dissolved in H₂O (50 mL) and EtOAc (50 mL). The organic layer was washed with sat. aq. NaHCO₃ and brine, dried over MgSO₄, filtered and concentrated *in vacuo*. The title compound was obtained after purification by RP-HPLC purification (linear gradient 40% → 60% ACN in H₂O, 0.1% TFA, 15 min) as a yellow oil (yield: 0.61 g, 0.97 mmol, 15.8%).

¹H-NMR (400 MHz, CDCl₃, Me₄Si) δ 9.32 (1H, s, CH_{ar}), 8.58 (1H, d, *J* = 6.0 Hz, CH_{ar}), 8.39 (1H, d, *J* = 6.4 Hz, CH_{ar}), 8.27 (1H, d, *J* = 7.2 Hz, CH_{ar}), 8.18 (1H, d, *J* = 8.0 Hz, CH_{ar}), 7.65 (1H, t, *J* = 7.6 Hz, CH_{ar}), 7.11 (4H, s, 4 x CH_{ar}), 3.99 (2H, s, CH₂), 3.65 (2H, t, *J* = 6.0 Hz, CH₂OH), 3.10 (2H, s, CH₂), 2.81 (2H, t, 6.0 Hz, CH₂), 2.09 (2H, t, *J* = 8.0 Hz, CH₂), 1.79 – 1.74 (2H, m, CH₂), 1.39 (9H, s, 3 x CH₃). ¹³C-NMR (101 MHz, CDCl₃) δ 152.94, 144.56, 139.76, 138.19, 134.37, 133.24, 132.80, 131.05, 129.12, 128.87, 127.87, 127.21, 126.10, 125.76, 121.93 (q, *J* = 275.73 Hz), 117.31, 80.78, 61.67, 45.76, 45.31, 41.48, 31.05, 30.06, 28.18 (q, *J* = 40.4 Hz), 28.10. HRMS: calculated for C₃₀H₃₄F₃N₅O₅S [M+H]⁺ 634.22327; found 634.22333.

***Tert*-butyl(Z)-(5-hydroxy-2-(4-(3-(trifluoromethyl)-3H-diazirin-3-yl)benzylidene)pentyl)(2-(isoquinoline-5-sulfonamido)ethyl)-carbamate (**19**)**

This compound was prepared in the same reaction as **18**. The title compound was obtained after purification by RP-HPLC purification (linear gradient 40% → 60% ACN in H₂O, 0.1% TFA, 15 min) as a yellow oil (yield: 0.44 g, 0.7 mmol, 14%). ¹H-NMR (400 MHz, CDCl₃, Me₄Si) δ 9.31 (1H, s, CH_{ar}), 8.59 (1H, d, *J* = 6.0 Hz, CH_{ar}), 8.45 (1H, d, *J* = 6.4 Hz, CH_{ar}), 8.37 (1H, d, *J* = 6.8 Hz, CH_{ar}), 8.14 (1H, d, *J* = 7.6 Hz, CH_{ar}), 7.60 (1H, t, *J* = 7.6 Hz, CH_{ar}), 7.19 (2H, d, *J* = 8.4 Hz, 2 x CH_{ar}), 7.10 (2H, d, *J* = 8.0 Hz, 2 x CH_{ar}), 6.15 (1H, s, CH), 3.85 (2H, s, CH₂), 3.57 (2H, t, *J* = 6.0 Hz, CH₂OH), 3.35 (2H, bs, CH₂), 3.12 (2H, t, *J* = 5.6 Hz, CH₂), 2.08 (2H, t, *J* = 7.2 Hz, CH₂), 1.67 (2H, bs, CH₂), 1.40 (9H, s, 3 x CH₃). ¹³C-NMR (101 MHz, CDCl₃) δ 153.01, 144.63, 139.57, 138.33, 134.45, 133.30, 132.95, 131.13, 129.16, 128.93, 128.78, 127.16, 126.21, 125.83, 121.98 (q, *J* = 275.73 Hz), 117.41, 61.93, 53.55, 46.41, 42.09, 30.95, 28.22 (q, *J* = 40.4 Hz), 28.15. HRMS: calculated for C₃₀H₃₄F₃N₅O₅S [M+H]⁺ 634.22327; found 634.22312.

***Tert*-butyl(*E*)-(5-azido-2-(4-(3-(trifluoromethyl)-3*H*-diazirin-3-yl)benzylidene)pentyl)(2-(isoquinoline-5-sulfonamido)ethyl)-carbamate (**20**)**

Alcohol **18** (0.16 g, 0.26 mmol) was dissolved in DCM (5 mL). After addition of TEA (1 eq., 36 μ L, 0.26 mmol) and DMAP (0.64 mg, 5 μ mol) the resulting mixture was cooled to -20 °C. A solution of TsCl (1 eq., 0.05 g, 0.26 mmol) in DCM (2 mL) was added dropwise and the reaction was stirred at -20 °C for 18h. Subsequently, 0.1 M aq. HCl (10 mL) was added and the layers were separated. The organic layer was washed with 0.1 M HCl (10 mL) and brine, dried over MgSO₄, filtered and concentrated under reduced pressure. The crude product was subjected to the next step without further purification.

The residue was dissolved in DMF (10 mL). To this was added NaN₃ (10 eq., 0.17 g, 2.6 mmol) and the reaction was stirred at room temperature for 5h before being concentrated. The resulting residue was purified by RP-HPLC gradient (linear gradient 40% \rightarrow 60% ACN in H₂O, 0.1% TFA, 15 min) and the title compound was obtained as light-yellow oil (yield: 0.44 g, 0.7 mmol, 14%). ¹H-NMR (400 MHz, CDCl₃, Me₄Si) δ 9.36 (1H, s, CH_{ar}), 8.68 (1H, s, CH_{ar}), 8.34 (1H, s, CH_{ar}), 8.29 (1H, d, *J* = 7.2 Hz, CH_{ar}), 8.20 (1H, d, *J* = 8.0 Hz, CH_{ar}), 7.67 (1H, t, *J* = 8.0 Hz, CH_{ar}), 7.16 – 7.09 (4H, m, 4 x CH_{ar}), 6.48 (1H, s, CH), 3.97 (2H, s, CH₂), 3.29 (2H, t, *J* = 6.4 Hz, CH₂N₃), 3.06 (2H, t, *J* = 5.6 Hz, NHCH₂), 2.78 (2H, bs, CH₂), 2.05 (2H, t, *J* = 6.8 Hz, CH₂), 1.78 – 1.75 (2H, m, CH₂CH₂N₃), 1.45 (9H, s, 3 x CH₃). ¹³C-NMR (101 MHz, CDCl₃) δ 162.54, 153.14, 145.03, 137.93, 134.30, 133.37, 132.92, 131.11, 129.20, 128.97, 128.73, 127.63, 126.31, 125.74, 122.00 (q, *J* = 275.7 Hz), 117.20, 81.17, 50.82, 45.66, 44.94, 41.87, 30.90, 28.23, 27.43. HRMS: calculated for C₃₀H₃₃F₃N₈O₄S [M+H]⁺ 659.22976; found 659.22963.

***(E)*-N-(2-((5-azido-2-(4-(3-(trifluoromethyl)-3*H*-diazirin-3-yl)benzylidene)pentyl)amino)ethyl)isoquinoline-5-sulfonamide (**3**)**

TFA (0.5 mL) was added to a solution of *tert*-butyl(*E*)-(5-azido-2-(4-(3-(trifluoromethyl)-3*H*-diazirin-3-yl)benzylidene)pentyl)-(2-(isoquinoline-5-sulfonamido)ethyl)-carbamate **20** (95 μ g, 0.14 mmol) in DCM (0.5 mL). After 1h TLC analysis indicated complete conversion of the starting material. Toluene was added and the mixture was co-evaporated under reduced pressure. In order to remove excess TFA the mixture was co-evaporated twice with toluene. The resulting mixture was purified by RP-HPLC (linear gradient 40% \rightarrow 60% ACN in H₂O, 0.1% TFA, 15 min) and the title compound was obtained as a yellowish oil (yield: 0.44 g, 0.7 mmol, 14%). ¹H-NMR (400 MHz, CDCl₃, Me₄Si) δ 9.29 (1H, s, CH_{ar}), 8.57 (1H, d, *J* = 4.8 Hz, CH_{ar}), 8.39 (1H, d, *J* = 5.2 Hz, CH_{ar}), 8.35 (1H, d, *J* = 7.6 Hz, CH), 8.15 (1H, d, *J* = 8.0 Hz, CH_{ar}), 7.64 (1H, t, *J* = 7.6 Hz, CH_{ar}), 7.18 (2H, d, *J* = 8.4 Hz, 2 x CH_{ar}), 7.11 (2H, d, *J* = 8.4 Hz, 2 x CH_{ar}), 6.63 (1H, s, CH), 3.74 (2H, s, CH₂), 3.28 (2H, bs, CH₂N₃), 3.19 (2H, t, *J* = 6.4 Hz, CH₂), 2.33 (2H, t, *J* = 8.4 Hz, CH₂), 1.67 – 1.60 (2H, m, CH₂). ¹³C NMR (101 MHz, CDCl₃) δ 153.96, 144.69, 136.72, 133.95, 133.71, 133.35, 132.62, 131.14, 128.92, 128.85, 128.52, 126.48, 126.03, 121.97 (q, *J* = 274.7 Hz), 177.40, 52.68, 50.70, 46.88, 39.07, 31.17, 28.27 (q, *J* = 41.4 Hz), 26.98, 25.90. HRMS: calculated for C₂₅H₂₅F₃N₈O₂S [M+H]⁺ 559.17733; found 559.17750.

***Tert*-butyl(*Z*)-(5-azido-2-(4-(3-(trifluoromethyl)-3*H*-diazirin-3-yl)benzylidene)pentyl)(2-(isoquinoline-5-sulfonamido)ethyl)carbamate (**21**)**

An identical method was used as for the synthesis of *tert*-butyl(*E*)-(5-azido-2-(4-(3-(trifluoromethyl)-3*H*-diazirin-3-yl)-benzylidene)-pentyl)(2-(isoquinoline-5-sulfonamido)ethyl)-carbamate except that compound **19** (0.39 g, 0.61 mmol) was used as starting material and the amounts of the other reagents were adjusted accordingly. Purification by RP-HPLC (linear gradient 40% → 60% ACN in H₂O, 0.1% TFA, 15 min) yielded the title compound as light yellow oil (yield: 0.44 g, 0.7 mmol, 14%). ¹H-NMR (400 MHz, CDCl₃, Me₄Si) δ 9.35 (1H, s, CH_{ar}), 8.65 (1H, d, *J* = 6.0 Hz, CH_{ar}), 8.43 (1H, d, *J* = 6.0 Hz, CH_{ar}), 8.39 (1H, d, *J* = 7.2 Hz, CH_{ar}), 8.18 (1H, d, *J* = 8.0 Hz, CH_{ar}), 7.63 (1H, t, *J* = 7.6 Hz, CH_{ar}), 7.19 – 7.13 (4H, m, 4 × CH_{ar}), 6.22 (1H, s, CH), 3.87 (2H, s, CH₂), 3.35 (2H, bs, CH₂N₃), 3.20 (2H, t, *J* = 6.4 Hz, CH₂), 3.11 (2H, bs, CH₂), 2.21 – 2.05 (2H, m, CH₂), 1.67 – 1.63 (2H, m, CH₂), 1.44 (9H, s, 3 × CH₃). ¹³C-NMR (101 MHz, CDCl₃) δ 153.06, 144.79, 138.71, 138.13, 134.41, 133.06, 131.23, 129.20, 128.78, 127.89, 127.56, 126.40, 125.83, 122.04 (q, *J* = 275.7 Hz), 117.37, 81.02, 53.44, 51.33, 46.09, 42.39, 28.24, 27.26, 25.78. HRMS: calculated for C₃₀H₃₃F₃N₈O₄S [M+H]⁺ 659.22976; found 659.22984.

***Z*-*N*-(2-((5-azido-2-(4-(3-(trifluoromethyl)-3*H*-diazirin-3-yl)benzylidene)pentyl)amino)ethyl)isoquinoline-5-sulfonamide (**4**)**

An identical method was used as for the synthesis of **3** except that *tert*-butyl(*Z*)-(5-azido-2-(4-(3-(trifluoromethyl)-3*H*-diazirin-3-yl)benzylidene)pentyl)(2-(isoquinoline-5-sulfonamido)ethyl)-carbamate (0.56 g, 0.85 mmol) was used as starting material and the amounts of the other materials were adjusted accordingly. Purification by RP-HPLC (linear gradient 40% → 60% ACN in H₂O, 0.1% TFA, 15 min) yielded the title compound as light yellow oil (yield: 0.44 g, 0.7 mmol, 14%). ¹H-NMR (400 MHz, CDCl₃, Me₄Si) δ 9.46 (1H, bs, CH_{ar}), 8.59 (1H, bs, CH_{ar}), 8.40 (1H, d, *J* = 7.2 Hz, CH_{ar}), 8.31 (2H, d, *J* = 8.0 Hz, 2 × CH_{ar}), 7.76 (1H, t, *J* = 7.6 Hz, CH_{ar}), 7.17 – 7.12 (4H, m, 4 × CH_{ar}), 6.74 (1H, s, CH), 3.82 (2H, s, CH₂), 3.31 (2H, t, *J* = 6.4 Hz, CH₂N₃), 3.12 (2H, s, CH₂), 2.98 (2H, s, CH₂), 2.37 (2H, t, *J* = 7.2 Hz, CH₂), 1.83 – 1.76 (2H, m, CH₂). ¹³C-NMR (101 MHz, CDCl₃) δ 150.45, 139.88, 136.78, 135.16, 134.62, 134.33, 133.80, 132.40, 132.15, 128.93, 128.59, 127.54, 126.77, 121.94 (q, *J* = 275.7 Hz), 119.69, 50.55, 46.71, 45.73, 38.87, 31.13, 31.07, 28.20 (q, *J* = 40.4 Hz), 26.98. HRMS: calculated for C₂₅H₂₅F₃N₈O₂S [M+H]⁺ 559.17733; found 559.17753.

Biochemistry

IC₅₀ and K_i determination by FRET assay

Kinase activity was measured using a FRET-based assay with a peptide from ribosomal protein S6 as substrate. 10 nM ULight-rpS6 peptide (Perkin-Elmer) was incubated with 100 μM ATP and 2 nM Eu-labeled anti-phospho-rpS6 antibody (Perkin-Elmer, recognizing pSer S6 at position 235 and 236) in HEPES buffer (50 mM HEPES pH 7.5, 1 mM EGTA, 10 mM MgCl₂, 2 mM DTT and 0.01% Tween-20) together with 0.5 nM/min AKT1 or 0.05 nM/min PKA (SignalChem), in the presence or absence of the probe or H-89. During incubation at RT, the intensity of the light emission was measured with intervals of 60 min on a

PE Envision reader using the Lance Ultra kinase assay settings (λ_{ex} 320 nm; λ_{em} 665 nm) and a secondary control emission was measured at 615 nm. In control experiments, no ATP was added to the buffer. Data was analyzed using GraphPad Prism 5 (GraphPad software, La Jolla, USA).

To determine the K_M for the kinases, the same assay was performed using a fixed concentration of probe or H-89 (2 μM) and 0, 0.1, 0.2, 0.5, 1, 2, 5, 10, 20, 50, 100, 200, 500, 1000 μM ATP. K_M values were calculated using GraphPad Prism 5 (GraphPad software, La Jolla, USA).

K_i values were calculated via equation 1.1:

$$K_i = \text{IC}_{50} / (1 + ([S]/K_M)) \quad (1.1)$$

where K_i is the inhibition constant, IC_{50} is the half maximal inhibitory concentration, S is the concentration of substrate and K_M is the Michaelis-Menten constant, which is the substrate concentration at which the reaction rate is half maximum. All experiments were conducted in triplicate and curves were corrected for background fluorescence of the solvent.

Photo-labeling of recombinant kinases (PKA, AKT1)

PKA (PKAc beta) and AKT1 were purchased from Signalchem, aliquoted, stored at -80°C and thawed only once for an experiment.

For pre-denatured samples the solutions were treated with 10% SDS (2 μL) and boiled for 5 min before addition of the probes. Non-irradiated samples were protected from light by wrapping in aluminium foil. Competition experiments were performed in triplicate, quantification of residual activity was achieved by fluorescent densitometry using the Biorad Image Lab software (version 5.2.1).

In a typical experiment, 100 ng (1 μL [100 ng/ μL] of recombinant enzyme were added to the assay buffer (17 μL) (20 mM HEPES, pH 7.5, 50 mM KCl, 10 mM MgCl_2 , 10% glycerol)(adapted). For competition experiments, the respective inhibitor (1 μL , 20X) was added next and the samples were incubated in the dark at RT for 30 min. For all experiments probe **3**, probe **4** (2 μL , 10X or 1 μL , 20X in competition experiments) or DMSO were added and the samples were incubated for 30 min at RT in the dark. For irradiation the samples were transferred to a clear, flat-bottom 96-well plate and diluted with 30 μL 100 mM HEPES, pH 7.5. The samples were then irradiated for 5 min at 0°C and transferred back into Eppendorf tubes, the concentration was further adjusted by adding 5 μL of 100 mM HEPES, pH 7.5; the untreated samples were diluted in the same way. For the attachment of the Cy5 fluorophore by click reaction samples were treated with "click mix" (6 μL /sample), prepared freshly as follows: 3 μL 25 mM CuSO_4 (aq.) were mixed with 1.8 μL 0.25 M sodium ascorbate, resulting in a brown solution, this was then vortexed until a colour change to bright yellow was achieved, indicating the reduction of the copper ion. Next, THPTA (0.6 μL , 25 mM in DMSO) was added and the mixture vortexed again. Finally, 0.6 μL of a 150X Cy5 alkyne (relative to the amount of probe used in the experiment) was added, the mixture vortexed again, added to the sample, mixed and incubated for 1h at RT in the dark. The final concentrations of the click reagents were 1.25 mM CuSO_4 , 7.5 mM sodium ascorbate, 250 μM THPTA

and 1.5 eq. Cy5 alkyne. The reaction was stopped by adding 20 μ L of SDS loading buffer and boiling for 5 min.

Samples were resolved by 10% SDS-PAGE, for in-gel detection of fluorescent bands, wet gel slabs were scanned with ChemiDoc MP system using Cy5 settings.

References

- ¹ T. Chijiwa, A. Mishima, M. Hagiwara, M. Sano, K. Hayashi, T. Inoue, K. Naito, T. Toshioka and H. Hidaka, *J. Biol. Chem.*, 1990, **265**, 5267.
- ² A. Lochner and J. A. Moolman, *Cardiovasc. Drug Rev.*, 2006, **24**, 261.
- ³ R. A. Engh, A. Girod, V. Kinzel, R. Huber and D. Bossemeyer, *J. Biol. Chem.*, 1996, **271**, 26157.
- ⁴ S. P. Davies, H. Reddy, M. Caivano and P. Cohen, *Biochem. J.*, 2000, **351**, 95.
- ⁵ J. A. Engelmann, *Nat. Rev. Cancer*, 2009, **9**, 550.
- ⁶ B. D. Manning and L. C. Cantley, *Cell*, 2007, **129**, 1261.
- ⁷ K. Moelling, K. Schad, M. Bosse, S. Zimmermann and M. Schweneker, *J. Biol. Chem.*, 2002, **277**, 31099.
- ⁸ C. Kuijl, N. D. L. Savage, M. Marsman, A. W. Tuin, L. Janssen, D. A. Egan, M. Ketema, R. van den Nieuwendijk, S. J. F. van den Eeden, A. Geluk, A. Poot, G. van der Marel, R. L. Beijersbergen, H. Overkleeft, T. H. M. Ottenhoff and J. Neefjes, *Nature*, 2007, **450**, 725.
- ⁹ G. Médard, F. Pachi, B. Ruprecht, S. Klaeger, S. Heinzlmeier, D. Helm, H. Qiao, X. Ku, M. Wilhelm, T. Kuehne, Z. Wu, A. Dittmann, C. Hopf, K. Kramer and B. Kuster, *J. Proteome Res.*, 2015, **14**, 1574.
- ¹⁰ J. F. Fischer, C. Dalhoff, A. K. Schrey, O. Y. Graebner, S. Michaelis, K. Andrich, M. Glinski, F. Kroll, M. Sefkow, M. Dreger and H. Koester, *J. Proteomics*, 2011, **75**, 160.
- ¹¹ J. F. Fischer, O. Y. Graebner, C. Dalhoff, S. Michaelis, A. K. Schrey, J. Ungewiss, K. Andrich, D. Jeske, F. Kroll, M. Glinski, M. Sefkow, M. Dreger and H. Koester, *J. Proteome Res.*, 2010, **9**, 806.
- ¹² T. Barf and A. Kaptein, *J. Med. Chem.*, 2012, **55**, 6243.
- ¹³ N. Liu, S. Hoogendoorn, B. van der Kar, A. Kaptein, T. Barf, C. Driessen, D. V. Filippov, G. A. van der Marel, M. van der Stelt and H. S. Overkleeft, *Org. Biomol. Chem.*, 2015, **15**, 5147.
- ¹⁴ US Pat., US20080096903(A1), 2008.
- ¹⁵ M. Wiegand and T. K. Lindhorst, *Eur. J. Org. Chem*, 2006, 4841.
- ¹⁶ A. M. C. H. van den Nieuwendijk, A. B. T. Ghisaidoobe, H. S. Overkleeft, J. Brussee and A. van der Gen, *Tetrahedron*, 2004, **60**, 10385-10396.; P. Zandbergen, A. M. C. H. van den Nieuwendijk, J. Brussee and A. van der Gen, *Tetrahedron*, 1992, **48**, 3977.
- ¹⁷ M. W. Karaman, S. Herrgard, D. K. Treiber, P. Gallant, C. E. Atteridge, B. T. Campbell, K. W. Chan, P. Ciceri, M. J. Davis, P. T. Edeen, R. Faraoni, M. Floyd, J. P. Hunt, D. J. Lockhart, Z. V. Milanov, M. J. Morrison, G. Pallares, H. K. Patel, S. Pritchard, L. M. Wodicka and P. P. Zarrinkar, *Nat. Biotech.*, 2008, **26**, 127.
- ¹⁸ Y. Luo, C. Blex, O. Baessler, M. Glinski, M. Dreger, M. Sefkow and H. Koester, *Mol. Cell. Proteomics*, 2009, **8**, 2843.

7

An affinity-based probe for kinase profiling: Fishing for Dasatinib targets

7.1 Introduction

Chronic lymphocytic leukemia (CLL) is the most common hematologic disease occurring among adults in the Western world. It is characterized by the clonal expansion of mature, $CD5^{+}$ - $CD23^{+}$ B cells in the peripheral blood, secondary lymphoid tissues, and bone marrow.¹ This malignancy is still considered incurable, although new treatment combinations of monoclonal antibodies and chemotherapy appear promising.² Two compartments can be distinguished in CLL: the peripheral blood, in which quiescent CLL cells accumulate, and the tumor microenvironment within the lymphoid tissues and bone marrow that contain proliferating B cells and act as tumor reservoirs.³

The tissue microenvironment plays a central role in the pathogenesis of CLL. CLL cell proliferation occurs in distinct microanatomical sites termed proliferation centers or pseudofollicles.⁴ In these areas, CLL cells are in intimate contact with non-tumoral accessory cells, such as bone marrow stromal cells (BMSCs),^{5,6} monocyte-derived nurse-like cells,^{7,8,9,10} follicular dendritic cells, endothelial cells¹¹ and CD40L expressing T cells^{12,13} that provide the necessary external signals that drive maintenance of the CLL cells.^{14,15,16,17} Among the various external stimuli in the tissue microenvironments, B-cell receptor (BCR) signaling has been recognized as a crucial pathologic mechanism. Activation of BCR triggers a cascade of signaling events that promotes survival and growth of the CLL clone.^{18,19} As a consequence, BMSCs create niches that protect CLL cells from cytotoxic anticancer drugs and this in turn causes resistance to current chemotherapeutics.^{15,20} Currently, a variety of novel kinase inhibitors aiming to target various components of the BCR signaling pathway have been designed and are in clinical development for CLL. In previous studies, dasatinib (**1**, Figure 1), an oral Src/c-Abl tyrosine kinase inhibitor, has been demonstrated to induce apoptosis and/or sensitize against cytotoxic drugs.^{20,21,22} Initially, dasatinib was approved for treatment of chronic myeloid leukemia and second-line treatment of Philadelphia chromosome-positive acute lymphoblastic leukemia on the basis of Bcr-Abl inhibition²³, but the activity of dasatinib (**1**) against additional kinases provides a rationale for investigating it in other hematologic malignancies, such as CLL. In model systems, such as the chronic myeloid leukemia (CML)-derived cell-line K562, the spectrum of kinases targeted by dasatinib (**1**) has been mapped.²⁴ A prominent binder besides Abl and Src family kinases was the TEC family kinase BTK.²⁵ Since these kinases are all implicated in BCR- and or CD40-mediated microenvironmental stimuli, it is interesting to determine the actual targets of dasatinib and their contribution in mediating CLL survival and chemoresistance.

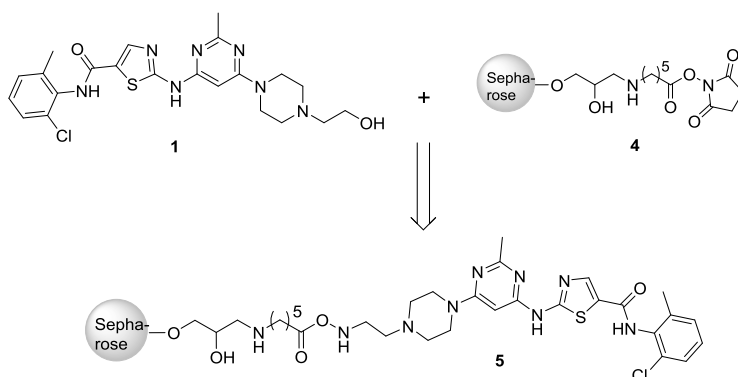


Figure 1. Affinity-based dasatinib probe **5**. Dasatinib **1** is immobilized by coupling it to sepharose beads **4**.

In this study, dasatinib (**1**) is coupled to an affinity matrix **4** to obtain the affinity-based kinase probe **5**, which is used to characterize its spectrum of targets in primary CLL by an affinity-based kinase profiling assay (Figure 2). In this assay, the immobilized dasatinib probe **5** binds noncovalently to its targets after exposure to CLL cell lysates. The interacting kinases are expected to be immobilized by affinity-chromatography, and non-binding proteins will be washed away. Next the retained proteins are washed from the affinity column under protein denaturing conditions and resolved on SDS PAGE. Bands from the gel are next excised, trypsinolysed and identified using mass spectrometry (MS).

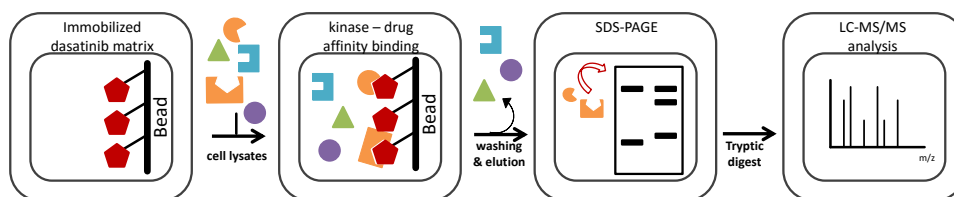
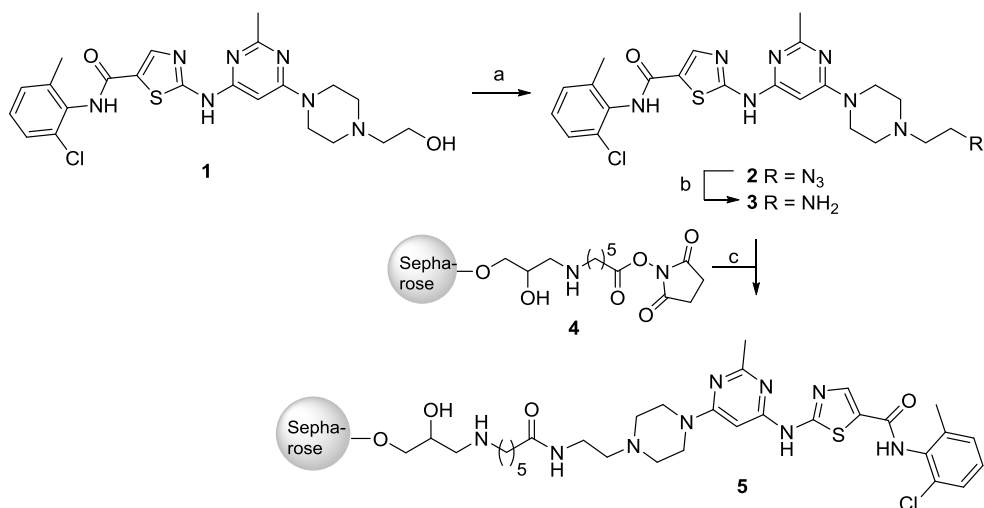


Figure 2. Affinity-based kinase profiling. Immobilized dasatinib matrix (**5**) is noncovalently bound to its cellular targets. After washing and elution, the targets are profiled by SDS-PAGE followed by LCMS for target identification.

7.2 Results and discussion

Synthesis of affinity-based dasatinib probe

In order to identify the interacting kinase(s) of dasatinib (**1**), this drug was modified and immobilized by covalent attachment to NHS-activated sepharose (**4**) via its free amine group (Scheme 1). Compound **3** was prepared via a slightly modified literature procedure of Kim D. *et al.*²⁶ First, dasatinib (**1**) was extracted from SprycelTM, which are tablets containing dasatinib, and converted to azide **2** via substitution of the corresponding mesylate with NaN_3 . A Staudinger reaction was performed to convert the azide **2** into its amine **3** using PMe_3 in $\text{DMF}/\text{H}_2\text{O}$. Finally, amine **3** was immobilized on NHS-activated Sepharose 4 Fast Flow beads **4**, which have a ligand density of 16-23 μmol NHS/mL drained gel, to obtain modified dasatinib **5**.



Scheme 1. Synthesis of immobilized dasatinib **3**. Reagents and conditions: a) i) MsCl, TEA, DMF, 0 °C – RT; ii) NaN₃, 41% after RP-HPLC; b) PMe₃, DMF/H₂O (2/1 v/v), 37% after RP-HPLC; c) **4**, DMSO, TEA.

Biological evaluation

In the first instance, the inhibitory potential of dasatinib-amine (**3**) was compared at different concentrations to the parent compound **1** by measuring the inhibitory effect on cell viability of K562 human CML cells, which are dependent on the Bcr-Abl fusion protein for survival³⁴. Figure 3 shows that dasatinib-amine (**3**) had identical activity as the parent compound **1**. Thus, it can be assumed that the targets that will be identified with the immobilized dasatinib **5** are identical for the parent compound **1** itself.

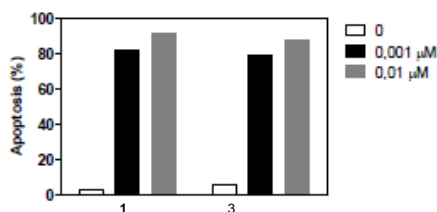


Figure 3. Dasatinib-amine (**3**) induces apoptosis of K562 human CML cells as effectively as the parent compound (**1**). K562 cells were treated with dasatinib (**1**) or dasatinib-amine (**3**) for 48 hr. Cell viability was measured by staining for DiOC6/PI. A representative experiment of two independent experiments is shown.

In the next set of experiments, the immobilized dasatinib **5** was used to identify the drug targets of dasatinib (**1**). Therefore, the immobilized dasatinib **5** was incubated with lysates of CD40 stimulated primary CLL cells. Without SDS-page analysis, the eluted proteins were

identified by liquid chromatography mass spectrometry (LC-MS) with subsequent database search of the analyzed MS spectra. Among the eluted kinases, c-Abl and BTK were identified as important targets of dasatinib (**1**) in the total lysates of CD40 stimulated CLL cells. Furthermore, other identified peptides mapping to the kinases were Lyn, Csk, Fyn, Yes, Src and Lck, which were previously described as specific targets of dasatinib in the CML line K562.³¹

Hereafter, Western blot analysis of pulldown experiments was used to confirm binding of c-Abl and BTK to immobilized dasatinib (**5**) in lysates of CD40-stimulated CLL cells. In agreement with previous studies, Lyn and p38MAPK were also identified as targets of dasatinib³¹ (**1**), whereas Syk and ZAP70, although abundantly expressed in CLL, did not bind to dasatinib-sepharose **5** (Figure 4A). As a control for specificity, competition experiments were performed in which lysates were preincubated with free soluble dasatinib **1** prior to exposure to immobilized dasatinib **5**. Western blot analysis confirmed competition of c-Abl, BTK, Lyn and p38MAPK from immobilized dasatinib (**5**) by free dasatinib (**1**) (Figure 4A, lane 4).

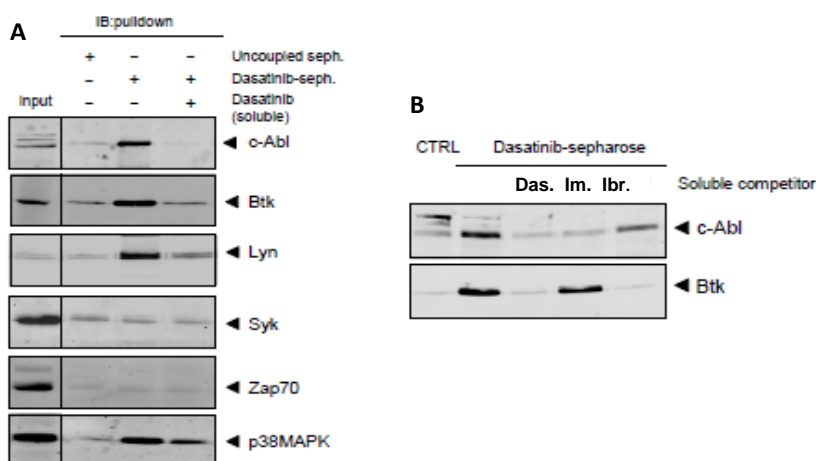


Figure 4. c-Abl and BTK are specific interactors of dasatinib in CD40-stimulated primary CLL. (A) Immunoblots of pull-down experiments with control Sepharose (uncoupled) and immobilized dasatinib **5** from lysates of CLL cells stimulated with CD40L for 48hrs. In lane 4, lysates were pretreated by addition of 10 μ M soluble dasatinib 30 minutes prior to exposure to dasatinib-sepharose. Western blots of eluates were probed for the presence of the indicated kinases. Input lane designates the total lysate. (B) c-Abl and BTK are specific targets of dasatinib in CD40L stimulated primary CLL. Anti-BTK and anti-Abl immunoblots of CLL pulldown series. Pretreatment was performed by addition of dasatinib (Das.), imatinib (Im.) or ibrutinib (Ibr.) to lysates 30 minutes prior to exposure to drug-affinity matrix. Representative figure is shown of at least 8 independent experiments.

Competition experiments were performed as well to compare the selectivity of the dasatinib (**1**) towards c-Abl and BTK with other CLL drugs imatinib and ibrutinib (Figure 2B). In these experiments CD40L stimulated primary CLL were treated with dasatinib, imatinib or ibrutinib prior to exposure to immobilized dasatinib **5**. Western blot of the eluates provided the kinases that are bound by immobilized dasatinib **5**. Imatinib, which shows greater selectivity than dasatinib for Abl kinase³⁵⁻³⁷ in earlier studies, was able to inhibit binding of Abl but not of BTK to immobilized dasatinib **5** in lysates of CD40-stimulated CLL cells (Figure 4B). In a complementary set-up, BTK but not Abl was fully competed by pretreatment with specific BTK-inhibitor ibrutinib prior to pulldown with solid-phase dasatinib.

7.3 Conclusion

In conclusion, an affinity-based probe based on dasatinib has been synthesized and can be used to identify the drug targets that are still unknown for primary CLL. This study has identified c-Abl and BTK as dominant drug targets of dasatinib in CLL upon stimulation with CD40 ligand using the affinity-based dasatinib **5**.

Experimental

General: Tetrahydrofuran (THF) was distilled over LiAlH_4 before use. Acetonitrile (ACN), dichloromethane (DCM), N,N-dimethylformamide (DMF), methanol (MeOH) and trifluoroacetic acid (TFA) were of peptide synthesis grade, purchased at Biosolve, and used as received. All general chemicals (Fluka, Acros, Merck, Aldrich, Sigma) were used as received. Traces of water were removed from reagents used in reactions that require anhydrous conditions by coevaporation with toluene. Solvents that were used in reactions were stored over 4 Å molecular sieves, except methanol and acetonitrile, which were stored over 3 Å molecular sieves. Molecular sieves were flame dried before use. Unless noted otherwise all reactions were performed under an argon atmosphere. Column chromatography was performed on Silicycle Silia-P Flash Silica Gel, with a particle size of 40 – 63 µm. The eluents toluene and ethyl acetate were distilled prior to use. TLC analysis was conducted on Merck aluminium sheets (Silica gel 60 F254). Compounds were visualized by UV absorption (254 nm), by spraying with a solution of $(\text{NH}_4)_6\text{Mo}_7\text{O}_{24} \cdot 4\text{H}_2\text{O}$ (25 g/L) and $(\text{NH}_4)_4\text{Ce}(\text{SO}_4)_4 \cdot 2\text{H}_2\text{O}$ (10 g/L) in 10% sulphuric acid, a solution of KMnO_4 (20 g/L) and K_2CO_3 (10 g/L) in water, or ninhydrin (0.75 g/L) and acetic acid (12.5 mL/L) in ethanol, where appropriate, followed by charring at ca. 150°C. ^1H - and ^{13}C -NMR spectra were recorded on a Bruker DMX-400 (400 MHz) or a Bruker DMX-600 (600 MHz) spectrometer. Chemical shifts are given in ppm (δ) relative to tetramethylsilane (^1H -NMR) or CDCl_3 (^{13}C -NMR) as internal standard. Mass spectra were recorded on a PE/Sciex API 165 instrument equipped with an Electrospray Interface (ESI) (Perkin-Elmer). High-resolution MS (HRMS) spectra were recorded with a Finnigan LTQ-FT (Thermo Electron). IR spectra were recorded on a Shimadzu FTIR-8300 and absorptions are given in cm^{-1} . Optical rotations $[\alpha]_D^{23}$ were recorded on a Propol automatic polarimeter at room temperature. LC-MS analysis was performed on a Jasco HPLC system with a Phenomenex Gemini 3 µm C18 50 x 4.6 mm

column (detection simultaneously at 214 and 254 nm), coupled to a PE Sciex API 165 mass spectrometer with ESI. HPLC gradients were 10 → 90%, 0 → 50% or 10 → 50% ACN in 0.1% TFA/H₂O. Chiral HPLC analysis was performed on a Spectroflow 757 system (ABI Analytical Kratos Division, detection at 254 nm) equipped with a Chiralcel OD column (150 x 4.6 mm). The compounds were purified on a Gilson HPLC system coupled to a Phenomenex Gemini 5 μm 250 x 10 mm column and a GX281 fraction collector. The used gradients were either 0 → 30% or 10 → 40% ACN in 0.1% TFA/water, depending on the lipophilicity of the product. Appropriate fractions were pooled, and concentrated in a Christ rotary vacuum concentrator overnight at room temperature at 0.1 mbar.

2-(6-{4-[2-Azidoethyl]piperazin-1-yl}-2-methylpyrimidin-4-ylamino)-N-(2-chloro-6-methylphenyl)thiazole-5-carboxamide (2).

Compound **1** was obtained by dissolving 20 pulverized Dasatinib tablets (Sprycel™ 70 mg) in H₂O (200 mL) prior to filtration. The residue was washed with DCM/MeOH (1/1 v/v, 5x 150 mL) followed by concentration under reduced pressure to give compound **1** (1.27 g, 91% recovery) as a white solid.

Compound **1** (0.89 g, 1.82 mmol) was dissolved in DMF (20 mL) and cooled to 0 °C. Pre-cooled TEA (3 eq., 0.76 mL, 5.47 mmol) and MsCl (1.5 eq., 0.21 mL, 2.73 mmol) were added dropwise. The reaction mixture was allowed to warm to RT in 5 hrs after which TLC analysis indicated a complete conversion. Hereafter, NaN₃ (10 eq., 1.20 g, 18.2 mmol) was added and the mixture was stirred at RT for 16 hrs until TLC analysis indicated a complete conversion. EtOAc and H₂O were added and the layers were separated. The aqueous layer was extracted with EtOAc (5x), dried over MgSO₄ and concentrated *in vacuo*. The title compound was obtained after RP-HPLC purification (gradient: 30% - 70% ACN/0.1% aq. TFA) as a white solid (yield: 0.38 g, 0.75 mmol, 41%). ¹H NMR (400 MHz, DMSO-*d*₆): δ = 11.64 (br s, 1H), 9.92 (s, 1H), 8.25 (s, 1H), 7.40 (d, *J* = 7.6 Hz, 1H), 7.27 (m, 2H), 6.17 (s, 1H), 3.82 (br s, 2H), 3.55 (m, 8H), 3.28 (m, 2H), 2.45 (s, 3H), 2.24 (s, 3H); ¹³C NMR (100 MHz, DMSO-*d*₆): δ = 165.44, 162.42, 161.99, 159.91, 157.24, 140.82, 138.83, 133.51, 132.45, 129.06, 128.22, 127.04, 125.96, 83.41, 54.39, 50.76, 45.08, 40.43, 25.56, 18.31. HRMS: calculated for C₂₂H₂₅ClN₁₀OS [M+ H]⁺ 513.16948; found 513.16930.

2-(6-{4-[2-Aminoethyl]piperazin-1-yl}-2-methylpyrimidin-4-ylamino)-N-(2-chloro-6-methylphenyl)thiazole-5-carboxamide (3).

PMe₃ (6 eq., 2.4 mL, 2.4 mmol, 1M in THF) was added to a solution of compound **2** (0.21 g, 0.4 mmol) in DMF/H₂O (1/1/ v/v, 6 mL). The mixture was stirred at RT until TLC analysis indicated complete consumption of starting material after 16 hrs and this was followed by concentration under reduced pressure. Compound **3** was obtained after RP-HPLC purification (20 – 50% ACN/0.1% aq. TFA) as a white solid (yield: 0.43 g, 0.89 mmol, 37%). ¹H NMR (400 MHz, DMSO-*d*₆): δ = 11.63 (br s, 1H), 9.92 (s, 1H), 8.24 (s, 1H), 8.09 (br s, 2H), 7.40 (d, *J* = 7.6 Hz, 1H), 7.27 (m, 2H), 6.17 (s, 1H), 3.76 (m, 6H), 3.17 (m, 6H), 2.44 (s, 3H), 2.24 (s, 3H); ¹³C NMR (100 MHz, DMSO-*d*₆): δ = 165.38, 162.46, 162.05, 159.92, 157.21, 140.82, 138.84, 133.52, 132.46, 129.07, 128.23, 127.04, 125.94, 83.31, 53.11, 51.24, 41.63, 34.08, 25.57, 18.32. HRMS: calculated for C₂₂H₂₇ClN₈OS [M+ H]⁺ 487.17898; found 487.17883.

Experimental procedures: biochemistry

Patient material

After informed consent, patient material was obtained during diagnostic or follow-up procedures at the Departments of Hematology and Pathology of the Academic Medical Center Amsterdam. This study was approved by the AMC Ethical Review Board and conducted in agreement with the Declaration of Helsinki. PB mononuclear cells of patients with CLL, obtained after Ficoll density gradient centrifugation (Pharmacia Biotech) were frozen and stored as previously described¹⁸. Expression of CD5 and CD19 (both Beckton Dickinson (BD) Biosciences) on leukemic cells was assessed by flow cytometry (FACScanto; BD Biosciences). CLL samples included in this study contained 81-99% CD5+/CD19+ cells.

Reagents

The pharmacological inhibitor ibrutinib was obtained under a Material Transfer Agreement from Pharmacyclics (Sunnyvale, CA 94085-4521). The kinase inhibitors imatinib and dasatinib were from Novartis (Basel, Switzerland) and Bristol-Myers Squibb (New York, NY), respectively.

Immobilization of dasatinib

The procedure for immobilization of dasatinib was performed as described by Rix et al²¹. Compounds were immobilized on NHS-activated Sepharose 4 Fast Flow (GE Healthcare) via their amine functionalities as follows: Beads were washed with dimethyl sulfoxide (DMSO) and incubated overnight at room temperature (RT) with 1 mM compound and 100 mM triethylamine (TEA). After complete coupling of the compound, the affinity matrix was blocked with 0.8 M ethanolamine, washed, and stored at 4°C until use.

Affinity purification

Cell lysates were prepared immediately prior to incubation with immobilized dasatinib in lysis buffer containing 50 mM Tris-HCl (pH 7.5), 100 mM NaCl, 1% NP-40 (Sigma). Cell suspensions were clarified by centrifugation before incubated with immobilized dasatinib or uncoupled control sepharose overnight at 4°C. Pretreatment was performed by addition of Dasatinib, Imatinib or ibrutinib to lysates 30 minutes prior to exposure to drug-affinity matrix. After incubation, sepharose was washed 3 times with lysis buffer, before beads were drained and retained proteins were eluted by heat denaturing with SDS sample buffer.

Western blot analysis

Western blot analysis was performed using standard techniques¹⁸. Membranes were probed with anti-Mcl-1 (Cell Signaling), anti-Noxa (Imgenex), anti-Bcl-XL (BD Biosciences), antiserum to β -actin (Santa Cruz Biotechnology), anti-A1/Bfl-1 (Cell Signaling) or Bim (Stressgen Bioreagents Canada). Blots were subsequently incubated with IRDye 680 or 800 labelled secondary antibodies for 1 hour. Odyssey Imager (Li-Cor Biosciences) was used as a detection method according to the manufacturer's protocol.

Statistical analysis

An unpaired two-tailed Student's T test was used to determine the significance of differences between two mean values. The one sample T test was used to determine the significance of differences between means and normalized values (100%). * $p < 0,05$; ** $p < 0,01$; *** $p < 0,001$.

References

- ¹ N. Chiorazzi, K. R. Rai and M. Ferrarini, *N.Engl.J.Med.*, 2005, **352**, 804.
- ² M. J. Keating, S. O'Brien, M. Albitar, S. Lerner, W. Plunkett, F. Giles, M. Andreeff, J. Cortes, S. Faderl, D. Thomas, C. Koller, W. Wierda, M. A. Detry, A. Lynn and H. Kantarjian, *J. Clin. Oncol.*, 2005, **23**, 4079.
- ³ F. Caligaris-Cappio and T. J. Hamblin, *J.Clin.Oncol.*, 1999, **17**, 399.
- ⁴ Stein H, Bonk A, Tolksdorf G, K. Lennert, H. Rodt and J. Gerdes, *J.Histochem.Cytochem.*, 1980, **28**, 746.
- ⁵ L. Lagneaux, A. Delforge, D. Bron, B. C. De and P. Stryckmans, *Blood*, 1998, **91**, 2387.
- ⁶ P. Panayiotidis, D. Jones, K. Ganeshaguru, L. Foroni and A. V. Hoffbrand, *Br.J.Haematol.*, 1996, **92**, 97.
- ⁷ N. Bhattacharya, S. Diener, I. S. Idler IS, T. F. Barth, J. Rauen, Z. Habermann, T. Zenz, P. Moller, H. Dohner, S. Stilgenbauer and D. Mertens, *Leukemia*, 2011, **25**, 722.
- ⁸ J. A. Burger, N. Tsukada, M. Burger, N. J. Zvaifler, M. Dell'Aquila and T. J. Kipps, *Blood*, 2000, **96**, 2655.
- ⁹ A. Burkle, M. Niedermeier, A. Schmitt-Graff, W. G. Wierda, M. J. Keating and J. A. Burger, *Blood*, 2007, **110**, 3316.
- ¹⁰ M. Nishio, T. Endo, N. Tsukada, J. Ohata, S. Kitada, J. C. Reed, N. J. Zvaifler and T. J. Kipps, *Blood*, 2005, **106**, 1012.
- ¹¹ G. Fabbri and R. Dalla-Favera, *Nat. Rev. Canc.*, 2016, **16**, 145.
- ¹² P. Ghia, G. Strola, L. Granziero, M. Geuna, G. Guida, F. Sallusto, N. Ruffing, L. Montagna, P. Piccoli, M. Chilosi, F. Caligaris-Cappio, *Eur.J.Immunol.*, 2002, **32**, 1403.
- ¹³ P. E. Patten, A.G. Buggins, J. Richards, A. Wotherspoon, J. Salisbury, G. J. Mufti, T. J. Hamblin and S. Devereux, *Blood*, 2008, **111**, 5173.
- ¹⁴ J. A. Burger and V. Gandhi, *Blood*, 2009, **114**, 2560.
- ¹⁵ A. V. Kurtova, K. Balakrishnan, R. Chen, W. Ding, S. SchnAbl, M. P. Quiroga, M. Sivina, W. G. Wierda, Z. Estrov, M. J. Keating, M. Shehata, U. Jager, V. Gandhi, N. E. Kay, W. Plunkett and J. A. Burger, *Blood*, 2009, **114**, 4441.
- ¹⁶ L. A. Smit, D. Y. Hallaert DY, R. Spijker, B. de Goeij, A. Jaspers, A. P. Kater, M. H. van Oers, C. J. van Noesel and E. Eldering, *Blood*, 2007, **109**, 1660.
- ¹⁷ F. Caligaris-Cappio, *Br. J. Haematol.*, 2003, **123**, 380.
- ¹⁸ J. A. Burger, P. Ghia, A. Rosenwald and F. Caligaris-Cappio, *Blood*, 2009, **114**, 3367.
- ¹⁹ Y. Herishanu, P. Perez-Galan, D. Liu D, A. Biancotto, S. Pittaluga, B. Vire, F. Gibellini, N. Njugana, E. Lee, L. Stennett, N. Raghavachari, P. Liu, J. P. McCoy, M. Raffield, M. Stetler-Stevenson, C. Yuan, R. Sherry, D. C. Arthur, I. Maric, T. white, G. E. Marti, P. Munson, W. H. Wilson and A. Wiestner, *Blood*, 2011, **117**, 563.
- ²⁰ D.Y. Hallaert, A. Jaspers, C. J. van Noesel CJ, M. H. van Oers, A. P. Kater and E. Eldering, *Blood*, 2008, **112**, 5141.

²¹ L. Amrein, T. A. Hernandez, C. Ferrario, J. Johnston, S. B. Gibson, L. Panasci and R. Aloyz, *Br.J.Haematol.*, 2008, **143**, 698.

²² A. M. McCaig, E. Cosimo, M. T. Leach and A. M. Michie, *Br.J.Haematol.*, 2011, **153**, 199.

²³ E. Weisberg, P. W. Manley, S. W. Cowan-Jacob, A. Hochhaus and J. D. Griffin, *Nat.Rev.Cancer*, 2007, **7**, 345.

²⁴ U. Rix, O. Hantschel, G. Durnberger, L. L. Remsing Rix, M. Planyavsky, N. V. Fernbach, I. Kaupe, K. L. Bennett, P. Valent, J. Colinge, T. Kocher and G. Superti-Furga. *Blood*, 2007, **110**, 4055.

²⁵ O. Hantschel, U. Rix, U. Schmidt U, T. Burckstummer, M. Kneidinger, G. Schutze, J. Colinge, K. L. Bennett, W. Ellmeier, P. Valent and G. Superti-Furga, *Proc.Natl.Acad.Sci.U.S.A*, 2007, **104**, 13283.

²⁶ D. Kim, Y. Yi, J. H. Kim, *J. Am. Chem. Soc.*, 2008, **130**, 16466.

8

Summary and Future Prospects

Kinases play a role in many diseases including cancer, diabetes and infection diseases. For this reason, kinases are interesting drug targets. Inhibitors for some kinases are already in use as clinical drugs, however due to resistance and side effects, but also to target kinases related to diseases for which there is currently no treatment, research on the discovery of new classes of kinase inhibitors is imperative. To achieve this, not only new inhibitor classes need to be designed and synthesized, but also tools to profile kinases in their physiological context and to determine the selectivity of inhibitors are required. The research in this thesis has focused on the development of more potent AKT1 and FLT3 kinase inhibitors and on the synthesis and application of new chemical tools for the profiling of kinases involved in various types of cancers and other diseases. A brief

description of the function and the role of the kinases subject of study in this thesis is given in **Chapter 1**.

Over the past decades, numerous chemical profiling methods have been developed and used to study the biological functional role of kinases, and to profile the selectivity and targets of kinase inhibitors. In **Chapter 2**, the principles of three chemical profiling methods applied for kinases are reviewed and compared: activity-based protein profiling (ABPP), photoaffinity labeling and affinity-based profiling (AfBP). These three methods formed the common thread throughout this thesis.

H-89, an isoquinolinesulfonamide-based compound, is a well-known, potent PKA inhibitor. Analogues of this compound have been proven to inhibit AKT1 and other kinases, including the oncological target, FLT3. **Chapter 3** deals with the design and synthesis of a new set of isoquinolinesulfonamide-based inhibitors for FLT3 (Figure 1). These compounds all contain the isoquinolinesulfonamide core and variations are at the phenyl moiety. Variations were introduced at the ortho, meta or para position by Suzuki coupling using 34 different bulky (hetero)aromatic boronic acids (leading in total to a focused library of 102 compounds).

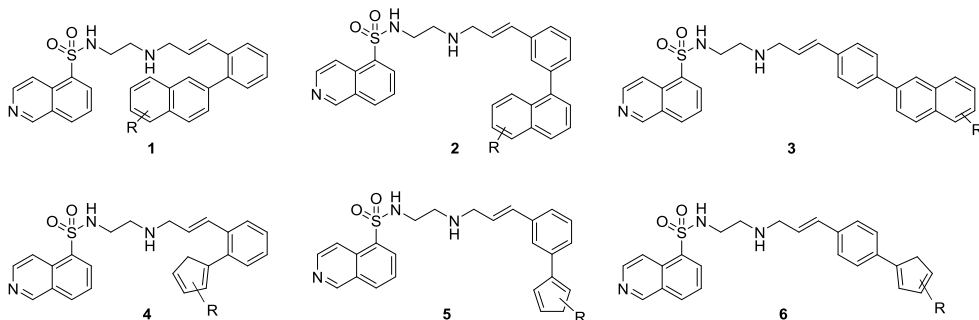
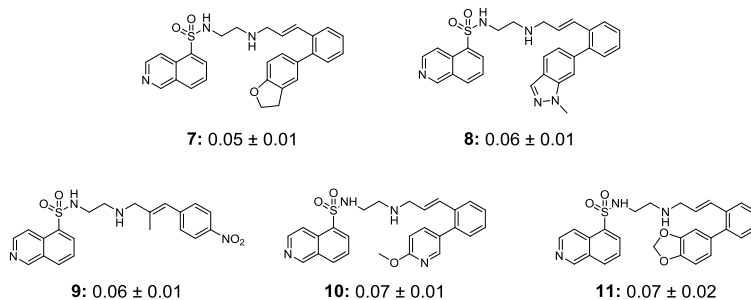


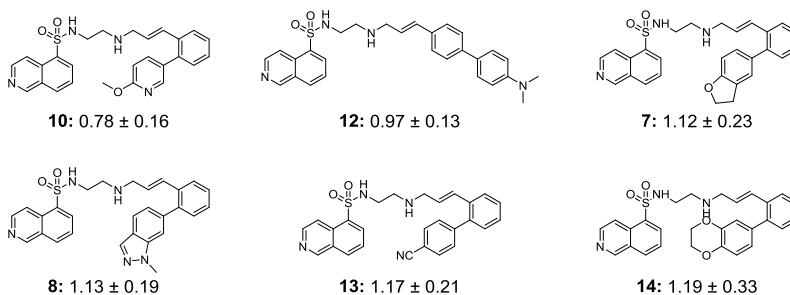
Figure 1. General structures (1 – 6) of the library containing 102 isoquinolinesulfonamide-based inhibitors for FLT3.

The inhibitory potency towards PKA, AKT1, AKT2 and FLT3 of the 102 newly synthesized isoquinolinesulfonamides together with 137 isoquinolinesulfonamides previously prepared¹ are discussed in **Chapter 4**. The effect of these 239 compounds on PKA, AKT1, AKT2 and FLT3 was evaluated using a TR-FRET kinase activity assay. The most active AKT1 and AKT2 inhibitors contain a bulky heteroaromatic group at the ortho position (Figure 2). It is clearly that both the kinases AKT1 and AKT2 favor the same kind of compounds, which make it hard to find active and selective inhibitors towards AKT1. The most active PKA inhibitors of the series proved to be compounds **15** and **16**. These compounds have the same conformation and contain an aromatic group at the para position, just like lead compound H-89. Apparently, electron-donating groups at this position are favourable for PKA inhibition.

AKT1



AKT2



PKA

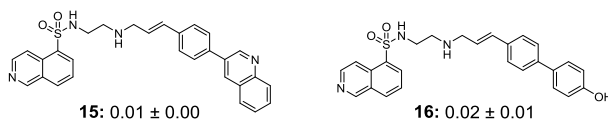


Figure 2. K_i values (μM) given for a selection of AKT1 (**7 – 11**), AKT2 (**7, 8, 10, 12 – 14**) and PKA (**15 – 16**) inhibitors, which are more active than lead compound H-89 based on their K_i values.

Inhibition of both AKT1 and AKT2 has been shown to be lethal in mice, and the ability to inhibit one selectively over the other is therefore of medical importance. The most selective AKT1 over AKT2 inhibitors proved to be compounds **17 – 19** (Figure 3). A methyl substituent at the linker alkene contributes to AKT1 selectivity over AKT2. Next to this, introduction of a para-halogen at the phenyl ring appears to improve the selectivity of AKT1 over AKT2. The configuration of the alkene moiety (E or Z) appears to play a role as well. Compounds **8, 10**, and **20 – 22** (Figure 3) are the most selective AKT1 over PKA inhibitors. These compounds contain aromatic groups having oxygen or nitrogen groups at the ortho position.

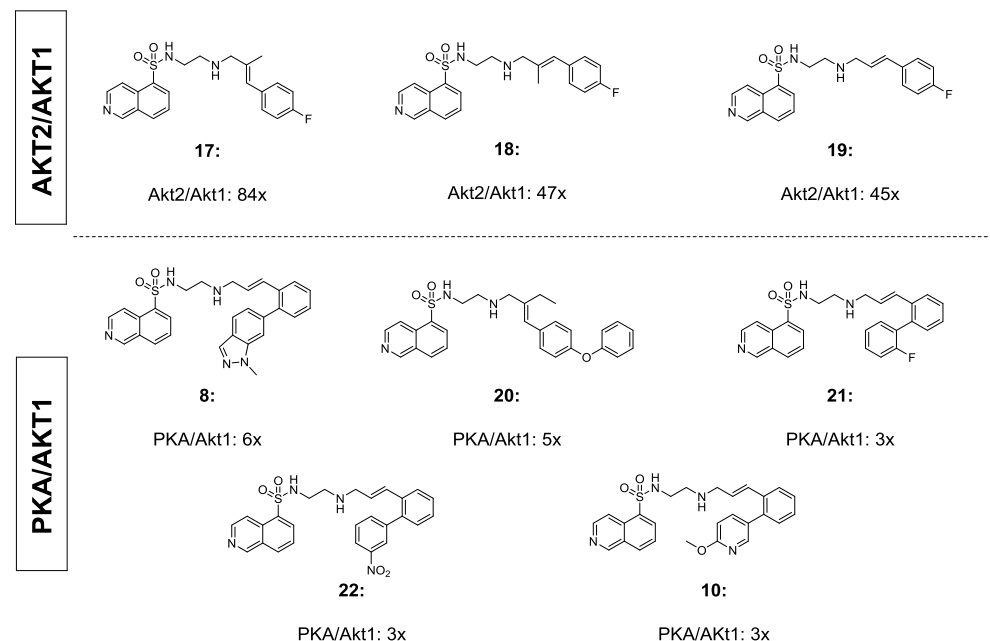


Figure 3. The most selective AKT1 over AKT2 (**17 – 19**) and AKT1 over PKA inhibitors (**8, 10 and 20 – 22**) based on their K_i value differences.

To obtain a more selective and active AKT1 inhibitor, it may be of interest to study the effect of incorporation of a fluorine group at the para position, which is important for selectivity, and a bulky heteroaromatic group at the ortho position, which contributes to enhancement of activity. Suggested compounds featuring these properties are **23** and **24** (Figure 4). Furthermore, a methyl group at the alkene site contributes to activity and selectivity as well, which suggests compounds **25** and **26** as future synthetic targets.

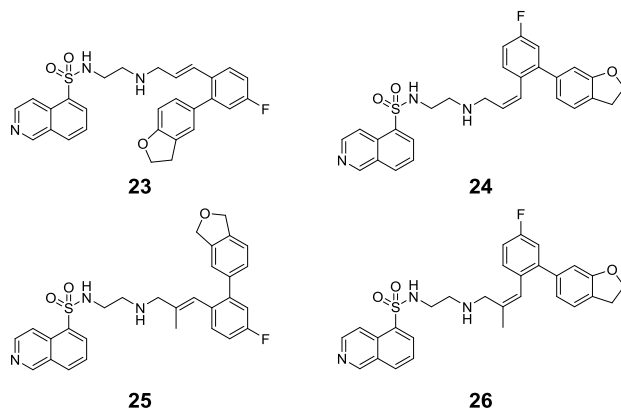


Figure 4. Suggested isoquinolinesulfonamide inhibitors selective for FLT3.

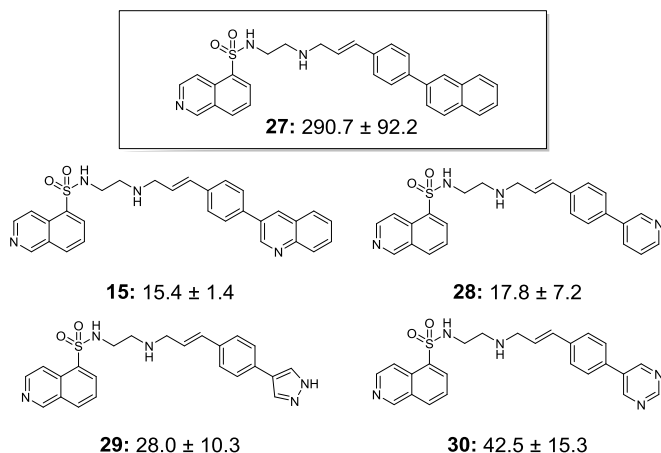


Figure 5. IC_{50} values (nM) given for a selection of FLT3 inhibitors (**15**, **28** – **30**), which are more active than lead compound **27** based on their K_i values.

Another kinase studied in this Thesis is FLT3. The most active inhibitors for this kinase are compounds **15**, **28** – **30** (Figure 5). They all have a heteroaromatic group at the para position and appeared to be at least 7 times more active as FLT3 inhibitors than the lead compound (**27**).

Based on these SAR findings, a new set of FLT3 inhibitors (**31** – **36**) can be designed having an electron donating nitrogen-atom containing aromatic group at the para position. Some proposed structural analogues are depicted in Figure 6.

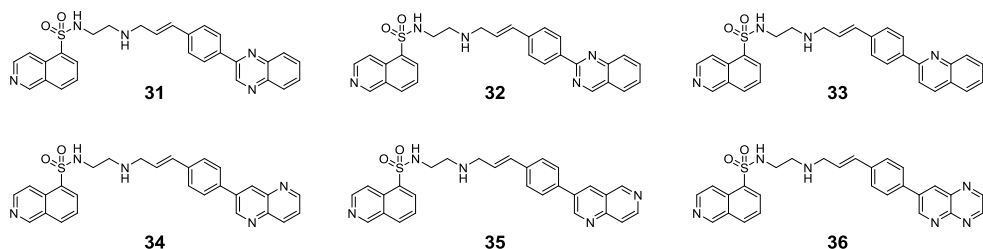


Figure 6. Suggested isoquinolinesulfonamide inhibitors selective for FLT3.

In the second part of this thesis, the synthesis and biological evaluation of chemical tools for profiling of kinases have been described. Three different methods for chemical profiling have been highlighted: ABPP, photo-affinity labeling and AfBP. **Chapter 5** describes the design and synthesis of two types of ABPs for labeling of Bruton's tyrosine kinase (BTK), namely direct (**37** and **38**) and two-step bioorthogonal (**39** – **41**) BTK activity-based probes (Figure 7).

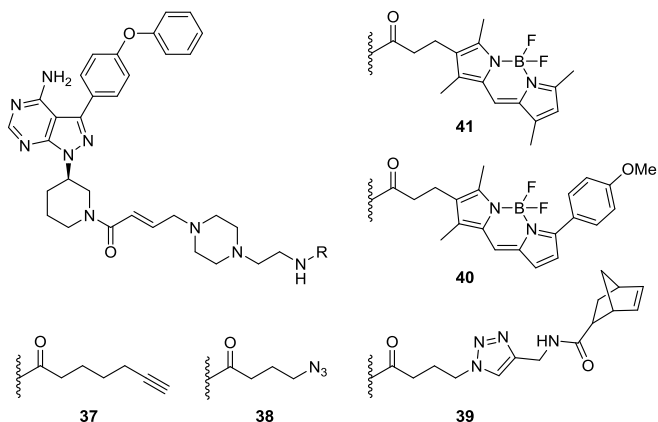
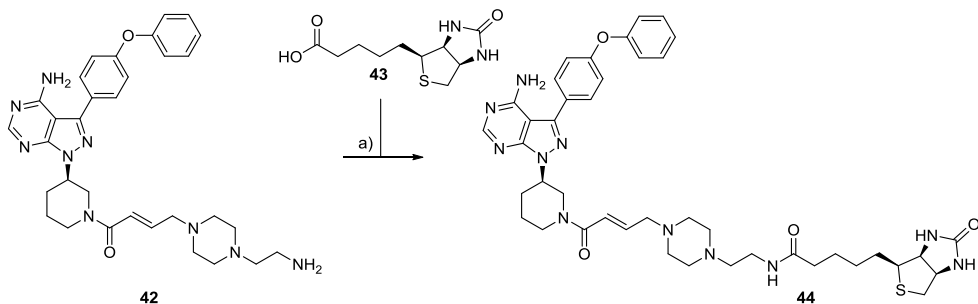


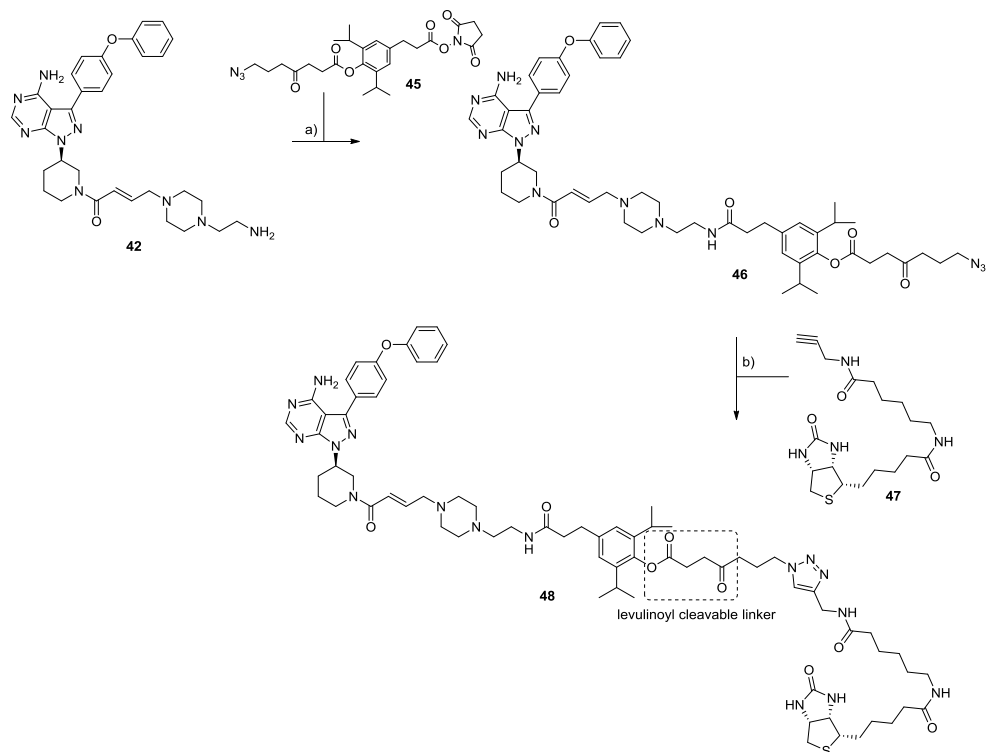
Figure 7. Structures of direct (**37** and **38**) and two-step bioorthogonal (**39** – **41**) BTK activity-based probes.

The core of these probes is based on the covalent inhibitor ibrutinib, which forms a covalent bond by attack of a cysteine thiol in the BTK active site to the acrylamide moiety of ibrutinib. All five probes (**37** – **41**) contain an acryl amide group as does ibrutinib, and all probes were able to label BTK. The direct probes **37** and **38** label BTK in Ramos cell extract and in living Ramos cells. Two-step bioorthogonal labeling of BTK using the probes **39** – **40** was also possible in *in vitro* and *in situ* experiments.

It is not always favorable to perform BTK labeling under fluorescent conditions, for instance when background fluorescence is an issue. In addition, an important method to identify target proteins and to determine the exact site and mechanism of ABP binding is by analysis of labeled proteins using mass spectrometry. In this case, it is usual to label proteins with a biotin-tagged ABP and subsequently enrich them by affinity-purification using streptavidin-beads. To allow for identification of the targets of ibrutinib, ibrutinib-biotin **44** has been synthesized by condensation (HATU, DiPEA) with biotin (**43**) (Scheme 1).



Scheme 1. Synthesis of ibrutinib-biotin **44**. Reagents and conditions: a) **43**, HATU, TEA, DMF, 26.5% after RP-HPLC.



Scheme 2. Synthesis of immobilized dasatinib **3**. Reagents and conditions: a) **45**, DiPEA, DMF, 36% after RP-HPLC; b) **47**, 1M CuSO₄, 1M Na L-ascorbate, 23% after RP-HPLC.

A disadvantage of ABPs featuring a biotin moiety is that the release of captured proteins from the beads requires harsh conditions and may result in contamination of the purified sample with endogenous biotinylated proteins. In such situations, an ABP containing a biotin in combination with a cleavable linker may form an attractive alternative. Therefore, ibrutinib-cleavable levulinoyl linker-biotin **48** was designed and synthesized (Scheme 2). This linker can be cleaved by treatment with an excess of hydrazine after protein enrichment.²

The synthesis of ibrutinib-cleavable levulinoyl linker-biotin **48** commenced with reacting crude amine **42** with the ester-based levulinoyl linker succinimide **45** to obtain azide **46**. A copper(I)-catalysed click ligation to alkyne-modified biotin **47** was then performed yielding the ibrutinib cleavable levulinoyl linker biotin **48** after HPLC purification. Both biotin probes (**44** and **48**) were able to select and visualize on SDS PAGE BTK from cell extracts. The utility of these probes in comparative and competitive ABPP on this drug target needs to be further investigated, though.

Not all kinases contain a nucleophilic moiety in the active site as BTK. To label these kinases covalently another type of chemical tool is required. **Chapter 6** describes the synthesis and biological evaluation of two diazirine-functionalized photocrosslinking probes (**49** and **50**, Figure 8) for labeling of PKA and AKT1, which are kinases without a nucleophilic group in the active site. Both probes are based on the core of H-89, which is proven to inhibit PKA and AKT1, and contain a diazirine group. Diazirine will bind covalently to the kinase upon UV activation. As well, these probes feature an azide group, which serves as a bioorthogonal ligation handle.

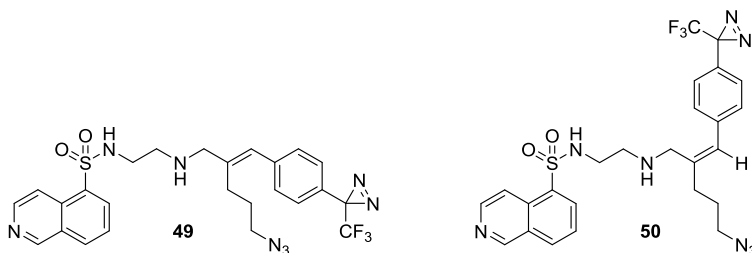
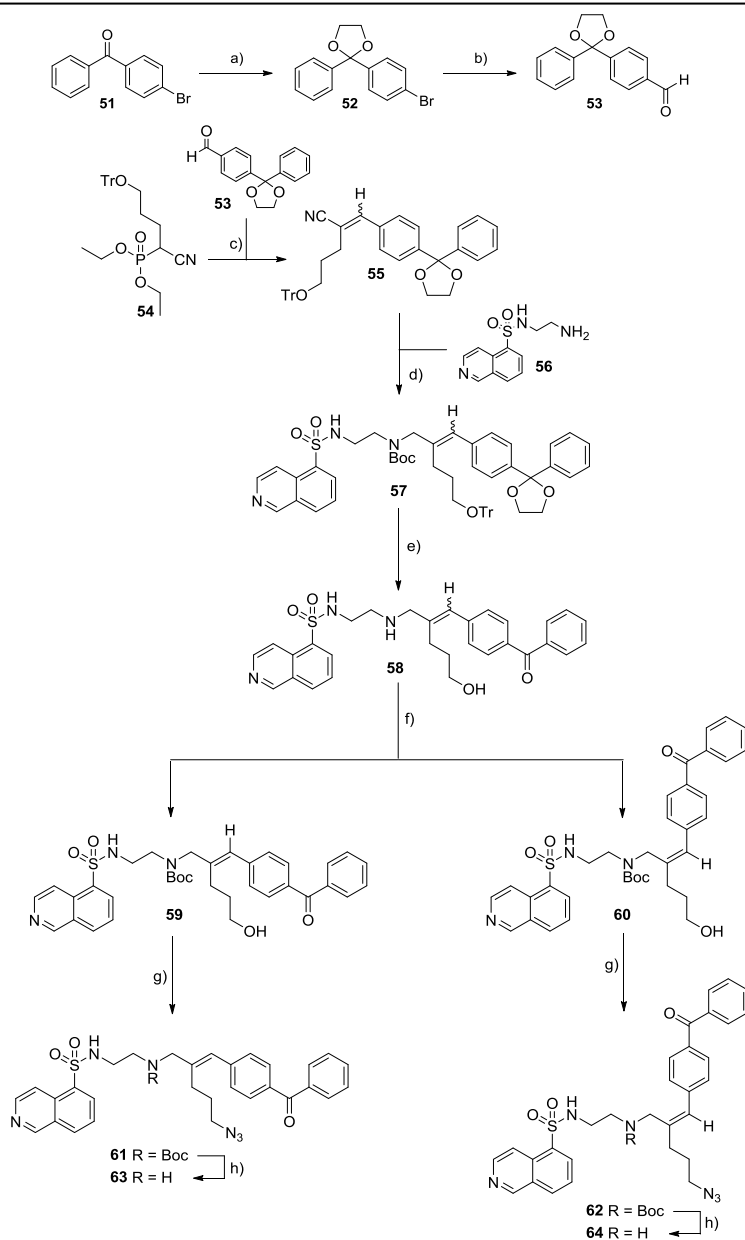


Figure 8. Structures of diazirine-functionalized photocrosslinking probes **49** and **50**.

According to a single point kinase active site-directed competition binding KinomescanTM assay, in which the capability of the probes to inhibit a panel of 111 human kinases was examined, both probes **49** and **50** have a preference to inhibit Ser/Thr kinases including PKA and AKT1. Following this, both photocrosslinking probes were subjected to labeling experiments in which they showed to photocrosslink recombinant PKA and AKT1 efficiently and specifically upon UV activation. Other photocrosslinking groups that have been used in the past include benzophenone moieties. It would be of interest to investigate the benzophenone analogues **63** and **64** (Scheme 3) on their differences with respect to inhibitory potency and labeling efficiency. For the synthesis of both the probes, the benzophenone part can be obtained by protection of bromo-ketone **51** under Dean-Stark conditions giving compound **52**. Compound **52** was in turn lithiated using *n*-BuLi before reaction with DMF to form aldehyde **53**. Next, a Horner-Wadsworth-Emmons (HWE) reaction between benzaldehyde **53** and phosphonate **54** resulted in α -substituted cinnamitrile **55** as a 1/1 mixture of *E/Z* isomers in 95% yield. Since separation of the isomers in the nitrile-stage was partially successful, and the nitriles were observed to isomerise during the ensuing transimination, the mixture of nitriles was used in the ensuing reaction. Subsequently, *E/Z* cinnamitrile mixture **55** was used in the four-step-one-pot trans-imation procedure according to Brussee *et al.*³, which has been described



Scheme 3. Synthesis of benzophenone-functionalized photocrosslinking probes **63** and **64**. Reagents and conditions: a) ethylene glycol, *p*-toluenesulfonic acid monohydrate, benzene, Δ , 71%; b) *n*-BuLi, DMF, THF, $-78\text{ }^{\circ}\text{C}$ – RT, 80%; c) NaH, **53**, $0\text{ }^{\circ}\text{C}$, THF, $E/Z = 1/1$, 95%; d) i) DiBALiH, $-78\text{ }^{\circ}\text{C}$, Et_2O ; ii) MeOH, $-100\text{ }^{\circ}\text{C}$; iii) **56**, MeOH, RT; iv) NaBH_4 , $-10\text{ }^{\circ}\text{C}$ to RT; e) THF, HCl, H_2O ; f) Boc_2O , TEA, DCM, $0\text{ }^{\circ}\text{C}$, 6.7% (**59**) and 18% (**60**) after RP-HPLC; g) i) TsCl, DCM, TEA, DMAP; ii) NaN_3 , DMF; h) DCM/TFA 1/1, v/v, RT, 44% (**63**) and 38% (**64**) after RP-HPLC.

in detail in Chapter 6, and the crude *E/Z* mixture of trityl protected isoquinolineamide **57** was obtained. The Boc-groups and trityl-groups in **57** were deprotected under acidic conditions to obtain a crude mixture of **58**, and installment of the Boc-group to yield isoquinolinesulfonamide **59** and **60** as crude *E/Z* mixture. HPLC purification allowed separation and isolation of both isomers. Both alcohols **59** and **60** were tosylated followed by substitution using NaN_3 to obtain compounds **61** and **62**. At last, deprotection of the Boc-group furnished the photo-affinity based probes **63** and **64** in 44% and 38% yield after HPLC purification. Probe **3** has the same double bond geometry as the parent inhibitor H-89 (**1**) and inhibits both PKA and AKT1 with a high potency. A change of the double bond configuration to (*Z*) does not have a significant influence on the inhibition of PKA but for AKT1 a partial loss of potency was observed. In this study, the recombinant kinases in pure form as well as in mixtures with control proteins could be labelled; additionally a variety of control experiments reveal that the probes act in an affinity-based manner on active enzymes and that UV activation is required for labeling have been performed.

A third chemical profiling method for kinases has been described in **Chapter 7**. An affinity-based probe (**65**, Figure 9) has been synthesized to investigate the drug targets of dasatinib in primary CLL. This affinity-based probe is obtained by coupling of the kinase inhibitor and clinical drug, dasatinib to NHS-activated sepharose beads. In this method, the targets are reversibly bound by the probe and are analyzed by SDS-PAGE and/or LC/MS after they are eluted from the immobilized dasatinib probe **65**.

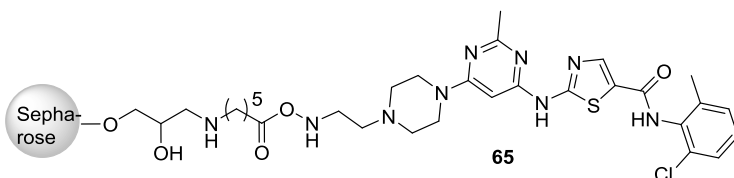
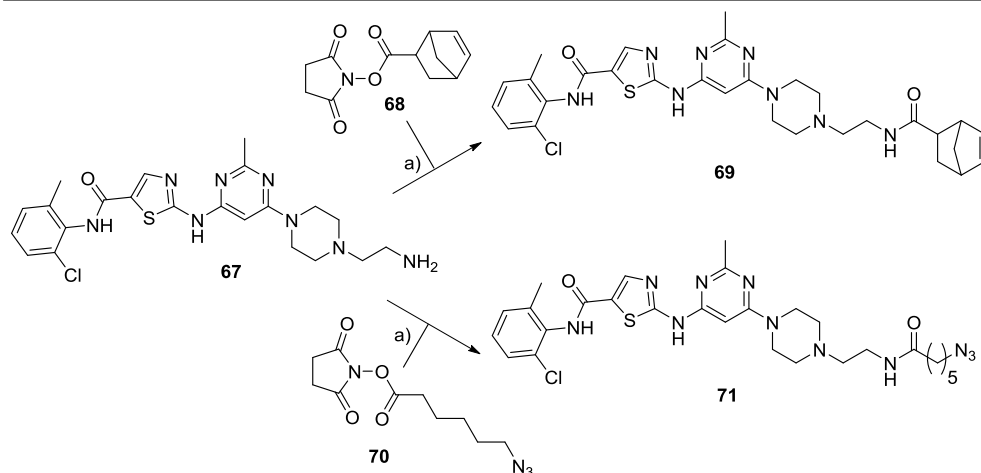


Figure 9. Structure of affinity-based probe **65**, which is based on the structure of dasatinib.

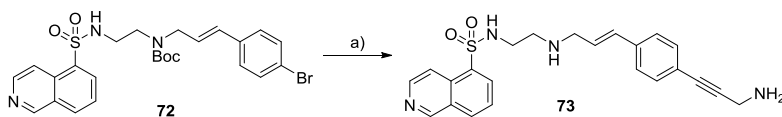
In this study it was found that the important targets of dasatinib in primary CLL were c-Abl and BTK. Furthermore, other identified peptides corresponded to the kinases Lyn, Csk, Fyn, Yes, Src and Lck.

An alternative strategy to identify the targets of dasatinib would be to use dasatinib-based probes containing a ligation handle. Two such two-step probes were designed and synthesized, one featuring a norbornene (**69**) and one containing an azide as ligation handles (**71**). The synthesis of both compounds is depicted in Scheme 4. Both probes were obtained by a reaction between the dasatinib-amine **67** with the corresponding OSu-functionalized tag. In the future, the utility of these probes needs to be studied in detail.



Scheme 4. Synthesis of dasatinib-norbornene **69** and dasatinib-azide **71**. Reagents and conditions: a) **68** or **70**, DiPEA, DMF, **69**: 18%; **71**: 28% after RP-HPLC.

Affinity-based protein profiling can also be useful to study the targets and investigate the drug mechanism of H-89. Therefore, the Boc-protected H-89 **72** was converted into the amine containing isoquinolineamide **73** by a Sonogashira cross-coupling (Scheme 5). This probe can be in turn immobilized by coupling to a NHS-Sepharose bead, which can then be used to isolate the targets of H-89.



Scheme 5. Synthesis of affinity-based probe **73**, based on H-89. Reagents and conditions: a) i) *N*-Boc-propargylamine, pyrrolidine, CuI, Pd(PPh₃)₄, DMF; ii) TFA/DCM 1/1 v/v, RT, 34% after RP-HPLC.

In this study, three chemical profiling methods to label kinases have been described including their advantages and disadvantages. To have a true comparison of these three methods, an affinity-based probe, a photoaffinity based probe and an activity-based probe have to be synthesized based on the same small molecule in the future. For example, next to the direct and two-step bioorthogonal ibrutinib probes (**37-41**), an affinity-based probe and a photoaffinity based probe, such as compounds **74** and **75**, respectively should be developed (Figure 10). For affinity-based profiling, the Michael-acceptor moiety has been displaced by an alkyl amine group, which in turn can be immobilized on a matrix. In the case of photoaffinity labeling, the acrylamide group has been displaced by the aryl diazirine, which serves

as the photoaffinity reactive group and by an azide group, which serves as the ligation handle.

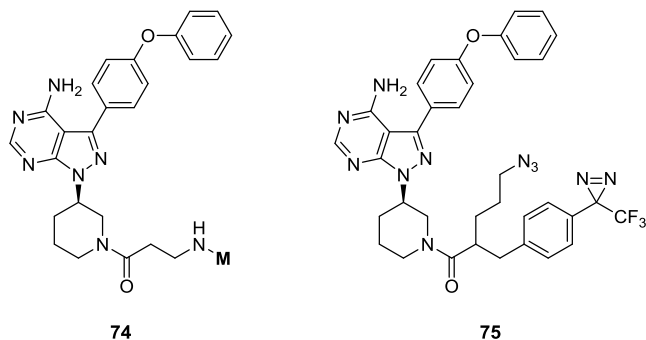


Figure 10. Designs of a ibrutinib-based affinity and photoaffinity probe **74** and **75**, respectively. **M** = matrix.

In this thesis, new powerful tools and assays have been developed that unite the fields of synthetic chemistry, protein biochemistry and cell biology for the global analysis of kinase expression and function. The value of chemical profiling as a method for functional proteome analysis has been further highlighted by its application as a screen to evaluate the potency and selectivity of kinase inhibitors. However, even though the numerous considerable advances that has been made to date, chemical approaches for kinome analysis still face significant technical challenges. Currently, 1D or 2D electrophoresis is mostly used to analyze probe-labeled proteins. A disadvantage of this method is the limited resolving power especially in cases where large number of proteins with similar molecular mass has to be analyzed. The use of LC-MS to analyze the large number of proteins overcome this problem due to its higher resolving power, but LC-MS has a much lower sample throughput. So the right strategy has to be chosen depending on the biological question being addressed. In addition, more selective probes are needed to explore the function of a particular kinase and also more general probes are needed that are able to label every single kinase in a cell, which are useful in studies of inhibitor selectivity. In either case, improvement of both the chemical and technical components of chemical profiling has to be made in the near future for a more in-depth analysis of the kinome and the targets of kinase inhibitors. These chemical tools, as developed in this thesis, provide new handles to define the biology of kinases in cells. The exploration of the chemical space around the H-89 building block shows how new and more specific inhibitors can be developed for this important enzyme class. The probes can then be used for profiling the *in vivo* effects.

Experimental

General: Tetrahydrofuran (THF) was distilled over LiAlH_4 before use. Acetonitrile (ACN), dichloromethane (DCM), N,N -dimethylformamide (DMF), methanol (MeOH) and trifluoroacetic acid (TFA) were of peptide synthesis grade, purchased at Biosolve, and used as received. All general chemicals (Fluka, Acros, Merck, Aldrich, Sigma) were used as received. Traces of water were removed from reagents used in reactions that require anhydrous conditions by coevaporation with toluene. Solvents that were used in reactions were stored over 4 Å molecular sieves, except methanol and acetonitrile, which were stored over 3 Å molecular sieves. Molecular sieves were flame dried before use. Unless noted otherwise all reactions were performed under an argon atmosphere. Column chromatography was performed on Silicycle Silia-P Flash Silica Gel, with a particle size of 40 – 63 μm . The eluents toluene and ethyl acetate were distilled prior to use. TLC analysis was conducted on Merck aluminium sheets (Silica gel 60 F254). Compounds were visualized by UV absorption (254 nm), by spraying with a solution of $(\text{NH}_4)_6\text{Mo}_7\text{O}_{24} \cdot 4\text{H}_2\text{O}$ (25 g/L) and $(\text{NH}_4)_4\text{Ce}(\text{SO}_4)_4 \cdot 2\text{H}_2\text{O}$ (10 g/L) in 10% sulphuric acid, a solution of KMnO_4 (20 g/L) and K_2CO_3 (10 g/L) in water, or ninhydrin (0.75 g/L) and acetic acid (12.5 mL/L) in ethanol, where appropriate, followed by charring at ca. 150°C. ^1H - and ^{13}C NMR spectra were recorded on a Bruker DMX-400 (400 MHz) or a Bruker DMX-600 (600 MHz) spectrometer. Chemical shifts are given in ppm (δ) relative to tetramethylsilane (^1H NMR) or CDCl_3 (^{13}C NMR) as internal standard. Mass spectra were recorded on a PE/Sciex API 165 instrument equipped with an Electrospray Interface (ESI) (Perkin-Elmer). High-resolution MS (HRMS) spectra were recorded with a Finnigan LTQ-FT (Thermo Electron). IR spectra were recorded on a Shimadzu FTIR-8300 and absorptions are given in cm^{-1} . Optical rotations $[\alpha]_D^{23}$ were recorded on a Propol automatic polarimeter at room temperature. LC-MS analysis was performed on a Jasco HPLC system with a Phenomenex Gemini 3 μm C18 50 x 4.6 mm column (detection simultaneously at 214 and 254 nm), coupled to a PE Sciex API 165 mass spectrometer with ESI. HPLC gradients were 10 \rightarrow 90%, 0 \rightarrow 50% or 10 \rightarrow 50% ACN in 0.1% TFA/ H_2O . Chiral HPLC analysis was performed on a Spectroflow 757 system (ABI Analytical Kratos Division, detection at 254 nm) equipped with a Chiralcel OD column (150 x 4.6 mm). The compounds were purified on a Gilson HPLC system coupled to a Phenomenex Gemini 5 μm 250 x 10 mm column and a GX281 fraction collector. The used gradients were either 0 \rightarrow 30% or 10 \rightarrow 40% ACN in 0.1% TFA/water, depending on the lipophilicity of the product. Appropriate fractions were pooled, and concentrated in a Christ rotary vacuum concentrator overnight at room temperature at 0.1 mbar.

Ibrutinib-biotin (44)

HATU (1.1 eq., 42 mg, 0.11 mmol) was added to a solution of biotin (2 eq., 50 mg, 0.20 mmol) and TEA (4 eq., 60 μL , 0.4 mmol) in DMF (0.4 mL) and the reaction mixture was allowed to stir for 1 min. A solution of crude amine **42** (42 mg, 0.1 mmol) in DMF (0.3 mL) was added and the resulting mixture was stirred overnight. EtOAc (10 mL) was added and the organic layer was washed with sat. aq. NaHCO_3 and brine, dried over MgSO_4 , filtered and concentrated under reduced pressure. The title compound was obtained after RP-HPLC purification (linear gradient 40% \rightarrow 60% ACN in H_2O , 0.1% TFA, 15 min) as a white solid (yield: 21.41 mg, 26.5 μmol , 26.5%). ^1H NMR (600 MHz, $\text{DMSO}-d_6$): δ 8.33 (s, 1H), 8.13 (br s, 1H), 7.66 (s, 2H), 7.44 (t, J = 8.4 Hz, 2H), 7.20 (t, J = 7.2 Hz, 1H), 7.17 (d, J = 8.4 Hz, 2H), 7.13 (d, J = 7.8 Hz, 2H), 6.82 (d, J = 11.4 Hz, 0.5H), 6.66 – 6.61 (m, 1H), 6.57 – 6.51 (m,

0.5H), 4.75 – 4.70 (m, 1H), 4.56 (d, $J = 10.8$ Hz, 1H), 4.32 (t, $J = 6.6$ Hz, 1H), 4.18 (d, $J = 10.8$ Hz, 1H), 4.13 (s, 1H), 4.06 (d, $J = 15$ Hz, 1H), 3.38 – 3.30 (m, 2H), 3.28 – 3.18 (m, 1H), 3.10 (s, 1H), 3.00 – 2.90 (m, 3H), 2.81 – 2.80 (m, 1H), 2.61 (s, 1H), 2.57 (s, 1H), 2.51 (s, 1H), 2.28 – 2.24 (m, 1H), 2.14 – 2.10 (m, 3H), 1.95 (d, $J = 13.2$ Hz, 1H), 1.61 – 1.58 (m, 2H), 1.53 – 1.45 (m, 4H), 1.26 (br s, 3H), 1.23 (s, 1H), 1.22 (d, $J = 13.2$ Hz, 1H), 1.11 (s, 2H). ^{13}C NMR (150 MHz, DMSO- d_6): δ 172.81, 163.85, 162.73, 157.34, 156.23, 153.57, 153.26, 144.18, 143.77, 130.18, 127.49, 123.89, 119.02, 97.27, 62.66, 61.06, 59.22, 55.43, 55.13, 52.88, 52.24, 50.38, 49.48, 49.22, 46.32, 45.76, 45.21, 44.77, 41.63, 40.43, 35.10, 31.31, 29.61, 29.44, 28.23, 28.07, 25.09, 24.91, 18.82. HRMS: calculated for $\text{C}_{42}\text{H}_{53}\text{N}_{11}\text{O}_4\text{S} [\text{M}+\text{H}^+]$: 808.40027; found: 808.40037.

Ibrutinib Levulinoyl ester-based cleavable linker azide (46)

DiPEA (3.5 eq., 0.12 mL, 0.70 mmol) and levulinoyl ester-based cleavable linker-OSu² **45** (2.2 eq., 0.22 g, 0.44 mmol) were added to a solution of crude amine **42** (84 mg, 0.2 mmol) in DMF (0.5 mL). The reaction mixture was stirred overnight before being evaporated. The title compound was obtained after RP-HPLC purification (linear gradient 40% \rightarrow 60% ACN in H_2O , 0.1% TFA, 15 min) as a white solid (yield: 69.7 mg, 71.0 μmol , 36%). ^1H NMR (600 MHz, DMSO- d_6): δ 8.36 (s, 1H), 8.11 (br s, 1H), 7.66 (s, 2H), 7.44 (t, $J = 7.8$ Hz, 2H), 7.19 (t, $J = 7.8$ Hz, 1H), 7.17 (d, $J = 7.2$ Hz, 2H), 7.13 (d, $J = 9.0$ Hz, 2H), 6.98 (s, 2H), 6.84 (d, $J = 18.0$ Hz, 0.5H), 6.69 (d, $J = 15.0$ Hz, 0.5H), 6.65 – 6.59 (m, 0.5H), 6.58 – 6.51 (m, 0.5H), 4.79 – 4.30 (m, 1H), 4.58 (d, $J = 18.0$ Hz, 0.5H), 4.19 (d, $J = 12.0$ Hz, 1H), 4.16 (d, $J = 12.0$ Hz, 0.5H), 3.54 (br s, 1H), 3.37 (br s, 4H), 3.30 (t, $J = 7.2$ Hz, 2H), 3.23 – 3.20 (m, 2H), 3.04 – 2.95 (m, 4H), 2.89 – 2.80 (m, 10H), 2.56 (t, $J = 7.2$ Hz, 3H), 2.41 (s, 3H), 2.26 (t, $J = 12.0$ Hz, 1H), 2.15 – 2.13 (m, 1H), 1.95 – 1.91 (m, 1H), 1.76 – 1.71 (m, 2H), 1.67 – 1.53 (m, 1H), 1.09 (s, 12H). ^{13}C NMR (150 MHz, DMSO- d_6): δ 207.98, 172.27, 171.52, 163.82, 157.31, 157.02, 156.63, 156.20, 153.96, 153.36, 144.13, 143.58, 143.12, 139.93, 138.75, 130.28, 127.36, 124.00, 123.22, 119.15, 97.00, 56.73, 55.12, 53.52, 51.87, 50.22, 50.00, 49.17, 38.60, 36.84, 36.52, 30.67, 27.35, 26.51, 22.58. HRMS: calculated for $\text{C}_{54}\text{H}_{68}\text{N}_{12}\text{O}_6 [\text{M}+\text{H}^+]$: 981.53848; found: 981.53856.

Ibrutinib Levulinoyl ester-based cleavable linker biotin (48)

Aqueous CuSO_4 (1.0 eq., 24.8 μL , 24.8 μmol , 1M) and aqueous sodium L-ascorbate (1.1 eq., 27.2 μL , 27.2 μmol , 1M) were added to a solution of azide **46** (24 mg, 24 μmol) and biotin-Ahx-propargylamide **47** (1.5 eq., 14.2 mg, 36 μmol) in DMF 0.8 mL. The reaction mixture was stirred at RT overnight and was concentrated *in vacuo*. The title compound was obtained after RP-HPLC purification (linear gradient 45% \rightarrow 65% ACN in H_2O , 0.1% TFA, 15 min) as a white solid (yield: 7.5 mg, 5.5 μmol , 23%). ^1H NMR (600 MHz, DMSO- d_6): δ 8.33 (s, 1H), 8.21 (t, $J = 5.4$ Hz, 1H), 8.07 (br s, 1H), 7.87 (s, 1H), 7.70 (t, $J = 5.4$ Hz, 1H), 7.66 (s, 2H), 7.44 (t, $J = 7.2$ Hz, 2H), 7.19 (t, $J = 7.2$ Hz, 1H), 7.18 (d, $J = 6.6$ Hz, 2H), 7.12 (d, $J = 7.8$ Hz, 2H), 6.98 (s, 2H), 6.82 (d, $J = 15.0$ Hz, 0.5H), 6.66 – 6.61 (m, 1H), 6.58 – 6.51 (m, 0.5H), 6.39 (s, 1H), 6.33 (br s, 1H), 4.79 – 4.68 (m, 1H), 4.58 (d, $J = 18.0$ Hz, 1H), 4.31 – 4.28 (m, 3H), 4.27 (d, $J = 6.0$ Hz, 2H), 4.18 (d, $J = 6.0$ Hz, 1H), 4.13 – 4.11 (m, 1H), 4.05 (t, $J = 12.0$ Hz, 1H), 3.25 – 3.22 (m, 3H), 3.11 – 3.07 (m, 3H), 2.99 (q, $J_1 = 7.2$ Hz, $J_2 = 13.2$ Hz, 3H), 2.95 – 2.88 (m, 2H), 2.87 – 2.83 (m, 3H), 2.82 – 2.79 (m, 6H), 2.62 – 2.58 (m, 2H), 2.39 (br s, 2H), 2.31 – 2.22 (m, 1H), 2.15 – 2.10 (m, 1H), 2.07 (s, 5H), 2.04 (t, $J = 7.8$ Hz, 2H), 1.99 (t, $J = 7.2$ Hz, 2H), 1.98 – 1.93 (m, 1H), 1.61 – 1.59 (m, 2H), 1.52 – 1.46 (m, 5H), 1.37 – 1.34 (m, 2H), 1.30 – 1.27 (m, 2H), 1.24 – 1.20 (m, 3H), 1.09 (s, 12H). ^{13}C NMR (150 MHz, DMSO- d_6): δ 207.79, 172.17, 172.00, 171.82, 171.55, 163.86, 162.70, 157.31, 156.22, 145.03, 143.37, 139.79, 138.96, 130.14, 127.52, 126.16, 123.86,

123.64, 122.63, 119.00, 118.02, 117.32, 115.79, 115.36, 97.23, 63.29, 61.05, 59.20, 56.82, 55.39, 52.87, 52.22, 49.52, 49.20, 48.50, 45.78, 45.21, 38.31, 36.87, 36.55, 35.21, 34.12, 30.69, 29.58, 29.37, 28.95, 28.19, 28.02, 27.34, 26.66, 26.12, 25.312, 25.16, 24.91, 24.14, 1.11. HRMS: calculated for $C_{73}H_{98}N_{16}O_9S$ $[M+H]^+$: 1375.74234; found: 1375.74244.

2-(4-Bromophenyl)-2-phenyl-1,3-dioxolane (52)

Ethylene glycol (1.1 eq., 6.13 mL, 110 mmol) and *p*-toluenesulfonic acid monohydrate (0.01 eq., 0.19 g, 1.0 mmol) were added to a solution of (4-bromophenyl)(phenyl)methanone **51** (26.11 g, 100 mmol) in benzene (40 mL) and the reaction mixture was refluxed with a Dean-Stark condenser for 48 hrs. The reaction mixture was poured into aqueous sodium bicarbonate and extracted with Et_2O . The organic layer was washed with aqueous sodium bicarbonate, water and brine before being dried over $MgSO_4$ and concentrated *in vacuo*. The residue was further purified by silica column chromatography (5% \rightarrow 20% DCM/pentane) to afford the title compound as a white powder (yield: 21.79 g, 71.3 mmol, 71%). 1H NMR (400 MHz, $CDCl_3$, Me_4Si) δ 7.49 – 7.46 (m, 2H), 7.43 – 7.36 (m, 4H), 7.31 – 7.22 (m, 3H), 3.98 (s, 4H). ^{13}C NMR (101 MHz, $CDCl_3$) δ 141.53, 141.25, 131.14, 128.11, 127.90, 125.90, 122.09, 108.85.

4-(2-phenyl-1,3-dioxolan-2-yl)benzaldehyde (53)

n-BuLi (1.2 eq., 10.4 mL, 16.60 mmol, 1.6 M in hexanes) was dropwise added to a solution of compound **52** (4.22 g, 13.83 mmol) in THF at $-78^\circ C$. The resulting mixture was stirred at $-78^\circ C$ for 30 min before dropwise addition of DMF (1.5 eq., 1.6 mL, 20.75 mmol). The reaction mixture was allowed to warm up to RT overnight. The mixture was poured into aqueous ammonium chloride (250 mL) and diluted with Et_2O . The layers were separated and the organic layer was washed with brine and water, dried over $MgSO_4$, filtered and evaporated. The obtained material was purified by column chromatography (2% \rightarrow 10% EtOAc/pentane) and the product was obtained as a white solid (yield: 2.81 g, 11.06 mmol, 80%). 1H NMR (400 MHz, $CDCl_3$, Me_4Si) δ 9.96 (s, 1H), 7.82 (d, J = 8.4 Hz, 2H), 7.70 (d, J = 8.4 Hz, 2H), 7.51 (d, J = 7.2 Hz, 2H), 7.33 – 7.24 (m, 3H), 4.06 – 4.02 (m, 4H). ^{13}C NMR (101 MHz, $CDCl_3$) δ 191.74, 148.66, 141.28, 135.81, 129.55, 128.23, 126.59, 125.79, 108.75, 64.90.

(*E/Z*)-2-(4-(2-phenyl-1,3-dioxolan-2-yl)benzylidene)-5-(trityloxy)pentanenitrile (55)

To an ice-cold suspension of NaH (1 eq., 0.23 g, 5.77 mmol, 60% mineral oil) in THF (20 mL) a solution of phosphonate **54** (1.25 eq., 3.44 g, 7.21 mmol) in THF (5 mL) was added dropwise and stirred for 30 min. Next, a solution of aldehyde **53** (1.47 g, 5.77 mmol) in THF (5 mL) was added and the reaction mixture was allowed to warm to RT and stirred overnight. The solution was quenched by addition of freshly prepared sat. aq. Na_2HSO_3 (30 mL) and diluted with H_2O (100 mL) and Et_2O (50 mL). The layers were separated and the aqueous phase was extracted with Et_2O (3 x 50 mL). The combined organic layers were washed with sat. aq. $NaHCO_3$ and brine, dried over $MgSO_4$, filtered and evaporated. The residue was further purified by column chromatography (80% \rightarrow 95% toluene/pentane) to afford the title compound as a white solid with an *E/Z* ratio of 1/1 (yield: 3.15 g, 5.46 mmol, 95%). 1H NMR (400 MHz, $CDCl_3$, Me_4Si) δ 7.59 – 7.50 (m, 10H), 7.43 – 7.37 (m, 12H), 7.29 – 7.09 (m, 26H), 7.08 (s, 1H), 6.78 (s, 1H), 3.95 (s, 8H), 3.12 (d, J = 5.2 Hz, 4H), 2.57 (t, J = 7.2 Hz, 2H), 2.47 (t, J = 7.2 Hz, 2H), 1.91 (d, J = 6.0 Hz, 4H).

^{13}C NMR (101 MHz, CDCl_3) δ 143.87, 143.78, 143.47, 143.35, 143.00, 141.57, 133.47, 133.23, 128.97, 128.38, 128.22, 128.06, 127.58, 126.77, 126.35, 125.83, 125.10, 120.08, 118.43, 115.36, 110.84, 108.82, 86.43, 86.32, 64.76, 64.72, 62.16, 61.56, 32.96, 29.50, 28.43, 28.24, 26.64. HRMS: calculated for $\text{C}_{40}\text{H}_{35}\text{NO}_3$ $[\text{M}+\text{H}]^+$ 578.26897; found 578.26883.

***Tert*-butyl (*E*)-(2-(4-benzoylbenzylidene)-5-hydroxypentyl)(2-(isoquinoline-5-sulfonamido)ethyl)carbamate (**59**)**

A solution of nitrile **55** (8.37 g, 14.49 mmol) in anhydrous Et_2O (75 mL) was cooled to -78°C . DiBAL-H (2 eq., 29 mL, 29 mmol, 1M solution in hexanes) was added dropwise and the reaction mixture was allowed to warm to 0°C and stirred for 2h, after which TLC analysis showed complete consumption of starting material. Next, the mixture was cooled to -100°C followed by rapid addition of MeOH (30 mL). After 5 min a solution of isoquinoline amine **56** (2.5 eq., 13.24 g, 36.25 mmol) in MeOH (10 mL) was added dropwise and the reaction mixture was allowed to stir at RT overnight. Hereafter, the reaction was cooled to -10°C and NaBH_4 (2 eq., 1.10 g, 29.0 mmol) was added and the mixture was allowed to stir for 3h at RT. The reaction mixture was diluted with 0.5 M aq. NaOH (100 mL) and the layers were separated. The aqueous layer was extracted with DCM (3 x 50 mL) and the combined organic phases were washed with H_2O (3 x 50 mL) and brine, dried over MgSO_4 , filtered and evaporated. The crude product **57** was subjected to the next step without further purification.

The crude product **57** was dissolved in THF (50 mL) and HCl (35 mL) was added. The reaction mixture was stirred for 1h at RT before addition of H_2O (40 mL), the resulting mixture was stirred for 30 min at RT. The mixture was diluted with aqueous NaOH (10 M) to pH14 before addition of CHCl_3 (100 mL). The layers were separated and the aqueous layer was extracted with CHCl_3 (2x 100 mL). The combined organic layers were washed with brine, dried over MgSO_4 , filtered and concentrated. The crude product **58** was subjected to the next step without further purification.

The residue **58** was dissolved in DCM (75 mL) and was cooled to 0°C . To this mixture Boc_2O (1.5 eq., 4.74 g, 21.75 mmol) and TEA (4 eq., 8.04 mL, 58.0 mmol) were added and the reaction was allowed to warm to RT and stirred overnight. The reaction mixture was concentrated under reduced pressure and re-dissolved in H_2O (150 mL) and DCM (150 mL). The organic layer was washed with sat. aq. NaHCO_3 and brine, dried over MgSO_4 , filtered and concentrated *in vacuo*. The title compound was obtained after purification by RP-HPLC purification (linear gradient 40% \rightarrow 60% ACN in H_2O , 0.1% TFA, 15 min) as yellow oil (yield: 0.61 g, 0.97 mmol, 6.7%).

^1H NMR (400 MHz, CDCl_3 , Me_4Si) δ 9.31 (s, 1H), 8.56 (s, 1H), 8.48 (d, $J = 6.0$ Hz, 1H), 8.40 (d, $J = 7.2$ Hz, 1H), 8.16 (d, $J = 8.0$ Hz, 1H), 7.65 (t, $J = 8.0$ Hz, 4H), 7.62 – 7.55 (m, 2H), 7.46 (t, $J = 7.6$ Hz, 2H), 7.30 (d, $J = 8.0$ Hz, 2H), 7.02 (t, $J = 6.8$ Hz, 1H), 6.24 (s, 1H), 3.89 (s, 2H), 3.61 (t, $J = 6.0$ Hz, 2H), 3.39 (s, 2H), 3.16 (s, 2H), 2.17 (s, 2H), 1.73 (s, 2H), 1.41 (s, 9H). ^{13}C NMR (101 MHz, CDCl_3) δ 210.61, 196.08, 152.81, 144.31, 141.27, 140.18, 137.22, 135.15, 134.35, 133.18, 132.77, 132.16, 130.94, 129.97, 129.61, 128.76, 128.17, 128.02, 125.76, 117.31, 80.37, 69.36, 61.73, 53.71, 46.30, 41.78, 31.51, 27.40. HRMS: calculated for $\text{C}_{35}\text{H}_{39}\text{N}_3\text{O}_6\text{S}$ $[\text{M}+\text{H}]^+$ 630.25596; found 630.25533.

***Tert*-butyl(*Z*)-(2-(4-benzoylbenzylidene)-5-hydroxypentyl)(2-(isoquinoline-5-sulfonamido)ethyl)carbamate (60)**

This compound was prepared in the same reaction as **59**. The title compound was obtained after purification by RP-HPLC purification (linear gradient 40% → 60% ACN in H₂O, 0.1% TFA, 15 min) as yellow oil (yield: 1.68 g, 2.67 mmol, 18%). ¹H NMR (400 MHz, CDCl₃, Me₄Si) δ 9.31 (s, 1H), 8.60 (s, 1H), 8.36 (d, *J* = 6.0 Hz, 1H), 8.26 (d, *J* = 7.2 Hz, 1H), 8.15 (d, *J* = 8.0 Hz, 1H), 7.81 – 7.75 (m, 4H), 7.65 – 7.57 (m, 2H), 7.48 (t, *J* = 7.6 Hz, 2H), 7.19 (d, *J* = 8.0 Hz, 1H), 6.56 (s, 1H), 4.07 (s, 2H), 3.67 (t, *J* = 6.0 Hz, 2H), 3.12 (t, *J* = 5.6 Hz, 2H), 2.81 (s, 2H), 2.12 (t, *J* = 7.2 Hz, 2H), 1.80 – 1.77 (m, 2H), 1.43 (s, 9H). ¹³C NMR (101 MHz, CDCl₃) δ 196.16, 153.09, 144.89, 141.29, 140.38, 137.55, 135.87, 134.37, 133.54, 133.18, 132.61, 131.25, 130.28, 130.07, 129.13, 128.87, 128.44, 126.01, 117.40, 81.15, 62.69, 45.97, 30.34, 28.41. HRMS: calculated for C₃₅H₃₉N₃O₆S [M+H]⁺ 630.25596; found 630.25609.

***(E)*-*N*-(2-((5-azido-2-(4-benzoylbenzylidene)pentyl)amino)ethyl)isoquinoline-5-sulfonamide (63)**

Alcohol **59** (0.16 g, 0.26 mmol) was dissolved in DCM (1 mL). After addition of TEA (1 eq., 36 μL, 0.26 mmol) and DMAP (0.64 mg, 5 μmol), the resulting mixture was cooled to -20 °C. A solution of TsCl (1 eq., 0.05 g, 0.26 mmol) in DCM (2 mL) was added dropwise and the reaction was stirred at -20 °C for 18h. Subsequently, 0.1 M aq. HCl (10 mL) was added and the layers were separated. The organic layer was washed with 0.1 M HCl (10 mL) and brine, dried over MgSO₄, filtered and concentrated under reduced pressure. The crude product was subjected to the next step without further purification.

The residue was dissolved in DMF (10 mL). To this was added NaN₃ (20 eq., 0.34 g, 5.2 mmol) and the reaction was stirred at room temperature for 5h before being concentrated. The resulting residue **61** was dissolved in DCM (2.5 mL) and TFA (2.5 mL) was added. The mixture was stirred for 1h at RT before it was co-evaporated with toluene (3x 10 mL). The resulting mixture was purified by RP-HPLC (linear gradient 40% → 60% ACN in H₂O, 0.1% TFA, 15 min) and the title compound was obtained as yellowish oil (yield: 0.06 g, 0.11 mmol, 44%). ¹H NMR (600 MHz, MeOD) δ 9.58 (s, 1H), 8.73 – 8.70 (m, 2H), 8.62 (d, *J* = 7.2 Hz, 1H), 8.54 (d, *J* = 7.8 Hz, 1H), 7.95 (t, *J* = 7.8 Hz, 1H), 7.82 (d, *J* = 8.4 Hz, 2H), 7.79 (d, *J* = 6.6 Hz, 2H), 7.66 (t, *J* = 7.8 Hz, 1H), 7.54 (t, *J* = 7.8 Hz, 2H), 7.49 (d, *J* = 8.4, 2H), 3.89 (s, 2H), 3.34 (t, *J* = 6.6 Hz, 2H), 3.28 – 3.24 (m, 4H), 2.50 (t, *J* = 7.8 Hz, 2H), 1.83 – 1.78 (m, 2H). ¹³C NMR (151 MHz, MeOD) δ 197.92, 153.18, 142.23, 141.73, 138.73, 137.81, 136.28, 135.91, 135.84, 135.75, 135.64, 133.97, 133.74, 133.49, 131.37, 131.12, 130.60, 129.80, 129.51, 128.69, 127.54, 120.31, 53.20, 51.96, 48.26, 28.25, 27.62. HRMS: calculated for C₃₀H₃₀N₆O₃S [M+H]⁺ 555.21001; found 555.21063.

***(Z)*-*N*-(2-((5-azido-2-(4-benzoylbenzylidene)pentyl)amino)ethyl)isoquinoline-5-sulfonamide (64)**

This compound was prepared in the same reaction as **63**. The title compound was obtained after purification by RP-HPLC purification (linear gradient 40% → 60% ACN in H₂O, 0.1% TFA, 15 min) as a yellow oil (yield: 0.08 g, 0.15 mmol, 38%). ¹H NMR (600 MHz, MeOD) δ 9.49 (s, 1H), 8.63 – 8.61 (m, 2H), 8.44 (t, *J* = 8.4 Hz, 2H), 7.85 (t, *J* = 7.8 Hz, 1H), 7.78 (t, *J* = 8.4 Hz, 2H), 7.75 (d, *J* = 7.2 Hz, 2H), 7.64 (t, *J* = 3.6 Hz, 1H), 7.50 (t, *J* = 7.8 Hz, 2H), 7.38 (d, *J* = 7.8 Hz, 2H), 6.91 (s, 1H), 3.97 (s, 2H), 3.44 (t, *J* = 6.6 Hz, 2H), 3.08 (t, *J* = 6.0 Hz, 2H), 3.03 (t, *J* = 5.4 Hz, 2H), 2.43 (t, *J* = 7.2 Hz, 2H), 1.93 – 1.88 (m, 2H). ¹³C NMR (151 MHz, MeOD) δ 197.77, 153.23, 142.51, 141.63, 138.56, 137.69, 136.01, 135.76, 135.62, 135.47, 134.77, 134.29, 133.86, 133.31, 131.52, 131.32, 130.99, 130.48, 129.77, 129.51, 128.95, 128.54, 120.07,

51.92, 47.70, 46.83, 39.54, 32.38, 28.08. HRMS: calculated for $C_{30}H_{30}N_6O_3S$ $[M+H]^+$ 555.21001; found 555.21021.

Dasatinib-norbornene (69)

DiPEA (3 eq., 12 μ L, 69 μ mol) and 2,5-dioxopyrrolidin-1-yl bicyclo[2.2.1]hept-5-ene-2-carboxylate (**68**) (2 eq., 11 mg, 45 μ mol) were added to a solution of Dasatinib-amine **67** (11 mg, 23 μ mol) in DMF (2 mL). The reaction mixture was stirred at RT overnight. The title compound was obtained after purification by RP-HPLC purification (linear gradient 20% \rightarrow 40% ACN in H_2O , 0.1% TFA, 15 min) as a white solid (yield: 2.67 mg, 4.4 μ mol, 18%). 1H NMR (400 MHz, DMSO- d_6) δ 11.76 (s, 1H), 10.04 (s, 1H), 8.36 (s, 1H), 7.52 (d, J = 7.2 Hz, 1H), 7.39 (d, J = 9.6 Hz, 2H), 6.28 (s, 1H), 5.32 – 3.87 (m, 10H), 3.35 – 3.21 (m, 2H), 2.66 (s, 6H), 2.56 (s, 3H), 2.35 (s, 3H), 2.03 (s, 3H). ^{13}C NMR (101 MHz, DMSO- d_6) δ 165.38, 162.45, 162.05, 159.91, 158.93, 157.19, 140.81, 138.84, 133.51, 132.45, 129.07, 128.23, 127.05, 125.94, 83.28, 53.15, 51.26, 41.70, 25.57, 21.09, 18.32. HRMS: calculated for $C_{30}H_{35}ClN_8O_2S$ $[M+H]^+$ 607.22922; found 607.22963.

Dasatinib-azide (71)

This compound was prepared in the same reaction as **69**. However, 2,5-dioxopyrrolidin-1-yl 6-azidohexanoate (**70**) was used instead of the norbornene-succinimide **68**. The title compound was obtained after purification by RP-HPLC purification (linear gradient 20% \rightarrow 40% ACN in H_2O , 0.1% TFA, 15 min) as a white solid (yield: 4.03 mg, 6.4 μ mol, 28%). 1H NMR (400 MHz, DMSO- d_6) δ 11.71 (s, 1H), 9.89 (s, 1H), 8.21 (s, 1H), 7.37 (d, J = 7.2 Hz, 1H), 7.23 (d, J = 10.0 Hz, 2H), 6.10 (s, 1H), 4.44 – 3.51 (m, 6H), 3.31 – 2.83 (m, 4H), 2.51 (s, 2H), 2.40 (s, 3H), 2.20 (s, 3H), 2.07 (t, J = 6.4 Hz, 2H), 1.88 (s, 2H), 1.54 – 1.43 (m, 4H), 1.33 – 1.24 (m, 2H). ^{13}C NMR (101 MHz, DMSO- d_6) δ 165.37, 162.05, 159.89, 157.16, 140.81, 138.82, 133.49, 132.43, 129.06, 128.22, 127.03, 50.54, 35.15, 28.03, 25.82, 24.63, 22.32, 21.09, 18.32. HRMS: calculated for $C_{28}H_{36}ClN_{11}O_2S$ $[M+H]^+$ 626.24627; found 626.24685.

(E)-N-(2-((3-(4-(3-aminoprop-1-yn-1-yl)phenyl)allyl)amino)ethyl)isoquinoline-5-sulfonamide (73)

In separate flasks, a solution of the *N*-Boc-propargylamine (1.5 eq., 93 mg, 0.6 mmol), isoquinolinephenyl bromide **72** (220 mg, 0.4 mmol) and pyrrolidine (3 eq., 0.10 mL, 1.2 mmol) in DMF (0.5 mL), a solution of CuI (0.1 eq., 8 mg, 40 μ mol) in DMF (100 μ L) and a solution of $Pd(PPh_3)_4$ (0.05 eq., 23 mg, 20 μ mol) in DMF (100 μ L) were flushed with argon for 1 hr in an ultrasonic bath. To the alkyne mixture were added subsequently the CuI and the $Pd(PPh_3)_4$ solutions and the resulting mixture was stirred at 80 $^{\circ}C$ overnight. The reaction mixture was filtered over a short silica column and was flushed with DCM/MeOH (1/1 v/v; 10x column volume). The eluate was concentrated and the crude product was subjected to the next step without further purification.

The residue was dissolved in DCM (2 mL) and TFA (2 mL) was added and the reaction mixture was stirred for 2h at RT. The mixture was then co-evaporated with toluene (5x). The title compound was obtained after purification by RP-HPLC purification (linear gradient 25% \rightarrow 45% ACN in H_2O , 0.1% TFA, 15 min) as a yellow oil (yield: 56.6 mg, 0.13 mmol, 34%). 1H NMR (600 MHz, DMSO- d_6) δ 9.60 (s, 1H), 8.75 (s, 1H), 8.70 (s, 1H), 8.61 (d, J = 7.2 Hz, 1H), 8.53 (d, J = 8.4 Hz, 1H), 7.94 (t, J = 7.8 Hz, 1H), 7.47 (s, 4H), 6.85 (d, J = 15.6 Hz, 1H), 6.36 – 6.33 (m, 1H), 4.05 (s, 2H), 3.86 (d, J = 7.2 Hz, 2H), 3.19 (s, 4H). ^{13}C NMR (151 MHz, DMSO- d_6) δ 152.86, 138.88, 137.77, 136.46,

136.04, 135.75, 133.56, 133.22, 133.08, 130.10, 128.81, 128.07, 123.01, 122.83, 122.45, 120.91, 87.36, 82.58, 50.33, 47.62, 40.11, 30.70. HRMS: calculated for $C_{23}H_{24}N_4O_2S$ $[M+H]^+$ 421.16200; found 421.16256.

References

- ¹ Synthetic studies on kinase inhibitors and cyclic peptides: strategies towards new antibiotics, Thesis, : Adriaan W. Tuin, 2008,
https://openaccess.leidenuniv.nl/bitstream/handle/1887/13365/Proefschrift%2BAW_Tuin%2Balles.pdf?sequence=7.
- ² P. P. Geurink, B. I. Florea, N. Li, M. D. Witte, J. Verasdonck, C-L. Kuo, G. A. van der Marel, and H. S. Overkleeft, *Angew. Chem. Int. Ed.*, 2010, **49**, 6802.
- ³ A. M. C. H. van den Nieuwendijk, A. B. T. Ghisaidoobe, H. S. Overkleeft, J. Brussee and A. van der Gen, *Tetrahedron*, 2004, **60**, 10385-10396.; P. Zandbergen, A. M. C. H. van den Nieuwendijk, J. Brussee and A. van der Gen, *Tetrahedron*, 1992, **48**, 3977.

Samenvatting

Kinasen spelen een belangrijke rol in vele ziekten, zoals kanker, diabetes en infectieziekten. Daarom zijn kinasen een interessante doelgroep voor geneesmiddelen ontwikkeling. Er zijn remmers voor verscheidene kinasen op de markt, maar wegens resistentie, bijwerkingen of gebrek aan remmers voor bepaalde kinase families is het noodzakelijk om onderzoek te doen naar nieuwe klassen van verbindingen gericht op kinasen. Om dit te bereiken moeten er niet alleen nieuwe remmers ontwikkeld worden, maar ook moleculair gereedschappen ("probes"). Deze probes kunnen gebruikt worden om de activiteit en aanwezigheid van kinasen in hun biologische omgeving vast te stellen, te kwantificeren en de selectiviteit van remmers te bepalen. Het in dit proefschrift beschreven onderzoek richt zich op de ontwikkeling van potentere AKT1 en FLT3 kinase remmers. Tevens heeft dit onderzoek als doel de synthese en toepassing van nieuwe

probes om de kinasen, die betrokken zijn bij de diverse kankersoorten en andere ziekten, in kaart te brengen. Een korte beschrijving over de functies en de rollen van de kinasen die een onderwerp zijn in dit proefschrift is gegeven in **Hoofdstuk 1**.

In de afgelopen decennia zijn er vele chemische benaderingen ontwikkeld voor het bestuderen van de biologische functionele rol van kinasen, en om de selectiviteit en de doeleiwitten van kinase remmers in kaart te brengen. **Hoofdstuk 2** beschrijft en vergelijkt de principes van drie chemische methodes toegepast op kinase onderzoek: “activity-based protein profiling” (ABPP), “photoaffinity labeling” en “affinity-based profiling (AfBP). Deze drie methodes vormen de rode lijn van dit proefschrift.

H-89, een isoquinolinesulfonamide gebaseerde verbinding, is een welbekende potente PKA remmer. Analogen van deze verbinding remmen tevens AKT1 en andere kinasen, waaronder het oncologische doelwit, FLT3. **Hoofdstuk 3** behandelt het ontwerp en de synthese van een nieuwe set van isoquinolinesulfonamide gebaseerde remmers voor FLT3. Deze verbindingen bevatten allemaal de isoquinolinesulfonamide kern, waarbij variatie is geïntroduceerd op de fenyl groep door gebruik te maken van Suzuki koppeling reacties op de ortho, meta of para positie. Er zijn 34 verschillende omvangrijke (hetero)aromatische boorzuren gebruikt, waardoor er 102 nieuwe isoquinolinesulfonamide analogen zijn ontstaan.

Het biologisch effect van de 102 nieuwe isoquinolinesulfonamides samen met 137 andere isoquinolinesulfonamide analogen, welke in voorafgaande onderzoek zijn gesynthetiseerd, wordt besproken in **Hoofdstuk 4**. De remmingspotentie van deze 239 verbindingen op PKA, AKT1, AKT2 en FLT3 is bepaald aan de hand van een TR-FRET kinase assay. De resultaten uit dit hoofdstuk tonen aan dat zowel AKT1 als AKT2 een voorkeur hebben voor remmers met een omvangrijke heteroaromatische groep op de ortho positie. Dit gegeven maakt het lastig om actieve en selectieve remmers te ontwikkelen voor AKT1. Het is belangrijk om selectieve AKT1 remmers te vinden, gezien eerder onderzoek heeft aangetoond dat remming van zowel AKT1 als AKT2 leidt tot de dood van muizen. In dit onderzoek is aangetoond dat de meest selectieve AKT1 remmers een methyl gesubstitueerde alkeen groep bevatten en de introductie van een halogeen groep op de fenyl ring op de para positie is ook bevorderlijk voor de AKT1 over AKT2 selectiviteit. Een ander kinase dat bestudeerd is in dit proefschrift is FLT3. De meest actieve remmers voor FLT3 bevatten een heterearomatische groep op de para positie van de fenylring.

In het tweede deel van dit proefschrift worden de syntheses en biologische evaluaties van de chemische probes beschreven. Drie verschillende chemische benaderingen worden uitgelicht namelijk: ABPP, AfBP en “photoaffinity labeling”.

Hoofdstuk 5 beschrijft het ontwerp en de synthese van twee typen “activity-based probes” (ABPs) om Bruton’s tyrosine kinase (BTK) te labelen, namelijk directe en tweestaps bioorthogonale ABPs. Directe ABPs bevatten een label, waarmee het doeleiwit direct kan worden gevisualiseerd of geïsoleerd. Tweestaps ABPs daarentegen bevatten

een kleine reactieve groep die kan worden gebruikt om het label in een later stadium te introduceren, nadat de ABP aan zijn doeleiwit heeft gebonden. De ABPs voor BTK zijn gebaseerd op de covalente remmer ibrutinib. Een covalente band wordt gevormd tussen BTK en ibrutinib door een nucleofiele aanval van de cysteine in de actieve holte van BTK op het acrylamide gedeelte van ibrutinib. Resultaten uit dit onderzoek tonen aan de directe probe BTK kan labelen in zowel Ramos cell extract als in levende Ramos cellen. Ook de tweestaps bioorthogonale probes waren in staat om BTK te labelen in *in vitro* en *in situ* experimenten. Labeling met behulp van de directe probes resulteerde in minder achtergrond labeling dan de tweestaps probes.

Niet alle kinasen zoals BTK bevatten een nucleofiele groep in de actieve holte. Om deze kinasen covalent te labelen zijn er andere type chemische gereedschappen vereist.

Hoofdstuk 6 behandelt de synthese en biologische toepassing van twee diazerine-gefunctionaliseerde fotoreactieve probes. Deze probes werden vervolgens gebruikt om PKA en AKT1 te labelen. Beide probes zijn gebaseerd op het chemische structuur van H-89, welke zowel PKA als AKT1 remt, en bevatten een aryl trifluoromethyl diazerine groep als de fotoreactieve groep. De diazerine ring gaat een covalente binding aan met zijn doeleiwit na UV belichting. Daarnaast bevatten deze verbindingen een azide groep, welke gebruikt wordt als de bioorthogonale ligatie handvat. Beide probes waren in staat recombinante PKA en AKT1 te labelen. De probe met een *E*-configuratie was potenter dan de probe met een *Z*-configuratie.

Een derde chemische methode om kinasen te labelen is beschreven in **Hoofdstuk 7**. Een affiniteits-gebaseerde probe werd gesynthetiseerd om doeleiwitten van dasatinib in primaire chronische lymfatische leukemie (CLL) te onderzoeken. Deze affiniteits-gebaseerde probe werd verkregen door een koppeling van de kinase remmer dasatinib aan de NHS-geactiveerde sepharose bollen. In deze methode werden de doeleiwitten reversibel gebonden door de probe en geanalyseerd door middel van SDS-PAGE en/of LC-MS nadat ze geëluëerd werden van de geïmmobiliseerde dasatinib probe. Uit deze studie is gebleken dat c-Abl en BTK de hoofddoeleiwitten van dasatinib in primaire CLL waren. Andere geïdentificeerde doeleiwitten waren: Lyn, Csk, Fyn, Yes, Src and Lck.

List of publications

- 1. Photo-crosslinking of clinically relevant kinases using H-89-derived photo-affinity probes**
N. Liu*, S. C. Stolze*, R. H. Wijdeven, A. W. Tuin, A. M. C. H. van den Nieuwendijk, B. I. Florea, M. van der Stelt, G. A. van der Marel, J. J. Neefjes, H. S. Overkleeft, *Molecular Biosystems*, 2016, **12**, 1809.
- 2. The novel β 2-selective proteasome inhibitor LU-102 decreases phosphorylation of I kappa B and induces highly synergistic cytotoxicity in combination with ibrutinib in multiple myeloma cells**
J. Kraus, M. Kraus, N. Liu, L. Bess, J. Bader, P. P. Geurink, G. de Bruin, A. F. Kisselev, H. S. Overkleeft, C. Driessen, *Cancer Chemotherapy and Pharmacology*, 2015, **76**, 383.
- 3. Direct and two-step bioorthogonal probes for Bruton's tyrosine kinase based on ibrutinib: a comparative study**
N. Liu, S. Hoogendoorn, B. van der Kar, A. Kaptein, T. Barf, C. Driessen, D. V. Phillipov, G. A. van der Marel, M. van der Stelt, H. S. Overkleeft, *Organic and Biomolecular Chemistry*, 2015, **13**, 5147.
- 4. Integrating chemical and genetic silencing strategies to identify host kinase-phosphatase inhibitor networks that control bacterial infection**
H. M. H. G. Albers, C. Kuijl, J. Bakker, L. Hendrickx, S. Wekker, N. Farhou, N. Liu, B. Blasco-Moreno, T. Scanu, J. den Hertog, P. Celie, H. Ovaa, J. J. Neefjes, *ACS Chemical Biology*, 2014, **25**, 414.
- 5. Bioorthogonal chemistry: applications in activity-based protein profiling**
L. I. Willems, W. A. van der Linden, N. Li, K.-Y. Li, N. Liu, S. Hoogendoorn, G. A. van der Marel, B. I. Florea, H. S. Overkleeft, *Accounts of Chemical Research*, 2011, **44**, 718.
- 6. Incorporation of fluorinated phenylalanine generates highly specific inhibitor of proteasome's chymotrypsin-like sites**
P. P. Geurink, N. Liu, M. P. Spaans, S. L. Downey, A. M. C. H. van den Nieuwendijk, G. A. van der Marel, A. F. Kisselev, B. I. Florea, H. S. Overkleeft, *Journal of Medicinal Chemistry*, 2010, **53**, 2319.

Curriculum vitae

Nora Liu werd op 4 juli 1986 geboren te 's-Gravenhage. Zij behaalde in 2004 het Gymnasium diploma (profiel Natuur & Gezondheid) aan het Christelijk Gymnasium Sorghvliet te 's-Gravenhage. In datzelfde jaar begon zij aan de bacheloropleiding Bio-Farmaceutische Wetenschappen aan de Universiteit Leiden, die zij in 2006 *cum laude* afrondde. In het kader van de bacheloropleiding werd in 2006 een korte onderzoeksstage verricht naar de ontwikkeling van spacer-moleculen voor Isotachophorese en Massa Spectrometrie in de vakgroep Analytische Bio-wetenschappen onder begeleiding van dr. P. Lindenburg en prof. Dr. U. R. Tjaden.

In 2006 begon zij aan de masteropleiding Bio-Farmaceutische Wetenschappen. Haar hoofdvakstage voerde zij uit in de vakgroep Bio-Organische Synthese onder begeleiding van dr. P. P. Geurink, prof. Dr. G. A. van der Marel en prof. dr. H. S. Overkleef. Het doel van dit onderzoek was het ontwikkelen van nieuwe fluor-bevattende covalente remmers voor het proteasoom. In het kader van de bijvakstage werd het onderzoek naar de ontwikkeling van actievere en specifiekere ENPP3 en ENPP4 fosfatase remmers om de groei van *Salmonella typhimurium* te stoppen uitgevoerd onder begeleiding van dr. C. Kuijl en prof. dr. J. Neefjes in de vakgroep Cel Biologie II bij het Nederlands Kanker Instituut (NKI). In augustus 2009 behaalde zij *cum laude* het Master of Science diploma.

Door de toekenning van de Mozaïek beurs in 2009 in het kader van de ontwikkeling van nieuwe PKB/AKT1 remmers, maakte het in dit proefschrift beschreven onderzoek mogelijk. In september 2009 begon zij als assistent in opleiding bij de vakgroep Bio-Organische Synthese onder leiding van prof. dr. G. A. van der Marel en prof. dr. H. S. Overkleef. Een deel van het beschreven onderzoek werd uitgevoerd op het NKI te Amsterdam in de vakgroep Cel Biologie II onder leiding van prof. dr. J. Neefjes. Delen van dit onderzoek zijn gepresenteerd door middel van posters op het EMBO Chemical Biology congres (Heidelberg, Duitsland, 2012) en de NWO-CW "Design and Synthesis" conferenties (Lunteren, 2009, 2010, 2012) en CHAINS (2011, 2013). Een mondeling presentatie werd gegeven op de West European Activity-Based Proteomics Meeting in Essen (Duitsland, 2012).

Van januari 2014 tot juli 2015 werd er als post-doc onderzoek verricht naar de ontwikkeling van opsplitsbare fixatie moleculen voor cellen, in samenwerking met prof. dr. R. P. H. Bischoff (afdeling Analytische Biochemie te Groningen) en dr. T. M. Luiders (Afdeling Neurologie, Erasmus Universiteit te Rotterdam).